



University
of Glasgow

Doonan, James Joseph (2014) *Fc gamma receptor mediated modulation of osteoclastogenesis*. PhD thesis.

<http://theses.gla.ac.uk/5579/>

Copyright and moral rights for this thesis are retained by the author

A copy can be downloaded for personal non-commercial research or study, without prior permission or charge

This thesis cannot be reproduced or quoted extensively from without first obtaining permission in writing from the Author

The content must not be changed in any way or sold commercially in any format or medium without the formal permission of the Author

When referring to this work, full bibliographic details including the author, title, awarding institution and date of the thesis must be given

Fcy receptor mediated modulation of osteoclastogenesis

James Joseph Doonan

A thesis submitted to the College of Medicine, Veterinary and Life Sciences, University
of Glasgow in fulfilment of the requirements for the degree of Doctor of Philosophy

June 2014

Institute of Infection, Immunity and Inflammation
University of Glasgow
120 University Place, Glasgow
G12 8TA

Abstract

Osteoporosis is a condition that results from substantially weakened bone, increasing an individual's risk of fracture. Post-menopausal osteoporosis is the most common form of the condition, affecting 30% of post-menopausal women over the age of 50. Following the menopause, female oestrogen levels decline and this perturbs bone homeostasis by promoting an environment that is biased towards bone erosion. Osteoclasts are the cells responsible for eroding bone and are normally inhibited by oestrogen. However, the decline in oestrogen production results in increased osteoclast differentiation and activity. This rapidly decreases the bone mineral density and results in fracture-prone bone. Osteoclasts are derived from mononuclear myeloid progenitors found in the blood and bone marrow, which fuse to form large multinucleated cells that reside in the bone cavity. These progenitor cells are also responsible for replenishing monocytes, macrophages and dendritic cells. One class of receptors present on the surface of these cells, which are capable of dictating a cell's function, are Fcγ receptors and modulation of Fcγ receptors has been shown to inhibit the differentiation of human monocytes to osteoclasts.

This thesis investigates Fcγ receptor modulation on murine osteoclastogenesis and in order to stimulate Fcγ receptors, both IgG and IgG complexes were used. IgG complexes were generated using *Staphylococcus aureus* Protein A (SpA) in combination with IgG to form SpA-IgG complexes (SIC). We show that IgG and SIC are capable of engaging with Fcγ receptors resulting in the inhibition of osteoclast differentiation. Furthermore, both IgG and SIC inhibit the transcription of mRNA essential for the fusion of progenitors and enzymes for the erosion of bone matrix. Therefore, IgG and SIC are capable of inhibiting murine osteoclastogenesis.

The murine model of osteoporosis was used to further investigate the ability of SIC to inhibit murine osteoclast differentiation. Previous studies have shown that when SpA is administered *in vivo* it is capable of binding circulating IgG to form SIC. We used this property to test the ability of SpA to bind to the surface of monocytes. SpA was found to bind with highest affinity to blood Ly6C^{high} monocytes, which are known to differentiate *in vitro* to OCs. IgG and SIC were also able to inhibit the *in vitro* osteoclastogenesis of Ly6C^{high} monocytes. It was hypothesised that SpA would co-opt IgG and inhibit the *in vivo* differentiation of progenitors to osteoclasts in the ovariectomy model of osteoporosis. To generate this animal model the ovaries were removed from the mice in order to simulate the menopause and induce bone loss. To assess the percentage of bone present after ovariectomy, we used micro-computer tomography and discovered that SpA was unable to prevent bone loss associated with ovariectomy.

Therefore, SpA can bind to the surface of osteoclast progenitors but is unable to inhibit bone loss in the model of osteoporosis.

In addition to studying the role of Fc γ receptor modulation of osteoclastogenesis, the role of Bcl-3 (a negative regulator of NF- κ B) in osteoclast differentiation and bone remodelling was also investigated. NF- κ B is an essential signalling molecule and transcription factor involved in osteoclast differentiation. Previous research has shown that in the absence of Bcl-3 (Bcl-3^{-/-}) aberrant cytokine responses to LPS and TNF- α occur. Therefore, RANKL stimulation of WT and Bcl-3^{-/-} osteoclast precursors was done to determine whether Bcl-3^{-/-} animals responded aberrantly to RANKL. WT and Bcl-3^{-/-} animals were able to generate *in vitro* osteoclasts, which were phenotypically and transcriptionally similar. However, comparison of *in vivo* osteoclast progenitors revealed that Bcl-3^{-/-} animals had reduced CD115⁺ osteoclast progenitors compared to WT animals. Examination of the trabecular bone present in the proximal tibia revealed that Bcl-3^{-/-} animals had a higher percentage of bone present than WT controls. Therefore, Bcl-3 does not effect *in vitro* osteoclast differentiation but further work needs to be done to understand the role of Bcl-3 in bone remodelling.

This thesis aimed to investigate whether SpA-IgG complexes or Bcl-3 could represent a novel avenue of therapeutic intervention in osteoporotic disease. In summation, SpA is able to form IgG complexes that can inhibit the differentiation of OCs *in vitro*; however, treatment of osteoporotic animals with SpA was unable to halt bone loss. This suggests that SpA-IgG complexes are able to modulate Fc γ receptors *in vitro* and skew progenitors from differentiation into osteoclasts but cannot overcome the prevailing pro-osteoclastogenic environment that results from ovariectomy. The presence of osteoclast progenitors was also shown to be partially dependent on Bcl-3 and as such Bcl-3 may be a novel target for therapeutic agents to target osteoclast progenitors in diseases like osteoporosis. However, the role of Bcl-3 in bone remodelling requires further investigation.

Table of Contents

Abstract.....	1
Table of Contents	3
List of Figures.....	6
List of Tables.....	7
Acknowledgements.....	8
Author's Declaration.....	9
Abbreviations	10
1 Introduction	15
1.1 Osteoimmunology	15
1.2 Post-menopausal osteoporosis.....	16
1.2.1 Therapies for post-menopausal osteoporosis	18
1.2.2 Animal models of osteoporosis	19
1.2.3 Pathogenesis of oestrogen deficiency.....	20
1.2.4 Oestrogen inhibits osteoclastogenesis	22
1.3 Osteoclast differentiation.....	24
1.3.1 Osteoclast progenitors	24
1.3.2 Macrophage-colony stimulating factor	27
1.3.3 Receptor activator of NF- κ B ligand.....	30
1.3.4 Osteoprotegerin	31
1.3.5 NF- κ B controls osteoclastogenesis.....	33
1.4 Osteoclast maturation	35
1.4.1 Co-stimulators of osteoclastogenesis.....	35
1.4.2 The role of T cells in osteoclastogenesis	37
1.4.3 ITAM co-stimulation.....	38
1.4.4 Multinucleation.....	40
1.4.5 Bone resorption	41
1.5 Fc γ receptors interactions	42
1.5.1 Fc γ receptors	42
1.5.2 Immunoglobulin G.....	45
1.5.3 Immune complexes and Fc γ receptors	47
1.6 Staphylococcus aureus Protein A.....	49
1.6.1 SpA immunomodulation	50
1.6.2 SpA IgG complex immunomodulation	51
1.7 Hypothesis and aims	52

2	Materials and methods	54
2.1	Animals.....	54
2.2	Osteoclast differentiation.....	54
2.2.1	RAW 264.7 cell differentiation to osteoclasts	54
2.2.2	Osteoclast differentiation from murine bone marrow	55
2.2.3	Monocyte enrichment	55
2.2.4	Blood and bone marrow mononuclear cell isolation	56
2.2.5	Isolation of non-adherent bone marrow	56
2.3	Tartrate resistant acid phosphatase staining.....	57
2.4	Assessing osteoclastogenesis.....	57
2.5	Bone resorption assay.....	58
2.6	SpA immunoglobulin complexes	58
2.6.1	BS ³ cross-linking	59
2.6.2	Coomassie stain	59
2.6.3	Size exclusion chromatography	59
2.7	Polymerase chain reaction	60
2.7.1	RNA isolation.....	60
2.7.2	cDNA generation	60
2.7.3	Primer design	60
2.7.4	End Point PCR.....	61
2.7.5	Quantitative PCR.....	61
2.8	Osteoporosis surgical model	63
2.9	Flow cytometry	63
2.10	ELISA	65
2.11	Biomechanical testing	66
2.12	Micro-computer tomography.....	66
2.13	Histology.....	67
2.13.1	Haematoxylin and eosin staining.....	67
2.13.2	Histological TRAP staining	68
2.14	Statistical analysis.....	68
3	Fcγ receptor interactions inhibit osteoclastogenesis	69
3.1	Introduction	69
3.2	Results	71
3.2.1	Optimisation of <i>in vitro</i> osteoclastogenesis	71
3.2.2	Fcγ receptor mediated inhibition of osteoclastogenesis	80
3.2.3	Comparison of Oplg and SIC	82
3.2.4	IgG inhibits osteoclastogenesis.....	85

3.2.5	Functional consequence of Fcγ receptor inhibition.....	87
3.2.6	The role of FcγRIII in Fcγ receptor mediated inhibition.....	89
3.2.7	Fcγ receptor modulation down-regulates osteoclast essential gene transcription.....	90
3.3	Discussion.....	94
4	SpA treatment in a murine model of bone loss.....	102
4.1	Introduction.....	102
4.2	Results.....	106
4.2.1	SpA interacts with blood and bone marrow monocytes.....	106
4.2.2	SpA and monocyte FcγRI.....	111
4.2.3	SIC inhibits Ly6C ^{high} monocyte differentiation to osteoclasts.....	114
4.2.4	Murine model of ovariectomy induced bone loss.....	116
4.2.5	CTX-1 is a marker of bone resorption.....	120
4.2.6	Biomechanical testing of OVX femurs.....	122
4.2.7	OVX bone loss measured by micro computer tomography.....	124
4.2.8	Oestrogen, SpA and monocyte composition.....	127
4.2.9	Fcγ receptor profiles and oestrogen deficiency.....	131
4.3	Discussion.....	135
5	NF-κB inhibitor Bcl-3 modulates bone remodelling.....	141
5.1	Introduction.....	141
5.2	Results.....	144
5.2.1	RANKL induces Bcl-3 mRNA transcription.....	144
5.2.2	Bcl-3 deficient osteoclastogenesis.....	145
5.2.3	RANKL induced transcription in Bcl-3 deficient animals.....	148
5.2.4	Fcγ receptor mediated osteoclast inhibition.....	151
5.2.5	Bcl-3 is required for osteoclast precursor homeostasis.....	154
5.2.6	Bcl-3 deficiency results in perturbed bone remodelling.....	163
5.3	Discussion.....	167
6	General discussion.....	172
6.1	Future work.....	175
6.2	Conclusion.....	176
	Appendix - Media, buffers and reagents.....	177
	References.....	179

List of Figures

Figure 1-1: Synthesis of oestrogens from cholesterol.	17
Figure 1-2: Differentiation of monocytes and osteoclasts from bone marrow progenitors.	29
Figure 1-3: Schematic of synergistic effect of cytokines and interactions involved in osteoclast differentiation.	32
Figure 1-4: Diagrammatic representation of IgG Fcγ receptor interactions.	43
Figure 1-5: Diagrammatic representation of SpA's interaction with IgG.	50
Figure 3-1: Enrichment of bone marrow monocytes does not induce the differentiation of osteoclasts.	74
Figure 3-2: Isolated blood and bone marrow monocytes respond to high concentrations of RANKL.	75
Figure 3-3: 30ng/ml M-CSF and 50ng/ml RANKL is not sufficient to differentiate osteoclasts. ...	76
Figure 3-4: Addition of IL-1β does not promote osteoclastogenesis.	77
Figure 3-5: Comparison of L929 culture media or M-CSF to differentiate osteoclasts.	78
Figure 3-6: Increasing concentrations of M-CSF induce osteoclastogenesis.	79
Figure 3-7: SIC and Oplg inhibit the differentiation of TRAP+ osteoclasts.	81
Figure 3-8: Cross-linking protein interactions between SpA and IgG results in IgG complex formation; OVA and IgG do not form complexes.	83
Figure 3-9: Fractionation of SpA, OVA and IgG using Sephacryl chromatography column demonstrates that OVA and IgG do not form complexes.	84
Figure 3-10: Murine IgG inhibits the differentiation of TRAP+ osteoclasts.	86
Figure 3-11: SIC inhibits the activity of osteoclasts on bovine cortical bone slices.	88
Figure 3-12: SIC inhibits the differentiation of TRAP+ FcγRIII ^{-/-} osteoclasts.	89
Figure 3-13: Primers designed for qPCR are specific for their target gene.	91
Figure 3-14: Fcγ receptor modulation of transcription in pre-osteoclasts.	92
Figure 3-15: IgG inhibits pre-osteoclasts transcript levels of osteoclast specific genes.	93
Figure 3-16: Diagrammatic representation of <i>in vitro</i> osteoclast inhibition.	101
Figure 4-1: Diagram representing oestrogen deficiency induced bone loss and treatment with SpA IgG complexes.	105
Figure 4-2: Gating strategies for the identification of monocytes and monocyte subsets.	108
Figure 4-3: Representative FACS plots of AF488 ⁺ monocytes and monocyte subsets.	109
Figure 4-4: Fluorescent SpA binds to Ly6C ^{high} monocytes in the blood.	110
Figure 4-5: Representative FACS plots of FcγRI expression on monocytes and monocyte subsets.	112
Figure 4-6: FcγRI expression is reduced on monocytes and monocyte subsets following SpA treatment.	113
Figure 4-7: Ly6C ^{high} monocytes are inhibited from differentiating to osteoclasts following Fcγ receptor modulation.	115
Figure 4-8: Diagrammatic representation of the OVX treatment regimes.	117
Figure 4-9: OVX surgery increased animal's weight.	118
Figure 4-10: Oestrogen deficiency decreases uterine weight.	119
Figure 4-11: OVX increases the plasma concentration of CTX-1.	121
Figure 4-12: The effect of OVX and treatment with SpA on bone integrity measured by three-point bend testing.	123
Figure 4-13: Representative images of μCT trabecular bone reconstructions from proximal tibia of sham and OVX animals.	125
Figure 4-14: μCT analysis of trabecular bone of proximal tibia of sham and OVX animals.	126
Figure 4-15: Representative FACS plots of three OVX treatment regimes.	128
Figure 4-16: Number of total monocytes following OVX and treatment with SpA.	129
Figure 4-17: Monocyte subset cell numbers following OVX and treatment with SpA.	130
Figure 4-18: Expression of FcγRI on monocyte subsets in blood and bone marrow following OVX.	132

Figure 4-19: Expression of FcγRII/III on monocyte subsets in the blood and bone marrow following OVX.	133
Figure 4-20: SpA modulates Fcγ receptors on monocytes.	134
Figure 5-1: Schematic of Bcl-3's hypothesised role in RANKL-RANK mediated signal transduction.	143
Figure 5-2: RANKL stimulation up-regulates Bcl-3 mRNA.	144
Figure 5-3: TRAP staining of osteoclast differentiation kinetics in WT and Bcl-3 ^{-/-} cultures.	146
Figure 5-4: Osteoclast differentiation kinetics in WT and Bcl-3 ^{-/-} cultures.	147
Figure 5-5: Osteoclast survival signals are unaffected in the absence of Bcl-3.	149
Figure 5-6: The transcription of osteoclast specific mRNA is unaffected in Bcl-3 ^{-/-} osteoclasts.	150
Figure 5-7: Representative TRAP staining for WT and Bcl-3 ^{-/-} osteoclasts.	152
Figure 5-8: Fcγ receptor modulation inhibits WT and Bcl-3 ^{-/-} osteoclast differentiation.	153
Figure 5-9: Gating strategy to identify blood and bone marrow monocytes.	156
Figure 5-10: WT and Bcl-3 ^{-/-} blood and bone marrow monocyte and neutrophil populations.	157
Figure 5-11: Number of total monocytes and neutrophils in WT and Bcl-3 ^{-/-} animals.	158
Figure 5-12: Monocyte subsets cell number in WT and Bcl-3 ^{-/-} animals.	159
Figure 5-13: Representative FACS plots of CD115 expression on monocytes and monocytes subsets.	160
Figure 5-14: CD115 expressing monocytes in WT and Bcl-3 ^{-/-} animals.	161
Figure 5-15: GM-CSF mRNA transcript is up-regulated in Bcl-3 bone marrow.	162
Figure 5-16: μCT analysis of trabecular bone of proximal tibia from WT and Bcl-3 ^{-/-} animals.	164
Figure 5-17: The presence of osteoclasts in Bcl-3 ^{-/-} tibias.	166

List of Tables

Table 1-1: Hormones involved in human and rodent reproductive cycles.	18
Table 1-2: Expression of surface markers on bone marrow subsets.	27
Table 1-3: Fcγ receptor subclasses, signalling potential and IgG binding affinities.	45
Table 2-1: List of primers sequences ordered from Integrated DNA Technologies Ltd and QIAGEN for qPCR analysis.	62
Table 2-2: List of flow cytometry reagents used.	65
Table 5-1: All μCT analysis parameters of trabecular bone of the proximal tibia in WT and Bcl-3 ^{-/-} animals.	165

Acknowledgements

Firstly, I would like to thank my supervisors Dr Carl Goodyear and Prof Margaret Harnett for their help and guidance throughout my PhD. As my primary supervisor, Dr Carl Goodyear deserves special thanks for his constant patience and mentoring over the last four years. He has taken so much time to help me develop into the scientist I am today (which has been a long and gruelling process) and for this I am very thankful. I would also like to thank the collaborators in the Universities of Edinburgh and Oxford who have made my PhD possible by providing training on μ CT machines and three-point bend testing. I would also like to thank Dr Ruaidhri Carmody for providing NF- κ B expertise and animals.

The Goodyear Lab deserves a lot of my thanks! Every member has at some point lifted my spirits and helped me when I have been in the depths of despair. Susan and Lindsay, you showed me everything I know: westerns, PCR and banjo playing. I doubt I could convey how much you have taught me and helped me over the last 4 years. You are both amazing - thank you! I couldn't continue without giving a resounding 'BIG UP' to Felix and Jen for donating their sleep to help with my 7am harvests (in exchange of coffee of course). Felix, sharing with you daily pictures of pygmy hedgehogs, cats, dogs, squirrels, rabbits, owls, mice, rats, chicks, hamsters, ducks, pandas both regular and red and anything else that makes me go 'd'awwwwwwwwwww' was a joy...for me. Jen, your cocktail making skills are off da hook and led to many a great night (I think). Pauline, you have been my science guardian angel, giving advice and chit chats when I needed it most: thank you. And of course other Goodyear Lab recruits both here and gone: Michelle, Ashley, Moeed, Katja, Cecilia, Louise, Simone, Mark, Hussain and Kevin. Thank you also to Trish for letting me be your new NF- κ Buddy, Kenny for our coffee dates and of course everyone on Level 3, without whom my experience would have been a poorer version.

All of my friends have had their part to play in my PhD, whether they know it or not, no matter how big or small. Each one has provided a welcome escape from my toils; assistance in reading drafts (Tristan and Lauren); or simply giving me a chance to relax, unwind and blow off steam. You are all always there for me, thank you all so much.

And finally, I have my very supportive family to thank. Without my family's unwavering love, support and freedom to let me be who and what I want, I would definitely not be where I am today.

Author's Declaration

I declare that, except where explicit reference is made to the contribution of others, that this thesis is the result of my own work and has not been submitted for any other degree at the University of Glasgow or any other institution.

Signature:

Printed Name: James Doonan

Abbreviations

23g	- 23 gauge
α-MEM	- alpha - minimum essential media
ANOVA	- Analysis of variance
AP1	- Activator protein 1
APC	- Antigen presenting cell
$\alpha_v\beta_3$	- Vitronectin receptor
CD115 (c-fms)	- Colony stimulating factor 1 receptor
BAFF	- B cell activating factor
Bcl-XL	- B cell lymphoma - extra large
Bcl-2	- B cell lymphoma 2
Bcl-3	- B cell lymphoma 3
BCR	- B cell receptor
BM	- Bone marrow
BMP	- Bone morphogenetic protein
BMU	- Basic multicellular unit
bp	- Base pair
BS³	- Bis-sulfosuccinimidyl suberate
BSA	- Bovine serum albumin
BV/TV	- Bone volume / tissue volume
Ca²⁺	- Calcium
CaMKIV	- Calcium calmodulin kinase IV
cAMP	- Cyclic adenosine monophosphate
Cath K	- Cathespin K
CD	- Cluster of differentiation
cDNA	- Complementary deoxyribonucleic acid
CMP	- Common myeloid progenitor
CIA	- Collagen induced arthritis
CO₂	- Carbon dioxide
C/EBP	- Ccaat enhancer binding proteins
CR3	- Complement receptor 3
CREB	- cAMP response element binding
CTX-1	- C terminal telopeptide of collagen type I
DAP12	- DNAX activating protein of molecular mass 12kDa
DC	- Dendritic cell
dH₂O	- Distilled H ₂ O
DAPI	- 4',6-diamidino-2-phenylindole
DC-STAMP	- Dendritic cell-specific transmembrane protein

D-MEM	- Dulbecco's modified eagle medium
DMSO	- Dimethyl sulphoxide
DNA	- Deoxyribonucleic acid
dNTPs	- Deoxynucleotide triphosphates
DXA	- Dual energy x-ray absorptiometry
EDTA	- Ethylenediaminetetraacetic acid
ELISA	- Enzyme linked immunosorbant assay
ERα/β	- Oestrogen receptor alpha or beta
ERE	- Oestrogen response element
ERK1/2	- Extracellular signal-regulated kinase 1 / 2
FACS	- Fluorescence-activated cell sorting
FasL	- Fas ligand
Fcγ	- Common gamma chain
FcγR	- Fc gamma receptor
FBS	- Foetal bovine serum
FMO	- Fluorescence minus one
FSc	- Forward scatter
FSH	- Follicle stimulating hormone
GAPDH	- Glyceraldehyde 3-phosphate dehydrogenase
GFP	- Green fluorescent protein
GSK3β	- Glycogen synthase kinase 3 beta
GM-CSF	- Granulocyte macrophage colony stimulating factor
GMP	- Granulocyte macrophage progenitor
GnRH	- Gonadotrophin releasing hormone
HRT	- Hormone replacement therapy
HSC	- Haematopoietic stem cell
HSD	- Hydroxysteroid dehydrogenase
IC	- Immune complex
ICAM-1	- Intracellular adhesion molecule 1
IFN-γ	- Interferon - gamma
IFN-γR	- Interferon - gamma receptor
Ig	- Immunoglobulin
IgG/M/D/A/E	- Immunoglobulin G / M / D / A / E
IκB	- Inhibitor of NF- κ B
K⁺	- Potassium
IL-10	- Interleukin 10
IL-12p40	- Subunit p40 of interleukin 12/23
IL-1R	- Interleukin 1 receptor
IL-1Ra	- Interleukin 1 receptor antagonist

i.p.	- Intraperitoneal
ITAM	- Immunoreceptor tyrosine based activation motif
ITAMi	- Inhibitory immunoreceptor tyrosine based activation motif
ITIM	- Immunoreceptor tyrosine based inhibitory motif
ITP	- Immune thrombocytopenic purpura
J	- Joules
KO	- Knockout
LH	- Luteinizing hormone
LPS	- Lipopolysaccharide
Ly6C	- Lymphocyte antigen 6 complex, locus C
Ly6G	- Lymphocyte antigen 6 complex, locus G
MAP Kinase	- Mitogen activated protein kinase
M-CSF	- Macrophage colony stimulating factor
MØ	- Macrophage
MDP	- Macrophage - dendritic cell progenitor
MHC II	- Major histocompatibility class II
MITF	- Microphthalmia-associated transcription factor
MFI	- Mean fluorescence intensity
mm	- Millimetre
MMP9	- Matrix metalloproteinase 9
MPa	- Mega Pascals of force
mRNA	- Messenger RNA
N	- Neutrons of force
µCT	- Micro computer tomography
µMT	- Mu MT mice (disruption Ig mu chain gene)
NA	- Non-adherent
NA BM	- Non adherent bone marrow
NFATc1 (NFAT2)	- Nuclear factor of activated T cells c1
NF-κB	- Nuclear factor κB
NIK	- NF-κB inducing kinase
OB	- Osteoblast
OC	- Osteoclast
OCPs	- Osteoclast progenitor population
OC-STAMP	- Osteoclast specific transmembrane protein
Oplg	- OVA with polyclonal IgG
OPG	- Osteoprotegrin
OSCAR	- Osteoclast associated receptor
OVA	- Chicken ovalbumin
OVX	- Ovariectomised mouse model of osteoporosis

PBS	- Phosphate buffered saline
PBMC	- Peripheral blood mononuclear cell
PBST	- Phosphate buffered saline with 0.01% tween
PCR	- Polymerase chain reaction
PI3K	- Phosphatidylinositol 3-kinases
PLZF	- Promyelocytic leukaemia zinc finger protein
PMO	- Post menopausal osteoporosis
PO₄³⁻	- Phosphate
Pre-OC	- precursors of OCs (all monocyte subsets and progenitors)
PTH	- Parathyroid hormone
qRT-PCR	- Quantitative real time polymerase chain reaction
RA	- Rheumatoid arthritis
RANK	- Receptor activator of NF-κB
RANKL	- Receptor activator of NF-κB ligand
RHD	- Rel homology domain
RPMI 1640	- Roswell park memorial institute 1640 medium
RNA	- Ribonucleic acid
RT	- Room temperature
SCF	- Stem cell factor
SD	- Standard deviation
Sham	- Sham operated mouse
SIC	- SpA immunoglobulin G complexes
siRNA	- Silencing RNA
SOFAT	- Secreted osteoclast factor of activated T cells
SpA	- <i>Staphylococcus aureus</i> protein A
sRANKL	- Soluble receptor activator of NF-κB ligand
SSc	- Side scatter
TAD	- Transcriptional activation domain
TAE	- Tris base, acetic acid and EDTA
TAK1	- Transforming growth factor β activated kinase 1
TBS	- Tris buffered saline
TBST	- Tris buffer saline with 0.01% tween
TCR	- T cell receptor
TGF-β	- Transforming growth factor β
TLR 4	- Toll like receptor 4
TNF-α	- Tumour necrosis factor α
TNFR1	- Tumour necrosis factor receptor 1
TNFRSF	- TNF receptor super family
TNT	- Tunnelling nanotubes

TRAF3	- TNF receptor associated factor 3
TRAF6	- TNF receptor associated factor 6
TRAP	- Tartrate resistant acid phosphatase
TREM2	- Triggering receptor expressed on myeloid cells 2
Vit D₃	- 1 α ,25-dihydroxyvitamin D ₃
WT	- Wild type C57Bl/6 animals

1 Introduction

1.1 Osteoimmunology

Osteoimmunology is the study of the interactions between the immune and skeletal system¹. Many factors produced by cells of the immune system promote immunity as well as being essential in the maintenance of bone integrity¹. Evidence is growing that the interactions between T cells, B cells, Macrophages (*MØ*), Osteoclasts (OC) and Osteoblasts (OB) within the bone marrow (BM) are vital for homeostatic bone remodelling¹. T and B cells from the adaptive immune system and *MØ* which bridge the innate and adaptive immune system interact with OCs and OBs, which are involved in bone modelling and remodelling¹. Despite arising from separate lineages, T cells and OCs share the same essential transcription factors², B cells and OBs secrete negative regulators of OC differentiation (see section 1.3.4)³ and *MØ* and OCs share the same progenitors prior to terminal differentiation⁴. However, this intimate link between the immune and skeletal system can become perturbed. In diseases like osteoporosis, oestrogen deficiency results in dysregulation of immune cells. This causes the production of factors which drive the differentiation of OCs, leading to global bone loss⁵. Therefore, establishing the interactions between immune and skeletal cells allows for dissection of osteoporotic pathogenesis.

In bone biology three main cell types remodel bone: OCs, OBs and osteocytes each play a vital role in modelling and remodelling the skeletal system. OCs differentiate from precursors of the monocyte lineage that are present in blood and reside within the BM⁴. Following the appropriate stimulation, monocytes will express essential osteoclastogenic proteins and begin to fuse (see sections 1.3 and 1.4)^{6,7}. Fusion results in the formation of a multinucleated OC which attaches onto the surface of the bone matrix⁷. OCs form a tightly sealed zone and a ruffled border creating an isolated section of bone matrix directly beneath the OC⁸. At this point the OC begins to acidify the matrix and secrete enzymes such as Tartrate resistant acid phosphatase (TRAP), Matrix Metalloproteinase 9 (MMP9) and Cathepsin K to resorb the bone⁷⁻¹².

In contrast, OBs differentiate from a mesenchymal origin and secrete organic molecules, such as collagen type I, osteocalcin and osteopontin, as they migrate over the surface of eroded bone matrix¹³. These organic molecules, mainly collagen type I, bind extracellular calcium ions (Ca^{2+}) which results in mineralisation and bone formation¹⁴. OBs can remain on the surface of eroded bone and allow themselves to become cocooned in the extracellular matrix. OBs which do this are then known as osteocytes¹³. Osteocytes are immobilised but remain connected to other osteocytes by

an extensive series of canals¹⁵. This shifts their role from bone formation to mechanical stress sensing in order to coordinate the bone remodelling process¹⁵.

Together these three cell types regulate bone homeostasis in a system called the basic multicellular unit (BMU)¹⁶. The BMU involves a coordinated series of events in which OCs differentiate and settle on bone, initiating the erosive phase of the BMU. OCs migrate across bone matrix and form trenches of eroded bone¹³. OCs have an average lifespan of 12 days before they apoptose allowing OBs to begin the lengthy process of secreting new organic matrix¹⁶. The bone formation phase of BMU can last as long as 3 months, as secreted organic matrix slowly binds circulating Ca^{2+} for mineralisation¹³. This temporal discrepancy in the bone resorption and formation phases of the BMU can become perturbed resulting in bone disorders. Despite, the rate at which bone formation and resorption occur, the purpose of bone modelling and remodelling is to maintain bone integrity¹⁶. Bone modelling occurs in order to respond to changes in mechanical load resulting in altered structure, size and shape of bones ensuring that the musculoskeletal system is able to meet the physical demands¹⁷. While, bone remodelling occurs to remove damaged bone and is stimulated by osteocyte death¹⁵. However, in diseases like osteoporosis bone loss exceeds bone formation resulting in pathologically weakened bone¹⁶.

1.2 Post-menopausal osteoporosis

Osteoporosis is a physical state in which there is sufficient bone loss to pose an increased risk of fracture. The disease can be categorised into either primary or secondary osteoporosis¹⁸. Primary osteoporosis is bone loss due to intrinsic factors such as menopause, aging or genetic factors¹⁹. While secondary osteoporosis occurs usually following medical intervention for other conditions such as Cushing's disease which requires long term glucocorticoid treatment resulting in osteoporotic fractures in 30-50% of patients²⁰. Osteoporotic fractures in the elderly are a major cause of disability and can increase mortality rates²¹. Clinical osteoporosis is diagnosed by measuring the percentage of bone present in femoral head by dual-energy x-ray absorptiometry (DXA)²². DXA uses x-ray images of the patient's femoral head and can provide insight into the micro-architecture of a patient's bones. To make a diagnosis, the percentage of bone present in the patient's femoral head is compared to that of a healthy sex-matched individual²². If the patient's percentage of bone is over 2.5 standard deviations or more below that of a healthy individual then that patient is diagnosed with osteoporosis. This method of diagnosis is referred to as the T score and this can be used to diagnose osteoporosis in both sexes²². The potential fracture risk increases as the mineral density of the bone decreases and studies have shown that the

lifetime risk of a female, aged 50 or over, suffering a hip fracture is 15%²². Thus diagnosing osteoporosis prior to fracture allows time for treatments to be initiated to slow the rate of bone loss and limit hazards which may lead to fractures.

Post-menopausal osteoporosis (PMO), or Type I osteoporosis, occurs in 30% of post-menopausal women and is caused by a decline in the production of oestrogen by the ovaries¹⁹. The ovaries are small nodular organs located either side of the uterine fallopian tubes which are involved in coordination of menstrual cycle. The release of follicle-stimulating hormone (FSH) from the pituitary glands induces oestrogen production by the ovaries and rising concentrations of oestrogen mark stages of the menstrual cycle²³. This cycle prepares the uterus for implantation and pregnancy. Several hormones are involved in the monthly cycle including gonadotrophin-releasing hormone (GnRH), FSH, luteinizing hormone (LH), oestrogen and progesterone (Table 1-1)²⁴. Rodents experience similar reproductive cycles to humans requiring the aforementioned hormones²⁵. However, unlike human menses, rodents reabsorb the uterus, rather than shed their menses, at the end of their oestrous cycles which lasts approximately 5-6 days for mice and 4-5 days for rats^{26,27}.

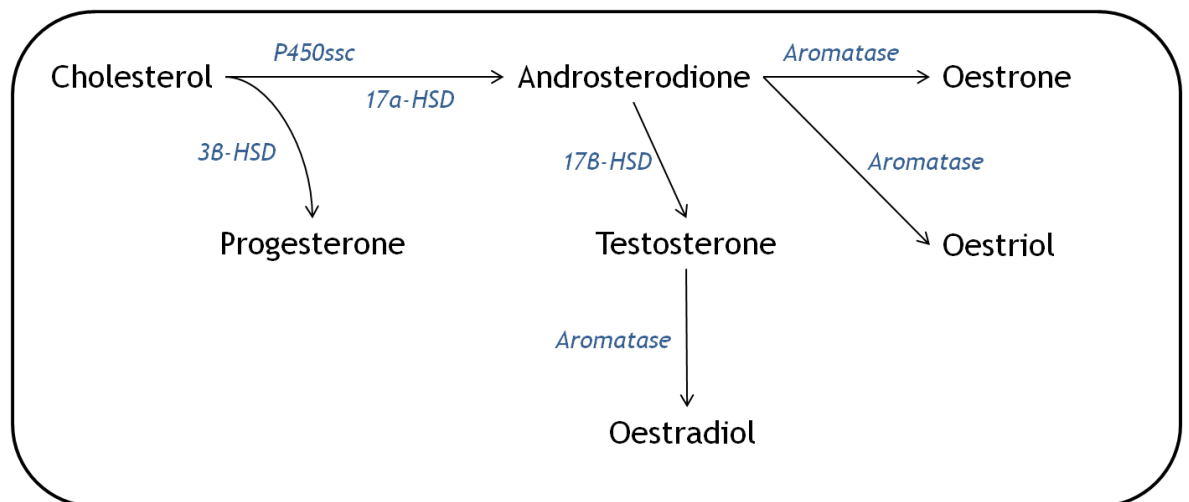


Figure 1-1: Synthesis of oestrogens from cholesterol.

Cholesterol is converted to multiple sex steroids depending on the physiological requirements of the body. Enzymes involved in producing sex steroids are in blue. Adapted diagram^{24,28}.

Oestrogen plays a pivotal role in both the menstrual and oestrous cycle. It is synthesised from cholesterol by thecal cells in the ovaries in response to FSH. However, oestrogen is the collective name given to three related hormones; oestrone, oestriol and the most

biologically active form oestradiol²⁸. Hereafter, the term oestrogen will be used to encompass all isoforms, unless specifically stated. The levels of oestrogen vary throughout the female menstrual cycle from 50ng/ml to 250ng/ml²⁹. The biosynthesis of oestrogen is a multi-step process in which cholesterol is converted to progesterone and the androgen, androsterodione²⁸. Androsterodione is then converted directly to oestrone or oestriol by aromatase or converted to testosterone by 17 β hydroxysteroid dehydrogenase (HSD)²⁸. Testosterone is then finally converted to oestradiol by aromatase (Figure 1-1)²⁸.

Hormone	Secretion	Function
Gonadotrophin-releasing hormone (GnRH)	Circulating E increases GnRH pulse frequency Circulating P decreases GnRH pulse frequency	<i>Released in pulses from hypothalamus to induce the release of FSH and LH</i>
Follicle-stimulating Hormone (FSH)	Slow GnRH pulse frequency increases FSH secretion	<i>Released by anterior pituitary gland to activate thecal cells to produce E and stimulate ovarian follicle development</i>
Lutenizing hormone (LH)	Fast GnRH pulse frequency increases LH secretion	<i>Released by anterior pituitary gland to stimulate oocyte development and release. Initiates P production by empty follicle</i>
Oestrogen (E)	FSH activates thecal cells surrounding oocytes to produce E	<i>E stimulates oocyte development and replenishment of the uterus following menses. Controls production of GnRH</i>
Progesterone (P)	LH stimulates the development of the corpus luteum which produces P	<i>P stimulates the secretory phase of the uterine wall and prepares uterus for implantation. Controls production of GnRH</i>

Table 1-1: Hormones involved in human and rodent reproductive cycles.

Adapted table²⁴.

1.2.1 Therapies for post-menopausal osteoporosis

The menopause refers to a period in the female reproductive cycle when the final oocyte is released by the ovary and the level of oestrogen decreases. The decline in oestrogen results in the commencement of menopausal symptoms such as hot flushes, neurological problems, weight gain and bone loss³⁰. In order to combat these symptoms and reduce the fracture risk hormone replacement therapy (HRT) is given. This supplies the body with oestrogen or oestrogen mimetics with or without progesterone derivatives³¹. These therapies are successful in preventing PMO; however, long term exposure to oestrogen and progesterone can increase the risk of cancer, cardiovascular disease and neurological issues³¹. Raloxifene, a non-hormonal selective oestrogen

receptor modulator has been shown to decrease fracture risk, however, there remained the increased risk of side effects including cramps and thromboembolisms³². Another group of drugs which is frequently used to treat osteoporosis are bisphosphonates which can bind to the bone matrix and upon resorption are ingested by OCs and induce apoptosis³³. Bisphosphonates effectively eliminate bone resorption. However, these drugs can have adverse side effects such as fever, oesophageal irritation, osteonecrosis, severely reduced bone remodelling and increased risk of cancer³⁴. Humanised monoclonal antibodies which target RANKL and sclerostin have been shown to be safe and effective at increasing bone mass in post-menopausal osteoporosis^{35,36}. However, these monoclonal antibodies are costly and must be administered in high doses to be effective^{35,36}. This has resulted in research focused at generating small peptides with the potential to engage the hinge region of RANK, preventing the conformational change which results in intracellular signalling, however, preclinical trials have still to be undertaken³⁷. Therefore, there is an absence of a safe, efficacious and ultimately cost effective therapeutic designed for the treatment of post menopausal osteoporosis. The research presented in this thesis will aim to demonstrate novel avenues of investigation.

1.2.2 Animal models of osteoporosis

In order to mimic human osteoporosis, animals are ovariectomised (OVX) thus removing the predominant source of oestrogen from their system²⁸. The rodent model of osteoporosis was first described by Salville in 1969³⁸. OVX surgery results in an oestrogen deficient system in which rapid trabecular bone loss is observed³⁹. Inducing osteoporotic disease by surgical removal of the ovaries has been studied in a range of mammals including monkeys, dogs, rats and mice⁴⁰. Monkeys in particular appear to be a good model organism for studying osteoporosis as they naturally undergo age-related bone loss and have a natural menopause⁴⁰. However, these are costly experiments with large waiting times before assessment of bone loss⁴⁰. Dogs are also used to study osteoporosis due to bone morphological similarities to humans⁴⁰. However, only age-related bone loss can be studied in dogs, as they are resistant to OVX induced bone loss⁴⁰. Rodents (rats and mice) are frequently used to study osteoporosis due to the rapid bone remodelling, reproducibility and ease of use⁴⁰. Rodents naturally do not develop 'osteoporosis' in a similar manner to humans; however, both rodents and humans lose bone mass with age⁴¹. The main difference is that human age and menopausal related bone loss can lead to fractures of the vertebrae and femoral head which does not occur in rodents¹⁹. Despite this difference both the rodent model and human osteoporotic disease results in loss of the trabecular structures of the femur, tibia and vertebrae due to over active OCs and an inability of OBs to replace eroded bone.

1.2.3 Pathogenesis of oestrogen deficiency

In recent years, and due to the availability of genetically engineered animals, the pathways involved in the rodent model of osteoporosis have been examined. In the rat model of OVX, early continuous treatment with oestradiol prevented bone loss by reducing OC numbers and stabilising the hormone balance⁴². Combined treatment of oestrogen and PTH was effective in the OVX model by preventing bone loss and increasing bone formation⁴². Administration of oestradiol to OVX mice prevents bone loss and as a consequence also decreases bone formation highlighting the tightly regulated nature of bone remodelling^{43,44}. Interestingly, OVX mice treated with oestradiol have reduced weight gain⁴⁵. These findings mirror results obtained from post-menopausal women receiving long term HRT, who had higher bone mineral density and decreased weight compared to placebo controls^{46,47}. Oestradiol also induces OPG secretion and as such, during PMO insufficient oestradiol levels result in lower OPG levels and increases the risk of developing osteoporosis⁴⁸.

The absence of oestrogen can cause systemic effects and one example of this is that oestrogen deficiency increases the number of CD25⁺ T cells present in the spleens of OVX animals, which arise in an IFN- γ dependent manner⁴⁹. M \emptyset taken from OVX animals are highly responsive to IFN- γ , producing pro-inflammatory cytokines IL-12 and IL-18, which are known to induce T cell proliferation and survival⁴⁹. This increase in T cell numbers and IFN- γ primed M \emptyset results in an activated immune state, with OVX animals possessing more than double the number of TNF- α producing T cells in the BM compared to controls⁴⁹. As previously mentioned, T cells are capable of expressing RANKL and initiating osteoclastogenesis⁵⁰. Interestingly, the roles of IFN- γ and IFN- γ Receptor (IFN- γ R) have not been fully elucidated. IFN- γ R^{-/-} C57Bl/6 animals suffer OVX induced bone loss while IFN- γ R^{-/-} DO11.10 animals are spared from OVX induced bone loss^{49,51}. However, Duque *et al* (2011) went onto show that IFN- γ given therapeutically can increase bone mass in sham and OVX operated C57Bl/6 mice⁵¹. This suggests that IFN- γ may negatively regulate OCs in a strain specific manner and further work must be done to fully elucidate IFN- γ 's effects on bone remodelling.

The importance of T cells in bone remodelling as already been discussed (see section 1.4.2), however T and B cells contribute to osteoporosis. T and B cell expansion and increased IL-7 production are hallmarks of human and OVX induced osteoporosis^{52,53}. IL-7 is an important regulator of T and B cell maturation produced by stromal cells and OBs. The absence of IL-7 results in significantly reduced T and B cell maturation *in vivo*⁵². Production of IL-7 by stromal cells and OBs is induced following stimulation by IL-1 and TNF- α ⁵⁴. This then acts on T cells to increase production of RANKL and TNF- α and drive

bone resorption^{54,55}. IL-7 has been shown to directly act via *in vivo* T cells in order to induce bone erosion^{55,56}. However, IL-7^{-/-} animals develop less trabecular bone with increased number of OC under steady state conditions and remain susceptible to OVX induced bone loss⁵⁷. The BM from IL-7^{-/-} animals also has an increased propensity to differentiate into OCs while treatment of IL-7 inhibits the differentiation of WT OC cultures⁵⁸. However, IL-7 neutralizing antibodies used in WT OVX animals were able to reduce OVX induced bone loss⁵⁶. Therefore, it would appear that IL-7 can indirectly drive OC differentiation and bone loss in osteoporosis. However, IL-7 has a complex role in the maintenance of bone remodelling under homeostasis.

With increasing age, and menopause, there is an increase in the secretion of IL-6, IL-1 and TNF- α by PBMCs⁵⁹. The role that IL-6, IL-1 and TNF- α play in OVX induced bone loss has been widely studied. Serum concentration of IL-6 positively correlates with serum concentrations of IL-1 β , TNF- α and the onset of the menopause⁵⁹. IL-6 is produced by stromal cells and OBs, and induces *in vitro* OC bone erosion⁶⁰. Interestingly, oestrogen effects on IL-6 production occur at a transcriptional level. Oestrogen binds to the oestrogen receptor and forms a complex (E/ER) (see section 1.2.4) which is capable of interacting with the promoter region of the IL-6 gene at NF- κ B and C/EBP regions to prevent the binding of p65 and c-Rel⁶¹. Thus in a state of oestrogen deficiency this transcriptional repression is lost and IL-6 is produced at higher concentrations. The link between IL-6 and OVX-induced bone loss was studied in IL-6^{-/-} mice. IL-6^{-/-} mice have a normal bone phenotype with faster remodelling than littermate controls, however OVX failed to induce bone loss in IL-6^{-/-} animals⁶². Therefore, IL-6 has a significant role in inducing bone loss following OVX.

As previously mentioned, TNF- α producing T cells are increased following OVX and the importance of this has been studied. TNF- α ^{-/-} animals have normal bone physiology but do not suffer from OVX induced bone loss⁶³. When soluble TNF- α receptor is used to treat OVX animals bone loss is limited, however, bone loss is prevented when TNF-binding protein (TNF-bp) is used⁶⁴. Adoptive transfer of WT T cells into TNF- α ^{-/-} animals resulted in TNF- α ^{-/-} animals becoming susceptible to OVX induced bone loss^{53,63}. These studies indicate that TNF- α , and TNF- α producing T cells have a central role in OVX induced bone loss. Transgenic mice which express human TNF- α spontaneously develop arthritis with increased bone loss. This bone loss can be prevented by treatment of OPG, suggesting that this bone loss is RANKL dependent^{65,66}. In addition, blockade of IL-6 receptor in TNF-transgenic animals was able to reduce the number of OC present in inflamed joints, but could not prevent bone erosion⁶⁷. Under steady state conditions treatment with TNF- α increases OC differentiation in the trabecular bone but this occurs in an IL-1 dependent manner⁶⁸.

TNF- α induced OC differentiation can be enhanced by treatment with IL-1 which acts on OBs to induce a positive feedback and allow secretion of TNF- α to drive osteoclastogenesis⁶⁸. IL-1 also stimulates BM M \emptyset to differentiate into OCs in the presence of TNF- α ⁶⁸. In fact, in the BM compartment, oestrogen deficiency in mice results in increased secretion of IL-1 and TNF- α by mononuclear cells which acts directly on stromal cells increasing their secretion of M-CSF^{69,70}. The concentration of M-CSF produced by oestrogen deficient stromal cells positively correlates with the degree of *ex vivo* osteoclastogenesis⁶⁹. The use of an M-CSF neutralisation antibody prevented OVX induced bone loss and inflammatory arthritis induced bone loss^{71,72}. In addition, the absence of IL-1 or IL-1 receptor (IL-1R), animals did not suffer OVX induced bone loss⁷³ and treatment with IL-1R antagonist (IL-1Ra) reduced bone loss after OVX surgery⁷⁰. Oestradiol significantly decreases murine splenic M \emptyset production of TNF- α , IL-6 and IL-1 β following LPS stimulation by reducing nuclear NF- κ B phosphorylation⁷⁴. In fact, serum oestradiol levels are inversely correlated to monocyte TNF- α mRNA transcript and oestradiol treatment decreases monocyte secretion of IL-1 α and IL-1 β ^{75,76}. This highlights the central role which oestrogen has in maintaining the homeostatic production of cytokines which can control bone remodelling.

1.2.4 Oestrogen inhibits osteoclastogenesis

Oestrogen can effect a variety of cells; however, it is also capable of directly acting on OCs. Interestingly the number of CD14⁺ monocytes increases during the menopause, following a reduction in ER expression, yet this effect was reversed in women using HRT⁷⁷. Thus oestrogen limits the pre-OCs found in the blood limiting the number of potential cells which differentiate into OCs. In fact, *in vitro* experiments using the leukemic monocytic cell line, THP-1, showed that treatment with oestradiol decreased the anti-apoptotic factor Bcl-2 expression⁷⁸. Therefore, oestradiol has the ability to reduce survival signalling.

E/ER interactions have genomic and non-genomic function. Oestrogen is able to enter the cell and bind intracellular ER where it forms the E/ER complex⁷⁹. This can then translocate to the nucleus for genomic E/ER activity by binding to oestrogen response elements (ERE) on the promoters of genes and either activate or inhibit transcription⁷⁹. One notable function of the E/ER complex is its ability to inhibit NF- κ B activity. As previously mentioned, TNF- α induced NF- κ B translocation and IL-6 transcription was inhibited by E/ER complex⁷⁴. As a member of the TNF receptor superfamily, RANK signalling via NF- κ B is essential in osteoclastogenesis therefore oestrogen may utilise a similar mechanism of action and inhibit NF- κ B activation. Treatment with oestrogen inhibited the activation of p65, RelB, c-Rel and partially blocked p52 *in vivo*⁸⁰. However,

oestrogen also increases Bcl-3 production which is known to bind and stabilize p50/p52 dimers on NF- κ B sites to modulate transcription⁸⁰. Treatment of the MCF-7 breast cancer cell line with oestrogen increases expression of NF- κ B p105 which acts as an I κ B protein and can block nuclear translocation of NF- κ B dimers⁸¹. This could be a mechanism which oestrogen uses to limit NF- κ B activation following RANK mediated signalling.

Oestrogen also exerts non-genomic effects which are due to expression of ER α and ER β on the cell surface⁸². Ligation of surface ER α results in dimerisation and signalling via PI3K/Akt and ERK⁸², which has been shown to reduce pro-apoptotic factors in cardiomyocytes^{83,84}. Oestradiol also has non-genomic effects on OCs by influencing potassium (K⁺) channels, namely the inwardly rectifying K⁺ channel, and results in the depolarisation of the OC membrane within seconds of activation⁸⁵. Pharmacological inhibitors of this channel prevent oestrogen induced depolarisation of the membrane⁸⁶. Oestrogen induced membrane depolarisation may cause the reduction in the secretion of H⁺ by H⁺ATPase and thus reduce OC activity. In addition, RAW 264.7 cells that were treated with oestradiol in RANKL stimulated cultures did not effect the differentiation to OCs but inhibited the transcription of Cathepsin K and TRAP, thereby reducing the OC capacity to function⁸⁷.

In an elegant study, Nakamura *et al* (2007) used an OC specific ER α KO animal (ER $\alpha^{\Delta OC/\Delta OC}$) to demonstrate that female ER $\alpha^{\Delta OC/\Delta OC}$ had reduced bone volume⁸⁸. Transgenic animals with Cre recombinase under the transcriptional control of Cathepsin K where bred with transgenic animals possessing LoxP sites that flanked the ER α gene⁸⁸. This resulted in a transgenic mouse which would only produce the Cre recombinase protein in OCs which could ultimately act directly on the LoxP sites to remove the ER α DNA from the genome, thus creating an OC specific ER α KO animal⁸⁸. This study demonstrated that oestrogen acts directly on OCs to regulate their *in vivo* function⁸⁸. Nakamura *et al* (2007) went onto show that this deficiency did not affect the ability of OCs to differentiate *in vitro* compared to littermate controls, but that addition of oestrogen to OC cultures induced the production of Fas Ligand (FasL), which could ligate Fas and induce apoptosis⁸⁸. Therefore, oestrogen is able to directly inhibit the function and survival of OCs *in vitro* and *in vivo* via production of FasL and induction of apoptosis.

1.3 Osteoclast differentiation

1.3.1 Osteoclast progenitors

Monocytes are typically thought of as the generic precursor of OCs (pre-OC) found in both the blood and BM⁸⁹. However, the view of a homogenous monocyte population has changed with recent evidence revealing that the differentiation of monocytes to MØ or OCs in health and disease occurs over a series of stages⁹⁰. Each step of differentiation produces a monocyte with a functionally different identity performing a role outlined by both the microenvironment and the receptors it expresses⁹¹.

Monocytes arise from haematopoietic stem cells (HSCs) that are self-renewing pluripotent progenitors found in the BM⁹⁰. Depending on the signals received, HSCs can differentiate into granulocyte-MØ progenitors (GMPs), common myeloid progenitors (CMPs) or MØ/Dendritic cell (DC) progenitors (MDPs)⁹⁰. However, with each subsequent differentiation the stem cell loses pluripotency and becomes more specialised until the final cell is terminally differentiated⁹⁰. In the case of monocytes, MDPs replenish the BM with monocytes which can migrate into the periphery to terminally differentiate into monocytes/MØ and DCs⁹⁰. However, prior to terminal differentiation, a number of transcription factors control this process. HSCs express high levels of the transcription factor promyelocytic leukemia zinc finger (PLZF) which represses myeloid differentiation by inhibiting transcription factors involved in stimulating monocytopoies⁹². However, in response to extracellular stimuli, such as cytokine signalling, HSCs can down-regulate PLZF expression allowing the HSC to enter the next stage in differentiation⁹². The repressive activity of PLZF allows HSCs to balance the maintenance of progenitors and newly differentiated cells⁹². Another transcription factor which is essential in the differentiation of monocytes, MØ and OCs is PU.1. Originally, Scott *et al* (1994) generated a PU.1 knockout (KO) mouse line and showed that PU.1 deletion was embryonic lethal and resulted in abnormal development of lymphoid and myeloid compartments⁹³. Tondravi *et al* (1997) later generated another PU.1 transgenic animal with a disrupted gene and demonstrated that PU.1 transgenic animals could reach full term but would die of septicaemia within 48 hours. This transgenic animal allowed observation of the skeleton which was void of OCs⁹⁴. These results showed that PU.1 was not only vital for the maintenance of the haematopoietic compartment but also for the differentiation of OCs. It is believed that this is due to PU.1's ability to control the expression of CD115, which is an essential receptor in survival and differentiation of monocytes and OCs (see section 1.3.2)⁹⁵.

The regulation of PLZF and PU.1 allow MDPs to differentiate into monocytes that express Ly6C at high levels (Ly6C^{high}) prior to their egress, in a CCR2-dependent manner, from the BM into the circulation^{96,97}. Ly6C^{high} monocytes are known as classical monocytes because they are typically involved in inflammatory responses by migrating to sites of inflammation and differentiating into MØ to assist the inflammatory response^{98,99}. In the absence of inflammatory signals, Ly6C^{high} monocytes down-regulate Ly6C and become non-classical Ly6C^{low} monocytes⁹⁷. Ly6C^{low} monocytes also down-regulate CCR2 and thus lose the capacity to migrate to sites of inflammation⁹⁷. However, Ly6C^{low} monocytes begin to express high levels of CX3CR1 which enhances monocyte survival and promotes Ly6C^{low} monocyte 'patrolling' behaviour^{100,101}. This behaviour is thought to allow the surveillance of the vascular system for signs of infection and removal of apoptotic cells¹⁰⁰. Ly6C^{low} monocytes are short lived cells and they were once believed to migrate into tissue and differentiate into tissue resident MØ, however, recently this has been disputed and it is now thought that tissue resident MØ are self-renewing and the monocyte compartment does not replenish this MØ population⁹⁷. A third subset of monocyte also exists that has intermediate expression of Ly6C (Ly6C^{int}) and expresses CX3CR1. These cells are believed to be Ly6C^{high} monocytes which have migrated to the BM and have begun the process of down-regulating Ly6C to become Ly6C^{low} monocytes⁹⁷. However, there is uncertainty as to whether Ly6C^{high} monocytes are required to return to the BM for Ly6C down-regulation to occur, as intermediary Ly6C monocytes can be found in both the blood and BM⁹⁷. Human monocyte biology is similar to the mouse as classical monocytes are identified by CD14^{bright} FcγRIII^{negative} while non-classical monocytes are CD14⁺ FcγRIII^{bright}⁹⁹. These cell types play similar roles in the human and mice. A similar intermediate monocyte population, defined as CD14^{bright} FcγRIII⁺, is believed to be a classical monocyte transitioning to non-classical⁹⁹. In this manner, Fc γ Receptors (FcγRs) can be used to distinguish between human classical and non-classical monocytes and other members of the FcγR family are expressed on the surface of monocytes and osteoclast progenitors⁹⁹.

An extra layer of complexity is added to the murine system as both Ly6C^{high} and Ly6C^{low} monocytes express CD115, the MØ-colony stimulating factor (M-CSF) receptor, which promotes monocyte function, survival and is essential in the differentiation of OCs^{97,102}. In fact, attempts have been made to determine whether an isolated subset of monocytes exist as a defined OC progenitor (OCPs) population and whether these cells arise from MDPs. Research by Charles *et al* (2012) and Jacome-Galarza *et al* (2013) has demonstrated that a separate, but phenotypically similar, cell subset exists in the BM which is highly osteoclastogenic when compared to Ly6C^{high} and Ly6C^{low} monocytes (Table 1-2)^{4,103}. Charles *et al* (2013) proposed a novel model for the differentiation of OCPs from MDPs based on the expression pattern of receptors essential for MØ and OC

function (Figure 1-2)¹⁰³. Subtle differences in surface receptor expression exist between monocytes and OCPs which could reflect their *in vivo* roles.

Of particular interest is the expression of CD11b, CD117 and CD135. CD11b is an integrin which forms as a heterodimer with CD18 known as the complement receptor 3 (CR3)¹⁰⁴. CR3 is able to bind the complement factor C3b and activate the complement cascade and ligate intravascular adhesion molecule-1 (ICAM-1) to mediate phagocytosis, chemotaxis and cytotoxicity¹⁰⁴. Both Ly6C^{high} and Ly6C^{low} monocytes require high expression of CD11b in order to fulfil their role as phagocytes⁹⁷. Yet, OCPs have no immediate requirement for CD11b, as they are not phagocytes and thus do not require CD11b expression. CD117 (c-kit) and CD135 (Flt3) are tyrosine kinase receptors expressed on BM progenitors¹⁰⁵. The ligand for CD117 is stem cell factor (SCF) which maintains the differentiation of progeny from progenitors¹⁰⁵. The ligand for CD135 is Flt3 Ligand (Flt3L) which is believed to promote progenitor viability in the BM and *in vitro* DC differentiation^{106,107}. Down-regulation of CD117 is typically believed to be conducive for maturation of haematopoietic cell yet some non-progenitor cells, for example, mast cells, retain high expression of CD117¹⁰⁵. However, CD117 expression on OCPs can identify CD117^{high} and CD117^{low} populations and when isolated CD117^{high} OCPs differentiated to OCs at a faster pace than CD117^{low} OCPs^{4,103}. While MDP expression of CD117 is known to identify them as a subset it is not possible to delineate CD117 high or low expressing populations of MDPs¹⁰³. Blocking antibodies against CD117 did not, however, inhibit the haematopoiesis or differentiation of stem cells to OCs *in vitro*¹⁰⁸. The one discerning difference between MDPs and OCPs is that OCPs lack CD135 (Table 1-2). Flt3L binds CD135 and induces receptor dimerisation and activation promoting cell survival¹⁰⁶. CD135 is mainly expressed on haematopoietic BM progenitors but is mostly involved in lymphocyte development, as CD135^{-/-} animals have regular peripheral blood population but altered B cells compartments^{109,110}. Investigation into BM progenitors expanded in the presence of Flt3L *in vitro* maintain the ability to differentiate into MØ, DCs and OCs¹¹¹. However, the loss of CD135 on the surface of OCPs *in vivo* suggests that OCPs are a distinct cell type from CD135 positive MDPs.

Interestingly, OCPs have been shown *in vitro* to differentiate into MØ and DCs under the correct conditions, thus retaining a certain degree of plasticity⁴. It is also worth noting that Ly6C^{high} monocytes can differentiate into OCs *in vitro* unlike Ly6C^{low} monocytes¹⁰³. Monocytes expressing CX3CR1 also migrate through the blood and relocate to BM prior to differentiation to OCs¹¹². In the blood and spleen, Ly6C^{high} monocytes which express high levels of CD115 and CD11b are highly capable of differentiating into OCs and may represent the OCP population present in the periphery⁴. Despite the current research,

further work needs to ascertain the exact origin of OCPs. Whether OCPs can be classed as a monocyte subset, arise separately or share the same lineage is yet to be established. Regardless of progenitor lineage, the differentiation of monocytes and OCPs to OC relies on a number of factors *in vivo*. The most accepted and researched factor is Receptor activator of NF- κ B ligand (RANKL) mediated OC differentiation (see section 1.3.3)¹¹³.

Protein	Gene	CD	Bone Marrow Subset			
			MDP	Ly6C ^{high}	Ly6C ^{low}	OCP
c-fms	<i>Csf1r</i>	CD115	+	+	+	+
ITGAM	<i>Itgam</i>	CD11b	-	+	+	low
Stem cell factor receptor	<i>C-kit</i>	CD117	+	-	-	high/low
Fractalkine Receptor	<i>Cx3cr1</i>	CX3CR1	+	int	high	+
Flt3 Receptor	<i>Flt3</i>	CD135	+	-	-	-
RANK	<i>Tnfrsf11a</i>	CD265	-	-	-	-
F4/80	<i>F4/80</i>	-	low	low	low	low
Ly6C	<i>Ly6c1</i>	-		+	low	+
CCR2	<i>Ccr2</i>	CD192		+	-	+
L-Selectin	<i>Sell</i>	CD62L		+	-	+
Leukosialin	<i>Spn</i>	CD43		+	high	

Table 1-2: Expression of surface markers on bone marrow subsets.

Adapted table^{90,91,103}.

1.3.2 Macrophage-colony stimulating factor

RANK ligand (RANKL) mediated osteoclastogenesis is driven by two factors: M-CSF and RANKL¹¹³. Although many factors are known to participate in osteoclastogenesis *in vivo*, the activity of M-CSF and RANKL acting on populations of pre-OCs, from the blood or BM, from many species results in OC differentiation *in vitro*^{3,114,115}. Consequently, we will explore the ability of RANKL to induce differentiation of OCs.

For OC differentiation to occur, M-CSF must be a co-stimulator. M-CSF is a cytokine released by monocytes, fibroblasts, T cells and B cells which binds to the receptor CD115 on the surface of monocytes/M \emptyset and OCPs^{1,116,117}. The importance of M-CSF in bone remodelling was first realised when the *op/op* mouse was generated. *op/op*

animals produce a non-functioning form of M-CSF which results in osteopetrosis due to a lack of functional OCs resulting in short stature, short tail and no tooth eruption *in vivo*^{118,119}. This phenotype is mirrored in the M-CSF deficient rat which has a mutation in the *Csf1* gene¹²⁰. These animals are termed toothless (*tl/tl*) due to the lack of tooth eruption and development of osteopetrosis¹²⁰. In mice, this osteopetrotic phenotype plateaus with age suggesting that other mediators of osteoclastogenesis compensate for the lack of M-CSF¹¹⁸. In fact, recently IL-34 was shown to ligate CD115 and successfully replace M-CSF in generating mature OCs in the presence of RANKL¹²¹. Additionally, IL-34 is up-regulated in aged *op/op* animals suggesting that IL-34 is able to rescue osteopetrosis in *op/op* animals¹²². Kodama *et al* (1991) found that the bone defect in *op/op* animals could be rescued by the daily injection of recombinant human M-CSF into young *op/op* pups¹²³. Mirroring this finding, Wiktor-Jedrzejczak *et al* (1990) implanted L929 (a murine fibroblast cell line that produces biologically active M-CSF) containing capsules intraperitoneally (i.p.) into *op/op* animals which partially restored OC populations and bone homeostasis¹¹⁹.

The M-CSF receptor CD115 is a tyrosine kinase receptor that dimerises upon ligation with M-CSF¹²⁴. The importance of CD115 in bone remodelling was verified by the generation of *Csf1r*^{-/-} mouse (deficient for CD115) which had severe osteopetrosis and altered BM cellularity¹⁰². Upon ligation, M-CSF induces CD115 dimerisation and auto-phosphorylation of seven tyrosine residues on the cytoplasmic tail of the receptor¹²⁵. These have been shown to interact with up to 150 adaptor proteins in a macromolecular protein complex¹²⁵. The most important mediators of CD115 signalling are Phosphoinositide 3-kinase (PI3K) and Extracellular signal-regulated kinases 1/2 (ERK1/2) (Figure 1-3)¹²⁵. Both of these signalling molecules are essential for M-CSF induced MØ proliferation which leads to phosphorylation of glycogen synthase kinase-3 beta (GSK3B) resulting in inhibition of cell cycle arrest^{125,126}. CD115 mediated signalling also induces the transcription factor PU.1 which is essential for the induction of OCs as well as self-regulating the expression of CD115^{1,95}. Another transcription factor which is known to be essential for osteoclastogenesis is Microphthalmia-associated transcription factor (MITF)¹²⁷. Genetic knockout of the MITF gene, *Mitf*^{mi/mi}, are unable to differentiate OCs in culture because upon ligation, CD115 activation results in MITF phosphorylation which has been shown to induce osteoclastogenesis and increase OC activity¹²⁷. M-CSF has also been shown to maintain nuclear integrity and stimulate chemotactic behaviour in mature OCs¹²⁸. Hodge *et al* (2011) demonstrated that mature OCs treated with RANKL alone could form sealing rings, but addition of M-CSF further enhanced this ability¹²⁹. Arai *et al* (1999) found that stimulation of BM mononuclear cells with M-CSF increased RANK mRNA within 24 hours which continued to increase for up to 72 hours⁶. In addition, Charles *et al* (2012) demonstrated that OCPs stimulated

with M-CSF for two days resulted in an increase in the surface expression of RANK¹⁰³. Taken together studies suggest that M-CSF induces RANK expression via the combined binding of PU.1 and MITF to the promoter region of the *RANK* gene, inducing transcriptional activity¹³⁰.

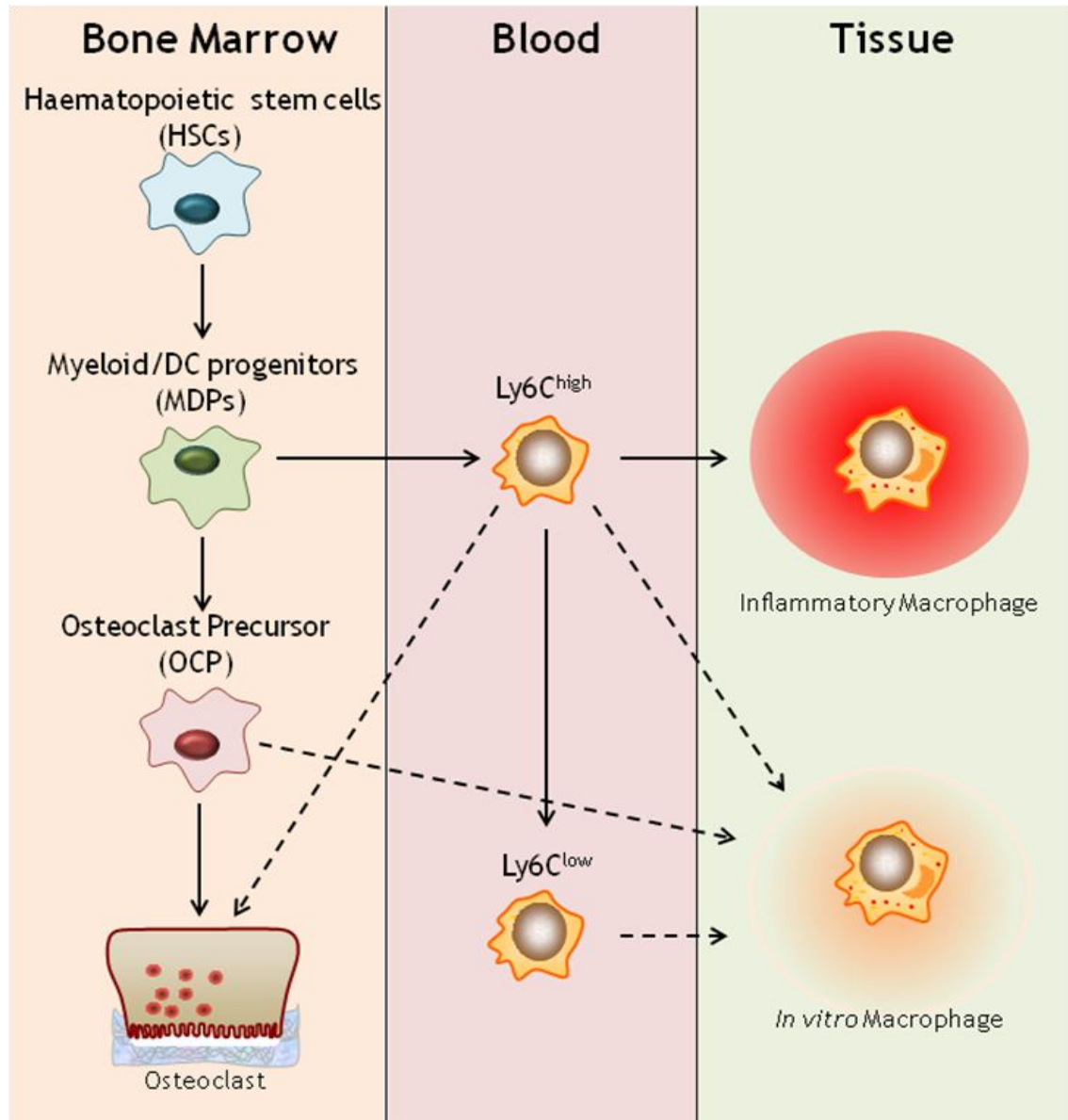


Figure 1-2: Differentiation of monocytes and osteoclasts from bone marrow progenitors. HSCs present in the BM self renew and parent MDPs. MDPs differentiate further into Ly6C^{high} monocytes which enter the circulation and migrate to sites of inflammation to terminally differentiate into inflammatory MØ. In the absence of inflammation, Ly6C^{high} monocytes migrate to the BM and down-regulated Ly6C expression becoming Ly6C^{low} monocytes which patrol the vasculature. Ly6C^{high} monocytes, but not Ly6C^{low} monocytes, can differentiate into OCs *in vitro*. OCPs are thought to arise from MDPs and can differentiate into OCs. OCPs are also able to differentiate into MØ, as are Ly6C^{high/low} monocytes *in vitro*. Solid arrows indicate *in vivo* differentiation pathways; dashed arrows indicate *in vitro* differentiation. Adapted diagram^{90,96,97,103}.

1.3.3 Receptor activator of NF- κ B ligand

RANKL is a cytokine expressed on the surface of OBs, stromal cells and activated T and B cells^{1,131}. RANKL present on the surface of cells interacts with the membrane bound receptor RANK on the surface of pre-OCs to stimulate osteoclastogenesis¹. However, RANKL can be cleaved by MMPs to form a soluble ligand, sRANKL, which has reduced efficacy at interacting with RANK and inducing osteoclastogenesis¹³²⁻¹³⁴. This reduced efficacy may be due to other surface molecules on the OBs interacting with OCs and thus enhancing osteoclastogenesis, instead of the difference between membrane anchored and soluble protein versions. The role of RANKL *in vivo* was highlighted by the creation of the RANKL deficient animal which was incapable of generating *in vivo* OCs and developed osteopetrosis¹³⁵. RANKL^{-/-} animals also have altered lymphocyte development and lymph node formation demonstrating that RANKL has a wider range of functions *in vivo*¹³⁵.

RANK is a transmembrane receptor that is part of the TNF- α receptor super family (TNFRSF) found on the surface of haematopoietic cells^{117,136}. RANK deficient animals have an inability to form OCs *in vivo* and also suffer from disturbed lymph node formation which demonstrates that RANK is essential in both the skeletal and immune systems¹³⁷. Interaction of RANKL and RANK activates TNF related activation factor (TRAF) adaptors¹³⁸, the most important of these adaptors being TRAF6 which forms a complex with c-Src promoting actin re-organisation (Figure 1-3)^{8,139}. Actin re-organisation is also mediated by CD115 through stimulation of c-Src which alters the cytoskeletal structure in preparation for multinucleation and pit formation⁸. The importance of TRAF6 in RANK signalling is highlighted by the perturbed bone remodelling in TRAF6^{-/-} animals¹⁴⁰. TRAF6^{-/-} animals also show impaired tooth eruption, cytokine signalling and OC function, highlighting TRAF6's essential role in osteoimmunology¹⁴⁰.

In addition to TRAF6, RANK activation stimulates mitogen activated protein kinase (MAP kinase) activation through transforming growth factor beta- activated protein 1 (TAK1) which activates Activator protein 1 (AP1) and MITF, both of which are essential for OC gene transcription^{1,12}. In particular p38, a MAP kinase, is vital for RANKL mediated OC differentiation, however, studies using pharmacological inhibitors demonstrated that inhibition of p38 does not inhibit mature OC activity^{141,142}. Another member of the MAP kinase family, ERK1, has been shown to positively regulate OC differentiation as *ERK1* deletion results in reduced *in vitro* RANKL mediated osteoclastogenesis¹⁴³. AP1 is a heterodimeric transcription factor essential in osteoclastogenesis. Phosphorylation of AP1 family member c-fos is mediated by Nuclear factor- κ B (NF- κ B) signalling and

animals deficient for c-fos suffer from severe osteopetrosis due to a deficit in the OC population^{144,145}. The most important transcription factor activated by RANK is nuclear factor of activated t cells c1 (NFATc1). NFATc1 transcription is up-regulated a few hours following RANKL-RANK engagement initiating the transcription of genes such as Cathespin K, as well as auto-regulating its own expression in a positive feedback loop¹⁴⁶. Deletion of NFATc1 is embryonic lethal but to test the effect of NFATc1 deficiency *in vivo*, NFATc1^{-/-} foetal liver cells were adoptively transferred into c-fos^{-/-} osteopetrotic animals¹⁴⁷. This adoptive transfer did not resolve the osteopetrosis of c-fos^{-/-} animals but when NFATc1^{+/-} cells were adoptively transferred into c-fos^{-/-} animals the osteopetrotic phenotype was rescued¹⁴⁷. This suggests that during osteoclastogenesis, NFATc1 is downstream of c-fos activation as NFATc1 activation could rescue osteopetrosis while c-fos deficient animals remained osteopetrotic¹⁴⁷. This pathway is under the regulation of NF-κB (see section 1.3.5) which is activated before downstream c-fos and NFATc1 activation¹⁴⁵. Taken together, RANK activates a broad signalling cascade with a variety of transcription factors that are responsible for the regulation of OC differentiation, survival and activity.

1.3.4 Osteoprotegerin

RANKL-RANK interactions are regulated by an endogenous competitive inhibitor known as osteoprotegerin (OPG)¹⁴⁸. OPG is secreted by OB, stromal cells and B cells in response to cytokines such as transforming growth factor (TGF-β) and bone morphogenic proteins (BMPs) to regulate the number of differentiating OCs¹⁴⁹. In fact, B cells are believed to responsible for up to 64% of the OPG production in the BM¹⁵⁰. OPG is a soluble decoy protein which is released into the extracellular fluid to bind to both sRANKL and membrane bound RANKL (Figure 1-3)¹⁵¹. In mice, OPG^{-/-} animals develop osteoporosis (bone loss) as the increase in uninterrupted RANKL-RANK signalling results in aberrant osteoclastogenesis¹⁵¹. Conversely, mice with artificially high levels of OPG in circulation have abnormally dense bone tissue⁴⁸. The use of OPG-Fc fusion protein decreased OC activity *in vivo* following injection of IL-1, TNF-α, parathyroid hormone (PTH), parathyroid-related hormone and Vit D₃. This cytokine cocktail was designed to simulate a pro-inflammatory environment of arthritic disease and treatment with OPG in this model was able to decrease OC differentiation and activity¹⁵². This study demonstrated that OPG is a negative regulator of osteoclastogenesis.

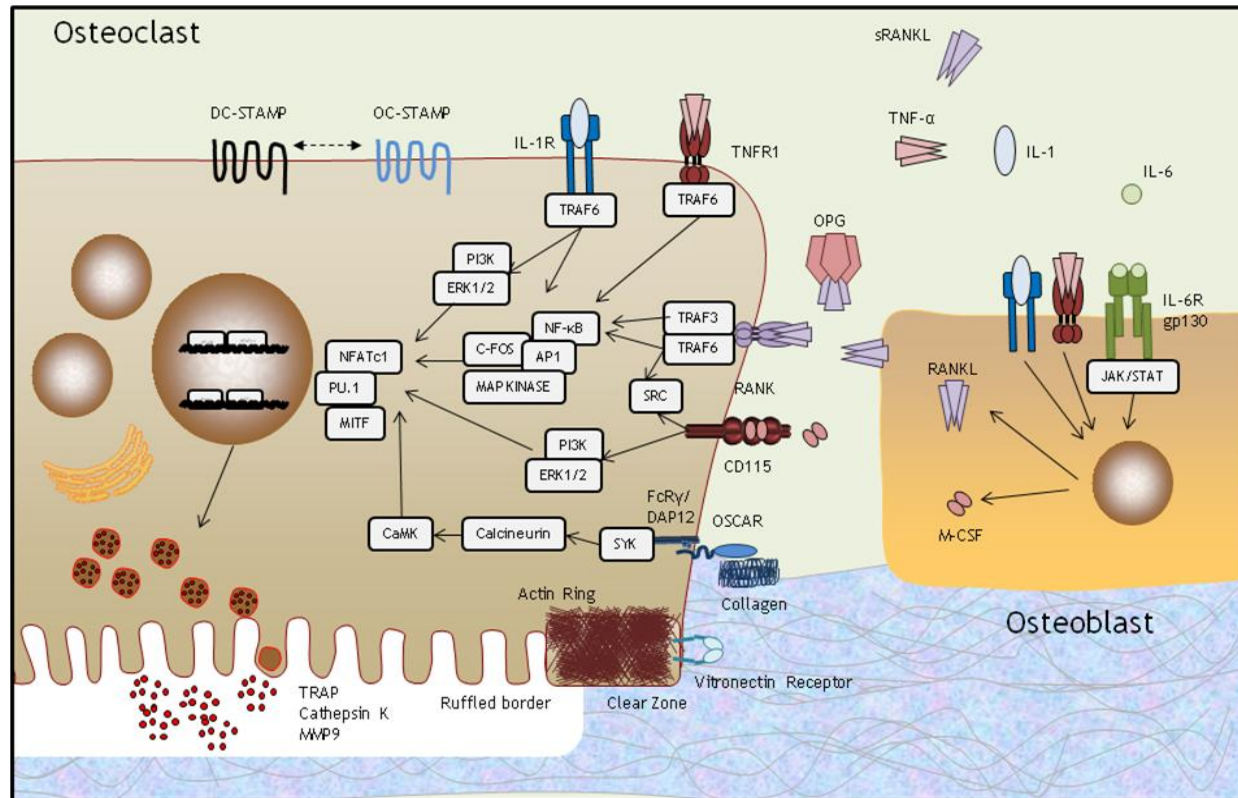


Figure 1-3: Schematic of synergistic effect of cytokines and interactions involved in osteoclast differentiation.

Each cytokine acts in synergy to stimulate transcription factors associated with osteoclastogenesis initiating differentiation. M-CSF and RANKL produced by OBs interact with CD115 and RANK on the pre-OC surface signalling to promote differentiation. TNF- α , IL-1 and IL-6 produced by a variety of cells can increase OB production of RANKL, in turn driving OC differentiation. TNF- α , IL-1 and IL-6 can also interact directly with pre-OCs to enhance differentiation and activity. Vitronectin and Collagen Type I present in the bone matrix can stimulate pre-OC attachment and differentiation via Vitronectin receptor and OSCAR-FcRy. DC-STAMP and OC-STAMP are essential for fusion of pre-OCs, however this mechanism remains to be elucidated. Together, these induce the transcription of genes which results in the production of enzymes and acidification of the bone matrix for degradation as well as production of actin ring to secure the resorption lacunae.

Adapted diagram^{12,125,153-155}.

1.3.5 NF- κ B controls osteoclastogenesis

NF- κ B is the ubiquitous signalling molecule and transcription factor that is vital for a variety of cellular processes¹⁵⁶. NF- κ B is pivotal in cell survival, stress responses and cytokine and growth factor signalling¹⁵⁷. The role of NF- κ B in osteoclastogenesis has been widely studied and as the name suggests RANK strongly activates NF- κ B by inducing gene transcription of proteins essential in the differentiation of OCs^{145,156}. NF- κ B is a dimer consisting of different combinations of five subunits: p105 (p50), p100 (p52), p65, RelB and c-Rel¹⁵⁸⁻¹⁶². These 5 subunits combine to form up to 15 homo- and hetero- dimers each with a specific function. Activated NF- κ B dimers can directly interact with NF- κ B sites on the promoter regions of genes to activate or suppress transcription^{163,164}.

The five NF- κ B subunits all contain Rel-homology domains (RHD) which enable interaction with NF- κ B sites on the DNA¹⁶⁵. Rel-B, c-Rel and p65 NF- κ B subunits all contain a transcriptional activation domain (TAD) which allows dimers containing these subunits to induce transcription¹⁶⁶. However, p50 and p52 NF- κ B subunits lack the TAD region and thus homo- and hetero- dimers of p50 and p52 repress transcription¹⁶⁷. However, p50 or p52 can combine with a TAD containing subunit which can induce transcription. Under steady state, p50/p52 dimers occupy NF- κ B sites. Activation of NF- κ B pathway, however, results in nuclear translocation of TAD containing dimers which replace p50/p52 dimers allowing the transcription of genes¹⁶⁷.

Inhibitors of κ B (I κ B) regulate NF- κ B signalling to prevent the nuclear translocation of NF- κ B¹⁶⁸. I κ B proteins have ankyrin repeats which are small protein domains that bind to the RHD on NF- κ B subunits and block translocation¹⁶⁸. The most prominent member of the I κ B family is I κ B α which predominantly sequesters p65:p50 NF- κ B dimers in the cytoplasm¹⁶⁹. The I κ B Kinase (IKK) complex regulates this process and initiates NF- κ B signalling¹⁶⁶. Activation of IKK results in phosphorylation of I κ Bs and targets them for degradation by the proteasome, allowing activation of NF- κ B and translocation to the nucleus¹⁶⁶. Rel-B, c-Rel and p65 are produced as active proteins: p50 and p52, however, are produced as the precursors p105 and p100, respectively¹⁶⁶. The degradation of these precursors to active NF- κ B subunits is a limiting factor in NF- κ B signalling and prevents aberrant gene transcription. Interestingly, the NF- κ B precursors p105 and p100 contain ankyrin repeats and have been shown to sequester NF- κ B dimers in the cytoplasm until the appropriate stimulation results in their degradation and NF- κ B activation¹⁶⁶. I κ B proteins can not only sequester NF- κ B in the cytoplasm but can prevent transcriptional activation by occupation of NF- κ B sites. In the case of Bcl-3, an atypical I κ B protein, the homo- and hetero- dimers of p50/p52 can be maintained on NF- κ B sites preventing

transcriptional activity of activatory NF- κ B dimers^{170,171}. Bcl-3 selectively binds to these p50/p52 dimers and forms a stable complex on NF- κ B binding sites¹⁶⁷. This Bcl-3:p50/p52 complex prevents the ubiquitination of p50/p52 halting its degradation and thus inhibiting activatory NF- κ B dimer binding¹⁶⁷. In the absence of Bcl-3, NF- κ B activity can become aberrant and uncontrolled¹⁶⁷.

NF- κ B activation can result in two distinct signalling pathways; the canonical and non-canonical pathways¹⁶⁶. The canonical pathway is rapid and occurs over a series of minutes to hours, while the non-canonical can require up to 8 to 12 hours following stimulation to initiate¹⁶⁶. This dual signalling is believed to potentiate stimuli responses and the signalling via canonical pathway provides the initiating first response¹⁶⁶. Once the initial response begins to dissipate the non-canonical pathway begins which results in long-term re-enforcement of the initial stimulus¹⁶⁶. RANKL stimulation of RANK activates both the canonical and non-canonical NF- κ B pathways¹⁶⁶. The canonical pathway relies on TRAF6 mediated signal transduction, rapid proteasomal degradation of I κ B α by IKK complex mediated ubiquitination and freeing of the p65:p50 NF- κ B dimer for nuclear translocation and gene transcription¹⁷². The non-canonical pathway requires degradation of TRAF3 before proteasomal processing of p100 which results in the production of the active NF- κ B subunit p52¹⁶⁰. p52 then forms a dimer with RelB and translocates to the nucleus for DNA binding and induction of transcription¹⁷³. Both pathways are essential for RANKL-induced osteoclastogenesis and the importance of NF- κ B in bone remodelling has been evaluated in numerous KO mice.

Animals deficient for p50 or p52 have no obvious skeletal abnormalities. Iotsova *et al* (1997), however, generated p50/p52 double KO (p50/p52^{-/-}) animal which were highly osteopetrotic and lacked *in vivo* OCs¹⁷⁴. p50/p52^{-/-} animals amassed RANK⁺ splenocytes *in vivo*, which were unresponsive to RANKL and could not differentiate to OCs *in vitro*¹⁷⁵. These studies demonstrated that the p50 and p52 subunits were vital in activating c-fos and NFATc1 and their absence resulted in the inhibition of osteoclastogenesis^{145,174}. Ablation of the p65 subunit is embryonically lethal and to overcome this p65^{-/-}TNFR1^{-/-} animals were generated¹⁶². p65^{-/-}TNFR1^{-/-} animals have a lifespan of approximately 3 weeks and radiation chimeras were created to study the effect of p65 deficiency in the haematopoietic cell compartment in wild type (WT) animals¹⁶². This revealed that there was no effect on bone volume when p65^{-/-} or p65^{+/+} chimeras were used. However, p65^{-/-} animals had half the number of OCs present *in vivo*¹⁶². RelB^{-/-} animals could not produce OCs *in vitro* but had similar bone architecture compared to WT animals¹⁷⁶. c-Rel is activated by the canonical NF- κ B pathway but does not translocate to the nucleus following RANKL stimulation and bone abnormalities have not been reported in c-Rel^{-/-} animals¹⁷⁷. Highlighting that the NF- κ B subunit c-Rel may

not be necessary for RANKL mediated osteoclastogenesis. In 2010, Muruyama *et al* generated animals deficient for p100 which has similar bone architecture to littermate controls and could differentiate to OCs *in vitro*¹⁶⁰. However, alymphoplasia (*aly/aly*) animals possessing an inactive form of the NF- κ B inducing kinase (NIK), which is unable to process p100 to p52, had less OCs present in the trabecular micro-architecture as well as increased bone volume¹⁶⁰. BM cells were also unable to differentiate into OCs in response to RANKL. This phenotype, however, could be overcome by transfection of *aly/aly* BM cells with p52 and an active form of NIK¹⁶⁰. This is believed to occur because p100 accumulates in the cytoplasm and prevents nuclear translocation of p65¹⁶⁶. Overall, this research demonstrates that NF- κ B is essential in bone remodelling and RANKL-RANK signalling.

1.4 Osteoclast maturation

1.4.1 Co-stimulators of osteoclastogenesis

RANKL is the main mediator of osteoclastogenesis; however, other cytokines are capable of working in synergy with RANKL or even directly initiating osteoclastogenesis. One example of this is TNF- α , an inflammatory cytokine that can be produced by a variety of cells and has been implicated in a number of diseases. TNF- α and its receptors TNFR1 and TNFR2, which are expressed on peripheral blood monocytes amongst other cells, belong to a superfamily of cytokines and cytokine receptors which includes RANKL/RANK^{136,178}. In osteoclastogenesis, TNF- α can work both in synergy with RANKL or independently to stimulate *in vitro* osteoclastogenesis but TNF- α cannot commit monocytes to OCs in RANKL^{-/-} mice, therefore, *in vivo* TNF α cannot replace RANKL mediated osteoclastogenesis^{9,179,180}. However, low concentrations of TNF- α used alongside RANKL can potentially increase *in vitro* osteoclastogenesis, increase actin ring formation and bone erosion¹⁷⁹. TNF- α binds to TNFR1 on the surface of M-CSF dependent BM cells and signals in synergy with RANKL to stimulate MAP Kinases, AP1, MITF and NF- κ B (Figure 1-3)¹⁷⁹. TNF- α signals, in a similar manner to RANKL, via TRAF6, TRAF5 and TRAF2 to activate p50/p52 NF- κ B to induce c-fos activation and NFATc1 transcription for OC differentiation¹⁴⁵. However, unlike RANKL, TNF- α only activates the canonical NF- κ B pathway which results in accumulation of the I κ B protein p100 which negatively regulates *in vitro* TNF- α induced osteoclastogenesis, therefore TNF- α mediated osteoclastogenesis is self-limiting¹⁸¹.

The synergistic activation of RANKL and TNF- α may explain certain inflammatory pathological diseases where the infiltrating M ϕ respond to the pro-inflammatory environment and produce TNF- α leading to increased OC activity¹⁸². In fact, the TNF- α

transgenic mouse which over-expresses human TNF- α spontaneously develops a bone erosive arthritic phenotype⁶⁶. These animals also have increased number of actively proliferating CD11b⁺ BM cells, which may help to account for the increased osteoclastogenesis¹⁸³. Treatment of WT animals with TNF- α increased the proliferation of a blood CD11b⁺ CD115⁺ monocyte population that could be used *in vitro* to differentiate OCs¹⁸³. Following treatment with TNF- α , the increase in CD115 expression could result in an increase in osteoclastogenesis as CD115 stimulation results in up-regulation of RANK¹⁸³. Anti-TNF- α therapies have proved very effective in treating inflammatory diseases and creating a less inflammatory milieu¹⁸⁴. An example of this is Infliximab (anti-TNF- α antibody) which is clinically used to treat patients with Rheumatoid arthritis (RA)¹⁸⁵. Removal of TNF- α from patients' systems results in decreased IL-6 and IL-1, decreased T cell responses, tissue destruction to bone and cartilage and importantly improved patients' disease severity¹⁸⁵.

Other cytokines which have been implicated in osteoclastogenesis include the Interleukin-1 (IL-1) family members, IL-1 α and IL-1 β . IL-1 α / β are both pro-inflammatory cytokines which bind to the IL-1R to induce TRAF6 activation resulting in activation of NF- κ B, AP1 and MAP Kinase p38 (Figure 1-3)¹⁸⁶. TRAF6^{-/-} animals have perturbed bone remodelling as well as altered IL-1 activation¹⁴⁰. Treatment of M \emptyset s with TNF- α can differentiate OCs, yet IL-1 α is also required to stimulate bone erosion¹⁸⁷. IL-1 can dose-dependently induce the multinucleation of monocytes and bone erosion via p50/p52 NF- κ B¹⁸⁸⁻¹⁹⁰. IL-1 enhances RANKL mediated OC differentiation and extends the lifespan of *in vitro* mature OCs, in a PI3K and ERK dependent manner¹⁹¹. *In vivo*, IL-1R can indirectly induce osteoclastogenesis; IL-1 activates IL-1R on OBs and stromal cells to increase RANKL expression while directly interacting with IL-1R on the surface of BM M \emptyset s stimulating p38 and enhancing RANKL induced osteoclastogenesis⁶⁸. As well as inducing RANKL production by OBs, IL-1 is also known to induce the production of pro-inflammatory cytokines. One important pro-inflammatory cytokine in osteoclastogenesis is Interleukin-6 (IL-6).

IL-6 is a pro-inflammatory cytokine produced by a variety of cells to elicit an immune response and initiate inflammation¹⁹². IL-6 binds to its receptor IL-6R α which signals via the adaptor protein gp130¹⁹². IL-6 activated signalling is mediated by JAK/STAT transcription factors as well as PI3K, MAP Kinases and Src activation¹⁹². The role of IL-6 in osteoclastogenesis was realised when IL-6 produced by OBs dose-dependently induced OC bone resorption when used along with IL-1⁶⁰. There is an interplay between these cytokines, as IL-6 can induce the secretion of IL-1 from human BM cells which results in the differentiation of OC-like cells in culture¹⁹³. Synergistic IL-6 and TNF- α treatment of BM M \emptyset can differentiate OCs in the absence of RANKL¹⁹⁴. However, direct stimulation of

BM MØ with IL-6 can suppress RANK signalling and thus inhibit osteoclastogenesis dose-dependently^{190,195}. Therefore, IL-6 alone is unable to induce osteoclastogenesis; however, in synergy with other cytokines and in the presence of OBs, IL-6 can strongly enhance the differentiation and erosive potential of OCs¹⁵³.

1.4.2 The role of T cells in osteoclastogenesis

During inflammation a number of pleiotropic cytokines are produced which can induce the production of pro-OC factors. IL-17 is produced by a subset of T cells called Th17 cells, which are implicated in the pathogenesis of autoimmune diseases¹⁹⁶. IL-17 is a recently discovered pro-inflammatory cytokine which induces the expression of TNF- α in the synovial membrane and stimulates OBs to express RANKL^{197,198}. Osteoporosis has been linked to an increase in the Th17 cell population in the BM as well as an increase in serum IL-17¹⁹⁹. The presence of IL-17 in the serum can induce the secretion of TNF- α and IL-1 β from human MØ as well as directly inducing osteoclastogenesis and the production of MMP9 and Cathepsin K^{197,200}. However, IL-17 appears to have a temporal effect on osteoclastogenesis: IL-17 treatment prior to RANKL enhances OC differentiation while IL-17 treatment after RANKL inhibits osteoclastogenesis¹⁹⁰. Therefore, IL-17 needs to be further examined to elucidate its role in bone remodelling. Another cytokine which is produced by T cells and has biphasic roles in osteoclastogenesis is Interferon- γ (IFN- γ)²⁰¹. IFN- γ is important in mediating adaptive immune responses and priming immune cells to initiate the immune response to infection²⁰². IFN- γ exists as a biologically active dimer which binds to its receptors IFN- γ R1 and IFN- γ R2 to stimulate JAK/STAT signalling²⁰². IFN- γ is a negative regulator of OC differentiation as it directly inhibits MØ differentiation to OCs by preventing RANKL signalling and OC inducible genes²⁰¹. However, pre-treatment of MØ with RANKL can render a cell resistant to IFN- γ and allow OC differentiation²⁰¹. Yet, IFN- γ indirectly enhances osteoclastogenesis via T cells activation⁵⁰. IFN- γ primed T cells produce TNF- α and RANKL which can directly interact with pre-OCs to drive *in vivo* OC differentiation in the BM⁵⁰.

Recently a novel T cell derived mediator of osteoclastogenesis was discovered. Secreted osteoclastogenic factor of activator of T cells (SOFAT) was discovered when fractionated supernatants of T cells, stimulated with CD28/CD3, was used in culture with OBs and monocytes²⁰³. One fraction of this media was shown to induce IL-6 production by OBs and increase OC differentiation from human monocytes¹⁵⁵. SOFAT was found to dose dependently induce osteoclastogenesis independent of RANKL, TNF- α and IL-6²⁰³. However, TNF- α was able to enhance SOFAT induced osteoclastogenesis²⁰³. SOFAT was also shown to induce the *in vitro* differentiation of functional OCs from RAW

264.7 cells, and *in vivo* formation of OCs^{155,203}. As yet, a receptor for SOFAT has not been identified nor has its mechanism of action. This novel mechanism highlights the wide-ranging interplay between the skeletal and immune system that is yet to be fully understood.

1.4.3 ITAM co-stimulation

A co-stimulatory immunoreceptor which has been implicated in osteoclastogenesis is OC associated receptor (OSCAR). OSCAR is a 282 amino acid long immunoglobulin (Ig)-like receptor with an Ig domain, an extracellular N terminal and a transmembrane domain containing an arginine residue, which binds to an adaptor protein²⁰⁴. The adaptor protein is typically either DNAX activating protein 12 (DAP12) or common γ -chain (FcR γ), which rely on immunoreceptor tyrosine-based activation motif (ITAM) signalling as OSCAR lacks the capacity to signal²⁰⁵. DAP12 and FcR γ are adaptor proteins typically found as a dimer which signal via an ITAM on the intracellular tail²⁰⁶. The ITAM motif consists of one tyrosine residue (Y) that is separated from a leucine (L) by two amino acids in duplicate (Y_{xx}L-Y_{xx}L)²⁰⁶. Upon stimulation, Src family tyrosine kinases phosphorylate the tyrosine residues on the ITAM motifs²⁰⁶. This results in activation of SYK leading to signalling via MAP Kinases, CREB, NFATc1 and NF- κ B (Figure 1-3, see section 1.5.1)²⁰⁷. When DAP12 or FcR γ is genetically ablated, OSCAR expression is lowered and osteoclastogenesis is altered but not inhibited²⁰⁸. However, when both DAP12 and FcR γ are deficient the result is osteopetrosis and a reduction in osteoclastogenic gene transcription²⁰⁸. OSCAR is found expressed solely on murine OCs but it is more widely distributed on humans monocytes, M \emptyset , OCs and DCs^{205,209}. A murine monoclonal antibody generated against OSCAR is capable of inhibiting OB mediated osteoclastogenesis, suggesting that OSCAR has a pivotal role in stimulating osteoclastogenesis²⁰⁵.

The ligand for OSCAR has recently been discovered as collagen type II¹⁵⁴. OSCAR recognises collagen motifs exposed on the bone surface allowing interaction of pre-OCs and bone matrix¹⁵⁴. Collagen ligation of OSCAR signals through Ca²⁺ release causing the activation of calcineurin and calcium-calmodium kinase IV (CaMKIV). This in turn causes a positive feedback loop amplifying NFATc1 and activating cAMP response element binding protein (CREB) (Figure 1-3)¹. Collagen interaction with OSCAR increases *in vitro* osteoclastogenesis and increased TRAP and Cathespin K mRNA¹⁵⁴. OSCAR expression is regulated by NFATc1 and is up-regulated by MITF, PU.1 and NF- κ B which are induced by M-CSF and RANKL stimulation²¹⁰. Genetic KO of PU.1 and NFATc1 has been shown to reduce osteoclastogenesis and prevent the expression of OSCAR^{94,210}.

OSCAR has been implicated in the pathogenesis of human diseases like osteoarthritis, osteoporosis and RA. Polymorphisms have been discovered in the OSCAR gene leading to increased incidence in osteoporosis in post-menopausal women suggesting that the genetic variation in the promoter region of the OSCAR gene was a risk factor in the development of osteoarthritis²¹¹. Interestingly, OSCAR and NFATc1 mRNA transcripts are up-regulated in murine BM cells when they were treated with synovial fluid from osteoarthritis patients²¹². In patients suffering from RA the expression level of OSCAR on monocytes correlated with the level of C-reactive protein in the serum, which is used as a marker of disease severity²¹³.

DAP12 is also associated with the surface receptor Triggering receptor expressed on myeloid cells 2 (TREM2) which is an Ig like receptor which signals via the ITAM on DAP12²¹⁴. TREM2 or DAP12 mutations in humans results in Nasu-Hakola disease which leads to brain abnormalities and osteoporotic fractures²¹⁵. TREM2^{-/-} animals were observed to have an osteoporotic phenotype²¹⁶. Investigation *in vitro* showed that transcription of TREM2 is induced by treatment with M-CSF and RANKL and may help OC multinucleation and migration²¹⁴. However, DAP12^{-/-} BM mononuclear cells failed to generate *in vitro* OCs following M-CSF and RANKL stimulation²¹⁷. One reason for this is that DAP12 associates with CD115 following stimulation by M-CSF²¹⁸. CD115 dimerisation and auto-phosphorylation of tyrosine 559 activates DAP12 phosphorylation and recruitment of SYK leading to reorganisation of the cytoskeleton²¹⁸. Thus, loss of DAP12 results in augmented *in vitro* osteoclastogenesis and *in vivo* DAP12^{-/-} leads to osteopetrosis²¹⁷. However, *in vivo* TREM2^{-/-} resulted in enhanced osteoclastogenesis due to its ability to negatively regulate proliferation in response to M-CSF and thus commitment to the OC lineage²¹⁶.

ITAM signalling is classically believed to be a co-stimulator in osteoclastogenesis and it can enhance late stage osteoclastogenesis²¹⁹. OSCAR-Ig fusion proteins (antagonist for OSCAR) can inhibit *in vitro* OC differentiation and suggests that OSCAR-FcRγ/DAP12 ITAM signalling enhances OC differentiation²⁰⁵. The downstream Ca²⁺ signalling associated with ITAM coordinates with M-CSF and RANKL to potentiate osteoclastogenesis as well as aiding in reorganisation of the OC cytoskeleton²¹⁸. However, TREM2^{-/-} animals have an increase in OC differentiation and activity that provides evidence that TREM2-DAP12 ITAM signalling may be a negative regulator of osteoclastogenesis.

1.4.4 Multinucleation

The fusion of mononuclear pre-OCs into multinucleated OCs results in a higher capacity for resorption. Without fusion pre-OCs remain functionally viable but have reduced activity⁷. Initially discovered as a receptor on the surface of DCs, DC-specific transmembrane protein (DC-STAMP) expression was believed to be a marker of DC activation²²⁰. DC-STAMP is a 470 amino acid protein with seven transmembrane domains expressed on the surface of the cell²²⁰. It was later found expressed on the surface of OCs and MØs and is essential in fusion as inhibition of DC-STAMP with siRNA inhibited multinucleation of RANKL treated RAW-D cells¹⁰. Its role in osteoclastogenesis was first highlighted when it was discovered to be a RANKL inducible protein under the control of NFATc1^{10,221}. However, Mensah *et al* (2009) published that DC-STAMP was constitutively expressed on the surface of BM MØ and that that RANKL induced the generation of two separate populations of BM MØ; DC-STAMP^{low} and DC-STAMP^{high}⁷. Hypothesising that RANKL induced the internalisation of DC-STAMP in a group of MØ (DC-STAMP^{low}) which would go onto act as the nuclear acceptors for DC-STAMP^{high} cells which are mononuclear donors⁷. DC-STAMP has been shown to traffic between RAW-D cells via tunnelling nanotubes (TNTs) and interaction via TNTs is essential of osteoclastogenesis in murine BM mononuclear cells thus presenting a mechanism by which DC-STAMP^{high/low} pre-OCs communicate²²². The research focusing of DC-STAMP was based mainly in murine studies; however, Zeng *et al* (2009) showed that human RANKL stimulates monocytes to increase DC-STAMP mRNA transcription²²³. The ligand for DC-STAMP is still unknown and the mechanism behind internalisation is yet to be elucidated (Figure 1-3).

Furthermore, OC-stimulatory transmembrane protein (OC-STAMP) was discovered which had sequence homology to DC-STAMP²²⁴. Yang *et al* (2008) found that directly blocking translation of OC-STAMP using siRNA reduced the number of multinucleated OCs in culture but not the number of TRAP positive (TRAP+) cells and provided evidence that OC-STAMP was required for multinucleation of OCs²²⁴. OC-STAMP was found expressed on tissues throughout the body including lung, brain, heart, liver but absent from the ovary²²⁵. Interestingly, oestrogen inhibited the expression of OC-STAMP and represents a possible mechanism for increased osteoclastogenesis and lowered bone density in post-menopausal women²²⁵. Another interesting observation regarding OC-STAMP and DC-STAMP is that in DC-STAMP^{low} groups OC-STAMP mRNA is up-regulated⁷. The predominant hypothesis regarding fusion of pre-OCs is that OC-STAMP up-regulation is dependent on the internalisation of DC-STAMP, allowing the fusion of DC-STAMP^{low} OC-STAMP^{high} and DC-STAMP^{high} OC-STAMP^{low} groups via TNTs (Figure 1-3)^{7,222}.

1.4.5 Bone resorption

In order for an OC to mature it must bind to the surface of the bone matrix and secrete enzymes onto the bone surface under its ruffled border. OCs bind the bone matrix via integrins to form the sealing zone. An important integrin in this process is $\alpha_v\beta_3$ (Vitronectin receptor), which is involved in osteoclastogenesis²²⁶. OCs express Vitronectin receptor which helps the attachment to matrix²²⁶. This results in the formation of an actin rich ring which seals the edge of the plasma membrane and bone interface in order to create the sealed ruffled border²²⁶. Interestingly, Vitronectin receptor expression is found on microvilli like structures on the leading edge of the cell, providing a possible mechanism for OCs migration prior to pit formation²²⁷. Inhibition of the Vitronectin receptor results in altered OC morphology²²⁷. Chin *et al* (2003) found that over expression of α_v subunit of Vitronectin receptor stimulated the *in vitro* differentiation of OCs, while Faccio *et al* (2003) found that β_3 deletion decreased OC activity^{228,229}. M-CSF is believed to act in synergy with the Vitronectin receptor as they share similar MAP kinase pathways and M-CSF treatment can restore $\beta_3^{-/-}$ deficient OC activity²²⁹. Therefore, the Vitronectin receptor is responsible for attachment and possible migration of OCs on bone matrix.

After attachment to the bone the formation of the actin ring results in a controlled microenvironment between the plasma membrane and the bone matrix. The polarisation of OCs allows the targeted secretion of enzymes and acidification into the microenvironment. This allows the mineralization of bone by secreted enzymes and the subsequent degradation of the organic matrix²³⁰. An essential regulator of the acidification process is cytosolic carbonic anhydrase (CAII), which hydrates CO_2 to form H^+ and HCO_3^- ²³¹. The H^+ are then secreted via the vacuolar H^+ ATPase proton pump (H^+ ATPase) into the resorption lacunae²³². CAII and H^+ ATPase are both regulated by RANKL activated c-Fos and NFATc1 signalling^{232,233}. The acidification of the bone matrix is completed by the $\text{HCO}_3^-/\text{Cl}^-$ exchanger which provides extracellular Cl^- to be transported to the resorption lacunae producing HCl with the H^+ present²³¹. The inhibition of H^+ release and CAII activity inhibits osteoclastogenic differentiation and activity on dentine slices proving that this acidification process is essential in bone erosion^{232,233}.

Cathepsin K is a cysteine protease enzyme which is involved in the cleavage of collagen, osteonectin, elastin and gelatine²³⁴. Cathepsin K in the serum of patients with RA positively correlates with the clinical disease²³⁵. Inhibitors of Cathepsin K activity have been shown to effectively treat osteoporosis, as they reduce the degradation of bone matrix²³⁶. This has been demonstrated in human clinical trials and in animal models of

disease^{234,236}. Regulation of Cathepsin K by the MITF is activated by M-CSF and RANKL signalling, as MITF^{-/-} mice have reduced Cathepsin K production²³⁷. Interestingly, MITF also regulates the transcription of TRAP which is an enzyme which works optimally in acidic conditions on a variety of substrates ranging from collagen, nucleotides, phosphor-proteins but mainly osteopontin *in vivo*²³⁸⁻²⁴⁰. OCs secrete the precursor TRAP 5a into the sealing zone which is cleaved by Cathepsins to produce TRAP 5b, the active form of the enzyme²⁴⁰. TRAP 5b is known to leach out of the sealing zone and enter the systemic circulation and can be used as a serum marker of bone remodelling in animals²⁴⁰. TRAP^{-/-} animals display a mild osteopetrosis with stunted limb growth, while over-expression of TRAP typically leads to osteoporosis with increased bone turnover^{241,242}. Due to altered bone remodelling, TRAP^{-/-} animals have altered collagen cross-linking which consequently results in perturbed Ca²⁺/Phosphate (PO₄³⁻) homeostasis²³⁸. In addition to Cathepsin K and TRAP, MMP9 is also produced by OCs to degrade bone matrix and is responsible for the degradation of collagen type IV and V²⁴³. MMP9 is expressed in many tissue and is typically responsible for tissue remodelling²⁴⁴. It is secreted as a pro-protein and cleaved extra-cellularly to an active form of the enzyme^{244,245}. These enzymes work in synergy within the acidified microenvironment to decalcify and remove organic proteins from areas of damaged bone in order to maintain bone integrity.

1.5 Fcγ receptors interactions

1.5.1 Fcγ receptors

Cells of the myeloid lineage, including monocytes, MØ, DCs and OCs express FcγRs and FcγRIII expression is able to delineate human monocyte subsets (see section 1.3.1). One method that cells of myeloid lineage use to respond to pathogens is by the interaction of Immunoglobulin G (IgG) with FcγR. FcγRs are found on phagocytes and function to capture the Fc regions of IgG bound to an antigen²⁴⁶. After engagement of FcγR by IgG, cells can then release cytotoxic products to kill a pathogen or phagocytose the antigen²⁴⁷. Differences exist between human and murine FcγR biology. Human FcγRs can be divided into six types; FcγRI, FcγRIIA, FcγRIIB, FcγRIIC, FcγRIIIA and FcγRIIIB (Table 1-3)²⁴⁸. However, there are only four members of murine FcγR; FcγRI, FcγRIIB, FcγRIII and FcγRIV (Table 1-3)²⁴⁸. Each type of FcγR has a unique signature and can bind IgG subclasses with varying affinities (Table 1-3)²⁴⁸. All FcγR have a similar structure in that they all have at least two extracellular Ig-like domains responsible for binding to IgG, and an intracellular tail, which either maintains the ability to signal or relies on an adaptor protein to signal²⁴⁹. However, activation of these receptors can only occur if multiple neighbouring FcγRs bind IgG, IgG aggregates or IgG containing immune

complexes (IC) simultaneously²⁵⁰. One exception to this rule is FcγRI which has an additional extracellular Ig-like domain enabling it to bind with higher affinity to monomeric IgG compared to the other FcγRs²⁵¹.

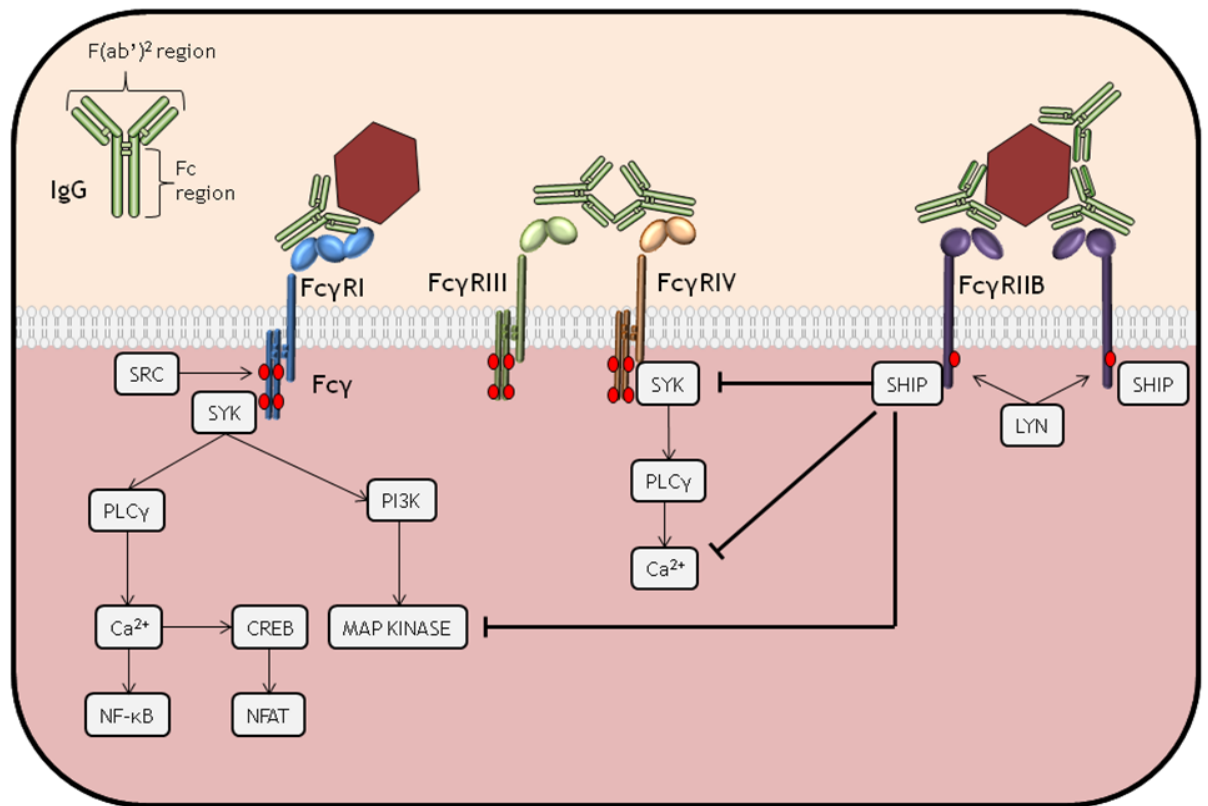


Figure 1-4: Diagrammatic representation of IgG Fcγ receptor interactions.

IgG is composed of two regions: F(ab')² region which binds antigen and the Fc region which is recognised by FcγRs. In mice, four FcγRs exist which have different IgG binding abilities and can bind IgG alone, aggregated IgG or IgG in complex with antigen. Activatory FcγRI, FcγRIII and FcγRIV signal via ITAM adaptor FcRγ molecule which is phosphorylated upon FcγR ligation. Cross-linking and activation of multiple FcγRs induces signalling. Phosphorylated ITAMs signal via PI3K, MAP Kinases, and Ca²⁺ activating effector functions. Inhibitory FcγRIIB contains an intracellular ITIM which is phosphorylated to activate phosphatases that remove phosphate groups from activated proteins. Thus SHIP is able to regulate SYK, PI3K and MAP Kinase activation. Adapted diagram^{249,252,253}.

FcγRs can be broadly categorised into activatory and inhibitory receptors. Murine activatory receptors, FcγRI, FcγRIII and FcγRIV lack the ability to signal and rely on the FcRγ ITAM to signal²⁵⁴. As previously mentioned ITAM signalling activates cellular responses and can enhance the differentiation of OCs *in vivo* and *in vitro* (Figure 1-4, see section 1.4.3)²⁰⁶. Unlike activatory FcγRs, FcγRIIB is capable of signalling without adaptor molecules²⁵⁰. FcγRIIB does not have the ITAM motif, instead it only has one Y_{xx}L motif on its intracellular tail, known as an immunoreceptor tyrosine based inhibitory motif (ITIM)²⁵⁵. Tyrosine kinases phosphorylate the tyrosine residues on the ITIM motif, leading to a signalling cascade which generates phosphatase enzymes like SHP-1, SHP-2 and SHIP that are able to remove phosphate groups from a large number of proteins

involved in cell activation²⁵⁵. In particular, activation of FcγRIIB is capable of inhibiting the activation of activatory FcγRs by removal of phosphate groups from ITAM motifs as well as inhibiting Ca²⁺ signalling, SYK and MAP Kinases²⁵⁶. However, recently use of IgG and IVIG (see section 1.5.3) have been shown to interact with activatory FcγRIII to recruit SHP-1 to the FcRγ resulting in formation of an 'inhibisome'^{257,258}. This novel mechanism has been shown to reduce MØ responsiveness to stimuli, phagocytosis and endocytosis and has been termed inhibitory ITAM signalling (ITAMi)^{257,258}. ITAMi signalling has also been shown to occur in IgA and FcαRI-FcRγ interactions and is thought to dampen the immune response to prevent aberrant inflammatory responses²⁵⁸. It is believed that this is a method of maintaining homeostasis as circulating IgG or IC can interact with FcγRIII on the surface of monocytes or MØ and induce the recruitment of SHPs to the hypo-phosphorylated ITAMs on FcRγ²⁵⁷. It is thought that for ITAMi signalling to occur, activatory and inhibitory FcγRs must be in close proximity, however, once the concentration of circulating IgG or IC increases ITAMs are fully phosphorylated and return to activatory signalling^{253,257,258}.

In mice, FcγRs are expressed on the surface of many immune cells. FcγRI has been shown to be highly expressed on monocytes, MØ and DCs; FcγRIIB is expressed on all myeloid cells as well as being the only FcγR present on B cells; FcγRIII is found to be expressed on all myeloid cells and on natural killer cells; FcγRIV is only expressed on the surface of Ly6C^{low} monocytes and MØ^{259,260}. Research regarding mature OC expression of FcγRs has caused debate. OCs have been shown to express FcγRs on the polarised membrane directly interacting with the bone matrix *in vivo*, while recently they have been shown to express activatory FcγRs *in vitro*^{261,262}. However, OCs in the presence of IgG coated red blood cells (RBCs) failed to induce rosette formation, suggesting that FcγRs on OCs are non-functional²⁶³. OCs are capable of endocytosing particles but are not able to phagocytose via an FcγR mediated pathway²⁶⁴. No evidence at present disproves that FcγR interactions influence mature OCs *in vivo*. Yet, *in vivo* the role of ITAM bearing adaptor proteins, including FcRγ, in bone biology has been investigated (see section 1.4.3). Animals deficient of FcRγ developed mild osteopetrosis in steady state but remained susceptible to oestrogen deficient bone loss²⁰⁷. FcRγ is required for the expression of activatory FcγRs, however, FcRγ is also associated with OSCAR and FcRγ^{-/-} animals suffer osteopetrosis which may result from inhibited OSCAR signalling^{209,265}.

Another human and murine Fc receptor which is essential for IgG homeostasis is the Fc neonatal receptor (Fc nR) which has a similar structure to MHC Class I receptors and is associated with a Beta-2-microglobulin (B2m)²⁶⁶. This structure allows the Fc nR to interact with albumin and IgG in acidic conditions (pH<6.5) but dissociation occurs in

neutral and alkali conditions²⁶⁷. This feature provides FcnR with its main ability, which is to transport IgG across epithelial barriers and prevent IgG degradation²⁶⁷. IgG that is pinocytosed by epithelial cells can bind FcnR in internalised vesicle which quickly becomes acidified²⁶⁷. This allows bound IgG to be secreted at the basolateral cell boundary, this process is particularly important for transferring maternal IgG to the foetus²⁶⁸. Binding of IgG to FcnR in this process also prevents IgG degradation in lysosomes; therefore, the FcnR can greatly increase the half-life of IgG present in serum²⁶⁸. FcnR is also expressed on monocytes, MØ and DCs, but has not been observed on OCS²⁶⁹.

FcγR	Gene	Signalling	IgG Affinity
Human			
FcγRI	<i>fcgr1a</i>	ITAM	IgG1 = IgG3 > IgG4
FcγRIIA	<i>fcgr2a</i>	ITAM	IgG1 > IgG3 > IgG2 > IgG4
FcγRIIB	<i>fcgr2b</i>	ITIM	IgG3 = IgG4 > IgG1 > IgG2
FcγRIIC	<i>fcgr2c</i>	ITAM	IgG3 = IgG4 > IgG1 > IgG2
FcγRIIIA	<i>fcgr3a</i>	ITAM	IgG2 > IgG3 > IgG1 = IgG4
FcγRIIIB	<i>fcgr3b</i>	Decoy receptor	IgG1 = IgG3
Mouse			
FcγRI	<i>fcgr1</i>	ITAM	IgG2a > IgG2b
FcγRIIB	<i>fcgr2b</i>	ITIM	IgG1 > IgG2b > IgG2a
FcγRIII	<i>fcgr3</i>	ITAM	IgG2a > IgG2b > IgG1
FcγRIV	<i>fcgr4</i>	ITAM	IgG2a > IgG2b

Table 1-3: Fcγ receptor subclasses, signalling potential and IgG binding affinities. Adapted table^{248,250}.

1.5.2 Immunoglobulin G

Immunoglobulins (Ig) are proteins produced by B cells and one of the main roles of these antibodies is to target epitopes on pathogens to aid in their clearance²⁷⁰. In order for B cells to produce Ig a series of cellular interactions must occur to facilitate an appropriate immune response²⁷⁰. During an infection, professional antigen presenting cells (APCs) such as MØ or DCs phagocytose and degrade microbes/pathogens²⁷⁰. A single peptide fragment from the degraded pathogens is then presented at the cell surface in a complex with MHC II²⁷⁰. For T cell activation to occur, peptide in the context of MHC II presented by APCs is recognized by the the T cell receptor (TCR) and is co-stimulated by CD4 and CD28 (ligand for CD80/86 on APCs)²⁷⁰. This interaction induces the clonal expansion of T cells specific for the peptide²⁷⁰. Cytokines such as IL-6, IL-12 and TGF-β are produced by APCs, with the particular cytokines produced influencing the differentiation of helper CD4⁺ T cells into specific T helper (Th) cell subsets. Each Th cell subset has differing roles within the immune response and different Th cell types

are induced depending on the type of response required²⁷⁰. B cells are also capable of presenting antigen in the context of MHC II, however, B cells can only present antigen which their BCR recognises²⁷⁰. B cells which have been exposed to BCR specific antigen are able to express peptide in MHC II on their surface but require co-stimulation to differentiate and produce antibody²⁷⁰. Helper T cells that have been stimulated by APCs and recognise the specific peptide can interact with the B cell by engagement of MHC II:peptide/TCR, co-stimulation through CD40/CD40L and cytokine release²⁷⁰. This initiates the differentiation of B cells into plasma cells which produce high quantities of Ig and also differentiates antigen specific memory B cells which will be easily activated upon secondary exposure to antigen²⁷⁰. There are 5 classes of Ig; IgD, IgM, IgA, IgE and IgG. Ig contains two highly variable F(ab) regions which are specific for an antigen and one constant Fc region which varies between subclass and is responsible for binding receptors, tissue distribution and mechanism of action (Figure 1-4)²⁷¹. The subclass of Ig produced is reliant on a number of factors including the type of immune response required, the Th cell type produced and the co-stimulation which occurs during the T and B cell interaction²⁷⁰.

IgD is the first Ig produced by B cells and it remains membrane bound to detect antigen for B cell differentiation²⁵⁰. IgM is the primary Ig produced in response to infection, it has a pentameric structure with the five Fc regions of IgM forming a ring and the F(ab) antigen binding sites directed outwards²⁵⁰. IgM is capable of initiating complement activation and agglutinating antigen for clearance by phagocytosis²⁵⁰. IgA can be produced as a dimer, with two IgA monomers binding at the Fc region²⁵⁰. IgA is secreted into mucous membranes and its structure allows it to be trafficked across epithelial surfaces²⁵⁰. IgE exists as a monomer and represents only a small fraction of the total Ig produced²⁵⁰. However, IgE is essential in allergic reactions and clearance of parasites by triggering degranulation of mast cells and basophils²⁵⁰. Finally IgG is the most abundant Ig present in circulation and has a similar structure to IgM, but exists as a monomer²⁵⁰. IgG is capable of binding antigen with high affinity and engaging Fcγ receptors (FcγRs) to initiate complement cascade or phagocytosis²⁵⁰. IgG can be further classified into subclasses each with more specific functions, however, species specific differences exist in these subclasses. Human IgG can be categorised into IgG1 to IgG4, while murine IgG exists as IgG1, IgG2a, IgG2b and IgG3²⁴⁸. Each has very specific abilities to activate complement cascade, opsonise pathogen and neutralise antigen^{248,250}.

IgG exists as approximately a 150kDa protein with two light peptide chains and two heavy peptide chains linked by disulphide bonds to form the typical Y shape of an antibody (Figure 1-4)²⁷². The light chains consist of two domains, one which varies and one which remains constant, while the heavy chain has one variable domain and three

constant domains²⁵⁰. The variable domains of the heavy and light chains both recognise antigen and are responsible for antibody:antigen binding, this is known as the F(ab')² region²⁵⁰. The constant domains provide the structure for the antibody and provide its function²⁵⁰. In humans, the lower hinge region which connects the F(ab) and Fc region is of the IgG molecule is involved in receptor engagement²⁴⁸. In particular, residues 234-237 in this region have been shown to be essential in receptor binding²⁷³. Another important factor which affects IgG binding abilities are carbohydrate modifications on constant heavy chain (CH2) domain of the Fc region of IgG^{248,274}. These are implicated in receptor binding affinity and it is thought that these post translation modifications are essential for IgG functions^{248,274}.

1.5.3 Immune complexes and Fcγ receptors

IC can be the result of multiple IgG molecules binding to one antigen forming a large protein complex with multiple IgG Fc regions exposed²⁷⁵. ICs ligate multiple FcγRs on the surface of cells, typically MØ or DCs, resulting in phagocytosis of the IC and degradation of bound antigen²⁵⁹. The ability of MØs to phagocytose relies on their plastic nature which can change depending on the conditions in which they were differentiated²⁷⁶. Treatment of MØ with IFN-γ, TLR4 agonists and TNF-α results in classically activated MØ which have strong cell-mediated effects allowing protection against microbial pathogens²⁷⁶. Classically activated MØ can secrete high levels of IL-1 and IL-6 which induces inflammatory damage²⁷⁶. MØ that are exposed to IL-4 tend to have wound healing properties by promoting extracellular matrix deposition and lowering production of inflammatory cytokines²⁷⁷. The final type of MØ is called the regulatory MØ which is believed to have a role in finalising the immune response as it is typically generated in the presence of TLR agonists and IC²⁷⁸. It is hypothesised that IC stimulation occurs towards the end of the adaptive immune response because high levels of antigen specific antibody will be present to engage the remaining antigen. This could result in the IC formation which would direct the regulatory MØ to produce high amounts of the anti-inflammatory cytokine IL-10 to resolve inflammation²⁷⁸. Unlike wound healing MØ, regulatory MØ can produce inflammatory cytokines to stimulate T cells, but do not contribute to the extracellular matrix²⁷⁶. However, treatment of MØ with variations of these stimulants induces hybrid MØ with mixed phenotypes. Engagement of FcγRs on the surface of MØ can therefore have multiple effects depending on the context of the stimulation.

The type of IC can also have an impact on the modulatory effect of FcγR stimulation. IC can take many forms, such as multiple antibodies bound to a single antigen, agglutinated antigens which are multiple antibodies bound to multiple antigens forming

a large mass and antibody aggregates which can form IC without the presence of antigen^{275,279}. However, artificially generated heat-aggregated antibodies which form IC in a denatured structure is used to test *in vitro* IC interactions²⁸⁰. The size of the heat aggregated IgG depends on the initial concentration of protein which can lead to ambiguity regarding whether the production of aggregates is consistent between studies if different studies use different concentrations²⁸⁰. Research conducted by Torbinejad *et al* (1979) demonstrated that bone loss could be induced by heat-aggregated human IgG when injected into the pulp chamber of feline incisors²⁸¹. In this case heat-aggregated human IgG induced inflammation which resulted in rapid bone loss from 7 to 28 days following the injection, this demonstrated that immune complexes were capable of modulating *in vivo* OC activity²⁸¹. More recently, Kuramoto *et al* (2012) used LPS in complex with rat anti-LPS IgG to induce inflammatory bone loss in rat model of periodontal disease²⁸². In this example, LPS would have stimulated TLRs and FcγRs to elicit inflammatory immune response in gingival tissue²⁸². The size of these antibody:antigen complexes can influence the complex's ability to bind to FcγRs and thus the ratio of antigen and antibody must be carefully controlled²⁷⁹. Both Torbinejad *et al* (1979) and Kuramoto *et al* (2012) indirectly induced bone loss because MØs would be the primary effector cells responding to ICs and thus would promote inflammation^{281,282}. Antibody:antigen complexes elicit strong responses in human monocyte cultures when a similar ratio of antibody and antigen are used²⁸³. This drives the production of IL-10 which has an autocrine function down-regulating IL-6, IL-1β and TNF-α production²⁸³. IL-10 pre-treated MØ reduce the expression of FcγRII following treatment with heat-aggregated IgG²⁸⁴. However, Ambarus *et al* (2012) used heat-aggregated human IgG prepared in a similar method to show that treatment of human MØ cultured in a variety of conditions did not change the baseline production of cytokines, while treatment of IgG alone was enough to skew MØ production of IL-10, TNF-α and IL-6²⁸⁴.

Intravenous immunoglobulin (IVIG) is an effective therapeutic which utilises high dose IgG to alter patient's with autoimmune disorders. IVIG is highly concentrated human polyclonal IgG purified from hundreds of donors. IVIG is generally injected directly into circulation of patients²⁸⁵. It is an expensive treatment and is given at a dose of up to 2g/kg to treat diseases like RA, immune thrombocytopenic purpura (ITP) and systemic lupus erythematosus²⁸⁶. The mechanism by which IVIG induces its anti-inflammatory effect is unknown but research has shown that post-translational modifications on around 5% of IgG, known as sialylations, may play a role²⁷⁴. Other studies have shown that the inhibitory FcγRIIB is required for IVIG induced protection in murine models of ITP²⁸⁷, while IVIG induces FcγRIII mediated ITAMi signalling which is thought to inhibit

cellular function²⁵⁷. One general theory of IVIGs mechanism is that IVIG floods the system with IgG displacing pathogenic IgG and blocking FcγRs from IC activation. It is also thought that IVIG co-opts FcγRs and allows the enhanced clearance of pathogenic antibodies from patients system relieving patient symptoms²⁸⁸. This therapy is a strong immunomodulator; however, extremely high doses are required to observe effects²⁸⁹. Therefore, a more precise and cost effective therapy is required to maximise the treatment of these diseases.

Overall, the experiments which use IC tend to use models which cross-link FcγRs in a non-species specific manner and use complexes of unknown conformation. However, one particular example of IC formation which can reproducibly generate species specific IC of a discreet size are produced the bacterial protein; *Staphylococcus aureus* Protein A.

1.6 *Staphylococcus aureus* Protein A

S. aureus is a gram positive, anaerobic bacteria commonly present as part of the normal skin flora and due to the rise in drug resistant has become a widespread virulent nosocomial bacterium²⁹⁰. *S. aureus* invades the host and causes a myriad of diseases from minor irritations to serious diseases such as skin infections, cellulitis, impetigo, pneumonia and endocarditis²⁹¹. One mechanism *S. aureus* has evolved to evade the hosts immune system is Protein A (SpA), a 47kDa membrane anchored protein that targets both the Fc and F(ab) regions of Ig with high affinity²⁹¹. In its cell bound form, SpA has 5 extracellular IgG binding domains (domains E, D, A, B and C), a transmembrane domain and a cell wall binding domain²⁹². Each of the 5 extracellular domains are able to bind the Fc region of IgG or F(ab) region in a non-competitive manner^{271,292,293}.

S. aureus, expressing SpA, coats itself with circulating Ig masking its presence as only host epitopes are exposed²⁹⁴. It has been hypothesised that the ability of *S. aureus* to co-opt IgG evolved to prevent the activation of complement cascade, inhibit opsonisation and prevent FcγR mediated phagocytosis²⁹⁰. However, in the recombinant soluble form SpA has been used for decades in the purification and production of antibodies. In 1978, Ey and Jenkins published a method which has become commonplace, in which SpA was conjugated to sepharose and used to isolate purified IgG²⁹⁵. This method demonstrated that fractions of IgG1, IgG2a and IgG2b could be isolated from mouse serum by incubation with SpA-sepharose and subsequent washes in solutions of decreasing pH²⁹⁵. SpA is able to bind to IgG with varying affinities dependent on subclass of Ig and host species^{296,297}. SpA binds to murine IgG2a, IgG2b and

IgG3 with higher and equal affinity than IgG1²⁹⁶. Naturally occurring IC are also capable of binding SpA, which has been immobilised in silica, with high affinity²⁹⁸.

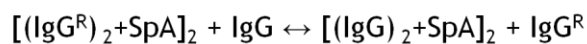
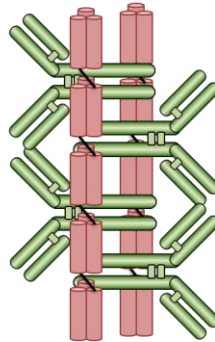


Figure 1-5: Diagrammatic representation of SpAs interaction with IgG.

Two molecules of SpA bind the CH2/CH3 region of four IgG molecules when IgG is present in excess. ^R denotes radio-labelled IgG. The continuous formation and dissociation of SpA and IgG in SIC is shown in the equation provided. Adapted diagram²⁹⁹⁻³⁰¹.

1.6.1 SpA immunomodulation

SpA's IgG binding ability was utilised in apheresis columns, which were clinically used to filter patient plasma and remove IgG and ICs³⁰². In a now discontinued model, 200mg of SpA was covalently bound to a silica matrix and was used to remove IgG, and some IgA and IgM, from circulation³⁰²⁻³⁰⁴. Use of SpA apheresis in patients with RA was highly effective despite only removing a small amount of IgG from circulation^{271,305}. However, other apheresis columns removed larger quantities of IgG and did not impact on patients' disease as effectively as SpA apheresis²⁷¹. Interestingly, it was discovered that during treatment approximately 200µg of SpA could leach from a column into the patient by proteolytic cleavage²⁹¹. This led researchers to investigate how SpA could be interacting with the immune system to resolve inflammation.

One aspect of SpA's ability to modulate the immune system is its ability to bind the F(ab) region of Ig. This is not an IC mediated pathway as SpA directly interacts with the B cell to modulate cellular function. SpA specifically interacts with one variant of the F(ab) region produced by the VH3 gene family²⁷¹. In humans this gene encodes approximately 14-50% of B cells, while only 3-5% of murine B cells express the variant^{306,307}. SpA specifically interacts with the IgM expressed on the surface of B cells (BCR) and induces super-antigenic apoptosis³⁰⁸. Once SpA engages the BCR, there is a down-regulation of co-stimulatory molecules CD19 and CD21³⁰⁸. This results in B cell activation and within hours there is a decrease in the mitochondria membrane potential resulting in the production of pro-apoptotic factor Bim which induces B cell

apoptosis^{308,309}. SpA induced cell death can be negated by co-stimulation of B cells using IL-4, CD40L and BAFF or even Bcl-2 overexpression³⁰⁹. In diseases such as RA, the removal of B cells from circulation via a SpA dependent manner may be beneficial as VH3 encoded B cells are implicated in producing auto-antibodies responsible for driving inflammation²⁷¹. In fact, Rituximab is an anti-CD20 monoclonal antibody, used clinically to deplete B cells in patients and successfully treat diseases like RA³¹⁰. Therefore, SpA mediated removal of B cells from patients maybe a viable treatment; however, it is not SpA's only method of immunomodulation.

1.6.2 SpA IgG complex immunomodulation

SpA has long been known to bind to the Fc region of IgG and form IgG complexes consisting of IgG bound to SpA at a 4:2 ratio³¹¹. These complexes are distinct from typical IC because SpA binds to the IgG Fc region and allows the formation of a distinct protein conformation³¹¹. While typically, IgG binds to an antigen via the F(ab) region and in the correct ratio of antibody:antigen results in either multiple antibodies binding to a single antigen or multiple antibodies bind to multiple antigens to form a large agglutinated mass²⁷⁵. Both of these forms of IC are distinct from the SpA IgG complexes (SIC) because these IgG complexes form without F(ab) binding (Figure 1-5). The interaction between SpA and IgG is dependent on molarity, because if SpA is in molar excess of IgG the ratio of binding becomes 1:1³⁰⁰. SpA binds the Fc portion of IgG at the CH2/CH3 hinge region while the hinge section linking the F(ab) and CH2 regions of IgG are important in interact with FcγRs^{292,312}. Deisenhofer (1981) used the B domain of SpA and Fc fragment of human IgG and demonstrated that the B domain interacted with the CH2/CH3 domains³¹¹. Further research demonstrated that mutations in murine IgG Fc region residues I253, H310, H433 and H434 were all involved in SpA binding, and this region overlapped with FcγR interactions^{313,314}. These four amino acid residues have been shown to reside in close proximity to the CH2/CH3 domains interface and thus provides different binding site from IgG/FcγRs interactions^{313,314}. Therefore, the use of SpA does not cause steric hindrance with the IgG Fc region and FcγRs (see section 1.5.2). The formation of SIC at a 4:2 occurs almost instantaneously upon administration²⁹⁹. In fact, SpA added to serum, purified IgG or Fc fragments can generate SIC almost instantaneously^{299,300}. Administration of radio-labelled SpA alone or in complex with IgG revealed an *in vivo* half life of approximately 9 hours²⁹⁹. However, administration of radio-labelled IgG alone or in complex with SpA revealed a half life of approximately 110 hours²⁹⁹. This identified SpA's promiscuous relationship with IgG, as it is proposed that SpA continually dissociates from bound IgG to form complexes with fresh IgG which accounts for the discrepancy in half lives²⁹⁹. This led to Dima *et al* (1983) proposing a model of SpA:IgG interactions (Figure 1-5)²⁹⁹.

However, more recently the ability of SIC to interact with FcγRs on the surface of immune cells to modulate cellular function has received attention³¹⁵. The use of murine SIC (SpA with murine IgG) in mouse MØ cultures was shown to skew the MØ from an inflammatory phenotype to a regulatory phenotype³¹⁶. SIC treated MØs produced high levels of IL-10 and decreased IL-12 production, as well as down-regulating MHC II expression³¹⁶. This would suggest that the SIC was capable of producing an anti-inflammatory MØ. SpA also demonstrated anti-inflammatory properties when used in a murine model of arthritis (collagen-induced arthritis - CIA)³¹⁶. In the murine model of CIA, SpA treatment reduced disease severity as measured by joint inflammation and reduced the number of OCs present at the inflamed joint³¹⁶. It remains unclear whether in this model, SpA interacted directly with OCs or pre-OCs to reduce OC numbers or whether the reduction in inflammation was responsible for the observed decrease in OCs. However, use of SIC generated with human IgG, was shown to inhibit the differentiation of human monocytes to OCs³¹⁶. This demonstrates that FcγR modulation in human monocytes can inhibit the differentiation of OCs.

Recently research using murine cultures has confirmed this observation and shown that FcγR modulation on pre-OCs can alter osteoclastogenesis. The use of heat aggregated rabbit IgG in cultures of pre-OCs was used to inhibit the *in vitro* differentiation of mature murine OCs³¹⁷. This result demonstrates that treatment of pre-OCs with FcγR stimulation prior to RANKL stimulation lead to a decrease in the cells ability to differentiate³¹⁷. It was also shown that the cross-linking of activatory FcγRI and IV using directed monoclonal antibodies leads to an increase in OC differentiation in pre-OCs that had already been cultured with RANKL²⁶². This discrepancy in temporal FcγR stimulation and lack of physiologically relevant stimulation has resulted in conflicting results. In order to understand the role of FcγRs in osteoclastogenesis, species specific interactions are vital in elucidating the complexity of FcγR biology. Therefore, IgG complexes derived from SpA and murine IgG will be used to examine the role of FcγRs in murine osteoclastogenesis.

1.7 Hypothesis and aims

The use of SpA to generate IgG complexes with human IgG can inhibit the differentiation of human OCs³¹⁶. Recently, the participation of FcγRs in murine osteoclastogenesis has received attention, however, these studies did not use species-specific IgG and thus conflicting results were achieved^{262,317}. To expand on this research IgG complexes were generated using murine IgG and SpA alongside murine osteoclast cultures. IC interactions with FcγRs have been well studied and are commonly used to treat a variety of inflammatory disease²⁸⁶. SpA is able to form IC *in*

vivo with endogenous IgG and engage monocytes and MØ to reduce inflammatory disease³¹⁶. However, the effect of SpA and FcγRs in non-inflammatory diseases has not been defined. Oestrogen deficiency induces excessive osteoclastogenesis resulting in lowered bone density and osteoporosis - which can be mimicked *in vivo* by removal of the ovaries⁴⁰. Monocytes and monocyte subsets express FcγRs and can differentiate into OCs *in vitro* and *in vivo* and play a central role in OVX mouse model of osteoporosis³¹⁸. Therefore, the use of SpA-IgG complexes may have potential in targeting osteoclast progenitors, via FcγRs, in osteoporotic diseases.

The differentiation of OCs relies heavily on RANKL mediated NF-κB activation¹⁵⁶. NF-κB activation results in nuclear translocation of activatory NF-κB dimers and gene transcription¹⁶⁴. However, recently Bcl-3 has been discovered as a regulator of cytokine stimulated NF-κB induced gene transcription¹⁶⁷. Bcl-3 prevents removal of p50/p52 NF-κB dimers from gene promoters preventing activatory NF-κB dimer gene transcription¹⁶⁷. As RANKL strongly activates both canonical and non-canonical pathways of NF-κB signalling Bcl-3 may regulate of this pathway. Therefore, as a negative regulator of NF-κB, Bcl-3 may potentially be a valid target in the search for novel drugs to treat osteoporotic diseases via disrupted RANKL signalling.

Aim: Do SpA-IgG complexes or Bcl-3 represent novel avenues of investigation in therapeutic intervention in osteoporotic disease?

2 Materials and methods

2.1 Animals

C57Bl/6 mice, between the ages of 6-24 weeks old, were either bred by the University of Glasgow's Central Research Facility or purchased from Harlan UK or Charles River UK. Bcl-3 deficient (Bcl-3^{-/-}) mice (C57Bl/6 background) between the ages of 6-24 weeks old were provided by Dr. Ruaidhri J. Carmody. Bcl-3^{-/-} C57Bl/6 / 129/SV mice originally obtained from Jackson Laboratory were backcrossed to C57Bl/6 mice for 12 generation and maintained at the University of Glasgow's Central Research Facility¹⁶⁷. Bcl-3^{-/-} were generated by selective deletion of the ankyrin repeats in the Bcl-3 genomic DNA of 129/SV mice which was replaced with a hygromycin resistance gene³¹⁹. This construct was then electroporated into embryonic stem cells before antibiotic selection with hygromycin³¹⁹. Embryonic stem cells with the disrupted bcl-3 gene survived hygromycin selection and were injected into C57Bl/6 blastocytes and transferred to surrogate C57Bl/6 mice³¹⁹. Fcγ receptor III deficient (FcγRIII^{-/-}) mice on a C57Bl/6 background were purchased from Charles River UK and bred by University of Glasgow's Central Research Facility. FcγRIII^{-/-} mice were generated in a similar manner to Bcl-3^{-/-} animals, except the exons encoding the extracellular and transmembrane domains were replaced with hydromycin resistance genes³²⁰. Mutant mice were then maintained on a C57Bl/6 background³²⁰. All animals were maintained at University of Glasgow's Central Research Facility and procedures were performed according to Home Office Regulations and the Animal (Scientific Procedures) Act 1986.

2.2 Osteoclast differentiation

2.2.1 RAW 264.7 cell differentiation to osteoclasts

The murine MØ cell line, RAW 264.7, was kindly provided by Dr. R. Carmody. Cells were maintained in complete Dulbeccos Minimum Essential Media (D-MEM, Gibco, Life Technologies, UK; see Appendix) at 37°C and 5% CO₂ in 75cm²/mm tissue culture flask (BD Biosciences, UK). RAW 264.7 cells were split once 80% confluent. To split RAW 264.7 cells, a cell scraper (Greiner Bio-one, UK) was used to dislodge adherent cells before transfer of non-adherent cells to a 50ml falcon tube and centrifugation at 400g for 5 minutes. Supernatant was aspirated and cells were re-suspended in 10ml of complete D-MEM, 1ml of cell suspension was added to 12ml of complete D-MEM and placed in a clean 75cm²/mm tissue culture flask.

To differentiate RAW 264.7 cells to OCs, RAW 264.7 cells were seeded onto tissue culture plates at differing cell densities in complete D-MEM. Cells were then incubated with 0, 50 or 100ng/ml RANKL (Peprotech, UK) for varying lengths of time with cultures being fed every third day.

2.2.2 Osteoclast differentiation from murine bone marrow

Mice were either euthanized by rising concentration of carbon dioxide (CO₂) or by cervical dislocation, in accordance to Home Office regulations. Reflexes were tested to ensure death before the long bones (femurs and tibias) were harvested and/or blood was removed via puncture of the exposed vena cava using a 23 gauge (23g) needle and 20µl of 0.5mM EDTA. Excess flesh was removed from the femurs and tibias. These bones were sprayed with 70% ethanol before storing in sterile phosphate buffered saline (PBS). In a sterile class II fume cabinet, the epiphysia were dissected and using a 23g needle and syringe with complete alpha-Minimum Essential Medium (α-MEM, Gibco, Life Technologies, UK; see Appendix), bone marrow (BM) was flushed from the bones into a 9cm Petri dish. The BM was then aspirated using the needle and syringe to create a single cell suspension. The suspension was passed through a 70µm cell strainer (BD Bioscience, UK) into a 50ml falcon tube to remove debris. The cell suspension volume was increased to 50ml with complete α-MEM and centrifuged at 400g for 5 minutes. Medium was removed and the cell pellet re-suspended in 10 ml of complete α-MEM. To count the number of cells obtained, 50µl of cell suspension was added to 200µl of complete α-MEM. This was further combined with 50µl of trypan blue at a 1:1 ratio. This mixture was then loaded onto a haemocytometer and the 16 squares from each of the four corners of the haemocytometer were counted and averaged. The value obtained was equal to the number of cells x 10⁶ in the 10ml single cell suspension.

2.2.3 Monocyte enrichment

BM was prepared as described in Section 2.2.2. To lyse red blood cells (RBCs), 1ml of Akt Lysis Buffer (Gibco, Life Technologies, UK) was added to pelleted BM cells and incubated at RT for 1 minute. Complete medium was then used to inactivate the lysis buffer and cells were centrifuged at 400g for 5 minutes prior to counting with trypan blue. With RBCs lysed, BM samples were negatively sorted by magnetic separation using Monocyte Enrichment Kit according to manufacturer's instructions (StemCell Technologies, UK). Briefly, BM cells were counted and re-suspended at a cell density of 1x10⁸ cells/ml in Separation Media (see Appendix) in a 6ml tube to which 50µl/ml of normal rat serum was added. 50µl/ml of mouse monocyte enrichment cocktail was added and incubated for 15 minutes at 4°C. Cells were centrifuged at 300g for 10

minutes and subsequently re-suspended at 1×10^8 cells/ml. 60 μ l/ml of Biotin Selection Cocktail was added to cells for 15 minutes at 4°C. Cells were vortexed before 150 μ l/ml of magnetic beads were added and incubated for 10 minutes at 4°C. The cell suspension volume was increased to 2.5ml and placed inside a magnet for 5 minutes. Unwanted cells remained bound in the tube to the magnet, while monocytes were poured off. Purity of the total monocyte population was assessed by flow cytometry (described in 2.9). Purified monocytes were plated out into tissue culture plates at a density of 1×10^5 or 1×10^6 cells/ml in complete α -MEM with 30ng/ml M-CSF (Peprotech, UK) and either 50 or 100ng/ml RANKL for 10 days, with media refreshed every third day.

2.2.4 Blood and bone marrow mononuclear cell isolation

For isolation of mononuclear cells, blood and BM was prepared as previously described (Section 2.2.2). Blood and BM cells were combined and this cell suspension was centrifuged once with room temperature (RT) PBS at 400g for 5 minutes before re-suspending in 1.5ml of PBS. This was layered onto 1.5ml of histopaque and centrifuged at 300g for 30 minutes without a centrifuge brake. Following centrifugation, the thin white layer ('buffy coat'), containing mononuclear cells was removed and these cells washed with PBS once more before counting using trypan blue and re-suspension at 1×10^5 cells/50 μ l. 50 μ l of this suspension was added to each well of a 96 well tissue culture plate and allowed to adhere for 2 hours before non-adherent cells were gently washed off using warm PBS. Adherent cells were cultured with complete α -MEM with 10ng/ml M-CSF and either 50 or 100ng/ml RANKL for 7 days.

2.2.5 Isolation of non-adherent bone marrow

BM was obtained as previously described in Section 2.2.2 and the suspension of murine BM cells was re-suspended to a cell density of 1×10^6 cells/ml in complete α -MEM. 9ml of this suspension was cultured overnight at 37°C with 30ng/ml M-CSF in a sterile 9cm non-tissue cultured treated Petri dish. Non-adherent (NA) BM cells were removed following the overnight incubation and these cells were centrifuged at 400g for 5 minutes and the cell pellet re-suspended in 10ml of complete α -MEM and counted using trypan blue as previously described (Section 2.2.2). The NA BM cells were then re-suspended at a cell density of 5×10^5 cells/ml and 200 μ l cell suspension containing 1×10^5 cells were cultured at 37°C in 96 well tissue culture plates along with M-CSF and/or RANKL at stated concentrations. Complete α -MEM was changed every 3rd day and experiments were terminated on various days (see results Section 3.2). In some experiments IL-1 β (Peprotech, UK) was added to cultures at a concentration of 10ng/ml.

L929 cell supernatant which contains M-CSF was used to differentiate OCs. L929 is a fibrosarcoma cell line that secretes M-CSF into the cell culture supernatant and this supernatant can be used to differentiate MØ³²¹⁻³²³. To generate L929 supernatant, L929 cells were cultured in 100ml of complete Roswell Park Memorial Institute Medium (RPMI, Gibco, Life Technologies, UK; see Appendix) until confluent. Cells were cultured for a further 4 days to increase the concentration of M-CSF in the supernatant at which point supernatants were removed and centrifuged at 400g for 5 minutes to remove cellular debris. Supernatant was aliquoted and frozen at -20°C until required. Once thawed, L929 cell supernatant was double filtered using a 0.2µm filter (Sartorius Stedim biotech, UK) before being diluted in complete α-MEM at a ratio of 2 parts L929 to 8 parts complete α-MEM. At this dilution, aliquots of 1x10⁶ cells/ml were plated out in tissue culture plates with or without 50 or 100ng/ml RANKL. Cells were cultured till day 7 with media refreshed every third day.

In order to maximise osteoclastogenesis careful screening of FBS was undertaken to ensure the terminal differentiation of cells. Ultimately, this involved the use of twice filtered FBS using 0.2µm filters in all OC culture media. Additionally, OC differentiation in various 96 well flat bottom tissue culture plates (Costar, Corning, UK) was also optimised in order to gain maximum OC differentiation.

2.3 Tartrate resistant acid phosphatase staining

To assess OC differentiation, cultures were stained for TRAP using Leukocyte Acid Phosphatase Kit (Sigma-Aldrich, UK) pre-warmed to RT and following manufacturer's instructions. Briefly, media was removed from cultures and cells were fixed with TRAP fixative solution (prepared following manufacturer's instructions, see Appendix), for 30 seconds. The fixative was then washed off three times with dH₂O at 37°C. The TRAP staining solution was prepared using the reagents provided in the kit (see Appendix) and warmed to 37°C. TRAP staining solution was incubated on fixed cells for 1 hour at 37°C. After incubation, the staining solution was removed and cultures were counter-stained with haematoxylin solution for 1 minute. The stained cells were rinsed in cold running water until water ran clear and plates were allowed to air dry.

2.4 Assessing osteoclastogenesis

TRAP stained OC cultures were imaged on an Olympus IX51 microscope (Olympus, UK) using Olympus TL4 Lamp (Olympus, UK) at 10x magnification. Images were captured using Cell[^]D Software (Olympus, UK) and four random images were taken of each well, which were then counted for the number of TRAP positive cells containing 3 or more

nuclei. The sum of each well was then averaged from the duplicates/triplicates of each condition to assess the level of osteoclastogenesis. ImageJ Analysis software (ImageJ, National Institute of Health, USA - <http://imagej.nih.gov/ij/>) was also used to calculate the size of OCs present in each field of view.

2.5 Bone resorption assay

NA BM cells were isolated as previously described (Section 2.2.5). NA BM cells were cultured in complete α -MEM with 75ng/ml M-CSF and 50ng/ml RANKL in 96 well plates on slices of bovine cortical bone (ImmunoDiagnostic Systems plc., UK). Bone slices were marked on their underside with pencil prior to culture and incubated at 37°C in complete α -MEM for an hour to equilibrate the bone. Cultures were maintained for 10 or 14 days with media refreshed every 3rd day. On the 10th day, bone slices were removed and stained for TRAP as previously described (Section 2.3). On the 14th day, media was removed and replaced with tap water for 2 hours at (RT) to lyse cells. A black marker pen was used to dye the non-pencilled side before quickly wiping off ink using tissue paper. Areas of erosion remain stained with ink while non-eroded areas wipe clean. For bone erosion analysis, five images of the bone slices were taken at 4x magnification and analysed using Image J software to calculate the area of erosion per bone slice and the area of the slice in the field of vision. The percentage area of erosion was then calculated.

2.6 SpA immunoglobulin complexes

SpA Immunoglobulin Complexes (SIC) were generated by incubating SpA (recombinant *Staphylococcus aureus* Protein A, rPA-50, RepliGen, USA) with ChromPure Murine IgG (Jackson ImmunoResearch, UK), at a molar ratio of 1:4 (37.5 μ M SpA: 150 μ M IgG). ChromPure Murine IgG is a preparation of whole IgG that has been isolated from non-immunised mice and therefore the composition of IgG subclasses present is representative of a healthy animal. For 3ml of media, 1.175 μ l SpA (4mg/ml) and 13.16 μ l Mouse IgG (5.7mg/ml) were incubated at 37°C for 1 hour to allow the formation of SIC after which, 15.6 μ l of PBS was added. SpA or OVA (Chicken Ovalbumin, Sigma, UK) alone (1.175 μ l SpA/OVA and 28.76 μ l PBS) were used to control for SpA. OVA with polyclonal mouse IgG (1.175 μ l OVA, 13.16 μ l Mouse IgG and 15.6 μ l of PBS) were used as a control for SIC. IgG alone was also used as a control which was used at 5.7mg/ml (13.16 μ l) in 16.84 μ l of PBS. Each treatment was made up to a volume of 30 μ l in PBS. Of which, 10 μ l was added to 1ml of culture medium which maintained IgG at a constant concentration of 25 μ g/ml. The research presented throughout this thesis utilised SpA in all *in vivo* experiments, while *in vitro* assays use SIC. IgG was centrifuged at 4000rpm

for 5 minutes prior to use to prevent naturally forming IgG aggregates interfering with the formation of complexes or interacting with cultures.

2.6.1 BS³ cross-linking

SIC was generated as mentioned in Section 2.6. 1.175µl SpA (4mg/ml) and 13.16µl Mouse IgG (5.7mg/ml) were incubated at 37°C for 1 hour in an eppendorf tube. This allowed sufficient time for complexes to form. At the same time Oplg, IgG, SpA, OVA and PBS controls were generated. Following the 1 hour incubation, protein interactions were fixed using BS³ cross-linker (ThermoScientific, UK). 1mM of BS³ cross-linker was added to each condition and incubated at RT for 30 minutes. 0.5M Tris-HCl was added to each condition to terminate the reaction.

2.6.2 Coomassie stain

In order to visualise cross-linked proteins, each sample was mixed with 4x LDS sample loading buffer (Invitrogen, UK) 15µl was loaded onto a 4-12% Bis-Tris gel (Invitrogen, UK) along with 10µl of Pre-stained protein standard (Invitrogen, UK). 1x MOPS running buffer (Invitrogen, UK) was added to the central reservoir of an electrophoresis gel tank and samples electrophoresed at 200V for 1 hour. Gels were cracked open and washed in dH₂O before addition of 20ml of Simply Blue SafeStain (Invitrogen, UK) and incubated with agitation at RT for 1 hour. Simply Blue SafeStain was washed off with dH₂O for 1 hour to remove background and enhance visualisation. Gels were imaged using an HP desktop scanner.

2.6.3 Size exclusion chromatography

To show the formation of SIC complexes from SpA and IgG, samples were run through a Sephacryl s-400 column (GE Healthcare, UK) using an ÄKTAprime plus (GE Healthcare, UK) to discriminate molecules based on size. Filtered PBS was used to wash the Sephacryl s-400 column prior to processing. 0.5ml of SIC was generated at 4mg/ml following 1 hour incubation at 37°C: 32.5µl SpA and 364µl IgG and loaded onto a column under the following conditions; flow rate - 0.2ml/ml; pressure limit - 0.5mPA; fraction size - 5ml; equilibrate volume - 120ml; sample injection - 0.5ml; elution volume - 200ml. The resulting readout shows protein concentration (UV - A₂₈₀) versus time. Oplg, IgG, SpA, OVA and PBS were also run under the same conditions as SIC. Sephacryl s-400 was cleaned using 20% ethanol in dH₂O. Results were visualised using PrimerView (GE Healthcare, UK) to establish the concentration and the time at which protein exited the column.

2.7 Polymerase chain reaction

2.7.1 RNA isolation

Murine NA BM derived OCs were differentiated as previously described (Section 2.2.5) until day 3. At this time, culture plates were centrifuged at 400g for 5 minutes, cell media removed and 700µl QIAzol Lysis Reagent (QIAGEN, UK) was added to each well to lyse cells. The lysates were transferred to 1.5ml eppendorfs and either immediately used for RNA extraction or stored at -20°C for later purification. RNA was isolated from lysates using a miRNeasy Mini Kit (QIAGEN, UK), as per manufacturer's instructions, 30µl of RNase free water was used in the final elution.

To ensure purified RNA had been isolated the samples were kept on ice and a Nanodrop 1000 (ThermoScientific) was used to detect the concentration of RNA present in each sample. Once the purity and concentration of RNA had been determined the samples were stored at -20°C.

2.7.2 cDNA generation

Purified RNA was used to generate cDNA using Affinity Script cDNA synthesis kit (Agilent Technologies, UK) following manufacturer's instructions. Using a PCR machine (Applied Biosystems 2720 Thermal Cycler, UK), random primers in the Affinity Script cDNA synthesis kit transcribed the RNA and generated cDNA. 200ng of RNA was used to generate cDNA and this was diluted in 50µl to give 4ng/µl cDNA template and stored at -20°C.

2.7.3 Primer design

A set of primers (forward and reverse) to generate a PCR product of 100-150 base pairs were designed using Primer3 Software (National Institute of Health, USA) and the NCBI nucleotide database (National Centre for Biotechnology Information, USA). Primers were designed to be between 18-23 base pairs in length have, a 40-60% GC nucleotide content, a melting temperature of between 59.5 and 61°C, a maximum self complementarity of 2 and a maximum 3' self complementarity of 1. Once primers had been designed and met these specific criteria, Primer BLAST software (National Centre for Biotechnology Information, USA) was used to determine their specificity of the primers and predict non specific amplification. Once a primer set had met all these criteria they were purchased from Integrated DNA Technologies Ltd. (IDT) and tested for specificity by end point PCR (Table 2-1). Primers for GM-CSF, Bcl-2 and Bcl-XL were obtained from QIAGEN and have been optimised for use with SYBR green.

2.7.4 End Point PCR

To ensure successful generation of cDNA and to test the specificity of primers, end point PCR was undertaken. A standard protocol was followed for the generation of a PCR master mix; the components of which were

- Nuclease free water - 35.5µl
- 5x GoTaq Buffer (Promega) - 10µl
- 10mM dNTPs (Promega) - 1µl
- Primer 1 (Forward) - 1µl
- Primer 2 (Reverse) - 1µl
- Go Taq Polymerase (Promega) - 0.5µl
- cDNA (4ng) - 1µl

Each sample was made up in a 0.2ml PCR tube and run on a PCR machine. The following thermal cycle was used; an initial 94°C for 5 minutes step followed by 35 cycles of 94°C for 10 seconds, 55°C for 30 seconds and 72°C for 30 seconds, terminating the reaction with 10 minutes at 72°C before holding at 4°C. After termination of the PCR, the samples were loaded into a 2% Agarose gel (see Appendix) with 5µl ethidium bromide added prior to pouring the solution onto the flat bed electrophoresis tank. Once the gel had cooled and set, 1Kb DNA ladder (Invitrogen, Life Technologies, UK) and PCR samples were loaded and the tank attached to a power pack set at 100V for 60 minutes. Gels were visualised using a UV light (Alpha Innotech, UK) to detect the presence of PCR products at correct molecular weight.

2.7.5 Quantitative PCR

For a 96 well qPCR plate (Starlabs, UK), each sample was run in triplicate with a master mix comprising of 10.4µl PerfeCTa SYBR Green FastMix (Quanta Bioscience, USA) or POWER SYBR Green (Life Technologies, UK), 0.8µl primer mix (0.4µl/primer) and 8.4µl nuclease free water per well. 56µl of this reaction mixture was then added to mixing wells along with 6µl of appropriate cDNA. This was mixed by pipette 20 times and 19µl was added to each of the triplicates. A non-template control (NTC) was used which contained nuclease free water in place of cDNA to ensure no contamination of the reagents. After loading, the plate was sealed using an adhesive PCR plate cover (Starlabs, UK) and centrifuged at 300g for 1 minute. A 9700HT qPCR machine (Applied Biosystems) was used to run the samples; the qPCR temperature cycle was 10 minutes at 94°C, followed by a 40 cycles of 94°C for 3 seconds and 60°C for 30 seconds. The final stage in this process is a dissociation curve which is an incremental increase in

temperature from 65°C up to 94°C which is designed to test the specificity of the primers in generating only one product. All genes were normalised to housekeeping gene glyceraldehyde 3-phosphate dehydrogenase (GAPDH). ΔC_t was measured for each sample by subtracting the gene of interest ΔC_t of an individual sample from the corresponding housekeeping gene ΔC_t sample. $\Delta\Delta C_t$ was calculated by subtracting the ΔC_t of a sample of interest from the control sample ΔC_t . Fold change was measured by inserting the $\Delta\Delta C_t$ of a sample into the power equation ($2^{-\Delta\Delta C_t}$).

Target Name	Direction	Tm (°C)	Product Size (bp)	Sequence
GAPDH	F	56.2	100	ACGCAAGGACACTGAGCAAG
	R	53.5		TATTATGGGGGTCTGGGATG
CD115	F	55	126	TGAAGGTGGCTGTGAAGATG
	R	58.2		AGGCTCCCAAGAGGTTGACT
RANK	F	53.2	102	TTTGTGGTTTTGGCCTCCTT
	R	54.3		CTGGCACCTTCATTTTGTCC
NFATc1	F	54.1	133	ACGCAAGGACACTGAGCAAG
	R	56.1		TATTATGGGGGTCTGGGATG
DC-STAMP	F	56.3	139	TCTGCTGTATCGGCTCATCTC
	R	56.6		ACTCCTTGGGTTCTTGCTT
TRAP	F	56.4	102	GGTATGTGCTGGCTGGAAAC
	R	59.0		GGTAGTAAGGGCTGGGAAGTC
MMP9	F	57.6	128	TCTACTGGGCGTTAGGGACA
	R	58.0		AGGAGTCTGGGGTCTGGTTT
Cathepsin K	F	54.9	122	GGAACGAGAAAGCCCTGAA
	R	56.0		CACACCTCTGCTGTAAACTGG
OSCAR	F	54.2	109	GTTTTGGGGGTTTGTTCGTT
	R	53.9		TTACCTGGGAGATGGGATTG
Bcl 3	F	62.9	102	CCGGAGGCCCTTACTACCA
	R	62.8		GGAGTAGGGGTGAGTAGGCAG
RANKL	F	56.0	100	ATGAAAGGAGGGAGCACG
	R	57.4		AGCAGGGAAGGGTTGGAC
Primers Ordered from QIAGEN				
Name	Product Code			
GM-CSF	PPM02990F-200 (csf2)			
Bcl-2	PPM02918F-200 (bcl2)			
Bcl - XL	PPM02920F-200 (bcl2l1)			

Table 2-1: List of primers sequences ordered from Integrated DNA Technologies Ltd and QIAGEN for qPCR analysis.

2.8 Osteoporosis surgical model

OVX or sham operations were performed on 8 week old anaesthetised female C57Bl/6 mice by Charles River UK. Mice were laid prone rostro-caudally away from the surgeon. The dorso-lumbar region was shaved, and sterilised with 70% ethanol before a ~20mm skin incision was made along the vertebral column. Approximately 10mm long incisions were made through the muscle wall on either side of the vertebral column and the peritoneal cavity exposed. The ovaries, located in a fat pad, were carefully excised. Once both ovaries were removed the skin incision was closed using wound clips. If Alzet Pumps™ (model 2004) were to be used; Alzet pumps™ were inserted into the peritoneal cavity prior to closing the incision with wound clips. The animals were allowed to recover for 7 days and subsequently delivered to the University of Glasgow's Central Research Facility. Sham and OVX animals were used in three treatment regimes. 100µg of SpA or OVA was given i.p. to animals in the Therapeutic Treatment Regime starting two weeks after surgery. This dose was given every second day up until week 6 when the experiment was terminated. The second treatment regime was the Continuous Treatment Regime in which 100µg of SpA or OVA was given i.p. to animals from the day of surgery until the termination of the experiment at week 6. The final treatment regime was the Alzet Pump™ Treatment Regime, in which Alzet Pumps™ containing 1.4mg of SpA or OVA was inserted into the peritoneal cavity at the point of surgery. Alzet Pumps™ secrete SpA/OVA over the course of 4 weeks. All operated mice were maintained for 6 weeks after surgery and after which they were euthanized by rising concentration of CO₂ according to Home Office regulations.

2.9 Flow cytometry

Blood and BM were harvested for analysis of cellular populations by flow cytometry. 200µl of blood was taken using EDTA flushed needles and RBCs lysed using ammonium chloride (1 part blood to 9 parts NH₄Cl - Stem Cells Technologies, France) on ice for 15 minutes. BM was prepared and lysed as previously described (Section 2.2.3). Lysis buffers were washed off by addition of excess complete media and centrifuged at 400g for 5 minutes. Cells were re-suspended in FACS Buffer (See Appendix). Cell numbers were determined by either the haemocytometer trypan blue method (Section 2.2.2) or by using a MACsQUANT (Miltenyi Biotec, Germany). After counting, 1x10⁶ cells were added to each FACS tube in technical duplicates and 1ml of FACS buffer added before centrifugation at 400g for 5 minutes. The buffer was aspirated off, tubes vortexed and non-specific binding by Fcγ receptors were blocked by using 50µl of 5% normal rat serum in FACS Buffer and incubating at 4°C for 15 minutes. Primary antibodies were used at stated concentrations and added to a master mix (Table 2-2). 50µl of master mix was

then added to each tube and cells stained for 15 minutes at 4°C. Antibody was washed off by addition of 1ml of FACS buffer and centrifugation at 400g for 5 minutes. Supernatant was aspirated and cell pellets were vortex and re-suspended in 300µl of FACS buffer for acquisition on the MACsQUANT (Miltenyi Biotec, Germany) or LSRII (BD Bioscience). If a secondary antibody step was required, the cells were stained with 50µl of diluted streptavidin conjugated fluorophore in FACS buffer and incubated for 15 minutes at 4°C, before being washed and re-suspended in 300µl of FACS buffer for acquisition. Prior to acquisition, cells were passed through Nitex to prevent cell aggregates blocking or interfering with the acquisition and analysis of the cell populations. In certain experiments dead cells were excluded from analysis, in order to do this, 3µl of DAPI (diluted 1/100 in FACS buffer - Sigma, UK) was added to 300µl of cells samples and briefly vortex prior to acquisition. Another method to exclude dead cells, which involved staining cells with Live/Dead Aqua Stain (Molecular Probes, Invitrogen, UK). Live/Dead Aqua Stain was prepared according to manufacturer's instructions, briefly, 50µl of DMSO was added to lyophilized dye and 1µl/ml of this solution was incubated with 1x10⁶cells/ml in PBS for 30 minutes on ice but protected from light. Cells were subsequently centrifuged for 5 minutes in excess FACS Buffer and re-suspended in FACS Buffer for acquisition. Analysis of FACS data was done using FlowJo software (TreeStar Inc., USA). This protocol was also used to examine purity following monocyte enrichment (outlined in Section 2.2.3).

A FACS Aria was also used to sort CX3CR1 GFP⁺ Ly6C^{high/low} monocytes for *in vitro* culturing. Blood and BM were isolated from CX3CR1 GFP animals after which cells were prepared for FACS. Dr. J. Montgomery stained and acquired cells on the FACS Aria, after which Ly6C^{high} and Ly6C^{low} monocytes were used for culturing. Sorted cells were used in an OC assay (as previously described in Section 2.2.5).

Antibody	Clone	Fluorophore	Dilution Factor	Isotype	Provider
B220	RA3-6B2	Alexa Fluor 488	1 / 100	Rat IgG2a	eBioscience
B220	RA3-6B2	APC Cy7	1 / 100	Rat IgG2a	eBioscience
B220	RA3-6B2	PE	1 / 100	Rat IgG2a	BD Biosciences
CD115	AFS98	Biotin	1 / 100	Rat IgG2a	eBioscience
CD11b	M1/70	APC Cy7	1 / 150	Rat IgG2b	BD Biosciences
CD11b	M1/70	qDOT	1 / 150	Rat IgG2b	BioLegend
CD11b	M1/70	PE	1 / 100	Rat IgG2b	eBioscience
CD117	2B8	Pacific Blue	1 / 100	Rat IgG2b	BioLegend
CD16/32	2.4G2	v450	1 / 150	Rat IgG2b	BD Biosciences
CD3e	A45-2C11	Alexa Fluor 488	1 / 100	Hamster IgG1	eBioscience
CD3e	A45-2C11	APC Cy7	1 / 100	Hamster IgG1	eBioscience
CD3e	A45-2C11	PE	1 / 100	Hamster IgG1	BD Biosciences
CD64	X54-5/7.1	APC	1 / 150	Mouse IgG1	BD Biosciences
Gr-1 (Ly6C/G)	RB6/8C5	APC	1 / 100	Rat IgG2b	BD Biosciences
Ly6C	AL-21	PerCP Cy5.5	1 / 150	Rat IgM	BD Biosciences
Ly6G	RB6/8C5	Alexa Fluor 700	1 / 150	Rat IgG2b	eBioscience

Streptavidin	qDOT	1 / 200	BioLegend
Streptavidin	APC	1 / 200	eBioscience
Streptavidin	PE	1 / 200	eBioscience
DAPI	v450	1 / 10000	Life Technologies
Live/Dead Aqua Stain	Pacific Blue	1µl/ml	Life Technologies

Table 2-2: List of flow cytometry reagents used.

2.10 ELISA

IFN- γ , TNF, IL-6, IL-1 β , Osteocalcin and CTX-1 ELISAs were performed on mouse plasma. Plasma was obtained at the time of culling by exsanguinating the mouse via the vena cava using a 23g needle flushed with 0.5M EDTA (see Appendix) and blood was kept on ice. Blood was centrifuged at 4,000rpm for 10 minutes and the clear plasma layer removed and stored at -20°C.

IFN- γ , TNF- α , IL-1 β and IL-6 ELISA kits (BD Bioscience, UK) were used and manufacturer's instructions were followed. Micro half-well high binding ELISA plates (Fisher Scientific) were used to reduce the volume of reagents required. Briefly, ELISA plates were coated with specific capture antibody diluted in appropriate coating buffer (see Appendix) overnight at 4°C. Plates were washed with PBS 0.05% Tween-20 (Sigma, see Appendix) a minimum of 3 times. Plates were then blocked with 5% FBS in PBS (Assay Diluent, see Appendix), to reduce non-specific binding, for 1 hour at RT. Plates were washed prior to incubation with protein appropriate standards and samples, diluted with assay diluents at appropriate dilution, and incubated at RT for 2 hours. Plates were washed using PBS 0.05% Tween-20 a minimum of 3 times. A detection antibody and a streptavidin-HRP were then used separately or in a working detector solution in assay diluents according to manufacturer's protocol. After 1 hour incubation at RT, plates were washed before tetramethylbenzidine (TMB, Kirkegaard & Perry

Laboratories, Inc., USA) solution was added to develop the ELISA and the reaction stopped using stop solution (2M H₂SO₄). The plate was read at 450nm using an ELISA reader (Sunrise ELISA Reader, Tecan, Switzerland) and a standard curve generated for each plate and sample concentrations calculated from the curve.

Osteocalcin and CTX-1 were both pre-coated ELISA plates purchased from Biomedical Technologies Inc., and Immunodiagnostic systems Ltd., respectively. Manufacturer's instructions were followed for both ELISAs. All samples and standards were run in duplicate and plasma samples were added at a 1:10 dilution with assay diluents provided (Osteocalcin) or added neat (CTX-1) to the appropriate pre coated ELISA plates. ELISA plates were read at 450nm on an ELISA plate reader and standard curves generated in order to calculate the concentration of protein in each sample. CTX-1 was an inverse competitive ELISA and required the use of a 4 way parameter logistic standard curve to calculate the sample concentrations of CTX-1.

2.11 Biomechanical testing

Left femurs were removed from OVX/Sham mice 6 weeks post surgery. Femurs were stored in 70% ethanol and stored at 4°C. Prior to biomechanical testing, femurs were rehydrated in PBS overnight and allowed to equilibrate to RT. All tissue was thoroughly removed from the femur to ensure that periosteum would not interfere with the strength of the bone. Three point bend testing was used as a measure of biomechanical integrity of bone using femurs loaded onto an Instron Dynamite hydraulic tester with data collected using Bluehill Software. Three point bend testing was performed under the supervision of Dr. N. Horwood at the Kennedy Institute of Rheumatology, Imperial College London. Femurs were placed ventral side down on two supports and a third support was slowly lowered from above to determine the force and time required to break the femur. Using this data, Bluehill software calculated Maximum Load (Newtons), Extension at Maximum Load (mm), Load at Break (N), Extension at Break (mm), Energy at Break (J) and Modulus (MPa - Mega Pascal's).

2.12 Micro-computer tomography

Tibiae were harvested from 12 week old C57Bl/6 or Bcl-3^{-/-} mice and C57Bl/6 mice 6 weeks post OVX/Sham surgery. Bones were fixed overnight in 4% formaldehyde in PBS (Fisher Chemicals, UK) before being stored in 70% ethanol at 4°C. To assess the micro-architecture of the trabecular bone in tibiae and vertebrae, the bones were scanned using a micro-computer tomography (µCT) system (Skyscan 1172 X-Ray microtomograph or Skyscan 1174 X-Ray microtomography, Aarteselaar, Belgium). µCT analysis was performed at the Institute of Genetics and Molecular Medicine, University

of Edinburgh, UK under the supervision of Dr. R. Van't Hof. Scans were obtained with an isotropic voxel size of 4.6 μm on a Skyscan 1172 or 8.3 μm on a Skyscan 1174 (60kV, 150 μA , 0.5mm aluminium filter, 0.5 rotation angle). NReconn software (Skyscan, Belgium) was used to reconstruct the X-Ray images into a 3D structure.

To analyse the trabecular bone of the tibiae, the growth plate of the tibia was used as a reference point in all samples. 20 sections below this reference point, 200 further sections were selected for analysis in CTAn software (Skyscan, Belgium). Using CTAn the trabecular regions underwent thresholding which was set at 80 - 255. The sample thresholds were set and analysed using CTAn software. The following parameters were analysed; bone volume (BV; μm^3), tissue volume (TV; μm^3), the percentage of trabecular (Bone volume/Tissue Volume; BV/TV; %), tissue surface (μm^2), bone surface (μm^2), bone surface density (BS/TV; μm), trabecular thickness (Tb.Th; μm), trabecular separation (Tb.Sp; μm), trabecular number (Tb.No; $1/\mu\text{m}$), structural model index (SMI), connectivity (Conn.), degree of anisotropy (DA) and connectivity density ($1/\mu\text{m}^3$).

2.13 Histology

Following euthanization, C57Bl/6 and Bcl-3^{-/-} animals had hind legs removed for histological analysis. Legs were fixed overnight in 4% formaldehyde in PBS and subsequently washed in PBS to remove any fixative. 15ml of decalcification solution (14% EDTA pH 8, see Appendix) was then added and agitated at 4°C. Decalcification solution was changed every week until legs were pliable to touch. Pliable legs were subsequently dissected and tibiae then embedded in paraffin wax using Shandon Citadel 1000 Tissue Processor (Fisher Scientific) and subsequently 20 μm sections cut (VWR, UK) using a Shandon Finesse 325 Microtome (Fisher Scientific) placed onto super frost glass slides.

2.13.1 Haematoxylin and eosin staining

Sections of paraffin embedded mouse legs were stained for H&E. Sections were heated to 65°C for 1 hour and then de-waxed in two changes of xylene for 3 minutes. Sections were then rehydrated in 100%, 90% and 70% ethanol for 5 minutes each, sections were subsequently rinsed in cold running tap water. Rehydrated sections were stained with haematoxylin for 2 minutes, and washed for 3 minutes in cold running tap water. Sections were immersed in 1% acid/alcohol (see Appendix) for a few seconds before rinsing in cold running water. Sections were immersed in Scotts Tap Water Substitute (see Appendix) for 30 seconds and then stained with 1% Eosin for 2 minutes. Excess stain was rinsed off using cold running tap water. Sections were dehydrated through graded alcohol (70%, 90% and 100%) for 5 minutes each and then placed in two changes of

xylene for 5 minutes each. Sections were mounted with coverslips using DPX (Leica Biosystems, UK). Stained sections were imaged on an Olympus IX51 microscope (Olympus, UK) using Olympus TL4 Lamp (Olympus, UK).

2.13.2 Histological TRAP staining

Coronal sections of the paraffin embedded proximal tibiae were cut and stained to determine the presence of OCs in the tibial trabeculae. Slides were heated to 65°C for 1 hour and de-waxed in Xylene for 10 minutes and re-hydrated in graded ethanol steps (100%, 90% and 70% ethanol for 5 minutes) followed by 2 minutes in 37°C dH₂O). Rehydrated sections were incubated in TRAP staining solution (see Appendix) for 4 hours. After incubation TRAP stain was rinsed off in 37°C dH₂O and counterstained with Meyer's Haematoxylin (CellPath, UK) for 1 minute. The excess haematoxylin was rinsed off in dH₂O and slides were allowed to air dry, removing excess dH₂O, prior to mounting in Vectashield mounting medium (Vector Laboratories, UK) and sealed with nail varnish. An Olympus IX51 microscope (Olympus, UK) using Olympus TL4 Lamp (Olympus, UK) was used to visualise OCs which were stained red/purple.

2.14 Statistical analysis

Statistical analysis was performed using GraphPad Prism4 software (GraphPad, USA). One Way ANOVA was used to compare more than two groups of data with Bonferroni's post hoc tests used to test for significance. Two Way ANOVAs were used to compare two sets of animals within two treatment groups and Bonferroni's post hoc tests were used to determine the significance between groups. Student's unpaired two-tailed t-tests were used to compare the results from two groups of animals. 95% confidence intervals were selected and p-values of < 0.05 were deemed significant. The appropriate statistical test used is described in the figure legends.

3 Fcγ receptor interactions inhibit osteoclastogenesis

3.1 Introduction

OCs are large multinucleated cells responsible for eroding the bone during skeletal remodelling¹. OCs originate from monocytes, MØ and OCPs found in the blood and BM and *in situ* differentiation can be driven by a number of cytokines and interactions¹. However, *in vitro* M-CSF and RANKL are known to be sufficient for OC differentiation³²⁴. M-CSF and RANKL act on their respective receptors, CD115 and RANK, on the surface of monocytes, MØ and OCPs to commit these cells to the OC lineage³²⁴. Stimulation via CD115 results in pro-survival signals¹²⁸ and increased expression of surface RANK leading to an increased potential for RANKL binding and signalling to promote osteoclastogenesis^{6,325}.

A myriad of factors are capable of driving/enhancing OC differentiation. Factors such as TNF- α ^{326,327}, IL-1³²⁸, IL-6³²⁹ and the presence of Collagen Type I in the bone matrix acting through OSCAR and the FcR γ ^{154,330} are known to enhance the *in vitro* differentiation of OCs. However, RANKL is mainly responsible for the differentiation of OCs through NF- κ B activation^{328,331}. NF- κ B is an umbrella term for five subunits which combine to form a combination of homo- and hetero- dimers each with distinct activities³³². RANKL mediated NF- κ B activation results in the p50 and p65 subunits forming a heterodimer which rapidly translocates to the nucleus³³¹, signalling the up-regulation of essential osteoclastogenic genes and activating NFATc1, which strongly induces osteoclastogenesis³³³. Up-regulated OC specific genes encode proteins like DC-STAMP⁷, OSCAR²¹³, MMP9³³⁴, TRAP^{239,335} and Cathepsin K^{336,337} which govern OC fusion and enzyme production required for the degradation of the bone matrix and bone resorption.

Monocytes and MØs are known to express Fc γ R that bind IgG in complex with antigen²⁴⁹. Mature murine OCs have also been shown to express all subsets of murine Fc γ Rs: Fc γ RI, Fc γ RIIB, Fc γ RIII and Fc γ RIV^{259,262}. Fc γ RI, the high affinity receptor, can bind monomeric IgG and signals via the FcR γ ²⁵¹. Fc γ RIIB, Fc γ RIII and Fc γ RIV are only able to bind IgG that has formed an IC with several IgGs bound to a single antigen, resulting in cross-linking of Fc γ Rs and intracellular signalling³³⁸. The effects of these interactions can range from phagocytosis of the bound antigen and production to cytokines to enhance the immune response³³⁹.

OCs are known to express activatory Fc γ RI, Fc γ RIII, Fc γ RIV and are able to phagocytose inert particles²⁶⁴ independently of Fc γ Rs²⁶². Therefore the role of these receptors on OCs is unknown. However, recent work by Seeling *et al* (2013) demonstrated that

cross-linking of activatory FcγRI or FcγRIV on RANKL stimulated MØ was able to increase differentiation to mature OCs by two fold²⁶². Grevers *et al* (2012) showed that treatment with heat-aggregated rabbit IgG could inhibit the differentiation of murine BM into mature OCs in a FcRγ dependent manner³⁴⁰. Seeling and Grevers both demonstrated that activatory FcγRs were able to respond differently to ligation. The mode of stimulation and differentiation state of the pre-OCs can cause the resulting effect to differ markedly^{262,340}.

In this study, IgG complexes generated by the combination of SpA and IgG will be investigated. SpA's natural ability to form a SIC at a ratio of two SpA to four IgG has been widely studied^{299-301,341-343}. Research investigating the potential of SIC to engage FcγRs on myeloid cells has shown that SIC can (a) modulate the polarisation state of the murine and human MØ, and (b) inhibit the *in vitro* differentiation of human OCs³¹⁶. Administration of SpA alone, *in vivo*, was also shown to reduce inflammation in the mouse model of CIA, and subsequently reduce the number of OCs in the inflamed joint³¹⁶. These effects are thought to be mediated via FcγRs; in particular, FcγRI. MacLellan *et al* (2011) showed that in the absence of FcγRI, SIC was unable to interact with *in vitro* MØ and pre-OCs³¹⁶. Thus SIC and heat-aggregated rabbit IgG used by Grevers *et al* (2012) would appear to utilise a similar mechanism of action³⁴⁰. FcγRI is an activatory receptor which depends on signal transduction through the FcRγ²⁶⁵. The FcRγ and a fellow adaptor protein DAP12 are both activatory ITAM signalling molecules and have been shown to regulate the differentiation and activity of OCs *in vitro* and *in vivo*³⁴⁴. Animals deficient for both the FcRγ and DAP12 become osteopetrotic due to deficient OSCAR stimulation^{154,330}. Despite research into the vital role of the FcRγ signalling pathways in OC differentiation, the effect of FcγRs has not been greatly studied.

The goal of the research presented in this chapter was to examine the effect of SIC on *in vitro* murine osteoclastogenesis. The principal aims were to:

1. Determine the optimal conditions for OCs' differentiation in a murine *in vitro* system.
2. Examine the effect of SIC on osteoclastogenesis.
3. Examine whether SIC has an effect on the transcription of OC specific genes.

3.2 Results

3.2.1 Optimisation of *in vitro* osteoclastogenesis

In order to examine the effect that SIC has on osteoclastogenesis, an *in vitro* assay had to be optimised due to marked variation in existing published data^{7,69,345}. In all instances, M-CSF and RANKL are necessary and sufficient to drive osteoclastogenesis³²⁴ but the exact concentrations needed to be empirically determined due to variations in published protocols. To define the appropriate amount of RANKL required, studies were initiated with a standard assay using immortal murine MØ cell line, RAW 264.7. The ability of RAW 264.7 cells to respond to RANKL and differentiate into OCs has been widely published³⁴⁶⁻³⁴⁸. The differentiation of OCs was assessed by the ability of RAW 264.7 cells to differentiate into large multinucleated OCs (greater than 3 nuclei) which stain positive for TRAP³⁴⁹. Stimulation of RAW 264.7 cells at 1×10^5 cells/ml in a 24 well plate while increasing the concentration of RANKL from 50 to 100ng/ml failed to differentiate OCs after 5 days of culture (data not shown). In order to further investigate RAW 264.7 cells differentiation into OCs, RAW 264.7 cell densities were changed from 7×10^4 up to 1×10^6 cells/ml while terminating the experiment at different time-points. Varying these factors failed to induce full osteoclastogenesis: RAW 264.7 cells would become TRAP positive but would not fuse and become multinucleated (data not shown). Due to the failure of RAW 264.7 cells to respond to RANKL, use of this cell line was discontinued to optimise the conditions for osteoclastogenesis using primary cells.

The generation of human OCs relies on the differentiation of purified CD14⁺ monocytes isolated from PBMCs. In contrast to this the published literature regarding murine OCs has shown that OCs can be differentiated from BM. Previous work in the lab using OC cultures has been conducted on human CD14⁺ monocytes. Accordingly, to comply with previous human studies, purified murine BM monocytes were isolated using negative magnetic selection, gaining approximately a 92% pure monocyte population. These monocytes were cultured at 1×10^5 and 1×10^6 cells/ml in the presence of either 50 or 100ng/ml RANKL alongside 30ng/ml M-CSF for 10 days. TRAP staining showed osteoclastogenesis in this purified population was low and cells did not appear to thrive (Figure 3-1). Due to the lack of OCs in the purified BM monocyte population, it was decided to isolate circulating murine mononuclear cells in a similar manner to the isolation of human CD14⁺ monocytes from blood. Murine blood was harvested in the presence of EDTA and combined with BM samples. The blood and BM mixture was subsequently centrifuged on a histopaque layer and the mononuclear cells isolated. When 1×10^5 mononuclear cells were cultured in the presence of 10ng/ml M-CSF and 0,

50 and 100ng/ml RANKL for 7 days there was a small degree of osteoclastogenesis (Figure 3-2) compared to the monocytes isolated from BM alone (Figure 3-1). However, the proportion of OCs that differentiated was minor and the number of mononuclear cells isolated from murine blood and BM was minute. This method of OC generation was considered unfeasible for the undertaking of larger scale OC assays. Consequently, a different method was sought.

To investigate an alternative method of inducing OC differentiation the literature was once again examined. According to Burger *et al* (1982) the optimal conditions for murine osteoclastogenesis involved using murine whole BM as a source of OCs progenitors alongside M-CSF and RANKL to stimulate osteoclastogenesis^{345,350}. An initial experiment which replicated these conditions was conducted. Murine BM was taken from C57Bl/6 animals and flushed from the long bones and cultured overnight at 1×10^6 cells/ml with 30ng/ml M-CSF. Following the overnight incubation, non-adherent (NA) BM cells were cultured at a cell density of 1×10^6 cells/ml until day 7 with 30ng/ml M-CSF and 50ng/ml RANKL. Assessment by TRAP staining showed very few OCs present in RANKL treated cultures (Figure 3-3). Due to the absence of osteoclastogenesis and lack of distinction between the RANKL treated positive control cultures and M-CSF alone negative control cultures, further investigation into the conditions which differentiate murine BM into OCs was needed.

To investigate these conditions, pro-OC factor IL-1 β was used to aid the induction of osteoclastogenesis using murine BM. IL-1 β is a known activator of OC activity and maturation³⁵¹. This activatory cytokine has been shown to stimulate osteoclastogenesis and multinucleation³⁵¹. NA BM cells were generated as previously described and cells were cultured with 30ng/ml M-CSF and 0, 50 or 100ng/ml RANKL, with or without 10ng/ml IL-1 β . The addition of IL-1 β in this culture system had no effect on the level of osteoclastogenesis (Figure 3-4). Interestingly, it was observed that increasing RANKL concentration had no added effect on osteoclastogenesis. Increasing RANKL concentration from 50ng/ml to 100ng/ml in cultures of purified monocytes and whole BM had no effect on the number of OCs differentiated (Figure 3-1, Figure 3-2 and Figure 3-4). Hence, RANKL was not the limiting factor in this culture system, so M-CSF was investigated to determine whether it could be a limiting factor in osteoclastogenesis.

Treatment with purified recombinant mouse M-CSF was compared to treatment with L929 cell supernatant. L929 is an immortal fibroblast cell line which secretes M-CSF and can be used to differentiate M ϕ s in culture^{321,323,352}. Supernatant from these cultures was kindly provided by Dr. J. Montgomery. As previously described, murine NA BM at 1×10^6 cells/ml were cultured in the presence of L929 supernatant or M-CSF at 30ng/ml

with 0, 50 or 100ng/ml RANKL for 7 days. Cells differentiated in the presence of L929 supernatant did not become OCs and only a small number of OCs differentiated with M-CSF at 30ng/ml in both 50 and 100ng/ml of RANKL (Figure 3-5). When 50ng/ml RANKL was used, there were, on average, 10 times more OCs present in M-CSF treated cultures than L929 cell supernatant cultures. While there were 14 times more OCs present in M-CSF treated cultures compared to L929 cell supernatant when used along with 100ng/ml RANKL. This stark difference indicated that purified recombinant mouse M-CSF was superior to L929 cell supernatant for the *in vitro* differentiation of OCs.

The generation of OCs in this culture system relied on the use of purified recombinant mouse M-CSF and the optimal concentration of M-CSF required for the differentiation of OCs was investigated. NA BM cells were cultured at 1×10^5 cells in 200 μ l of complete α -MEM in 96 well tissue culture plates. Cells were cultured with 50ng/ml RANKL and increasing concentrations of M-CSF (30ng/ml, 50ng/ml, 75ng/ml and 100ng/ml) for 5 days at 37°C. There was a dramatic increase in the size and multinucleation of OCs differentiated in 75ng/ml and 100ng/ml M-CSF compared to 30ng/ml and 50ng/ml (Figure 3-6A). Interestingly, this huge difference in appearance was not as obviously mirrored in the number of OCs enumerated. When compared, there was no difference between the M-CSF concentrations used (Figure 3-6B). However, due to the intensely TRAP+ multinucleated large OCs present in cultures treated with >75ng/ml M-CSF, this concentration of M-CSF in conjunction with 50ng/ml RANKL was chosen as the optimal conditions for the generation of OCs and future experiments were modelled on this system.

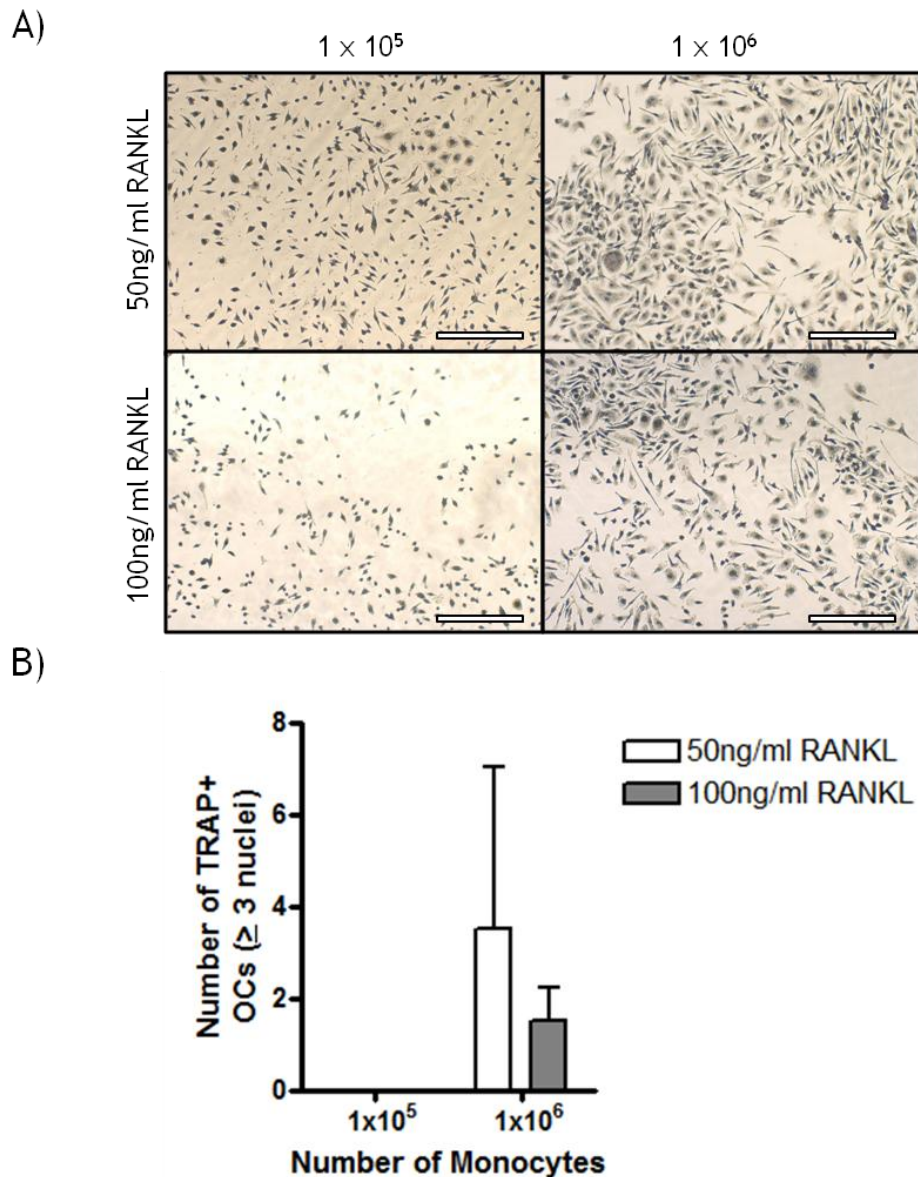


Figure 3-1: Enrichment of bone marrow monocytes does not induce the differentiation of osteoclasts.

Murine BM cells were harvested and RBCs were lysed using Akt Lysis Buffer. Monocytes were then enriched using EasySep Mouse Monocyte Enrichment Kit. Flow cytometry confirmed a 92.4% purity post separation. Purified monocytes (either 1×10^5 or 10×10^5 cells) were cultured with 30ng/ml M-CSF and either 50 or 100ng/ml RANKL for 10 days in 37°C with media renewed every third day. Cultures were stained for the presence of TRAP. A) Representative images of TRAP stained cultures. B) TRAP+ OCs with ≥ 3 nuclei were counted and the sum total of 8 fields of view per condition, in duplicate. Data represents mean \pm SD of experimental duplicates. Scale bar; 200 μ m.

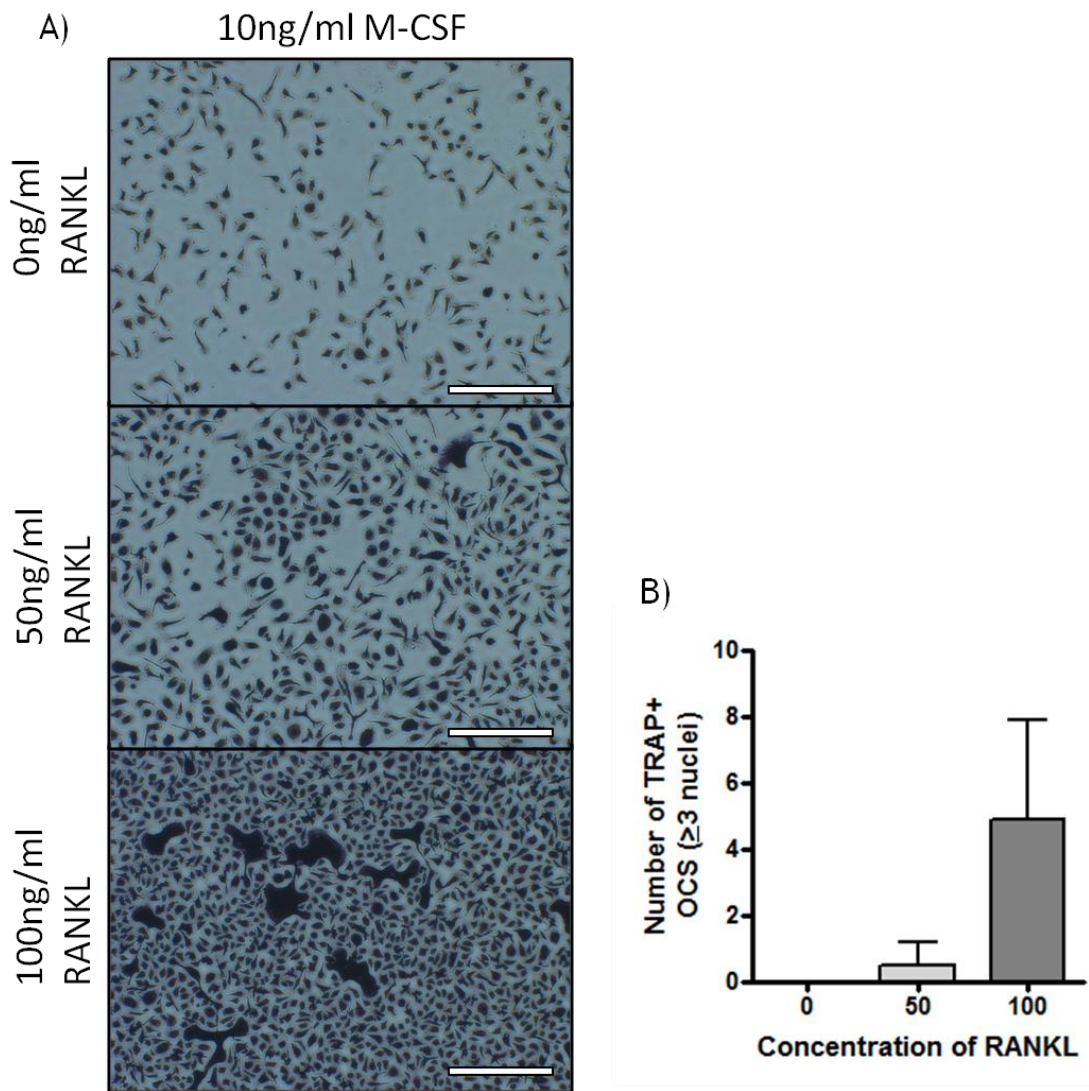


Figure 3-2: Isolated blood and bone marrow monocytes respond to high concentrations of RANKL.

Murine blood was taken using EDTA and BM was taken as previously described. Mononuclear cells were isolated using gradient centrifugation on a histopaque layer. The resulting 'buffy coat' was removed and 1×10^5 mononuclear cells in $50 \mu\text{l}$ was allowed to adhere to tissue culture plate wells at 37°C for 2 hours. Non-adherent cells were gently washed using warm PBS. Complete α -MEM with 10ng/ml M-CSF and 0, 50 or 100ng/ml RANKL were added to cultures in duplicate. Cultures were maintained at 37°C for 7 days with media refreshed on day 3. Cultures were stained for the presence of TRAP. A) Representative images of TRAP stained cultures. B) TRAP+ OCS with ≥ 3 nuclei were counted and the sum total of 4 fields of view per condition, in duplicate. Data represents mean \pm SD of experimental duplicates. Scale bar; $200 \mu\text{m}$.

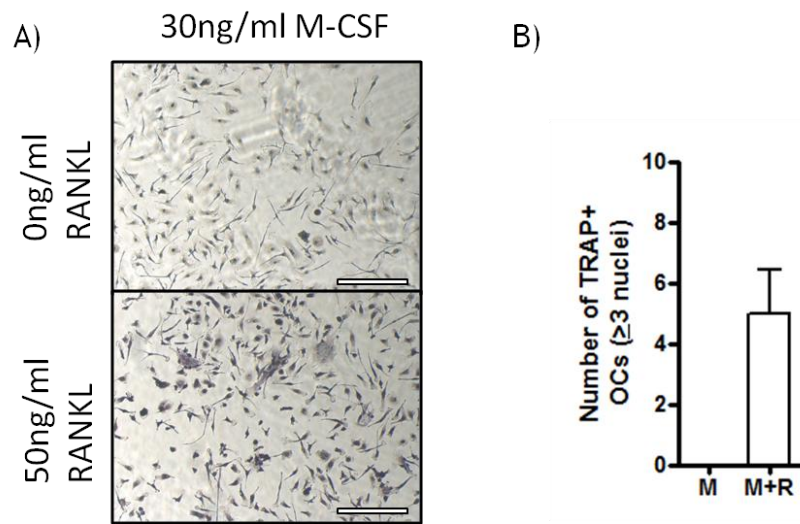


Figure 3-3: 30ng/ml M-CSF and 50ng/ml RANKL is not sufficient to differentiate osteoclasts. 1×10^6 murine NA BM cells were cultured with 30ng/ml M-CSF and 50ng/ml RANKL for 7 days in 37°C with media renewed on day 4. A) Cultures were stained for the presence of TRAP; representative images of cultures are shown. B) TRAP+ OCs with ≥ 3 nuclei were counted and the sum total of 4 fields of view per condition, in duplicate. Data represents mean \pm SD of experimental duplicates. Scale bar; $200\mu\text{m}$.

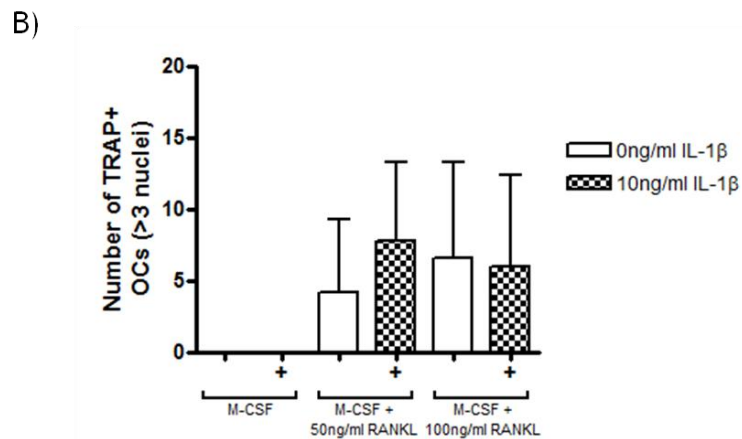
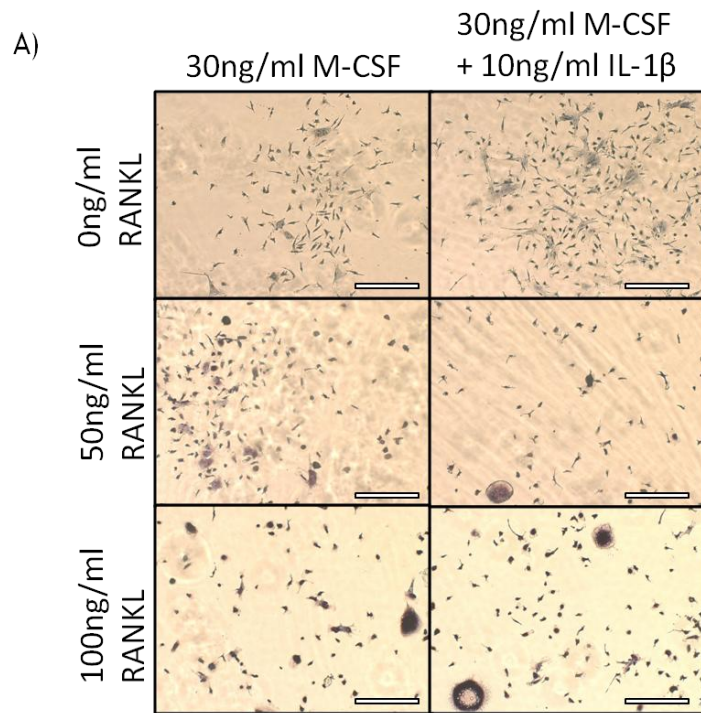


Figure 3-4: Addition of IL-1 β does not promote osteoclastogenesis.

1×10^6 murine NA BM cells were cultured with 30ng/ml M-CSF and 0, 50 or 100ng/ml RANKL. 10ng/ml IL-1 β was also added to cell media. Cultures were maintained for 7 days in 37°C with media renewed every third day. Cultures were stained for the presence of TRAP. A) Representative images of TRAP stained cultures. B) TRAP+ OCs with ≥ 3 nuclei were counted and the sum total of 5 fields of view per condition were used. Data represents mean \pm SD of 5 fields of view in one experiment. Scale bar; 200 μ m.

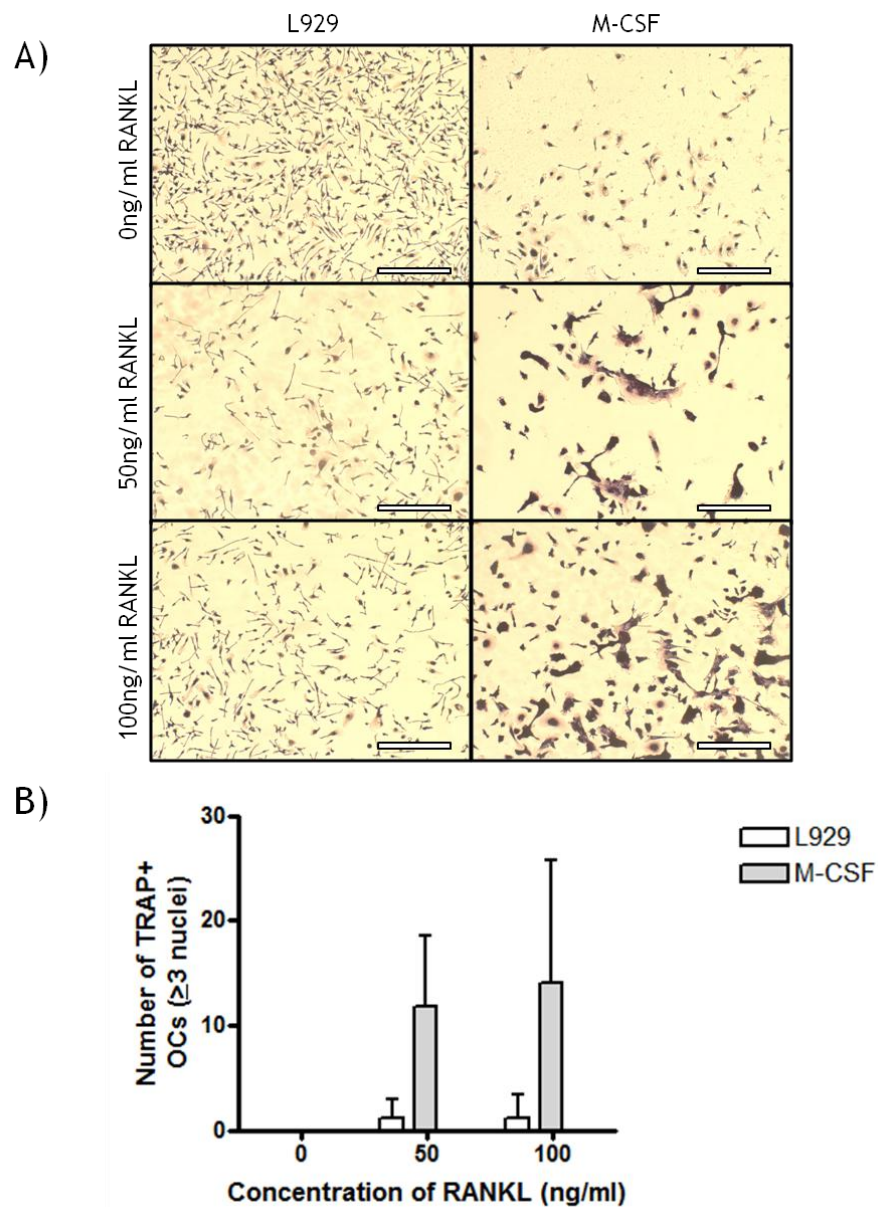


Figure 3-5: Comparison of L929 culture media or M-CSF to differentiate osteoclasts. 1×10^6 murine NA BM cells were cultured with either L929 (2 parts L929 to 8 parts media) or 30ng/ml M-CSF and 0, 50 or 100ng/ml RANKL for 7 days in 37°C with media renewed every third day. Cultures were stained for the presence of TRAP. A) Representative images of TRAP staining. B) TRAP+ OCs with ≥ 3 nuclei were counted and the average number of OCs in 5 fields of view per condition. Data represents the mean \pm SD of experimental duplicates of one experiment. Scale bar; 200 μ m.

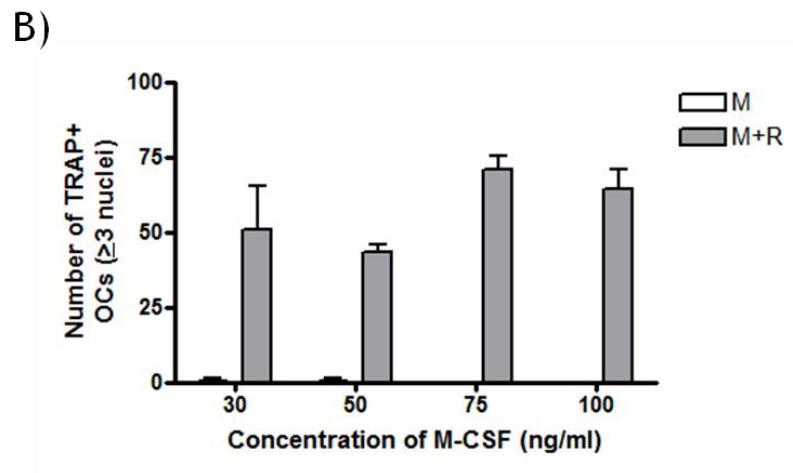
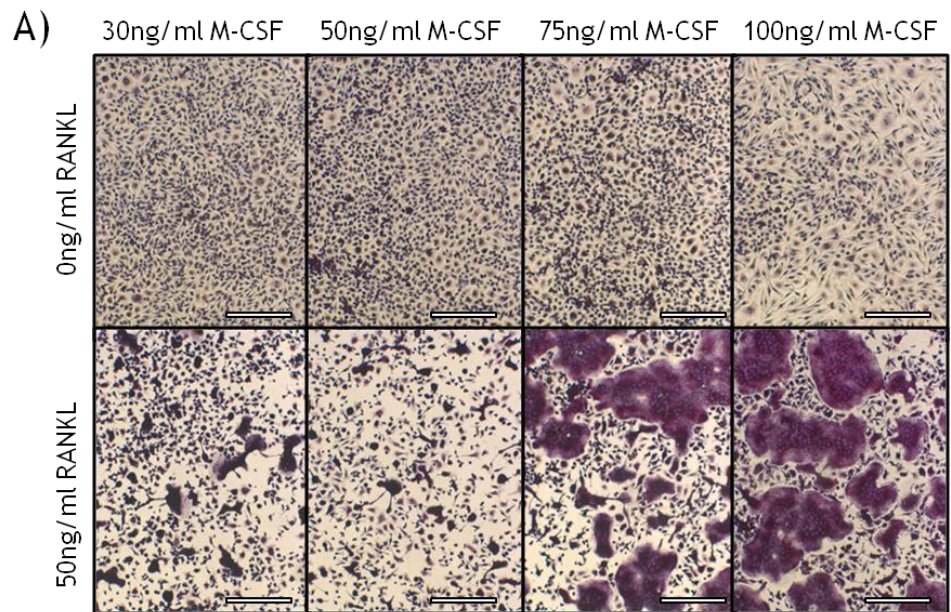


Figure 3-6: Increasing concentrations of M-CSF induce osteoclastogenesis.

1×10^5 murine NA BM cells were cultured with 30, 50, 75 or 100ng/ml MCSF and either 0 or 50ng/ml RANKL for 5 days in 37°C with media renewed on day 4. Cultures were stained for the presence of TRAP. A) Representative images of TRAP stained cultures. B) TRAP+ OCs with ≥ 3 nuclei were counted and the sum total of 4 fields of view per condition in duplicate were used. Data represents mean \pm SD of experimental duplicates of one experiment. Scale bar; 200 μ m.

3.2.2 Fcγ receptor mediated inhibition of osteoclastogenesis

The optimised OC culture system was used to test the affect that SIC could exert on the differentiation of OCs. 1×10^5 NA BM cells in 200 μ l were cultured with 75ng/ml M-CSF and 50ng/ml RANKL for 5 days. In conjunction with the addition of M-CSF and RANKL, the cells were treated with SIC or control treatments Oplg and SpA. SIC, Oplg and SpA were generated as described in section 2.6 and added to cultures at a concentration which reflected 25 μ g/ml of IgG per condition. A significantly high level of osteoclastogenesis was observed in the M-CSF and RANKL treated cultures (mean OCs \pm SD; 115.6 ± 23.6) compared to the M-CSF alone treated control (0 ± 0 ; $p < 0.001$) (Figure 3-7B). The differentiated OCs in the M-CSF and RANKL treated positive control cultures were large multinucleated and stained intensely for TRAP (Figure 3-7A). Treatment of these cultures with SpA alone did not alter osteoclastogenesis (114.6 ± 14.3) and did not affect the appearance of the differentiated OCs. Interestingly, a significant inhibition of osteoclastogenesis was observed in cultures treated with Oplg (36 ± 10 ; $p < 0.001$) and SIC (27 ± 8.1 ; $p < 0.001$) compared to M-CSF and RANKL treated positive controls (Figure 3-7B). The OCs that differentiated in the presence of Oplg and SIC were not only scarce, but smaller in size compared to the M-CSF and RANKL treated positive control (Figure 3-7A). Thus, in this culture system Oplg and SIC are able to inhibit osteoclastogenesis.

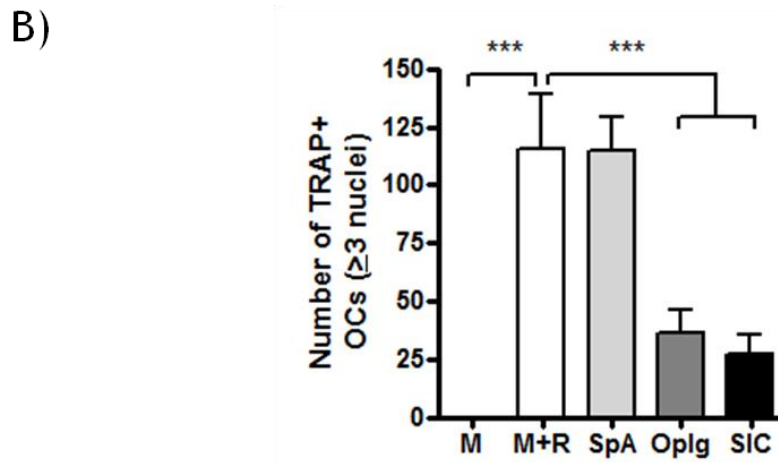
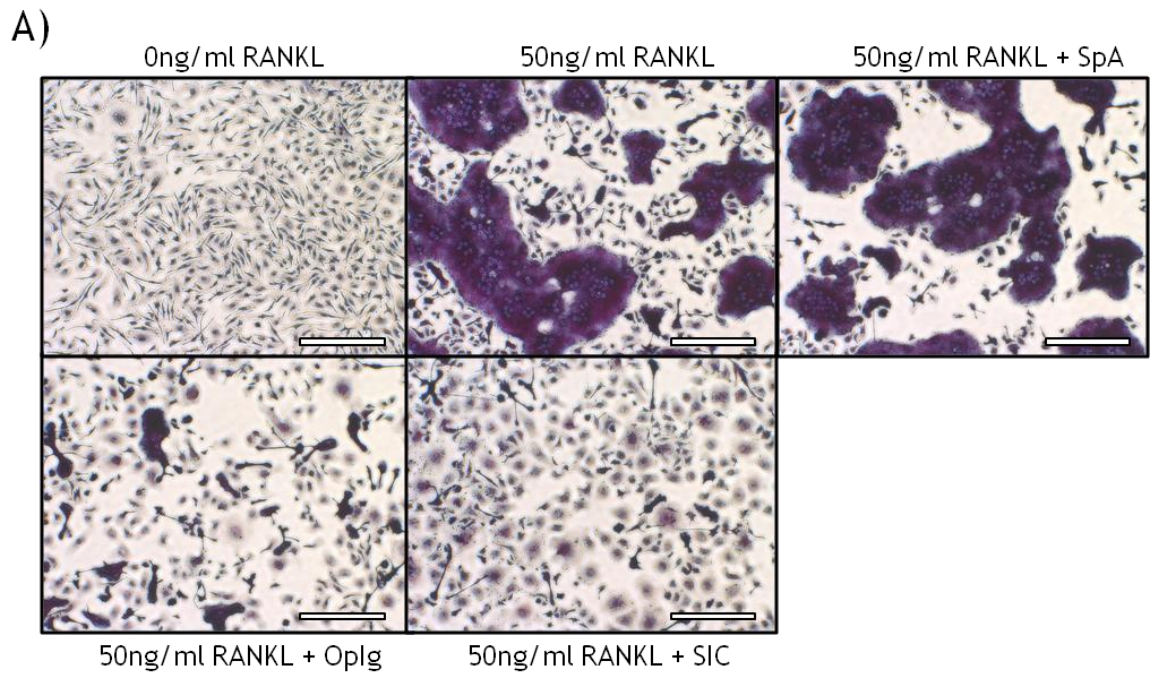


Figure 3-7: SIC and Oplg inhibit the differentiation of TRAP+ osteoclasts.

1×10^5 murine NA BM cells were cultured with 75ng/ml M-CSF and/or 50ng/ml RANKL for 5 days in 37°C with media renewed on day 4. Treatment with SpA, Oplg and SIC was given at day 1 and 4 alongside M-CSF and RANKL. Cultures were stained for the presence of TRAP. A) Representative images of TRAP stained cultures. B) TRAP+ OCs with ≥ 3 nuclei were counted and the sum total of 4 fields of view per condition in triplicate. One way ANOVA with Bonferroni's post tests; $p < 0.001$ (***)). Data represents pooled mean \pm SD of three individual experiments. Scale bar; 200 μ m.

3.2.3 Comparison of Oplg and SIC

Oplg and SIC can both inhibit *in vitro* osteoclastogenesis. Examination of whether the generation of Oplg created IC formation between OVA and IgG in a similar manner to SpA generated complexes was conducted. To ensure complexes were generated, protein interactions were cross-linked using a BS³ (Bis-sulfosuccinimidyl suberate) cross-linking reagent. BS³ contains two amine reactive esters that are able to covalently bind amine groups on proteins that are within close proximity³⁵³. Samples of SpA, OVA, IgG, Oplg and SIC were either cross-linked with BS³ or incubated with PBS. Samples were then loaded onto a gel, electrophoresed in non-reducing conditions and coomassie stained. All samples that had not been cross-linked migrated through the gel to the same extent as their constituent parts (Figure 3-8). OVA (42kDa), SpA (47kDa) and IgG (150kDa), as well as the OVA, SpA and IgG within Oplg and SIC samples, all migrated to their appropriate protein size as demarked by a protein ladder (Figure 3-8). Without cross-linking Oplg and SIC any protein interactions were separated; when the samples were cross-linked using the BS³ cross-linking reagent there was a large molecule observed at the top of the SIC lane (Figure 3-8). At a predicted size of approximately 694kDa, SIC was unable to migrate through the gel and remained close to the well at the top of the gel (Figure 3-8). However, protein aggregates appear in both cross-linked IgG and Oplg samples (Figure 3-8). It is unclear whether these are cross-linked IgG aggregates or whether IgG molecules have become cross-linked due to their close proximity, both explanations would account for the visible protein smear (Figure 3-8). The use of western blots could identify whether OVA and SpA are present in the large molecule weight cross-linked proteins present in these samples.

In order to verify that SpA, and not OVA, is able to form large molecular weight IgG complex, samples underwent size exclusion fractionation. OVA, SpA, IgG, Oplg and SIC were individually loaded into an ÄKTAprime and processed through a Sephacryl column under pressure. When using this method, samples do not require cross-linking as the forces used in this process will not separate interacting molecules. This process allows for the discrimination of proteins based on molecular weight as indicated by the length of time the protein requires to move through the column. Larger molecules are able to pass through the column more quickly than smaller molecules which become trapped in the column resin. The concentration of protein was measured by UV₂₈₀ as samples exit the column. OVA and SpA are 42 and 47kDa, respectively and required ~400 minutes in order to pass through the column, while 150kDa IgG molecules required ~350 minutes to exit the column (Figure 3-9). Oplg passed through the column and was observed to exit the column between 350-400 minutes (Figure 3-9). This indicates that both IgG and OVA exit the column at the same speed as the individual constituents (Figure 3-9).

Interestingly, SIC only required 200 minutes for the sample to begin its exit and had fully left the column by 400 minutes (Figure 3-9). This demonstrates that SIC can form a large molecular weight complex without protein cross-linking, unlike Oplg. However, in the SIC sample there is excess IgG which is also present in the Oplg samples (Figure 3-8 and Figure 3-9). Prior to use, all IgG samples were centrifuged to remove protein aggregates, however, the IgG present may still form small molecular weight complexes that could interact with cells in culture media. Despite this disparity SIC and Oplg were both able to inhibit osteoclastogenesis.

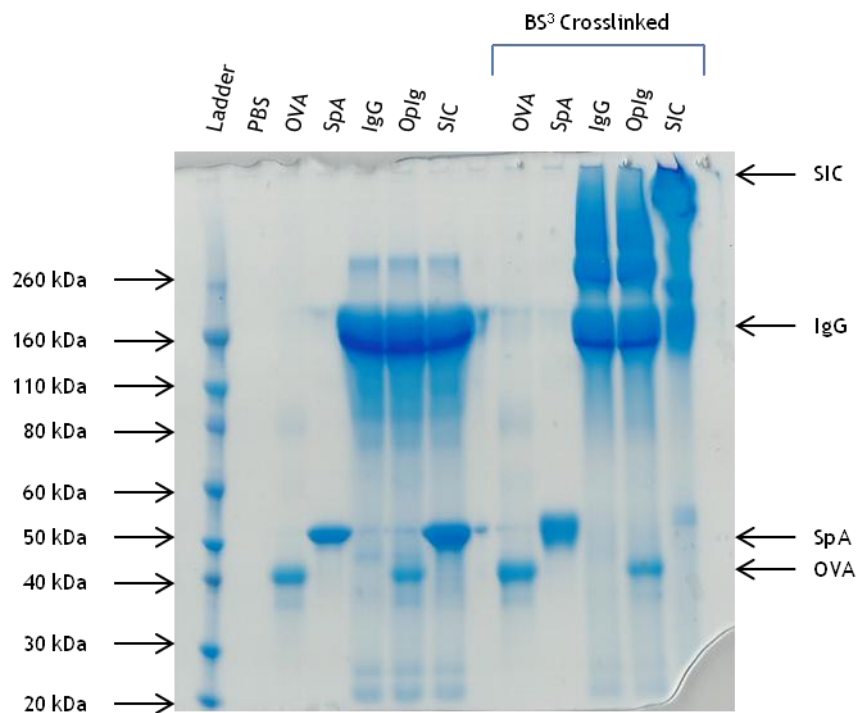


Figure 3-8: Cross-linking protein interactions between SpA and IgG results in IgG complex formation; OVA and IgG do not form complexes.

PBS, OVA, SpA, IgG, Oplg and SIC were incubated at 37°C for 1 hour. Protein interactions were cross-linked in the samples by addition of 1mM BS³ cross-linker for 30 minutes at RT. The reaction was quenched by incubation for 15 minutes in 0.5mM Tris-HCl. Samples that were not cross-linked had equivalent volumes of PBS added. 4x LDS sample buffer was added and samples were run on a 4-12% Bis-Tris gel with a protein ladder for 2 hours at 200V. Gel was subsequently stained using Simply Blue SafeStain and de-stained in dH₂O. Image represents one experiment.

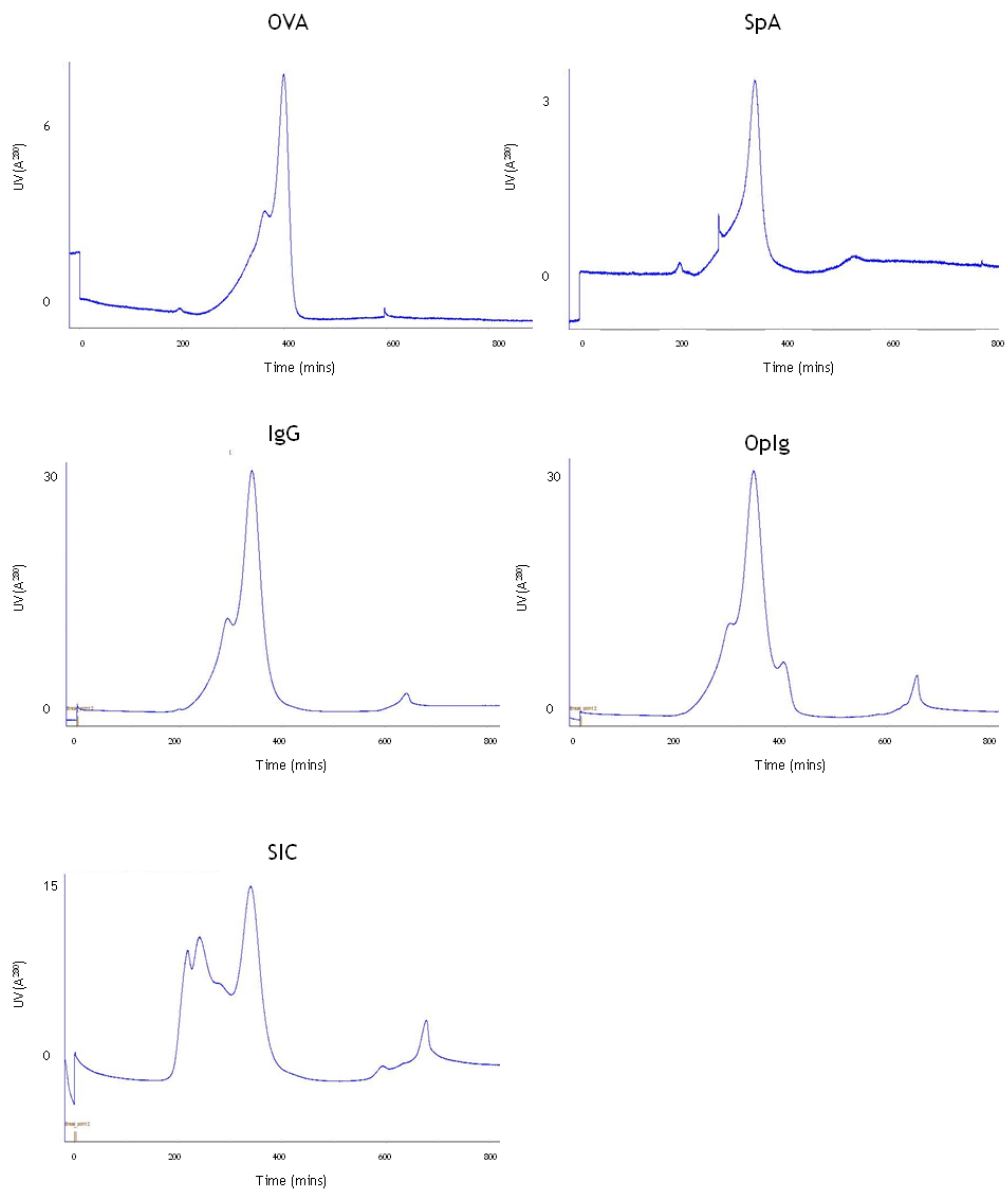


Figure 3-9: Fractionation of SpA, OVA and IgG using Sephacryl chromatography column demonstrates that OVA and IgG do not form complexes.

OVA, SpA, IgG, Oplg and SIC samples were individually processed through a Sephacryl column which discriminates protein size into separate fractions for collection - large proteins move more quickly through the medium. 2mg of OVA, SpA, IgG, Oplg and SIC in 500 μ l of PBS were used. Graphs represent the concentration of protein, measured by UV (at A²⁸⁰), in each fraction collected over time (minutes). Graphs shown are from one experiment.

3.2.4 IgG inhibits osteoclastogenesis

FcγRI has the ability to engage monomeric IgG²⁵¹, so, it was decided to test whether the inhibition associated with SIC and Oplg could be due to the excess IgG present in both of these treatments. SpA, IgG, Oplg and SIC were prepared as previously described and added to cultures of 1×10^5 NA BM cells in 200μl alongside 300ng/ml M-CSF and 50ng/ml RANKL. Following 5 days of culture, cells were stained for TRAP and it was shown that IgG, Oplg and SIC were all able to significantly inhibit osteoclastogenesis (Figure 3-10). Despite the supra-physiological concentrations of M-CSF, treatment with IgG was able to inhibit osteoclastogenesis by 48.9% ($p < 0.05$), while addition of Oplg could inhibit osteoclastogenesis by 68.9% ($p < 0.01$). As previously shown the only constituents of Oplg are IgG and OVA which do not interact. Therefore, the difference in inhibition may be due the large variation in data spread in IgG treated groups (mean OC number \pm SD; 39 ± 24.9) compared to Oplg (23.6 ± 9.0). Consequently, treatment of NA BM with SIC was able to significantly inhibit osteoclastogenesis by 80.3% ($p < 0.001$; 15 ± 3.6 - Figure 3-10). To verify whether the presence of OVA in Oplg was having an effect on osteoclastogenesis, NA BM was cultured for differentiation into OCs in the presence of SpA, OVA, Oplg and SIC. The presence of OVA in these cultures had no effect on the level of osteoclastogenesis, while treatment with Oplg and SIC significantly inhibited osteoclastogenesis (Figure 3-10). It remains to be elucidated whether OVA present in Oplg can interact with IgG and contribute to Oplg inhibitory capacity; however OVA alone cannot alter osteoclastogenesis (Figure 3-10).

Despite the differences in efficacy of IgG, Oplg and SIC to inhibit osteoclastogenesis, the presence of IgG (at 25μg/ml) is able to inhibit osteoclastogenesis. Nevertheless, treatment with ICs in the form of SIC was most successful at *in vitro* OC inhibition. Subsequent experiments were undertaken using Oplg as both a control for SIC and also a treatment to test the effect of monomeric IgG.

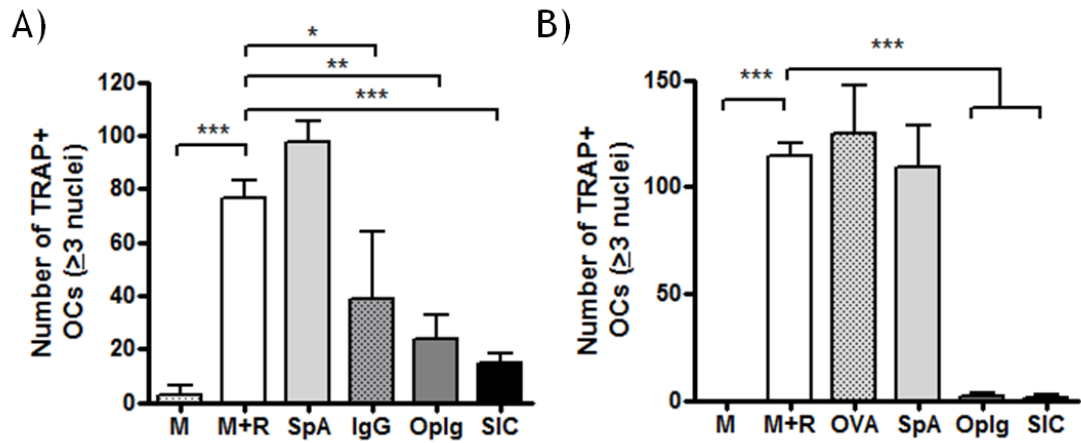


Figure 3-10: Murine IgG inhibits the differentiation of TRAP+ osteoclasts.

A) 1×10^5 murine NA BM cells were cultured with 300ng/ml M-CSF and 50ng/ml RANKL for 5 days in 37°C with media renewed on day 4. Treatment with SpA, IgG, Oplg and SIC was given at day 1 and 4 alongside M-CSF and RANKL. Cultures were stained for the presence of TRAP. TRAP+ OCs with ≥ 3 nuclei were counted and the sum total of 4 fields of view per condition, in triplicate. One way ANOVA with Bonferroni's post tests used; $p < 0.05$ (*), $p < 0.01$ (**), $p < 0.001$ (***). Data represents mean \pm SD of one experiment. B) 1×10^5 murine NA BM cells were cultured with 75ng/ml M-CSF and 50ng/ml RANKL for 5 days in 37°C with media renewed on day 4. Treatment with OVA, SpA, Oplg and SIC was given at day 1 and 4 alongside M-CSF and RANKL. Cultures were stained for the presence of TRAP. TRAP+ OCs with ≥ 3 nuclei were counted and the sum total of 4 fields of view per condition, in triplicate. One way ANOVA with Bonferroni's post-hoc tests; $p < 0.001$ (***). Data represents mean \pm SD of three separate experiments.

3.2.5 Functional consequence of Fc γ receptor inhibition

IgG, in the form of Oplg and SIC, has been shown to inhibit the differentiation of OCs from murine BM on tissue culture plates. This is a convenient medium to culture cells; however, it is an isolated environment in terms of cell growth. Culturing OCs on bone discs provides a valid growth platform resembling the physiological microenvironment of the bone. Present on the bone surface are stromal factors, among these is Collagen Type II which is able to promote osteoclastogenesis via the OSCAR receptor on pre-OCs¹⁵⁴. Therefore, the effect of Oplg and SIC on the differentiation of OCs on bovine bone discs was investigated. NA BM cells were cultured with 75ng/ml M-CSF and 50ng/ml RANKL with the addition of SpA, Oplg and SIC on bovine bone discs. After 10 days of culture, bone slices were removed and stained for TRAP (Figure 3-11A). This revealed that there was a large variation in the number of OCs present on the surface of the bone slices (Figure 3-11C). It also showed that Oplg and SIC were both unable to stop the differentiation of OCs cultured on bone discs (Figure 3-11C).

In parallel with this study, OCs were cultured on bone slices until day 14 in order to maximise their erosive capacity. Bone slices were then washed with dH₂O to remove any cells before areas of erosion were visualised (Figure 3-11B). This showed that the area of erosion varied markedly between experimental and biological triplicates, resulting in a large data spread. Cells grown in the presence of M-CSF and RANKL alone (mean % of erosion \pm SD; 14.9 \pm 11.2) had similar erosive capacity to cells grown in the presence of SpA (12.3 \pm 11.2) and Oplg (13.9 \pm 11.3) (Figure 3-11D). Interestingly, cells grown in the presence of SIC appeared to have a substantial reduction in the percentage of erosion (5.4 \pm 4.4). However, a comparison of all data sets revealed that there were no significant differences in the groups treated with SpA, Oplg and SIC compared to M-CSF and RANKL positive control group. However, when a less stringent method of analysis was used SIC treated samples have significantly reduced bone erosion ($p < 0.05$) compared to positive controls. Further work needs to be done to increase the replicates and determine conclusively whether SIC can inhibit *in vitro* bone erosion. This suggests that SIC may limit the activity, but not differentiation, of OCs cultured on bone discs. Therefore, SIC may be able to overcome the additional stimulation that OCs receive when cultured on bone discs that monomeric IgG in Oplg cannot overcome.

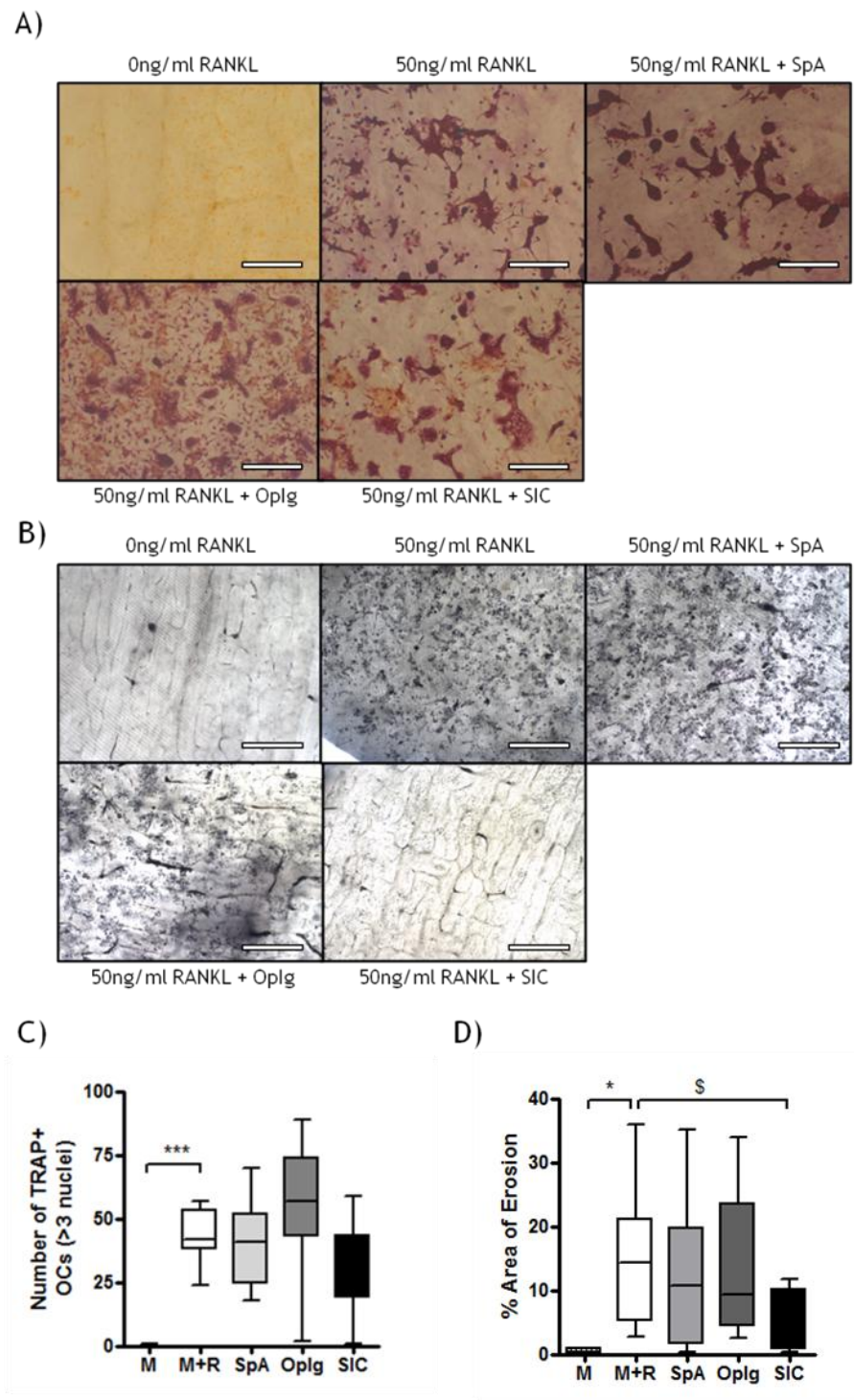


Figure 3-11: SIC inhibits the activity of osteoclasts on bovine cortical bone slices.

1×10^5 murine NA BM cells were cultured on bone slices with 75ng/ml M-CSF and 50ng/ml RANKL for 10 to 14 days in 37°C with media refreshed every 3rd day. Treatment with SpA, Oplg and SIC was given at day 1 alongside M-CSF and RANKL and upon every media change. A) Representative images of TRAP staining on bone slices at day 10 and C) TRAP+ OCs with ≥ 3 nuclei were counted at day 10 and the sum total of 4 fields of view per condition, in triplicate. One way ANOVA with Bonferroni's post-hoc tests used; $p < 0.001$ (***). B) Representative images of areas of bone erosion at day 14. D) 5 images per bone slice were taken and % area of erosion was measured by calculating the area of the image over the eroded area per field of view. One way ANOVA with Bonferroni's post-hoc tests; $p < 0.05$ (*). Data represents C) pooled median and range of data of three experiments, $n=3$, and D) pooled median and range of data of three experiments, $n=9$. Scale bar; A) 200 μ m and B) 500 μ m. \$ represents unpaired two tailed t tests between M+R and SIC treated samples; $p < 0.05$.

3.2.6 The role of FcγRIII in Fcγ receptor mediated inhibition

To further investigate the differences between Oplg and SIC, their role in inhibiting osteoclastogenesis using FcγRIII^{-/-} BM was investigated. NA BM from FcγRIII^{-/-} mice was cultured with 75ng/ml M-CSF and 50ng/ml RANKL in the presence of SpA, Oplg and SIC. FcγRIII deficiency had no impact on osteoclastogenesis observed in the M-CSF and RANKL treated positive control group (mean OCs; 85.3 ± 11.5) (Figure 3-12). Treatment of FcγRIII^{-/-} cultures with SpA (95.3 ± 17.4) and, importantly, Oplg (49.6 ± 19.1) had no significant effect on osteoclastogenesis, while treatment with SIC (25.3 ± 5.5) was able to significantly inhibit osteoclastogenesis (p<0.01). This accounts for a 70.3% inhibition of osteoclastogenesis in FcγRIII^{-/-} cultures which is comparable to the 76.6% inhibition of osteoclastogenesis observed in WT cultures treated with SIC (Figure 3-10 and Figure 3-12). FcγRIII is mainly involved in IC interactions²⁴⁹ and the inability of Oplg to inhibit osteoclastogenesis in FcγRIII^{-/-} cells suggests that it may be small IgG aggregates present in Oplg which are responsible for this inhibition. This also demonstrates that SIC can inhibit osteoclastogenesis independently of FcγRIII. It is likely that other FcγRs (including FcγRIII) are involved in this inhibitory effect. Without investigation into the interaction of other FcγRs this inhibitory effect will not be fully understood.

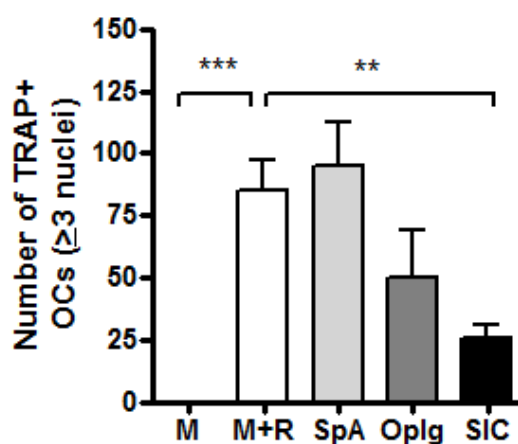


Figure 3-12: SIC inhibits the differentiation of TRAP+ FcγRIII^{-/-} osteoclasts.

1x10⁶ murine NA BM cells from FcγRIII^{-/-} mice were cultured with 75ng/ml M-CSF and 50ng/ml RANKL for 5 days in 37°C with media renewed on day 4. Treatment with SpA, Oplg and SIC was given at day 1 and 4 alongside M-CSF and RANKL. Cultures were stained for the presence of TRAP. TRAP+ OCs with ≥3 nuclei were counted and the sum total of 4 fields of view per condition in triplicate used. One way ANOVA with Bonferroni's post test; p<0.01 (**). Data represents pooled mean ± SD of three experiments.

3.2.7 Fcγ receptor modulation down-regulates osteoclast essential gene transcription

SIC and Oplg have been shown to inhibit the differentiation of murine BM into OCs. SIC limits the activity of OCs when cultured on bone. In order to understand the further potential differences between these treatments, OCs were differentiated in the presence of these treatments for 3 days and mRNA extracted. cDNA was synthesised from the mRNA and the presence of specific target mRNA was examined.

In order to do this, suitable primers against mRNA were designed. mRNA of genes which were of interest to us were located in the NCBI database and Primer 3 software was utilised to design primers that could potentially amplify a specific PCR product. Table 2.1 lists all the primers designed and used in this study. To test the specificity of the designed primers, end-point PCR was used to detect a PCR product of known size (Figure 3-13). Equal levels of mRNA for CD115, RANK, NFATc1 and Bcl-3 were present in MØ (M-CSF treated) and OC (M-CSF and RANKL treated) samples, while mRNA for OC specific genes TRAP, Cathepsin K, MMP9, DC-STAMP and OSCAR were only present at detectable levels in OC samples as they require RANKL for their induction (Figure 3-13).

Firstly the genes involved in the induction of osteoclastogenesis were examined. Transcription of CD115 and RANK mRNA play vital roles in the differentiation and survival of OCs and transcription of these genes was shown to be unaffected by treatment with SpA, Oplg and SIC (Figure 3-14). As mentioned, RANK signals via NF-κB and one important inhibitor of NF-κB signalling is Bcl-3^{167,331}. If NF-κB activation is inhibited by Oplg or SIC then Bcl-3 transcription may be up-regulated. Following three days of RANKL stimulation, Bcl-3 mRNA levels were increased compared to M-CSF alone treated samples ($p < 0.05$), however treatment with SpA, Oplg or SIC did not affect Bcl-3 transcription (Figure 3-14). Another transcription factor of interest is NFATc1 which is activated by NF-κB and strongly induces OC differentiation³³³. Interestingly, the data suggests that SIC, and to a small degree Oplg, were able to down-regulate NFATc1 mRNA compared to M-CSF and RANKL positive control; however this was shown to be not significant (Figure 3-14).

After three days of RANKL stimulation, mRNA transcripts were examined and treatment with SIC and Oplg down-regulated the transcription of OC genes. mRNA transcript levels of Cathepsin K, TRAP, DC-STAMP and OSCAR were all strongly increased in the M-CSF and RANKL treated positive control compared to M-CSF alone (Figure 3-15). This induction of mRNA was significantly inhibited when cells were cultured in the presence of SIC and Oplg (Figure 3-15). mRNA transcript level for MMP9 appeared to be reduced

following treatment with Oplg and SIC, however, this failed to reach significance (Figure 3-15).

Therefore, M-CSF and RANKL treatment in cultures committed to the OC lineage up-regulate transcription of genes essential for osteoclastogenesis. FcγR modulation inhibits this effect preventing the differentiation of mature OCs from murine BM.

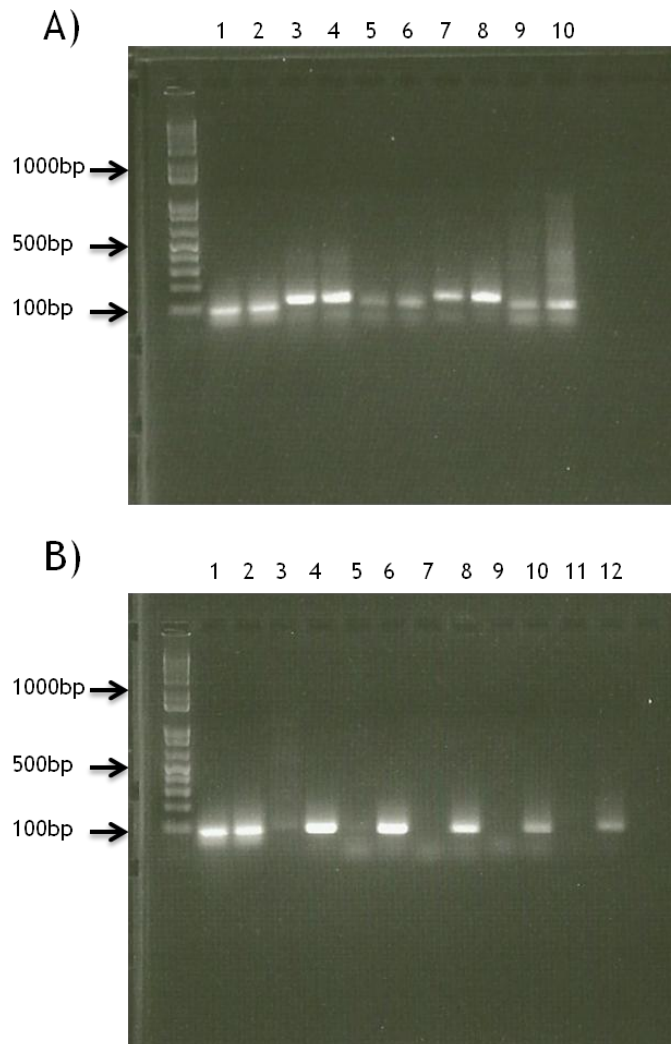


Figure 3-13: Primers designed for qPCR are specific for their target gene.

1×10^6 murine NA BM cells were cultured with 75ng/ml M-CSF and/or 50ng/ml RANKL for 5 days in 37°C with media renewed on day 4. Cultures were lysed using QIAzol Lysis Reagent, mRNA was extracted using QIAgent miRNEasy mini kit and cDNA generated. cDNA was added to a PCR master mix, with specific primer sets, using Go Taq Polymerase and end point PCR was used to amplify the PCR product. All odd numbered lanes are M-CSF treated MØ, while even numbered lanes are M-CSF and RANKL treated OCs. A) Primer sets used are 1+2) GAPDH, 3+4) CD115, 5+6) RANK, 7+8) NFATc1, 9+10) Bcl-3. B) Primer sets used are 1+2) GAPDH, 3+4) TRAP, 5+6) Cathepsin K, 7+8) MMP 9, 9+10) DC-STAMP, 11+12) OSCAR.

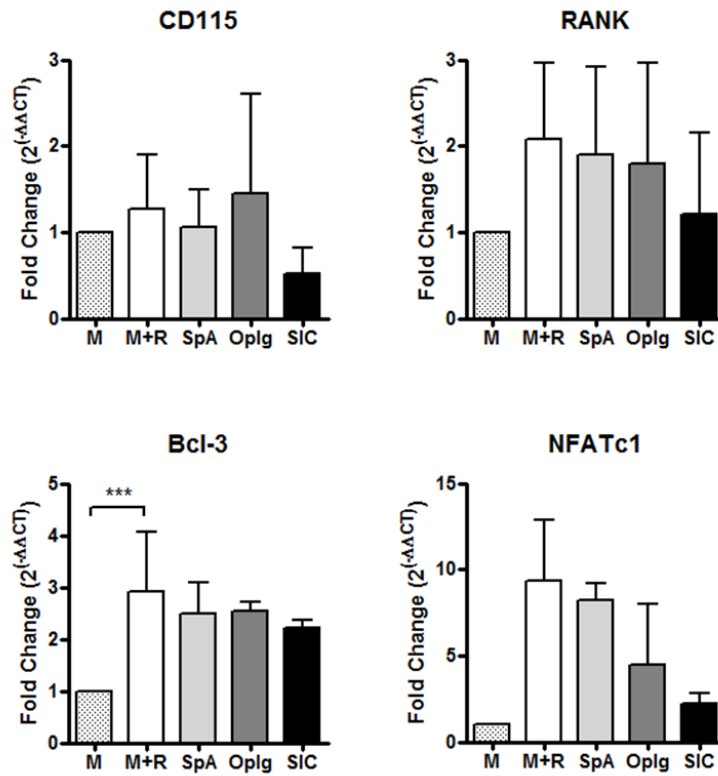


Figure 3-14: Fcγ receptor modulation of transcription in pre-osteoclasts.

1x10⁶ murine NA BM cells were cultured with 75ng/ml M-CSF and 50ng/ml RANKL for 3 days in 37°C. Treatment with SpA, Oplg and SIC was given at day 1. Cultures were lysed on day 3. For qPCR, all samples were run in triplicate. GAPDH was used as the housekeeping control and non-template controls were run for each gene. Fold Change (2^{-ΔΔCT}) was measured by normalising samples of each primer to the housekeeping control and subsequently normalising all samples to M-CSF alone to obtain the ΔΔCT. This was then used to obtain the fold change. One way ANOVAs with Bonferroni's post tests were performed on ΔCT values; p<0.001 (***). Data represents pooled mean ± SD of three experiments.

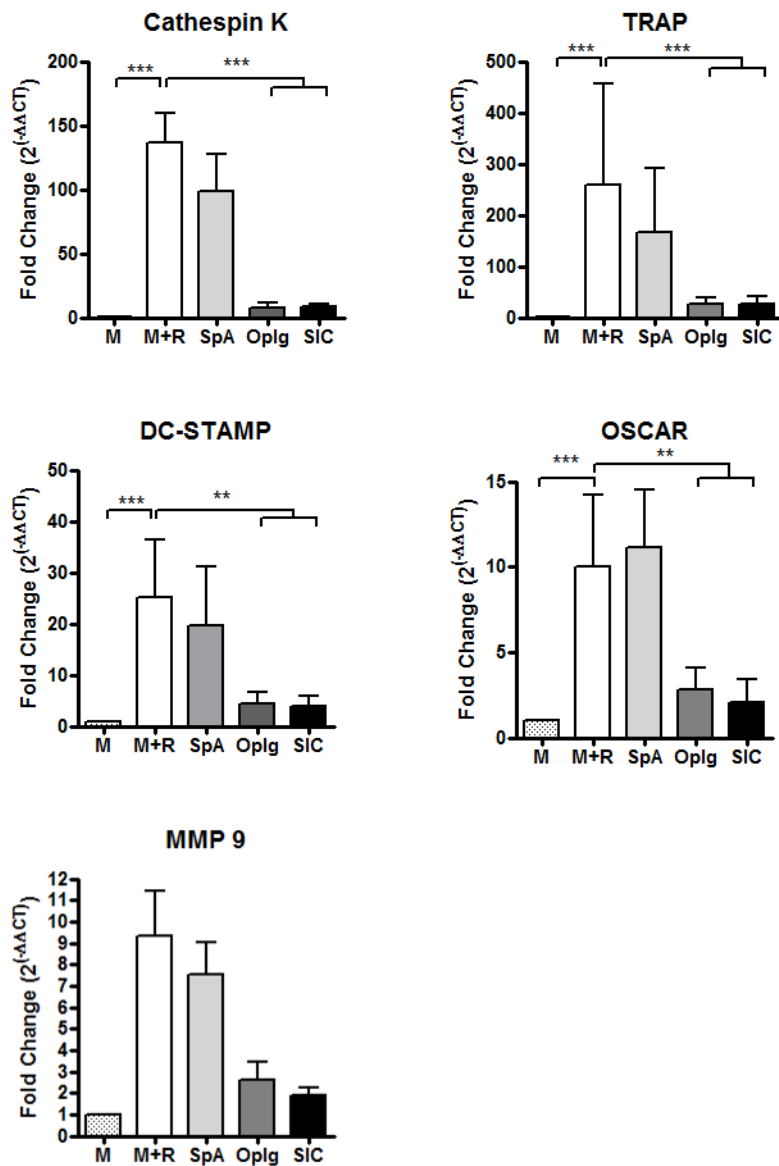


Figure 3-15: IgG inhibits pre-osteoclasts transcript levels of osteoclast specific genes.

1×10^6 murine NA BM cells were cultured with 75ng/ml M-CSF and 50ng/ml RANKL for 3 days in 37°C. Treatment with SpA, Oplg and SIC was given at day 1. Cultures were lysed on day 3. For qPCR, all samples were run in triplicate. GAPDH was used as the housekeeping control and non-template controls were run for each gene. Fold Change ($2^{-\Delta\Delta CT}$) was measured as previously mentioned. One way ANOVAs with Bonferroni's post tests were performed on ΔCT values; $p < 0.01$ (**), $p < 0.001$ (***). Data represents pooled mean \pm SD of three experiments.

3.3 Discussion

SIC formed by incubation of SpA with IgG has been shown to inhibit human osteoclastogenesis³¹⁶ and now we show that SIC will inhibit murine osteoclastogenesis. Optimisation of an assay to differentiate murine OCs was undertaken and revealed that culturing BM with 75ng/ml M-CSF and 50ng/ml RANKL optimal (Figure 3-6). Treatment of BM cells with SIC or Oplg, a control treatment, could inhibit the differentiation of TRAP+ OCs. While, the generation of SIC produced large protein complexes this did not occur with Oplg. Subsequently, IgG was shown to be capable of inhibiting the *in vitro* differentiation of OCs. However, SIC, and not Oplg, inhibited the activity of OCs on bone slices. Transcription of OC specific mRNA transcripts (Cathepsin K, DC-STAMP, OSCAR and TRAP) were down-regulated following treatment with SIC when compared with untreated cultures. Importantly, the effects seen with SIC treatment were also observed with Oplg. This indicates that IgG alone could be mediating the observed FcγR mediated inhibition.

In this chapter the ability of SIC to inhibit murine osteoclastogenesis was tested. This required the optimisation of an *in vitro* protocol for the generation of OCs which had previously not been done in the lab. Early experiments demonstrated that murine osteoclastogenesis was unlike human osteoclastogenesis where MacLellan *et al* (2011) used purified human CD14⁺ monocytes in the presence of M-CSF and RANKL to differentiate OCs³¹⁶. Murine monocytes purified from BM using a commercially available kit (Figure 3-1); monocytes isolated from blood and BM using gradient centrifugation and histopaque (Figure 3-2); treatment of NA BM cells with 30ng/ml M-CSF and increasing concentrations of RANKL (Figure 3-3); treatment of NA BM cultures with IL-1β alongside M-CSF and RANKL (Figure 3-4); culture of NA BM in L929 supernatant and RANKL to test the source of M-CSF all failed to induce osteoclastogenesis (Figure 3-5). It was not until the concentration of M-CSF added to cultures of NA BM was increased that osteoclastogenesis became evident (Figure 3-6).

The standard protocol that was developed used murine whole BM to derive a population of pre-OCs. Treatment of murine BM with 30ng/ml M-CSF overnight was able to induce the proliferation of NA mononuclear phagocytes with high OC potential^{354,355}. This generated NA BM which could be cultured with 75ng/ml of M-CSF and 50ng/ml RANKL for five days to generate OCs. When the concentration of M-CSF was increased from 30 to 100ng/ml it was shown that higher concentrations of recombinant M-CSF could increase osteoclastogenesis and impact on the cells ability to fuse. M-CSF interacts with CD115 on the surface of monocytes and without additional stimulation directs the monocyte to proliferate and differentiate into a MØ³⁵⁶. A higher concentration of M-CSF

may have lead to heightened signalling via CD115 resulting in phosphorylation of the transcription factor MITF which is known to increase pre-OC fusion and activity¹²⁷. In *op/op* mice, a dysfunctional M-CSF protein is produced resulting in decreased *in vivo* monocyte, MØs and OCs numbers¹¹⁹. These *op/op* mice become osteopetrotic due to a lack of OC differentiation¹²³. An increase in M-CSF will result a greater stimulation of PU.1, the transcription factor activated by CD115 which can enable the initiation of commitment to the OC lineage and has a major role in osteoclastogenesis as PU.1 deficient animals are osteopetrosis^{94,357}. This is because CD115 signalling through PU.1 directly interacts with the RANK promoter increasing RANK expression³⁵⁸. The role of M-CSF in mature OCs has also been observed as M-CSF is required to increase OC motility and prevent apoptosis^{128,129}. Therefore in this culture system M-CSF was the limiting factor affecting osteoclastogenesis.

An optimised OC culture assay allowed the effect of SIC to be investigated. OCs differentiated from NA BM in the presence of 75ng/ml M-CSF and 50ng/ml RANKL were treated with SIC. This treatment was shown to inhibit of differentiation of OCs (Figure 3-7). However, treatment of NA BM with Oplg also resulted in inhibition of osteoclastogenesis. Oplg consists of IgG and OVA, which is a non-reactive protein of a similar molecular weight as SpA. OVA is intended to be a control of the SpA present in SIC and should not interact or aggregate with IgG, yet Oplg has the ability to inhibit osteoclastogenesis. Therefore, to confirm that OVA was not inducing IgG aggregation in the Oplg samples we examined the constituents of Oplg and SIC.

SpA binds IgG from many mammalian species and forms both soluble and insoluble complexes by Fc and Fab mediated interactions^{294,295,301,343,359}. Atkins *et al* (2008) proposed a mechanism of SpA and IgG binding in a 2:4 ratio via the Fc region³⁰¹. SpA bound IgG is still able to interact with FcγRs in the form of this IgG complex that has been named SIC³¹⁶. Cross-linking of protein interactions showed that SIC but not Oplg could form large molecular weight complex (Figure 3-8). Another finding observed in this experiment, was that cross-linking of IgG and Oplg resulted in proteins larger than 150kDa. This may indicate that cross-linking has allowed IgG to form protein aggregates. Therefore investigation into whether IgG was able to form complexes in these samples using size exclusion chromatography was undertaken. By fractionating samples based on size it was shown that IgG and Oplg failed to make naturally occurring large molecular weight complexes. SIC was able to form a large IgG complex that rapidly exits the column (Figure 3-9). Despite the lack of large molecular weight protein aggregates the IgG present in Oplg may still interact and form low molecular weight proteins which could be responsible for the observed inhibition of osteoclastogenesis. Langone *et al* (1985) used a similar technique to demonstrate that SpA can form large complexes with

human purified IgG and serum³⁰⁰. Using both gel electrophoresis and size exclusion chromatography it was shown that in the samples of SIC there was an excess amount of unbound IgG. This suggests that it is the presence of excess IgG in SIC and Oplg that inhibits osteoclastogenesis and that the SIC may not be required for this effect.

To robustly test whether IgG alone could inhibit murine osteoclastogenesis, OCs were differentiated in the presence of IgG, Oplg or SIC. This demonstrated that alone IgG could inhibit osteoclastogenesis (Figure 3-10A). IgG, Oplg and SIC all significantly inhibited osteoclastogenesis, however, SIC was shown to be superior in this ability. This suggests that an IC is able to interact with FcγRs inhibiting osteoclastogenesis to a greater extent than IgG alone. Interestingly, investigation into whether Oplg and SIC could influence the bone erosion capacity of OCs proved insightful. Neither Oplg or SIC were able to prevent the differentiation of OCs when cultured on bone. However, importantly only SIC was able to reduce the OCs capacity to erode bone. SIC was able to overcome co-stimulatory signals that the OCs were receiving while differentiating on bone, which Oplg could not. In a similar experiment, Grevers *et al* (2012) differentiated OCs from murine BM on bone slices and was able to inhibit the erosive capacity of OCs using heat-aggregated rabbit IgG while monomeric IgG did not inhibit bone erosion³⁴⁰. Thus FcγR modulation is capable of inhibiting murine osteoclastogenesis in an FcγR dependent manner.

The method used to generate SIC resulted in an IgG complex of defined size and conformation in an excess of IgG. Dima *et al* (1983) demonstrated that SpA was able to continually bind and dissociate IgG to form SIC in a dynamic process both *in vitro* and *in vivo*²⁹⁹. Therefore, SpA requires excess IgG for the formation of SIC. This method of IC formation differs from the heat-aggregated rabbit IgG which Grevers *et al* (2012) demonstrated could inhibit osteoclastogenesis³⁴⁰. Heat-aggregated rabbit IgG is a large IC with an indefinable conformation³⁴⁰. Heat treatment of IgG is commonly used to denature the IgG and allow the individual molecules to interact and form an IC which remains able to engage FcγRs³⁶⁰. However, both SIC and heat-aggregated rabbit IgG inhibit osteoclastogenesis when BM cultures are treated from initiation of culture³⁴⁰. In contrast, Seeling *et al* (2013) used streptavidin linked biotinylated antibodies specific for FcγRI and FcγRIV to bind the FcγRs and induce cross-linking²⁶². This method of IC formation resulted in enhanced osteoclastogenesis in cells which had previously been stimulated with M-CSF and RANKL²⁶². Could, as Seeling demonstrated, the addition of SIC to cells that had previously received M-CSF and RANKL inhibit or enhance osteoclastogenesis? Likewise, could cross-linking of activatory FcγRI and FcγRIV from initiation of culture inhibit or enhance osteoclastogenesis? As interesting as these

differences are, the message from both these studies remains constant; activatory FcγRs can be used to modulate the differentiation of OCs^{262,316,340}.

Differences between IgG and SIC interactions with FcγRs exist between human and murine monocytes³¹⁶. Oplg was incapable of inhibiting human CD14⁺ monocytes from differentiating into OCs while SIC inhibits human osteoclastogenesis³¹⁶. In these human studies, SIC and Oplg were generated in the same manner as the murine studies except with use of species specific IgG. The reason for the difference observed when Oplg is used in human and murine OC studies is most likely due to IgG and FcγR biology differences in these species. Human monocytes express activatory FcγRI, FcγRIIA, FcγRIIC and FcγRIIIA with an inhibitory FcγRIIB receptor; murine monocytes express activatory FcγRI, FcγRIII and FcγRIV with an inhibitory FcγRIIB²⁶⁰. These receptors can be further classified by their ability to bind to IgG; in mice and humans FcγRI is the high affinity receptor capable of binding monomeric IgG²⁶⁰. The other FcγRs, in mice and humans, can only bind IC in conjunction with neighbouring FcγRs²⁶⁰. To further complicate this classification, murine and human IgG subclasses are also variable, in that murine IgG consists of IgG1, 2a, 2b and 3, while human IgG subclasses include IgG1, 2, 3 and 4²⁶⁰. In mice IgG2a binds with the highest affinity to FcγRI, while IgG1 fulfils this role in the humans²⁶⁰. SpA has been shown to bind to all subclasses of murine and human IgG with high affinity²⁹⁶. Thus, depending on the composition of IgG subclasses interacting with SpA, the addition of murine IgG to murine monocytes may well have a different effect than human IgG with human monocytes. The composition of IgG used is dependent on the batch which was purchased. As differences between preparations of IgG exist this too may be another reason for the differences observed in human and murine Oplg treated samples.

Another difference that has been observed is that in the absence of FcγRI, fluorescently labelled SpA in complex with murine IgG could not bind to monocytes/pre-OCs³¹⁶. Importantly, fluorescently labelled OVA in the presence of IgG could not bind to either WT or FcγRI^{-/-} monocytes/pre-OCs³¹⁶. This marries with the idea that the OVA present in the Oplg treatment had no effect on osteoclastogenesis because OVA could not interact with the cell surface and again suggests that it is IgG which is interacting with the cells. FcγRI is capable of binding monomeric IgG, as well as ICs in conjunction with other FcγRs, it can be assumed that the IgG present in Oplg and SIC is interacting with this receptor leading to an activatory signal skewing the cell from OC differentiation²⁵¹. Repeating a similar experiment to MacLellan *et al* (2011) and using fluorescently labelled IgG alone, or in the presence of OVA or SpA would allow the identification of the monomeric IgG or SIC ability to bind monocytes/pre-OCs³¹⁶.

Studies contained within this chapter also investigated the role of activatory FcγRIII in OCs differentiation in the presence of Oplg and SIC. SIC maintained the ability to inhibit osteoclastogenesis in FcγRIII^{-/-} cultures, while Oplg could not inhibit osteoclastogenesis, highlighting that FcγRIII is not required for SIC's mechanism of action. Thus suggesting that in WT cultures engagement of FcγRIII in conjunction with FcγRI may be sufficient for inhibition but is not necessary. This data also demonstrates that Oplg may require FcγRIII in order to inhibit OC differentiation. As mentioned, FcγRIII is a low affinity receptor for IgG and is only known to ligate ICs³³⁹. Therefore, the presence of small IgG aggregates could be acting via FcγRIII and thus inhibiting osteoclastogenesis which may account for the effects of Oplg.

In order to elucidate which FcγRs SIC and Oplg require for OC inhibition the use of genetic KO or siRNA could be utilised. SIC requires FcγRI to bind to the surface of MØ and pre-OCs³¹⁶, but the differentiation of FcγRI^{-/-} OCs in the presence of SIC is yet to be done and therefore it remains to be determined whether SIC requires FcγRI to inhibit osteoclastogenesis. Importantly, the use of FcγRI^{-/-} pre-OCs could determine further differences between SIC and Oplg's ability to inhibit osteoclastogenesis. Another receptor which is of interest is FcγRIIB, the inhibitory receptor, which negatively regulates effector functions, yet, ligation of FcγRIIB was shown to be insufficient for inhibiting murine osteoclastogenesis using heat-aggregated rabbit IgG^{340,361}. It would be interesting to differentiate FcγRIIB^{-/-} OCs in the presence of Oplg and SIC and determine whether murine IgG alone or in the form of SIC could still prevent osteoclastogenesis. However, it was not possible to obtain these transgenic animals. The use of FcγRs siRNA to elucidate the interactions which underpin SIC's mechanism of inhibition were the next experiments to be undertaken.

To evaluate the mechanisms of action associated with inhibition of osteoclastogenesis via SIC and Oplg we evaluated the effect of mRNA transcription essential for osteoclastogenesis. Treatment with IgG in the form of SIC or Oplg was able to down-regulate the transcription of DC-STAMP, Cathepsin K, OSCAR and TRAP, all of which are necessary for OC function^{7,154,242,336}. Animals which are deficient for TRAP and DC-STAMP develop osteopetrosis due to the differentiation of non-functioning OC^{242,362}. The down-regulation of mRNA transcripts for DC-STAMP could prevent OC fusion as DC-STAMP interacts with OC-STAMP allowing RANKL stimulated mononuclear cells to fuse and become multinucleated^{220,363}.

Recently, it was shown that the ligand for OSCAR is Collagen Type II, as SIC down-regulates OSCAR mRNA transcript it is also able to inhibit the erosive capacity of OCs on bone¹⁵⁴. The data would suggest that SIC is able to interfere with

OSCAR/Collagen Type II signalling which is known to aid OC differentiation¹⁵⁴. OSCAR signals through the FcγR or DAP12^{154,330}. FcγRI also signals through the FcγR and is required for SIC interaction on monocytes³¹⁶. This demonstrates that despite the similarities between OSCAR and FcγR signalling, SIC may co-opt this pathway and inhibit the differentiation of OCs. As the FcγR is required for the surface expression of activatory FcγRI and FcγRIII, an interesting experiment would have been to evaluate the effect of SIC on OCs in FcγR^{-/-} animals. FcγR^{-/-} animals have normal bone architecture and OC function, but would only express the FcγRIIB which would allow investigation into whether SIC could inhibit osteoclastogenesis in the absence of activatory FcγRs²⁶⁵.

The ability of FcγR modulation to inhibit osteoclastogenesis did not affect the transcription of CD115, RANK, NFATc1 or Bcl-3 mRNA after three days of culture. Previous work demonstrated that human monocytes stimulated with M-CSF and RANKL and treated with SIC for 24 hours, down-regulated RANK mRNA (unpublished data). This time point may have been too late to observe the effect SIC or Oplg treatment may exert on transcription of genes which induce osteoclastogenesis. Earlier time points may provide a better representation of how FcγR modulation changes mRNA transcription. As shown, SIC and Oplg were unable to influence the expression of CD115. It was not expected for SIC or Oplg to influence the expression of this factor greatly as M-CSF mediated signalling through CD115 is integral to cell survival¹²⁸. However, MacLellan *et al* (2011) observed that following 6 hours of treatment SIC the surface expression of CD115 was down-regulated in human monocytes stimulated with M-CSF and RANKL³¹⁶. Due to time constraints it was not possible to focus on the earlier time-points and surface expression of CD115 on murine cells in order to verify this effect in the mouse.

As has been previously stated, there are caveats regarding the comparison of human and murine cells which are most likely due to species differences FcγR biology. Despite the observations in human OCs of CD115 surface expression down-regulation, RANK mRNA transcript level down-regulation and inability of Oplg to inhibit osteoclastogenesis, a fresh insight has been gained regarding the interaction between FcγR modulation and murine OC differentiation.

A hypothesis which may explain the observations described in this chapter is that *in vivo* monomeric IgG is found in abundance at concentrations of 10mg/ml in the blood²⁹⁹ as well as in the extracellular space (Figure 3-16A). The constant interaction between IgG and FcγRs on monocytes as well as stimulation within the microenvironment may not stimulate monocyte's differentiation but could contribute to a 'threshold' level of activation by FcγRs³⁶⁴ (Figure 3-16B). However, removal of cells from this natural environment results in a homogeneous population of cells in culture media stimulated

only by M-CSF and RANKL (Figure 3-16C-D). In this culture system, the 'threshold' for FcγR activation may have been lowered. As a result stimulation by monomeric IgG, in the form of Oplg (Figure 3-16E) can activate an effector function which can skew the monocyte from differentiation into an OC, by preventing transcription of OC essential genes. In this system, addition of SIC results in enhanced FcγR activity and further inhibition of osteoclastogenesis (Figure 3-16F). Together, the data presented in this chapter demonstrates that the presence of IgG alone or in complex is able to inhibit the differentiation, activity and mRNA transcription of OCs in an optimised *in vitro* culture system.

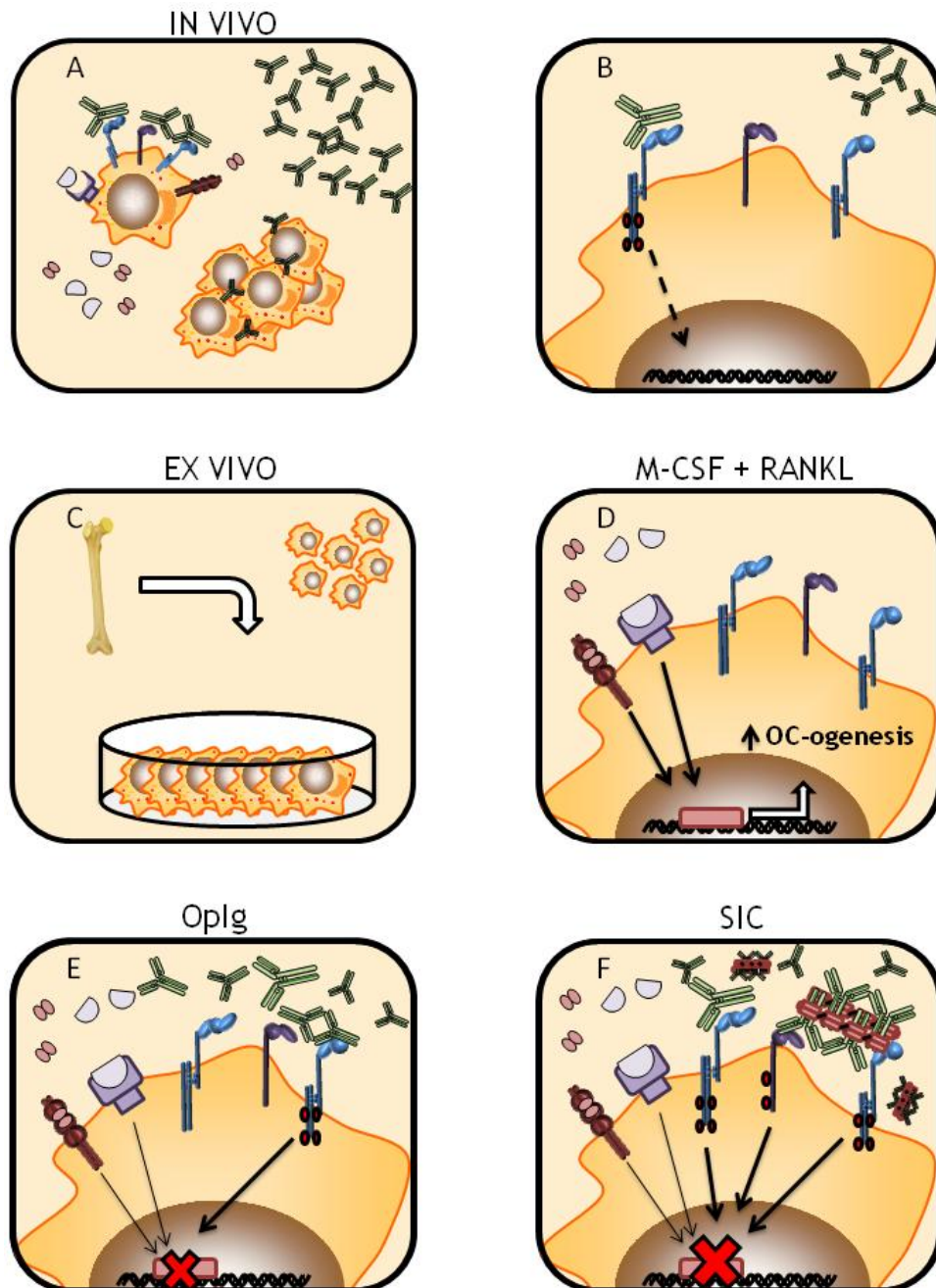


Figure 3-16: Diagrammatic representation of *in vitro* osteoclast inhibition.

A) *In vivo*, monocytes exist in a microenvironment containing, amongst other factors, IgG, which interacts with monocytes constantly. B) *In vivo*, monocytes are able to bind free IgG which creates a high threshold for cellular activation. C) Monocytes removed from animals are used to create a homogeneous population of cells in an artificial culture system, which does not generally have large amounts of IgG. D) *In vitro*, the monocytes only exogenous stimuli include M-CSF and RANKL in order to differentiate cells to OCs, thus creating a low threshold of activation. E) Addition of IgG in the form of Oplg, results in Fc γ R ligation and due to the low threshold of activation results in inhibition of osteoclastogenesis and decreased OC specific mRNA production. F) Addition of SIC, further enhances Fc γ R ligation and in the lower threshold of activation state further allows interactions between free and IgG complexes to alter the differentiation of monocytes, thus inhibiting osteoclastogenesis.

4 SpA treatment in a murine model of bone loss

4.1 Introduction

OCs differentiate from circulating monocytes in the blood and BM⁸⁹. As previously mentioned, *in vitro* stimulation of monocytes/MØ with pro-osteoclastogenic factors M-CSF and RANKL differentiates OCs^{113,324,365,366}. However, other factors can act in synergy with M-CSF and RANKL to enhance the differentiation of OCs. Cytokines like IL-6¹⁹³, TNF- α ^{187,367}, IL-1¹⁹¹, and TGF- β ³⁶⁸, produced by a variety of cells, including stromal cells found in the BM, can stimulate pre-OCs alongside M-CSF and RANKL to drive OC differentiation³⁶⁷. Upon stimulation pre-OCs commit to the OC lineage by expressing DC-STAMP and OC-STAMP allowing mononuclear precursor cells to fuse, forming large multinucleated bone eroding OCs^{7,10,220,362}.

Although, blood and BM derived monocytes have the ability to differentiate into OCs, they are a heterogeneous population⁹⁷. Subsets of monocytes have different phenotypes and functions depending on their anatomical position and immune status^{369,370}. The integrins Ly6C and CD11b can be used to identify Ly6C^{high} CD11b^{high} classical monocytes (hereafter known as Ly6C^{high} monocytes); circulating Ly6C^{high} monocytes migrate into inflamed tissue to resolve infection^{98,99}. However, in the absence of inflammation, circulating Ly6C^{high} monocytes down-regulate their surface expression of Ly6C³⁷¹. Ly6C^{high} monocytes differentiate into Ly6C^{low} CD11b^{high} non-classical monocytes (hereafter known as Ly6C^{low} monocytes) which 'patrol' the peripheral vasculature before exiting circulation and terminally differentiating into tissue MØs³⁷². These two subsets have definable *in vivo* phenotypes as Ly6C^{low} monocytes producing higher levels of TNF- α than Ly6C^{high} monocytes in response to TLR4 stimulation³⁷³. Ly6C^{high} monocytes have also been shown to express higher levels of CCR2 than Ly6C^{low} monocytes which is essential for migration to sites of inflammation⁹⁶. When Ly6C^{high} monocytes down-regulate expression of Ly6C to become Ly6C^{low} monocytes they up-regulate expression of CX3CR1¹⁰⁰. CX3CR1 is an essential adhesion molecule, not only promoting monocyte survival, but also adhesion and rolling on the vascular endothelium¹⁰¹.

Recently, a third population of monocyte, Ly6C^{high} CD11b^{low}, has been shown to be highly responsive to M-CSF and RANKL stimulation compared to both Ly6C^{high} and Ly6C^{low} BM monocytes⁴. Interest in identifying a specific monocyte subset as an *in vivo* OC progenitor (OCP) population arose from recent work undertaken by Jacquin *et al* (2006), Jacome-Galarza *et al* (2013) and Charles *et al* (2012) which demonstrated that the Ly6C^{high} CD11b^{low} monocytes present in BM were a definable OCP population capable of reconstituting *nfatc1* ^{Δ/Δ} animals with functional OCs^{4,103,116}. This population of OCPs in

the BM also express high levels of OC specific proteins like TREM-2, MDL-1 and PIR-A/B¹⁰³. Thus, in the murine system, the Ly6C^{high}, Ly6C^{low} and OCP populations represent three potential sources of pre-OC each with distinct properties and responsiveness to M-CSF and RANKL stimulation whose role in bone disorders has not been fully elucidated.

Oestrogen is an umbrella term for three related sex steroids which can regulate bone remodelling. Normally, oestrogen acts on OBs and OCs to regulate bone integrity; increasing OB activity³⁷⁴ and inducing OC apoptosis³⁷⁵. However, in post-menopausal women the ovarian production of oestrogen declines, causing a multitude of immune factors to become dysregulated leading to bone loss and the development of osteoporosis³⁷⁶. The murine model of ovariectomy-induced osteoporosis (OVX) is commonly used to interrogate the effect of oestrogen deficiency on bone remodelling³⁷⁷. In health, oestrogen enters cells and forms a complex with the oestrogen receptor (ER) which translocates to the nucleus allowing for activatory or inhibitory genomic effects. In the absence of oestrogen, many systems are perturbed. OBs increase production of TNF- α , IL-6, M-CSF, RANKL, and IL-7 while decreasing OPG and TGF- β secretion⁵⁵. T cells respond to IL-7 and produce IFN- γ which stimulates monocytes and M \emptyset to increase MHC II expression resulting in co-stimulation of T cells^{49,378}. Consequently, there is an increase in circulating TNF- α^+ /RANKL⁺ activated T cells and activated M \emptyset which produce IL-12, IL-6, IL-1, TNF- α ^{49,54,62,63,378,379}. Monocytes of the blood and BM become primed by the production of the numerous osteoclastogenic cytokines which leads to increase in OC differentiation, survival and bone resorption (Figure 4-1). Oestrogen deficiency observed in the OVX model rapidly increases OC activity resulting in loss of trabecular bone from the tibia similar to that seen in human osteoporosis³⁹. The increase in bone resorption results in decreased bone strength and trabecular bone which, in human osteoporosis, leads to an increased risk of fracture³⁸⁰.

ERs are expressed in myeloid cells of the blood and BM³⁸¹, yet the effect of oestrogen deficiency on monocyte populations has not been well characterised. Menopause has been associated with an increase in the number of circulating monocytes which express both ER α and ER β ⁷⁷. *In vitro* models of oestrogen withdrawal have shown that E/ER complex can negatively regulate Fc γ RIII expression on monocytes and in the absence of oestrogen expression of Fc γ RIII is heightened³⁸². This increase in Fc γ RIII may allow additional interaction with IC. However, as a heterogeneous population, monocyte expression of Fc γ Rs varies³⁸³. In mice Fc γ RI, RIIb, RIII and RIV are expressed at varying levels on circulating monocytes and OCs^{259,262}. However, expression of Fc γ Rs on the OCP population has not been investigated, nor has the effect of oestrogen on the monocyte populations.

Thus the effect of SpA derived IgG complexes in a model of oestrogen deficiency was examined. SpA forms ICs with IgG (SIC) upon injection and has been shown to reduce the number of OCs present in the inflamed joints of CIA animals^{299,316}. Previously, SIC was shown to inhibit the differentiation of murine BM cells to OC in an FcγRIII independent manner, however, SIC may work in concert with multiple FcγRs including FcγRIII. This inhibition also resulted in the down-regulation of OC essential genes such as DC-STAMP, OSCAR, Cathepsin K and TRAP. Research has also shown that SIC reduces MØ responsiveness to IFN-γ and down-regulated surface expression of MHC II, while increasing the production of IL-10 compared to IL-12 which is perturbed in the OVX model³¹⁶. SIC down-regulates the surface expression of CD115³¹⁶ and RANK on human pre-OCs and inhibits RANK mediated p38 signalling (unpublished observations) which are highly important in oestrogen deficient bone loss. These observations provide evidence for the potential of SpA to interfere with OC differentiation in this model. Models of inflammatory diseases have been associated with an increased presence of OCPs, yet the OCP population has not been studied in the oestrogen deficiency model^{103,183}. Likewise, the effect of SpA on pre-OCs has not been examined in a non-inflammatory disease, like the oestrogen deficiency model of osteoporosis.

With a diverse range of potential targets in the OVX induced oestrogen deficiency model, the use of SpA focuses on the pool of monocytes in the blood and BM. It is hypothesised that treatment with SpA will induce the formation of IC that will interact with monocytes in the blood and BM. This will ultimately prevent the differentiation of OCs in OVX animals and rescue the bone loss observed in this model (Figure 4-1). The research presented in this chapter examines the effect of SpA on murine monocytes and monocyte subsets during homeostasis and the OVX mouse model of oestrogen deficiency. The principal aims were to:

1. Determine which monocyte populations SpA interacts with in blood and BM.
2. Investigate whether SpA affects the phenotype of circulating monocytes and monocyte subsets in the blood and BM.
3. Investigate whether SpA can prevent the bone loss observed in the OVX mouse model of oestrogen deficiency.
4. Determine whether oestrogen deficiency and treatment with SpA has an effect on circulating populations of monocytes.

OVX INDUCED OESTROGEN DEFICIENCY

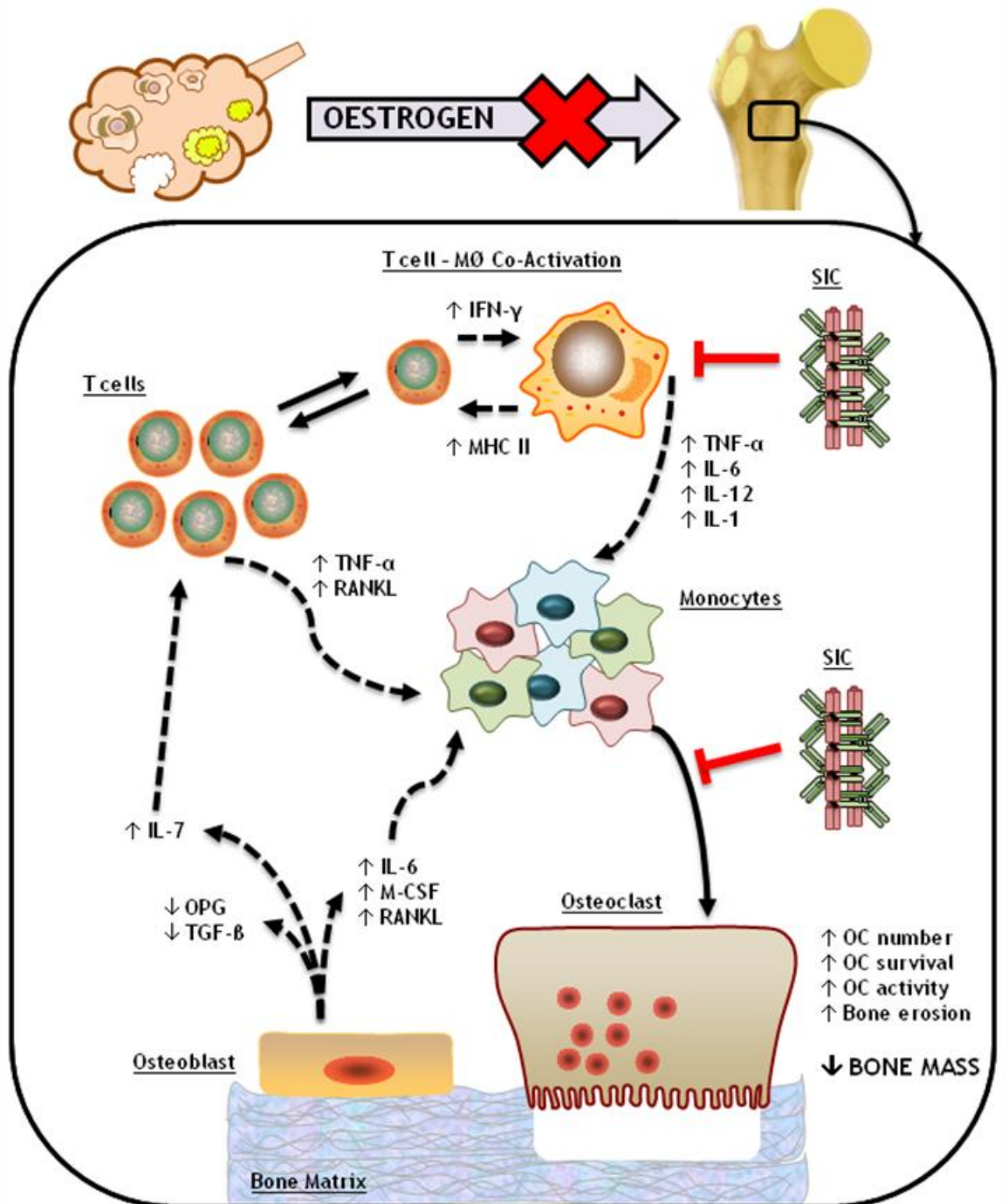


Figure 4-1: Diagram representing oestrogen deficiency induced bone loss and treatment with SpA IgG complexes.

Following OVX-induced oestrogen deficiency, IL-7 is produced by OBs and stromal cells. This induces T cell proliferation leading to Mφ activation. The overall effect is the production of IL-6, TNF-α, IL-1, M-CSF and RANKL which induce osteoclastogenesis from monocytes leading to increased OC activity and thus bone loss. In this microenvironment, it is hypothesised that SIC will prevent the differentiation of monocytes to OCs and reduce Mφ responsiveness to IFN-γ stimulation. Overall, SpA treated oestrogen deficient animals should not lose bone mass.

4.2 Results

4.2.1 SpA interacts with blood and bone marrow monocytes

In order to examine the ability of SpA to bind blood and BM monocyte subsets, a flow cytometry gating strategy, based on previous research, was developed. Due to accepted nomenclature, a naming system was used which reflected the definition of Ly6C^{high} and Ly6C^{low} monocytes, while both expressing high levels of CD11b⁹⁹. The gating strategy isolated monocyte subsets *ex vivo* which could also identify Ly6C^{high} monocytes expressing low levels of CD11b^{4,384}; this monocyte subset was termed the OCP after the observed functions of the BM population. In the blood, Jacquin *et al* (2006) demonstrated that Ly6C^{high} monocytes were more responsive to M-CSF and RANKL compared to Ly6C^{low} monocytes⁴. However, the osteoclastogenic potential of Ly6C^{high} CD11b^{low} monocytes found in the blood has not been determined. Despite this, these cells were referred to as OCP as demarked by their expression of Ly6C and CD11b, with note that in the blood Ly6C^{high} monocytes have been shown to differentiate into OCs. During the isolation of these monocyte subsets, a Ly6C^{negative} CD11b^{negative} population was present, however, Charles *et al* (2012) showed that this population has no osteogenic potential therefore this double negative population was not included in data analysis¹⁰³. This strategy of identification allowed analysis of monocytes free from contamination with neutrophils (Ly6G⁺), T cells (CD3⁺) or B cells (B220⁺) in the blood (Figure 4-2A) and BM (Figure 4-2B).

Using this flow cytometry panel, the ability of SpA to bind monocytes *in vivo* was investigated. SpA, or the control protein OVA, was conjugated to the fluorescent dye Alexa Fluor 488 (AF488). Fluorescently labelled OVA-488 or SpA-488 was then injected *i.p.* into C57Bl/6 mice, after 2 hours blood and BM was taken and prepared for FACS analysis (Figure 4-2A). Injection with SpA-488 resulted in a large percentage of AF488⁺ monocytes in the blood compared to OVA-488 (Figure 4-3A). The absolute number of AF488⁺ monocytes and monocyte subsets in the blood was calculated from the percentage of AF488⁺ monocytes. It was shown that in the blood Ly6C^{high} and Ly6C^{low} monocytes were interacting with SpA-488 (Figure 4-4A). However, the average intensity of SpA binding in the AF488⁺ cells remained equal with that of OVA-488 treated animals (Figure 4-4C). This suggests that even although there were a higher number of SpA-488⁺ cells, there was a low level of binding to these cells (Figure 4-3 and Figure 4-4). Importantly, SpA did not interact with OCP population (Figure 4-4A). However, due to a lack of biological replicates in the SpA-488 treatment group statistically analysis of the blood could not be done (Figure 4-4A).

Treatment with OVA-488 and SpA-488 did not affect percentage of AF488⁺ monocytes in the BM (Figure 4-3). This was reflected in the absolute cell numbers of AF488⁺ monocytes and monocyte subsets of OVA-488 and SpA-488 treated animals (Figure 4-4B). Yet, OVA-488 treated animals had significantly increased AF488 MFI on total monocytes compared to SpA-488 (Figure 4-4D). This revealed that Ly6C^{low} and OCP populations were responsible for the increased interactions of OVA-488 in the BM (Figure 4-4D). OVA protein is inert and thus should not bind to cells. However, resident MØ and phagocytic cells in the BM were not excluded from analysis due to exclusion of F4/80 from gating strategy. These phagocytic cells may have ingested OVA-488 in order to clear it from the system. While SpA-488 has already been co-opted by circulating monocytes and so will not be found at the same concentrations as OVA-488 in the BM. This demonstrates that within the total monocyte population, subsets are able to interact with SpA-488 IC and OVA-488 within their microenvironment to delineate these populations. Previous work done in the lab demonstrated that SpA-488 interacted highly with monocytes in the blood and BM 2 hours following i.p treatment³¹⁶. The present results show a limited level of interaction with Ly6C^{high} and Ly6C^{low} monocytes in the blood and BM. However, there appeared to be no interaction between OCPs and SpA-488 in this study in the blood and BM.

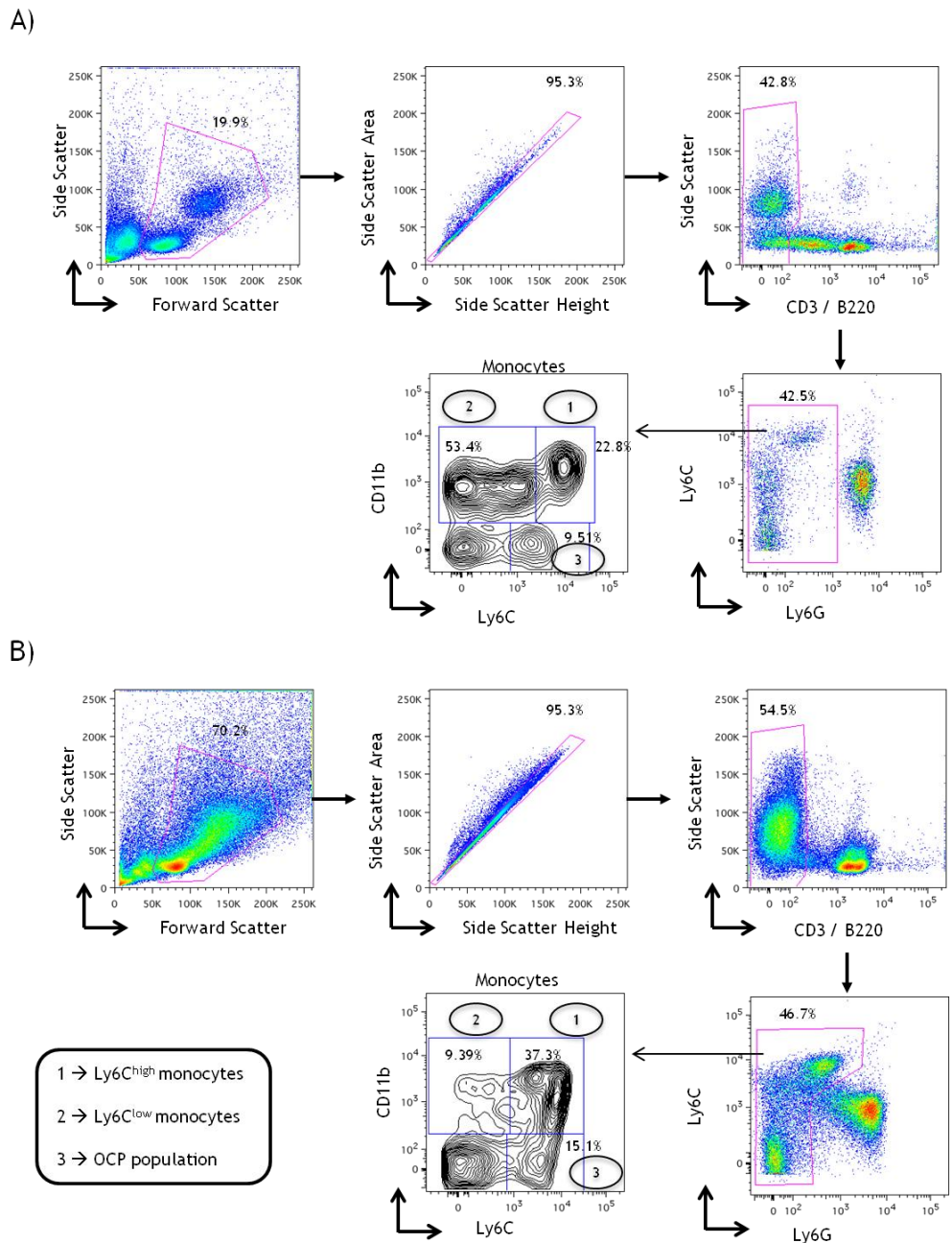


Figure 4-2: Gating strategies for the identification of monocytes and monocyte subsets. Representative FACS plots of gating strategies employed to distinguish monocytes. A) Blood and B) BM cells were isolated from C57Bl/6 mice and FACS stained for CD3, B220, Ly6G, Ly6C and CD11b. Doublets were isolated from single cells by exclusion of events which had a non-linear relationship with Side Scatter Area versus Side Scatter Height, T and B cells were excluded by their expression of CD3 and B220, and Neutrophils were excluded by their expression of Ly6G. Total Monocytes (CD3-B220-Ly6G-) and their subsets were analysed by their expression of CD11b and Ly6C; Ly6C^{high} CD11b^{high} (1 - Ly6C^{high} Monocytes), Ly6C^{low} CD11b^{high} (2 - Ly6C^{low} Monocytes) and Ly6C^{high} CD11b^{low} (3 - OCP population).

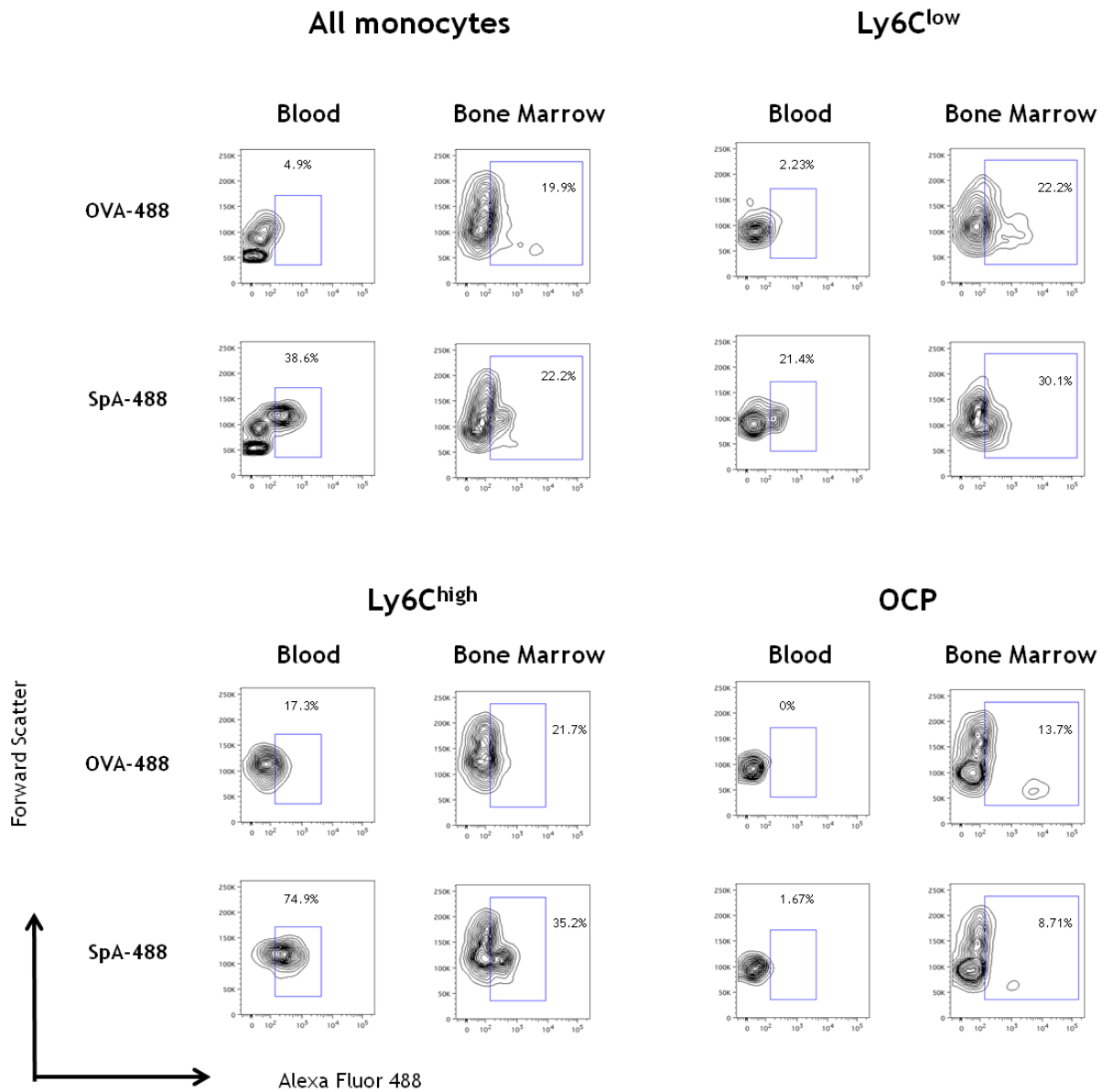


Figure 4-3: Representative FACS plots of AF488⁺ monocytes and monocyte subsets. SpA and OVA were conjugated to fluorescent dye AF488. 600µg of OVA-488 or SpA-488 in PBS was injected i.p. into C57Bl/6 mice. After 2 hours, blood and BM were isolated and prepared for flow cytometry. The gating strategy previously shown (Figure 4-2) was used to isolate total monocytes and their subsets for analysis of OVA-488 and SpA-488 binding. Representative FACS plots of OVA-488⁺ and SpA-488⁺ cells in blood and BM monocytes and monocytes subsets is shown from one individual experiment.

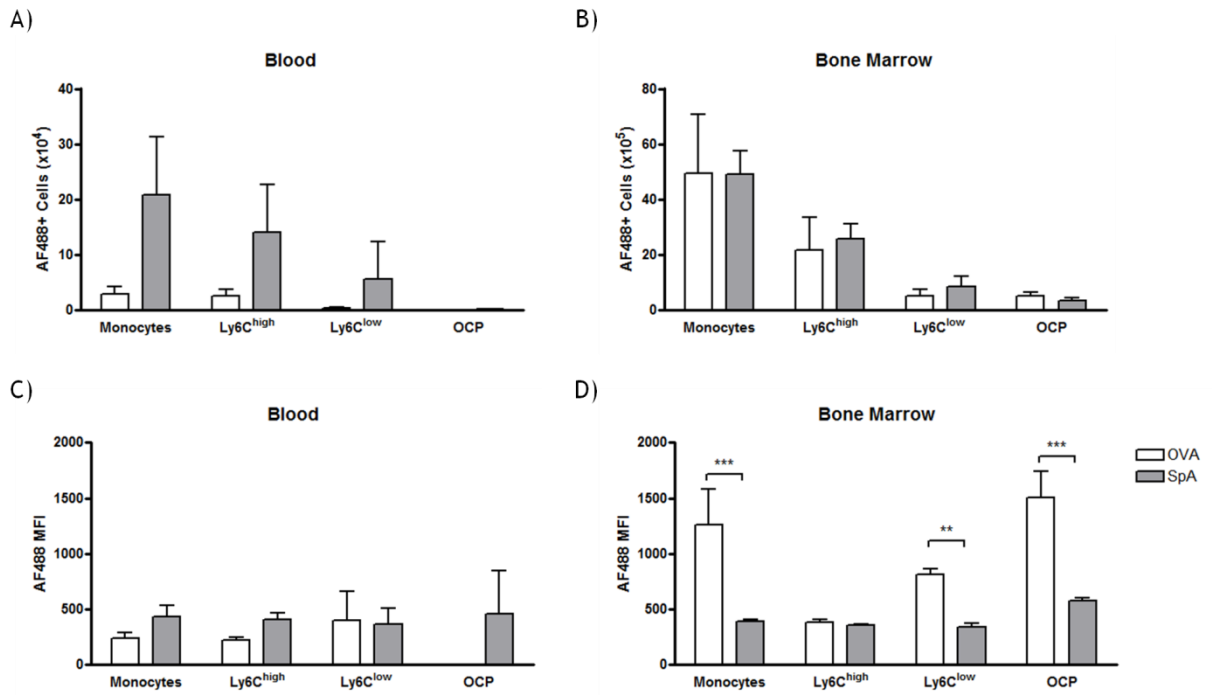


Figure 4-4: Fluorescent SpA binds to Ly6C^{high} monocytes in the blood.

C57Bl/6 mice were injected i.p. with 600 μ g of OVA-488 or SpA-488 in PBS. After 2 hours, blood and BM were isolated and prepared for flow cytometry. Gating strategy previously shown (Figure 4-2) was used to isolate total monocytes and their subsets for analysis of OVA-488 and SpA-488 interactions (Figure 4-3). The number of AF488⁺ cells in A) Blood and B) BM monocytes and monocyte subset populations was calculated from the % of AF488⁺ cells and the total number of cells isolated from each animal. C) Blood and D) BM MFI of AF488 in OVA-488 and SpA-488 on monocytes and monocytes subsets in treated animals. Two way ANOVA's with Bonferroni's post-hoc tests used to test BM OVA versus SpA monocyte subsets; $p < 0.01$ (**), $p < 0.001$ (***). Data represents mean \pm SD, blood OVA-488 (n=2) and SpA-488 (n=3) and BM OVA-488 (n=3) and SpA-488 (n=3). Data represents one individual experiment.

4.2.2 SpA and monocyte FcγRI

Due to the documented ability of SpA to interact with FcγRI³¹⁶, the expression of FcγRI was investigated. Following OVA-488 and SpA-488 treatment, the percentage of FcγRI⁺ monocytes and monocyte subsets in the blood and BM was evaluated (Figure 4-5). In the blood, SpA treatment had no effect on the number of FcγRI⁺ cells in total monocytes or subsets. Yet, the absolute number of FcγRI⁺ cells showed that Ly6C^{high} monocytes were the most abundant FcγRI⁺ monocyte subset (Figure 4-6A), and upon treatment with SpA-488, the expression of FcγRI was reduced (42%) (Figure 4-6C). The expression of FcγRI on the surface of Ly6C^{low} monocytes was also reduced (49%). Interestingly, OCPs do not appear to express FcγRI, this may account for the lack of interaction in SpA-488 binding (Figure 4-4C and Figure 4-6C).

A similar effect in FcγRI expression was observed in the BM with the number of FcγRI⁺ monocyte population significantly reduced following SpA-488 treatment (37.5%, $p < 0.01$) (Figure 4-6B). Upon further examination, Ly6C^{high}, Ly6C^{low} and OCP all had significantly reduced FcγRI expression following SpA-488 treatment (38%, $p < 0.001$, 34%, $p < 0.001$ and 25%, $p < 0.05$, respectively) (Figure 4-6D). The reduction in FcγRI expression on monocytes may be a by-product of SpA-488 IgG complexes co-opting FcγRI and thus masking the epitope for antibody binding. Therefore, after 2 hours of treatment, SpA was able to bind to monocytes in the blood and BM. Down-regulation of FcγRI on the surface of all monocyte subsets in the BM suggests that SpA is present in the BM and interacting with monocytes despite the obvious presence of SpA-488 binding to these cells (Figure 4-3 and Figure 4-4). BM OCPs express FcγRI, while in the blood OCPs don't express FcγRI, demonstrating that these cells are phenotypically different.

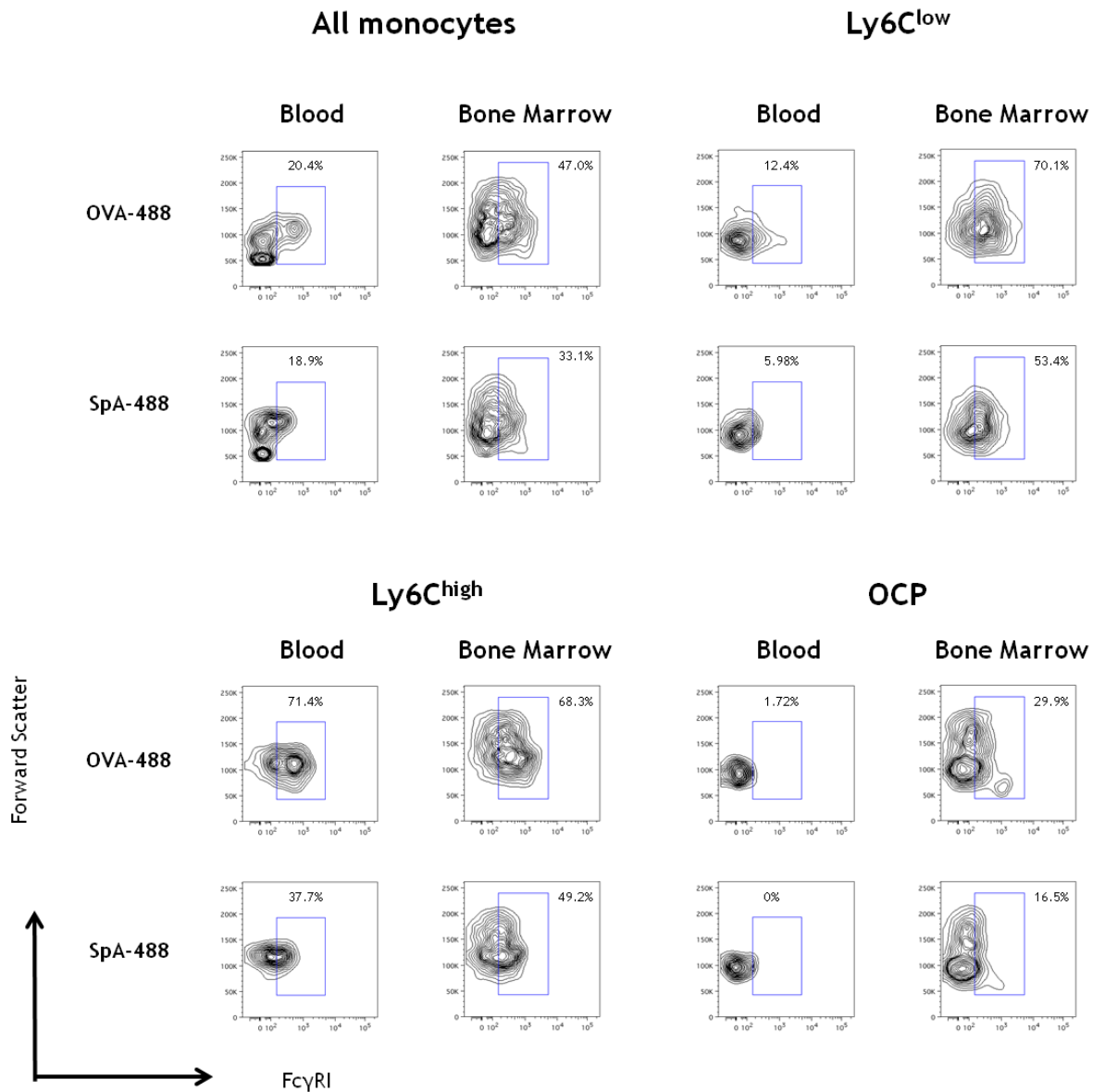


Figure 4-5: Representative FACS plots of Fc γ RI expression on monocytes and monocytes subsets.

600 μ g of OVA-488 or SpA-488 in PBS was injected i.p. into C57Bl/6 mice. After 2 hours, blood and BM was isolated and prepared for flow cytometry. Gating Strategy previously shown (Figure 4-2) was used to isolate total monocytes and their subsets for analysis of Fc γ RI expression. Representative FACS plots of Fc γ RI⁺ cells in blood and BM monocytes and monocytes subsets are shown from one individual experiment.

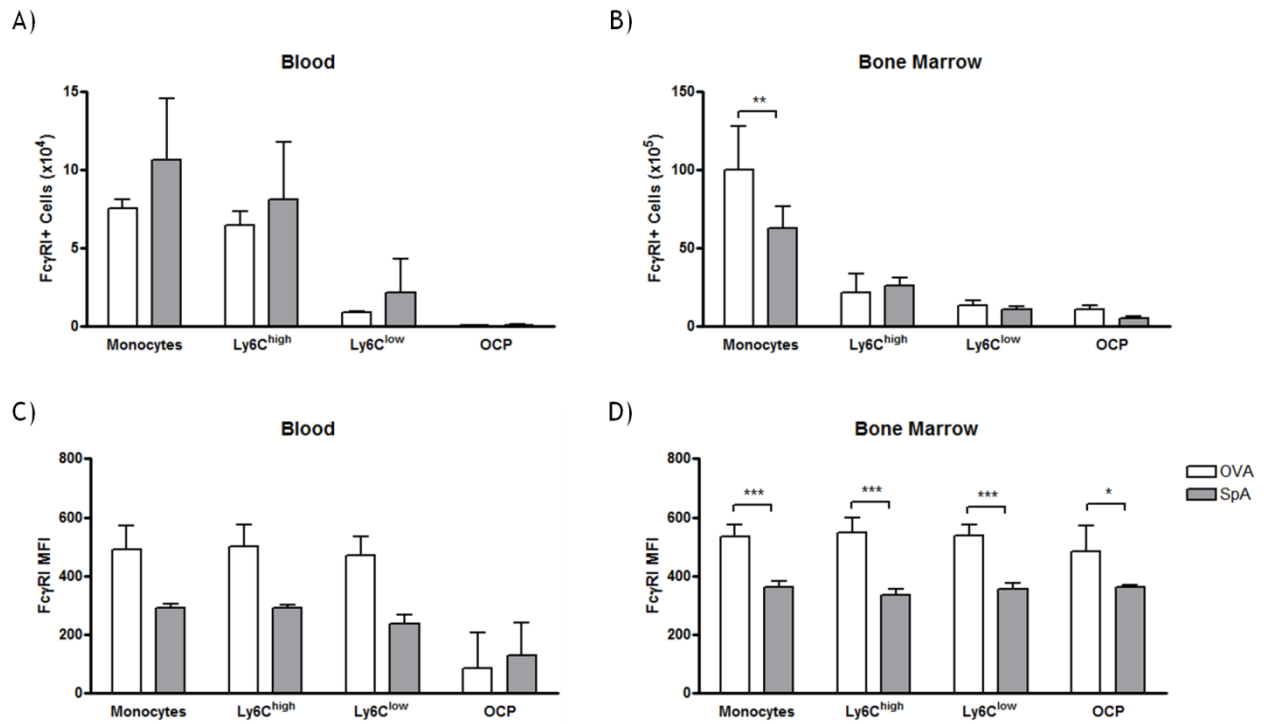


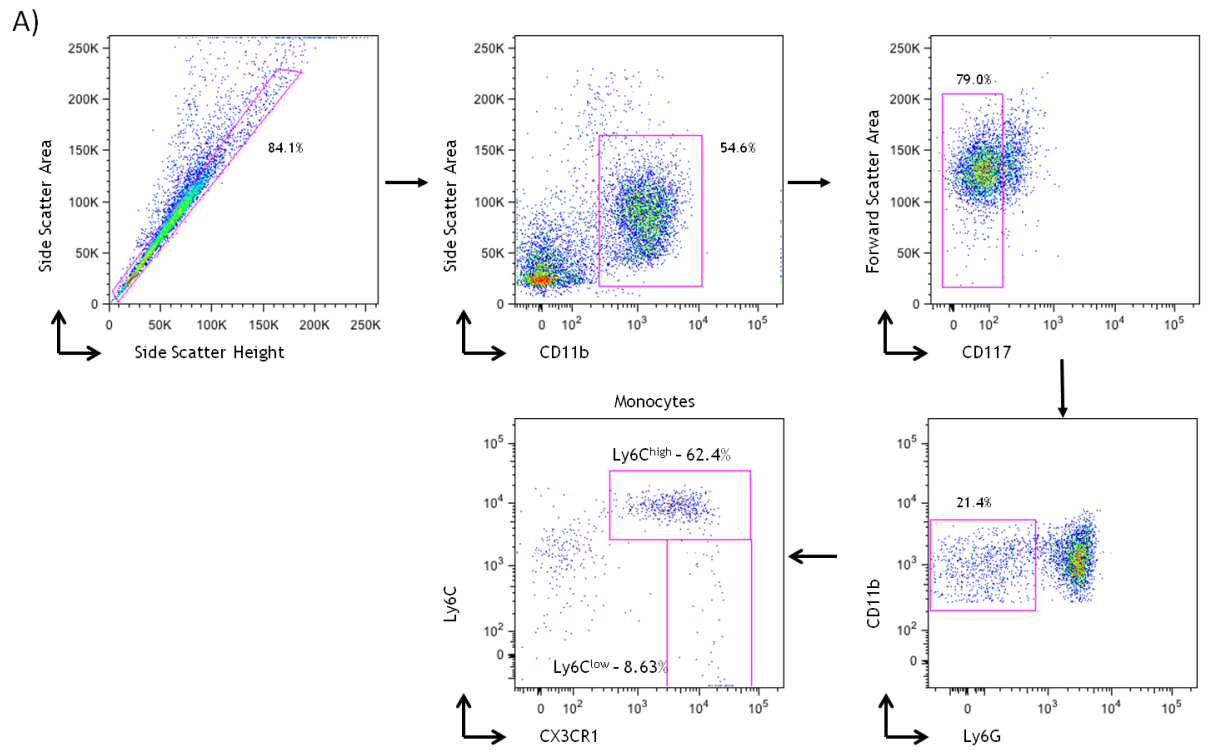
Figure 4-6: Fc γ RI expression is reduced on monocytes and monocyte subsets following SpA treatment.

600 μ g of OVA-488 or SpA-488 in PBS was injected i.p. into C57Bl/6 mice. After 2 hours, blood and BM was isolated and prepared for flow cytometry. Gating strategy shown (Figure 4-2) was used to isolate total monocytes and monocyte subsets for analysis of Fc γ RI (Figure 4-5). The number of Fc γ RI⁺ cells in A) Blood and B) BM monocytes and monocyte subset populations was calculated from the % of Fc γ RI⁺ cells and the total number of cells isolated from each animal. C) Blood and D) BM MFI of Fc γ RI in OVA-488 and SpA-488 on monocytes and monocytes subsets in treated animals. Two way ANOVA's with Bonferroni's post-hoc tests used on BM OVA versus SpA monocyte subsets; $p < 0.05$ (*), $p < 0.01$ (**), and $p < 0.001$ (***). Data represents mean \pm SD, blood OVA-488 (n=2) and SpA-488 (n=3) and BM OVA-488 (n=3) and SpA-488 (n=3). Data represents one individual experiment.

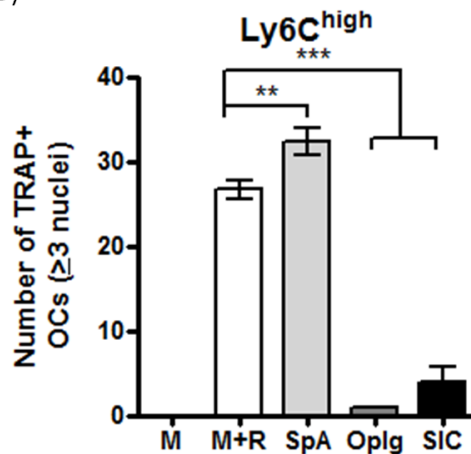
4.2.3 SIC inhibits Ly6C^{high} monocyte differentiation to osteoclasts

To investigate the effect of SpA on monocyte populations, Ly6C^{high} and Ly6C^{low} monocytes were isolated from blood and BM of CX3CR1-GFP C57Bl/6 animals. Using a FACS Aria, monocytes were isolated based on their expression of CX3CR1-GFP, Ly6C, Ly6G, CD11b and CD117 (Figure 4-7A). Monocyte sorting on a FACS Aria was performed by Dr. J. Montgomery. Single cells which were CD11b⁺ CD117⁻ Ly6G⁻ CX3CR1⁺ Ly6C^{high} or Ly6C^{low} were sorted. Ly6C^{high} and Ly6C^{low} monocytes were cultured using 75ng/ml M-CSF and 50ng/ml RANKL to differentiate cells to OCs. SpA, Oplg and SIC were added to Ly6C^{high} monocyte cultures in triplicate. Due to the low number of cells isolated, Ly6C^{low} monocytes could only be cultured in duplicate and only with or without SIC treatment. Following 5 days of culture, cells were stained for TRAP, revealing that Ly6C^{high} monocytes cultured in the presence of M-CSF and RANKL could differentiate into OCs (Figure 4-7B). Ly6C^{high} monocytes differentiation into OC was inhibited by treatment with Oplg (96% - $p < 0.001$) and SIC (85% - $p < 0.001$) (Figure 4-7B). Previously, it was shown that IgG alone present in the Oplg, as well as IgG complexes in SIC, could inhibit osteoclastogenesis. This demonstrates that these cell populations are prevented from differentiation to OCs in the presence of M-CSF and RANKL by addition of IgG alone or in complex. Treatment of Ly6C^{high} monocytes with SpA alone resulted in a slight but significant increase osteoclastogenesis ($p < 0.01$). Comparison between Ly6C^{high} and Ly6C^{low} monocytes differentiation wasn't analysed due to a lack of experimental replicates (Figure 4-7C). However, the data would suggest that Ly6C^{low} monocytes are far less osteoclastogenic than Ly6C^{high} monocytes as there were a third of cells produced when differentiated in the same conditions.

SIC has been used to inhibit the *in vitro* differentiation of OCs from pre-OCs by preventing the transcription of OC specific genes and now has been shown to directly prevent Ly6C^{high} monocytes from differentiating to OCs. SpA can bind to the surface of Ly6C^{high} and Ly6C^{low} monocytes in the blood and reducing the expression of FcγRI in the BM. As monocytes are important pre-OCs, the ability of SpA to interact with these cells and prevent the *in vivo* differentiation and function of OCs was examined using a murine model of disease.



B)



C)

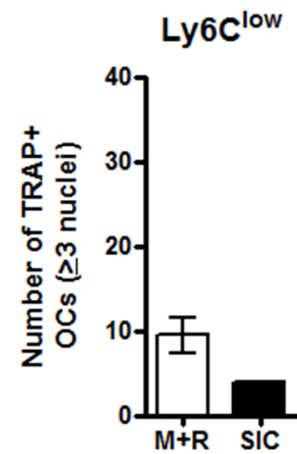


Figure 4-7: Ly6C^{high} monocytes are inhibited from differentiating to osteoclasts following Fc γ receptor modulation.

Blood and BM was isolated from CX3CR1 GFP C57Bl/6 mice and prepared for flow cytometry. Ly6C^{high} and Ly6C^{low} monocyte subsets were sorted based on their expression of CD11b⁺ CD117⁻ Ly6G⁻, CX3CR1 GFP. Monocyte cells were isolated by Dr. J. Montgomery. A) Representative FACS plots of the monocyte sort on the FACS Aria. B) and C) Isolated Ly6C^{high} and Ly6C^{low} monocytes were cultured at 1×10^5 cells in 200 μ l of complete α -MEM with 75ng/ml M-CSF and 50ng/ml RANKL for 5 days at 37°C with media refreshed on day 4. SIC (and controls) were added on day 1 and 4. Cultures were stained for TRAP and TRAP⁺ cells with ≥ 3 nuclei were counted. The sum total of 4 fields of view per culture well were recorded. Ly6C^{high} monocytes were cultured in triplicate and Ly6C^{low} monocytes were cultured in duplicate. One Way ANOVA with Bonferroni's post-hoc test were used on Ly6C^{high} monocytes only; $p < 0.01$ (**) and $p < 0.001$ (***). Data represents mean \pm SD from one experiment. Scale bar; 200 μ m.

4.2.4 Murine model of ovariectomy induced bone loss

The effect of SpA was examined in a non-inflammatory model of bone loss. The OVX model of oestrogen deficiency results in an increase in pro-osteoclastogenic factors enhancing the differentiation of OCs thus promoting bone loss⁶⁹. SpA's ability to alter the disease severity in the OVX model was examined.

Three separate methods of SpA administration were investigated (Figure 4-8). These regimes were designed to test the potential of SpA to influence disease progression. The Therapeutic Treatment Regime was designed to test the ability of SpA to recover the initial bone loss incurred 2 weeks following surgery (Figure 4-8A). The Continuous Treatment Regime was considered to be a 'prophylactic' regime to test whether SpA treatment from initiation of disease could overcome OVX induced bone loss (Figure 4-8B). The third treatment regime was designed to test the method of administration; Alzet PumpsTM (model 2004) with SpA or control protein OVA were inserted i.p at the time of surgery thus allowing the secretion of SpA/OVA at a constant rate of 0.25µl/hour over a 4 week period (Figure 4-8C). All treatment regimes lasted 6 weeks following surgery at which time the experiments were terminated.

Following surgery, animal's weights were monitored weekly ensuring that no treatment caused detrimental effects beyond those observable in the model (Figure 4-9). The weights of all animals steadily increased over the 6 week period. The difference in weight (Δ weight change) from the initiation to termination was calculated to evaluate weight gain over the treatment course. This revealed that oestrogen deficient animals in the Therapeutic and Continuous Treatment Regimes significantly increased weight compared to their sham operated counterparts (Figure 4-9C, F). Treatment with SpA had no additional effect on the weights observed in these treatment regimes (Figure 4-9). No difference in weight was observed in animals in the Alzet PumpTM Treatment Regime (Figure 4-9I). Following termination of the treatment regimes each animal had their uterus removed and weighed. In the event of a successful ovariectomy, oestrogen deficiency will cause the uterus to atrophy, as shown in the representative image (Figure 4-10A). Uterine weights revealed that the OVX groups had significantly lighter uteri when compared to sham operated animals regardless of treatment regime (Figure 4-10B-D). Treatment with SpA had no additional effect on the weight of the uteri.

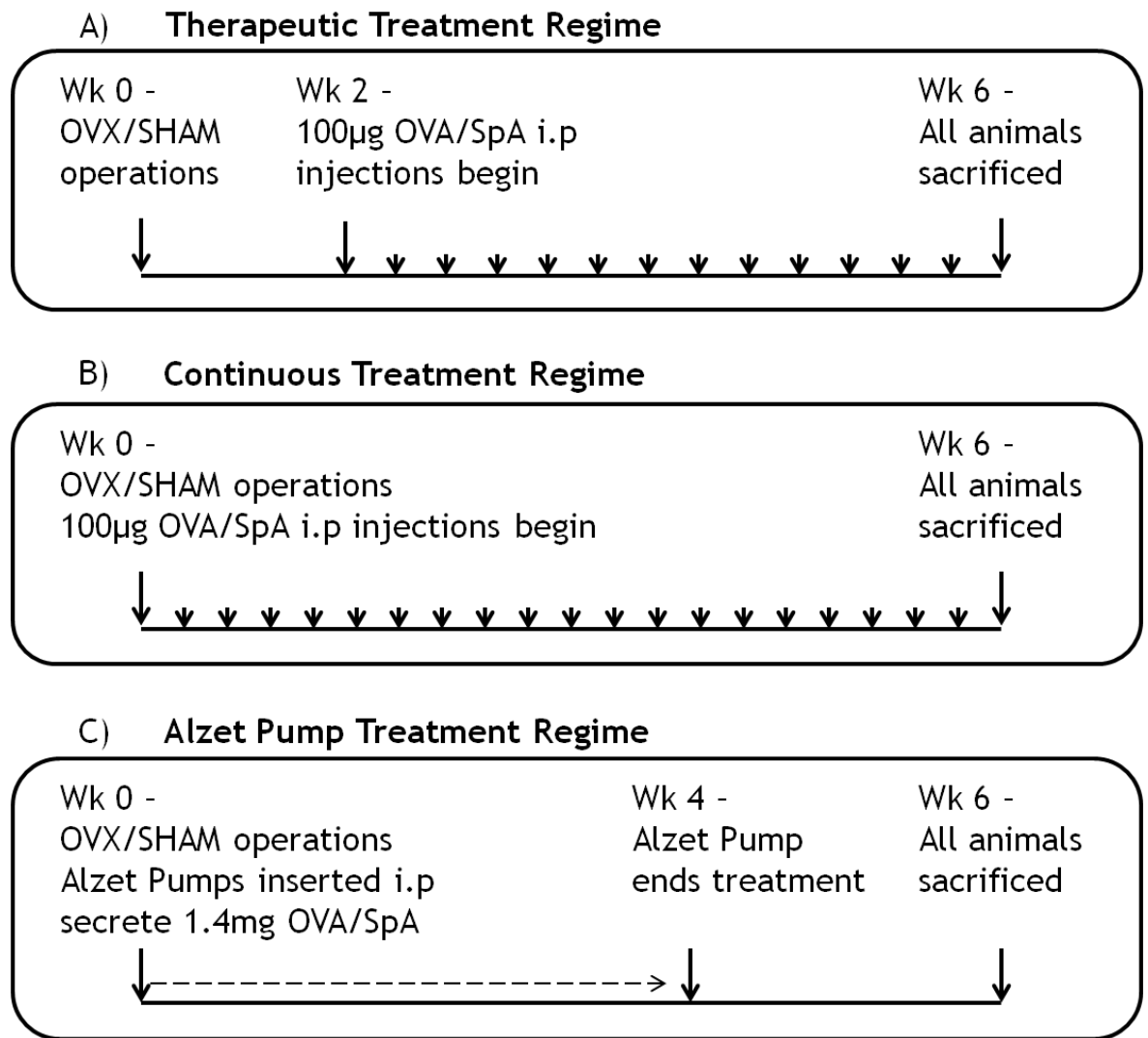


Figure 4-8: Diagrammatic representation of the OVX treatment regimes.

All animals were OVX or sham operated at week 0. Disease onset began from point of surgery and all animals were sacrificed at week 6. Three treatment regimes were utilised to test the effect of SpA on this model. A) Therapeutic Treatment Regime; 100µg of SpA or OVA in 100µl of PBS was injected i.p. every 2nd day two weeks after surgery - and the onset of disease - until the end of the experiment. B) Continuous Treatment Regime; 100µg of SpA or OVA in 100µl of PBS was injected i.p. every 2nd day from the point of surgery until the end of the experiment. C) Alzet PumpTM Treatment Regime; Alzet PumpsTM (model 2004) containing 1.4mg of SpA or OVA was inserted into the peritoneal cavity at the point of surgery. The Alzet PumpTM secretes at a rate of 50µg over the course of a day (100µg every 2nd day) for 4 weeks after which point animals were allowed to recover prior to the end of the experiment.

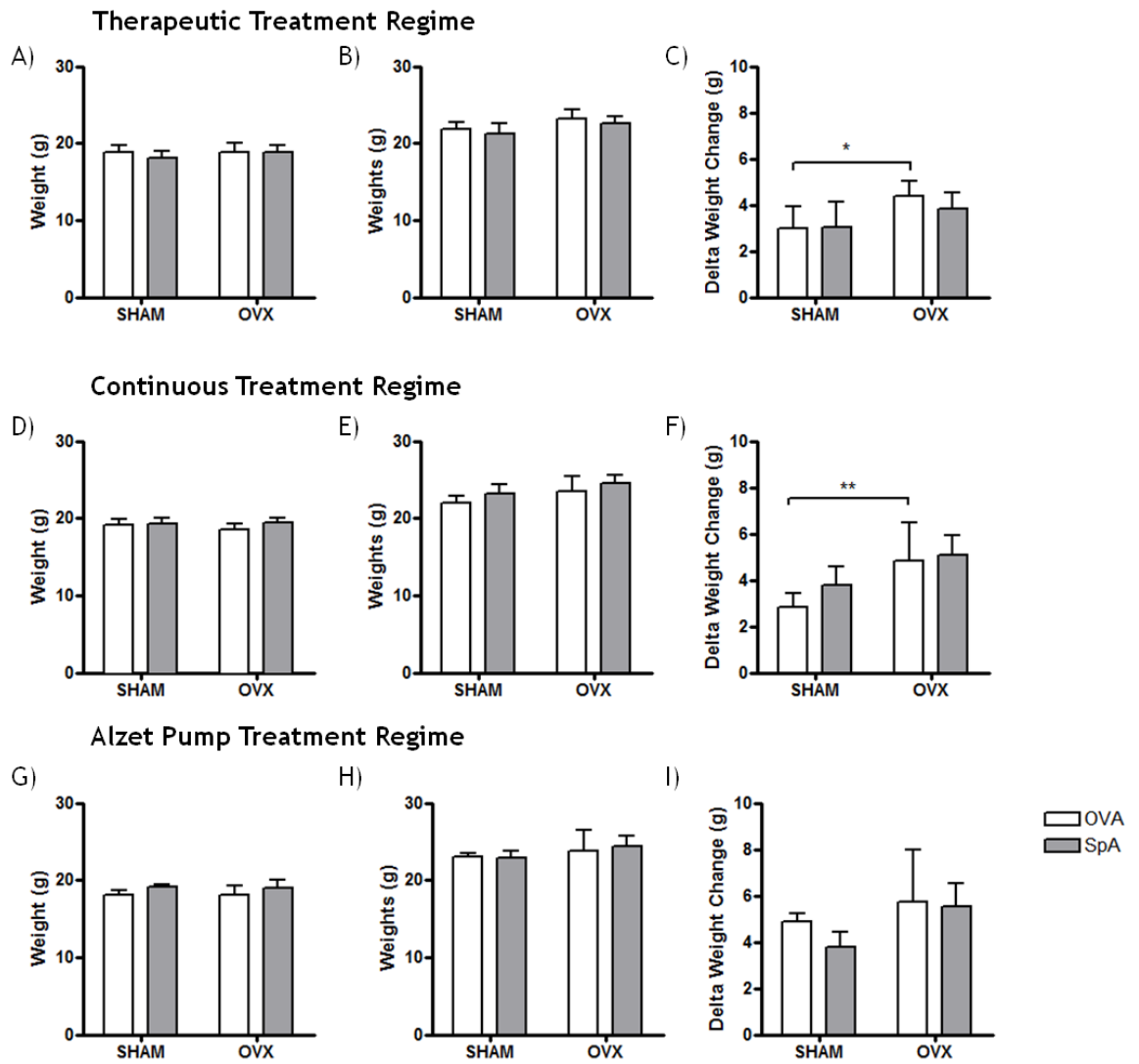


Figure 4-9: OVX surgery increased animal's weight.

Therapeutic Treatment Regime. A) Start weights (g) recorded at the time of surgery. B) Final weights of animals recorded 6 weeks after surgery. C) The change in weight (g) from start to the end was calculated (Final weight - Start weight = Delta Weight Change). Continuous Treatment Regime. D) Start weights (g) recorded at the time of surgery. E) Final weights of animals recorded 6 weeks after surgery. F) The change in weight (g) from start to the end was calculated (Final weight - Start weight = Delta Weight Change). Alzet Pump™ Treatment Regime. G) Start weights (g) recorded at the time of surgery. H) Final weights of animals recorded 6 weeks after surgery. I) The change in weight (g) from start to the end was calculated (Final weight - Start weight = Delta Weight Change). Two Way ANOVAs with Bonferroni's post-hoc tests used to compare treatment groups; $p < 0.05$ (*) and $p < 0.01$ (**). Data represents means \pm SD, $n = 7-8$.

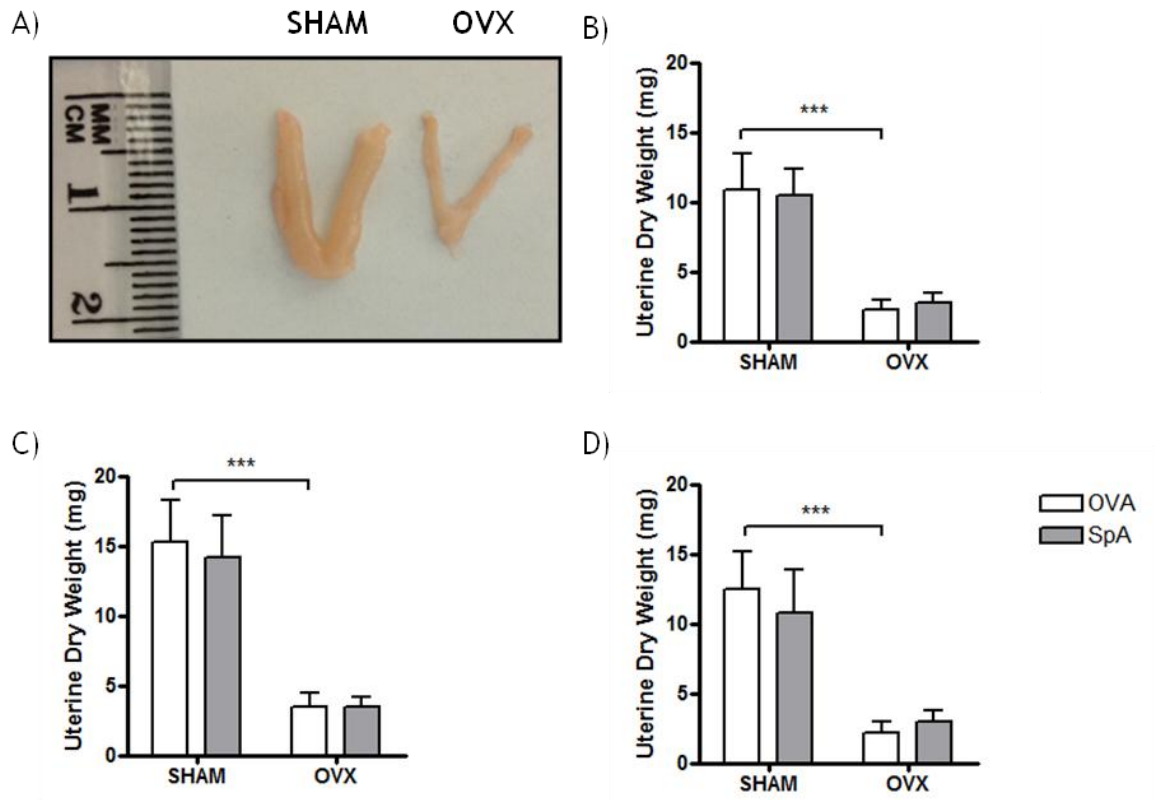


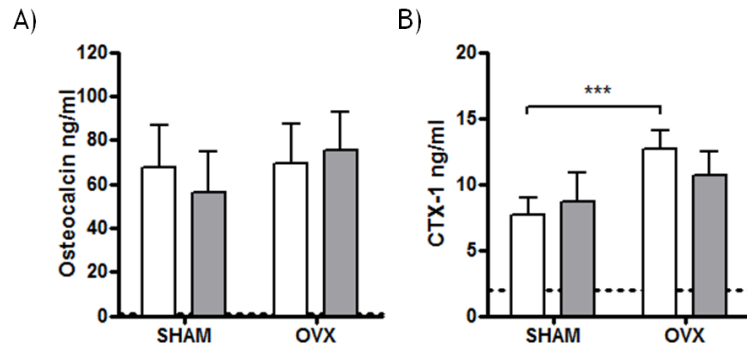
Figure 4-10: Oestrogen deficiency decreases uterine weight.

Six weeks after OVX/sham surgery, uteri were removed from animals. Excess fat and tissue was removed from each uterus prior to desiccation overnight. A) Representative image of uterus removed from sham and OVX operated animal prior to desiccation. B) Dry weights (mg) of uteri from animals in the Therapeutic Treatment Regime. C) Dry weights (mg) of uteri from animals in the Continuous Treatment Regime. D) Dry weights (mg) of uteri from animals in the Alzet Pump™ Treatment Regime. Two Way ANOVA with Bonferroni's post-hoc tests used to compare treatment groups; $p < 0.001$ (***). Data represents mean \pm SD, $n = 7-8$.

4.2.5 CTX-1 is a marker of bone resorption

The effect of SpA treatment on OVX induced bone remodelling was evaluated by examining two proteins; Osteocalcin and C-telopeptide fragment of Collagen Type 1 (CTX-1). Plasma from sham and OVX animals was taken at the termination of treatment regimes. OBs secrete Osteocalcin as part of the bone formation process, however, a small quantity is leached into circulation as a by-product³⁸⁵. Measurements of Osteocalcin concentration by ELISA showed that OVX and treatment with SpA had no effect on the rate of bone formation in either the Therapeutic or Alzet PumpTM Treatment Regimes (Figure 4-11A, C). Bone resorption was measured by the plasma concentration of CTX-1 which is released into circulation as a by-product of bone erosion³⁸⁶. The concentration of CTX-1 was measured by ELISA and in the Therapeutic and Alzet PumpTM Treatment regimes, oestrogen deficiency increased CTX-1 in plasma compared to sham operated animals (Figure 4-11B, D). SpA treatment in both sham and OVX animals had no effect on the level of CTX-1 in circulation (Figure 4-11B, D). Due to availability of these ELISA reagents, it was not possible to use plasma samples from the Continuous Treatment Regime. The detection for pro-OC cytokines TNF- α , IL-6, IL-1 β and IFN- γ was performed in all treatment regime samples. However, the concentration of these cytokines in all samples remained below the limit of detection and thus no conclusions could be drawn from these experiments (data not shown). Overall results show that in the context of the whole animal bone resorption is increased while the bone formation rate remains stable.

Therapeutic Treatment Regime



Alzet Pump Treatment Regime

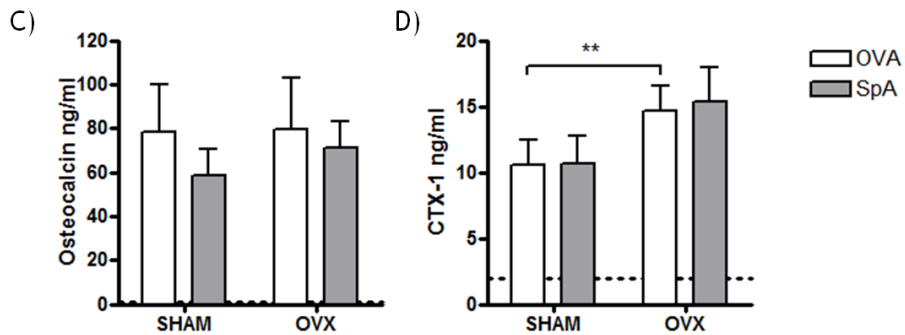


Figure 4-11: OVX increases the plasma concentration of CTX-1.

Plasma was collected from animals six weeks after OVX/sham surgery by draining blood from the vena cava with a needle and 20 μ l of 0.5M EDTA. Blood was centrifuged at 4,000rpm for 10 minutes and the clear plasma layer removed. Plasma concentration of Osteocalcin and CTX-1 were measured by ELISA. A) Osteocalcin and B) CTX-1 were measured from plasma collected from the Therapeutic Treatment Regime and measured by ELISA. C) Osteocalcin and D) CTX-1 were measured from plasma collected from the Alzet Pump™ Treatment Regime by ELISA. Two way ANOVA with Bonferroni's post-hoc tests were used to compare all treatment groups; $p < 0.01$ (**) and $p < 0.001$ (***). Data represents mean \pm SD, $n = 5-8$.

4.2.6 Biomechanical testing of OVX femurs

Oestrogen deficiency is known to induce bone loss which can result in a decrease in bone strength³⁸⁷ and as such the biomechanical properties of OVX animal's femurs were tested. Femurs from the Therapeutic Treatment Regime were taken at termination and exposed to three point bend testing. Three point bend testing is used to determine the integrity and overall strength of bone as measured by the Maximum Load - the peak Newtons of force (N) exerted on the bone before it breaks³⁸⁷⁻³⁸⁹. This process also records the Modulus (MPa - MegaPascals) - a measure of intrinsic stiffness in the bone regardless of size; Extension at Max Load (mm - millimetre) - the displacement required to reach the peak force necessary to break; Load at Break (N) - this is the force exerted when the bone fractures; Extension at Break (mm) - The displacement required to reach the Load to Break; Energy at break (J - Joules) - the energy the bone can absorb prior to fracture and is an indication of toughness. These parameters were shown to be unchanged following OVX or treatment with SpA (Figure 4-12). Three point bend testing is a destructive method to measure bone strength and can only provide limited data regarding cortical bone strength. Therefore, another more accurate method of measuring the effect of oestrogen deficiency on bone loss was required.

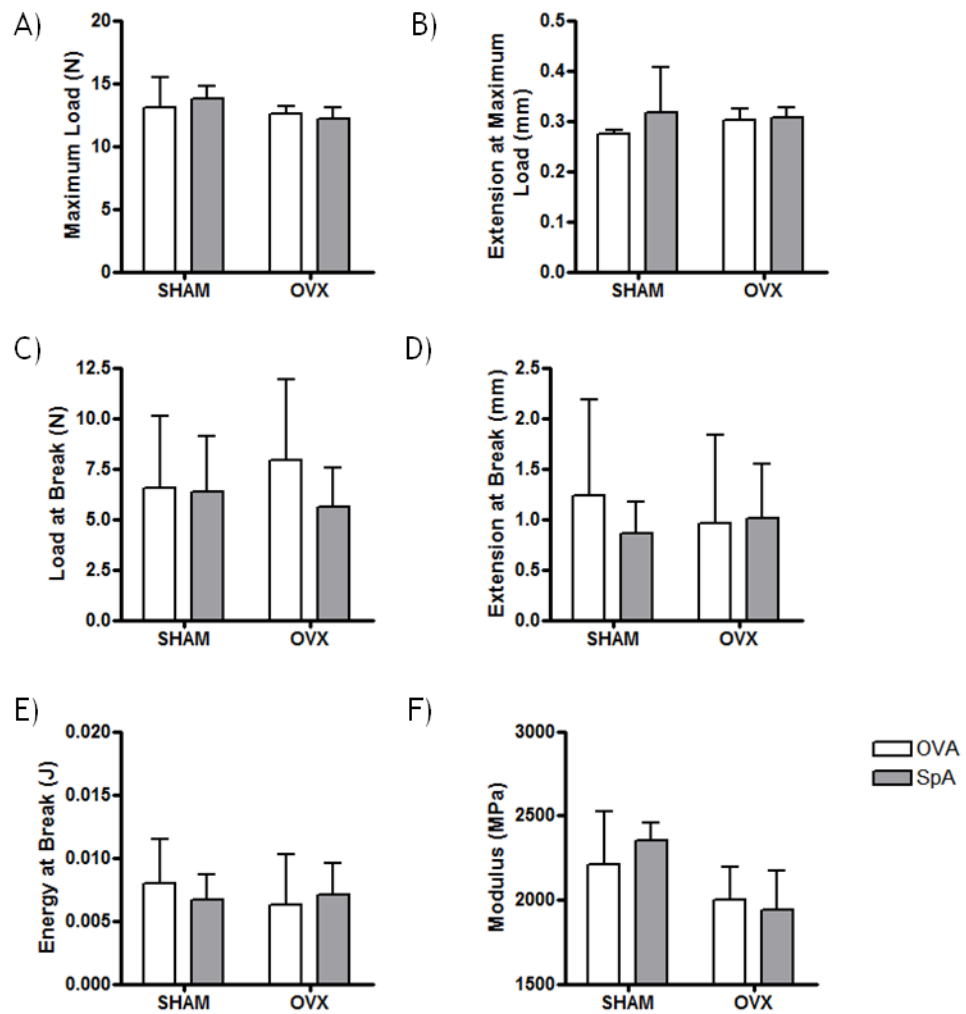


Figure 4-12: The effect of OVX and treatment with SpA on bone integrity measured by three-point bend testing.

Femurs were taken from Therapeutic Treatment Regime animals six weeks after OVX/sham surgery. Femurs were stripped of flesh and were stored in 70% ethanol at 4°C. The bones then underwent three-point bend testing by carefully mounting femurs on an Instron Mechanical Testing Stage using a third pressure point lowered slowly to the top of the femur. The force exerted on the bone and resistance of the bone were measured and the following parameters were calculated by Bluehill software. A) Maximum load (N), B) Extension at Maximum Break (mm), C) Load at Break (N), D) Extension at Break (mm), E) Energy at Break (J) and F) Modulus (MPa). Two Way ANOVAs with Bonferroni's post-hoc tests were used to compare all treatment groups. Data represents mean \pm SD, n=4-6 from one experiment.

4.2.7 OVX bone loss measured by micro computer tomography

The most sensitive method for examining bone micro-architecture is micro computer tomography (μ CT) which uses a series of X-ray images of a rotated structure to create a 3 dimensional image that can be manipulated and examined. Using this technology, tibias from sham and OVX animals were analysed (Figure 4-13). The trabecular sections of the proximal tibias (shown in coronal cross-section) were isolated and analysis was focused on a standardised region of interest of trabecular bone shown in the black box (Figure 4-13). μ CT allows for the analysis of a number of parameters including; percentage of trabecular bone, a commonly used parameter to measure the degree of osteoporotic disease in this model³⁹⁰. The percentage of trabecular bone examines the bone tissue volume (BV) in the trabecular section and normalises it for the overall tissue volume (TV) in the section (also known as BV/TV). OVX animals were shown to have approximately 30% less trabecular bone present when compared with sham operated animals ($p < 0.001$), which treatment with SpA was unable to alter. This was seen in all three treatment regimes (Figure 4-14A, E, I). Oestrogen deficiency also induced a decrease in bone volume in OVX groups compared to sham operated animals in all treatment regimes (Figure 4-14B, F, J).

Another measure of bone disease in the OVX model is trabecular number, the average number of trabeculae present in the trabecular bone section. Increased OC activity erodes trabeculae and thus decreases the number of trabeculae. In all treatment regimes, the number of trabeculae was significantly decreased in OVX compared to sham operated animals and treatment with SpA was unable to rescue this decrease (Figure 4-14C, G, K). As trabecular number decreases with OVX disease, the separation between each trabeculum increases and this parameter was shown to significantly increase by approximately 20% in OVX animals in the three treatment regimes (Figure 4-14D, H, L). The observed decrease in trabecular bone volume, trabecular number and increase in separation between trabeculae all demonstrate that each of the OVX surgeries successfully induced bone loss (Figure 4-14). A number of other parameters were also measured which all verify that OVX reduced the animals tibial bone volume (data not shown). OVX induced oestrogen deficiency resulted in bone loss in the proximal tibia that SpA treatment was unable to prevent.

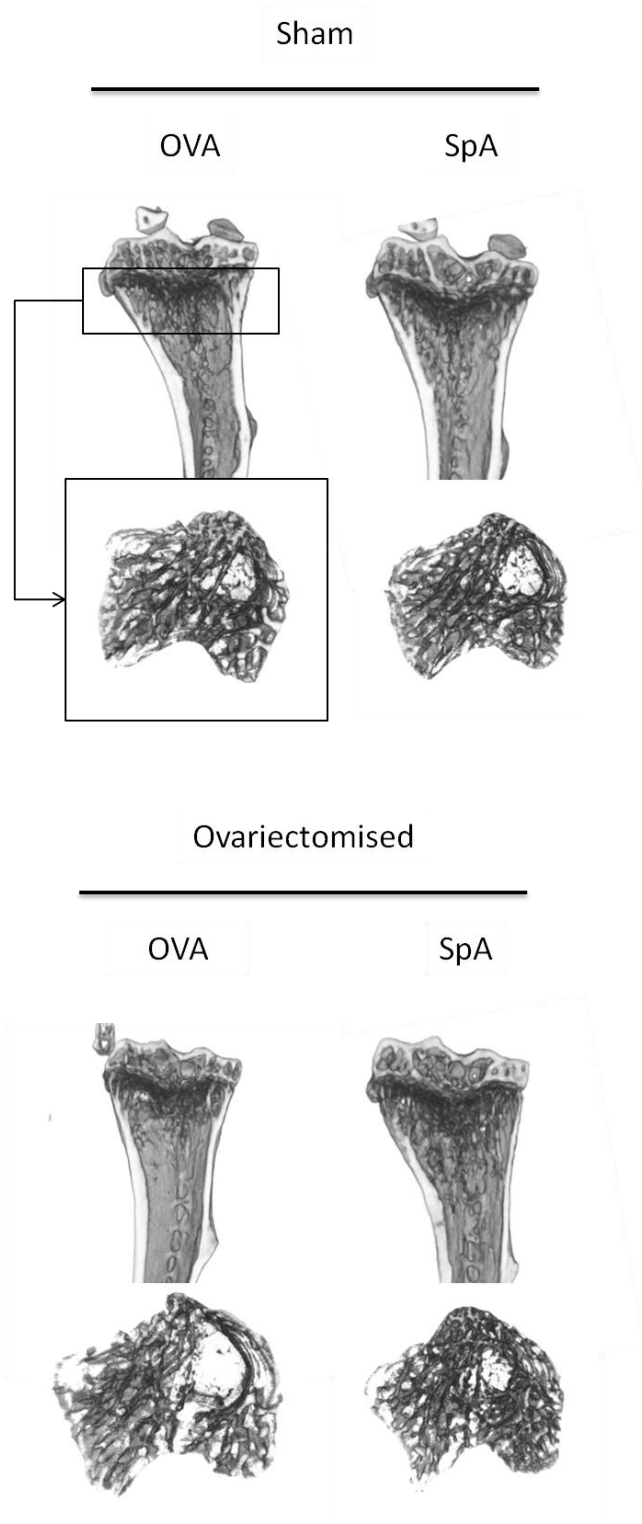
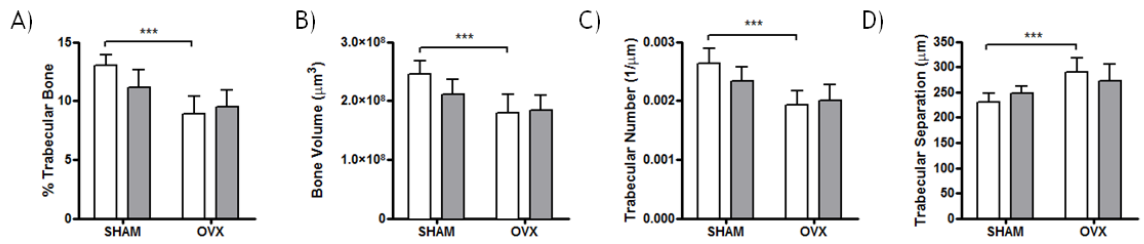


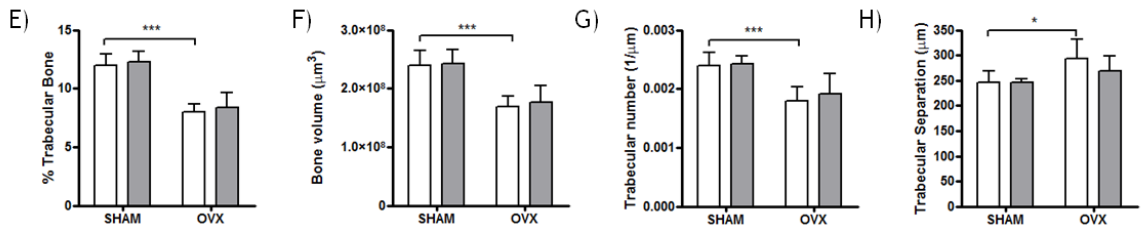
Figure 4-13: Representative images of μ CT trabecular bone reconstructions from proximal tibia of sham and OVX animals.

The left tibia of each animal was taken six weeks after OVX/sham surgery. Tibias were fixed overnight in 4% para-formaldehyde before being stored in 70% ethanol. Bones were scanned using a SkyScan 1172 μ CT scanner. This generated a series of X-ray images which could be manipulated using NReconn software to create a 3D structure of the tibia (shown in the coronal cross-section of the proximal tibia). The trabecular bone present in this tibia could be further examined by isolating the specific region of interest using CTAn software to create a 3D model of the trabecular bone (shown in the dorsal transverse section - black box) which can be processed to give a number of measurable parameters.

Therapeutic Treatment Regime



Continuous Treatment Regime



Alzet Pump Treatment Regime

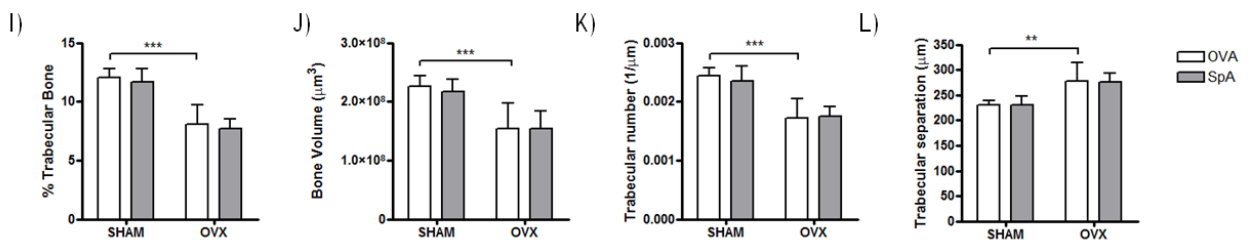


Figure 4-14: μ CT analysis of trabecular bone of proximal tibia of sham and OVX animals.

As described in Figure 4-13, trabecular bone was identified and the properties of which quantified by SkyScan CTAn software. The three treatment regimes are shown above. A), E) and I) Bone volume / tissue volume (BV/TV); the percentage of trabecular bone present. B), F) and J) Bone Volume (μm^3) present in the trabecular region. C), G) and K) The number of trabeculae present in the trabecular region, normalised to the trabecular volume. D), H) and L) The trabecular separation represents the average distance between each trabeculae in the trabecular region. Two Way ANOVA with Bonferroni's post-hoc tests were used to compare all treatment groups; $p < 0.05$ (*), $p < 0.01$ (**), $p < 0.001$ (***) Data shown represents mean \pm SD, $n = 7-8$.

4.2.8 Oestrogen, SpA and monocyte composition

SpA was unable to prevent OVX induced bone loss, however the effect of oestrogen deficiency on monocytes was evaluated. FACS analysis was done to analyse the effect that oestrogen deficiency exerts on monocytes and their subsets in blood and BM. Blood and BM was taken from animals and the total number monocytes was determined by flow cytometry (Figure 4-15). Each treatment regime required a slightly altered method of gating to isolate monocytes, but, this did not impact on the ability to isolate monocytes and their respective subsets within each sample.

Analysis revealed that the BM monocyte compartment was unaffected by oestrogen deficiency in all of the treatment regimes (Figure 4-16B, D, F). Interestingly, circulating monocytes from animals in each treatment regime vary. In the Therapeutic Treatment Regime, oestrogen deficiency had no effect on the number of total monocytes (Figure 4-16A). In the Continuous Treatment Regime oestrogen deficiency doubled the number of monocytes ($p < 0.05$) (Figure 4-16C), while the Alzet Pump™ Treatment Regime OVX groups had a decreased percentage of blood monocytes compared to sham controls (Figure 4-16E). In the Alzet Pump™ model, cell counts were not performed on the blood, so the total number of monocytes could not be quantified. Beyond the effects oestrogen exerts on monocytes, treatment with SpA in all treatment regimes had no impact on the number of monocytes in the blood or BM (Figure 4-16).

To further investigate the effect that oestrogen deficiency has on monocytes the composition of subsets was evaluated. Using the gating strategy previously outlined (Figure 4-15), monocyte subsets were isolated and the number of cells present within each group was quantified. In the Therapeutic Treatment Regime, SpA increased the number of Ly6C^{low} monocytes present in the blood of sham and OVX animals ($p < 0.05$ and $p < 0.001$, respectively) and BM of sham operated animals ($p < 0.001$) (Figure 4-17A-B). Analysis of the Continuous Treatment Regime demonstrated that oestrogen deficiency and treatment with SpA had no effect on blood monocytes, however, both oestrogen deficiency and treatment with SpA could increase the number of Ly6C^{high} monocytes in the BM compared to sham operated animals ($p < 0.01$) (Figure 4-17C-D). The BM of the Alzet Pump™ Treatment Regime showed no change on monocyte subset numbers, while oestrogen deficiency decreased the percentage of monocytes in the blood ($p < 0.05$) (Figure 4-17E). Overall, oestrogen deficiency did not exert any consistent effect on monocyte composition from one predominant cell type to another in any treatment regime (Figure 4-17).

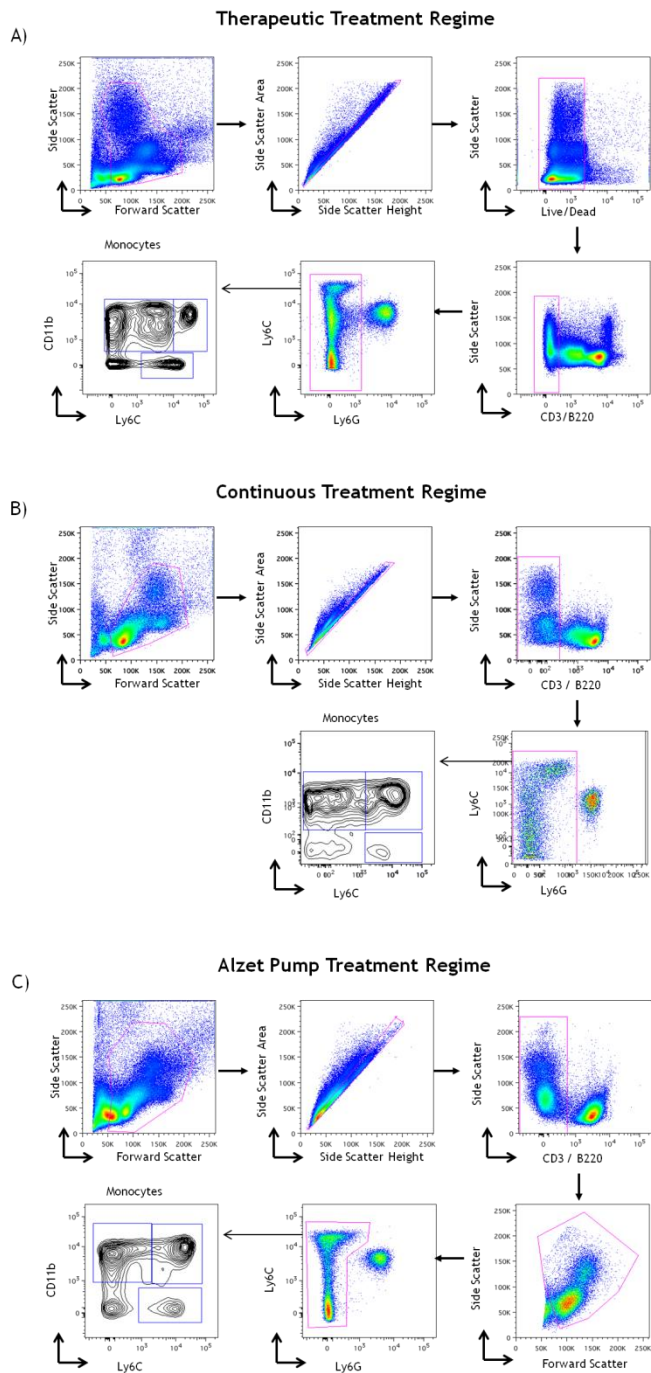
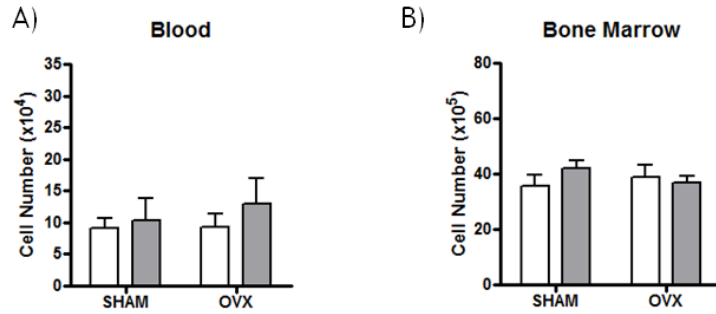


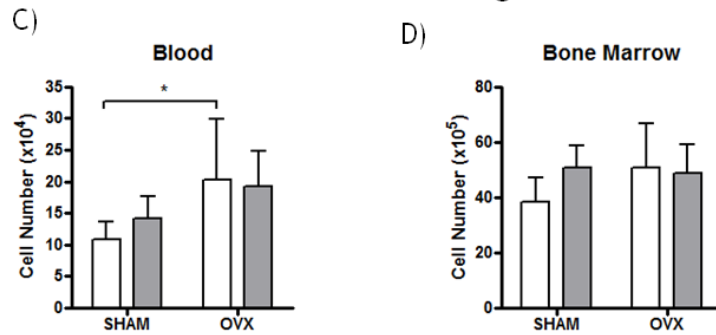
Figure 4-15: Representative FACS plots of three OVX treatment regimes.

A) Blood from Therapeutic Treatment Regimes were isolated from C57Bl/6 mice and FACS stained for Live/Dead, CD3, B220, Ly6G, Ly6C and CD11b. Representative FACS plots of gating strategies employed to distinguish monocytes. Doublets were isolated from single cells, Live Cells were selected on low expression of Live/Dead exclusion marker, T and B cells were excluded by their expression of CD3⁺ and B220⁺, and Neutrophils were excluded by their expression of CD3-B220-Ly6G⁺. Total Monocytes (CD3-B220-Ly6G⁻) and their subsets were analysed by their expression of CD11b and Ly6C. B) Blood from Continuous Treatment Regimes were isolated from C57Bl/6 mice and FACS stained for CD3, B220, Ly6G, Ly6C and CD11b. Representative FACS plots of gating strategies employed to distinguish monocytes and their subsets. C) Blood from Alzet Pump™ Treatment Regimes were isolated from C57Bl/6 mice and FACS stained for CD3, B220, Ly6G, Ly6C and CD11b. Representative FACS plots of gating strategies employed to distinguish monocytes. Monocyte subset populations were identified as described in Figure 4-2.

Therapeutic Treatment Regime



Continuous Treatment Regime



Alzet Pump Treatment Regime

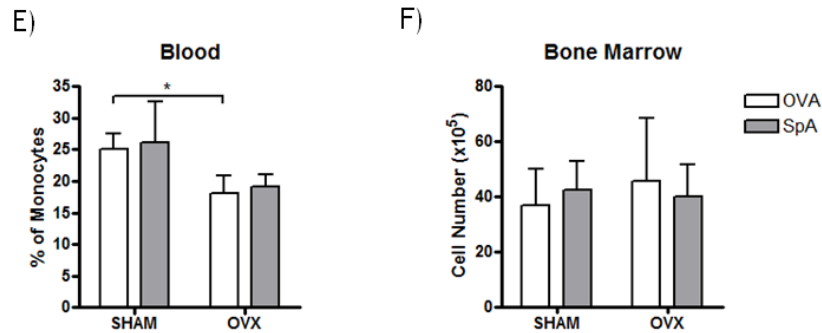


Figure 4-16: Number of total monocytes following OVX and treatment with SpA.

Blood and BM was isolated from animals six weeks after surgery and prepared for analysis by flow cytometry. Red blood cells were lysed using ammonium chloride or Akt Buffer. Cells were counted then stained for FACS and a gating strategy previously shown (Figure 4-15) was used to isolate the number of total monocytes. The % of monocytes defined by FACS analysis was used to calculate the absolute number of monocytes present in both the blood and BM. The number of total monocytes from the Therapeutic Treatment Regime in A) Blood and B) BM are shown. The number of total monocytes from the Continuous Treatment Regime in C) Blood and D) BM are shown. The percentage of and number of total monocytes from the Alzet Pump™ Treatment Regime in E) Blood and F) BM are shown. Two Way ANOVAs with Bonferroni's post-hoc tests were used to compare treatment groups; $p < 0.05$ (*). Data represents mean \pm SD, $n = 7-8$.

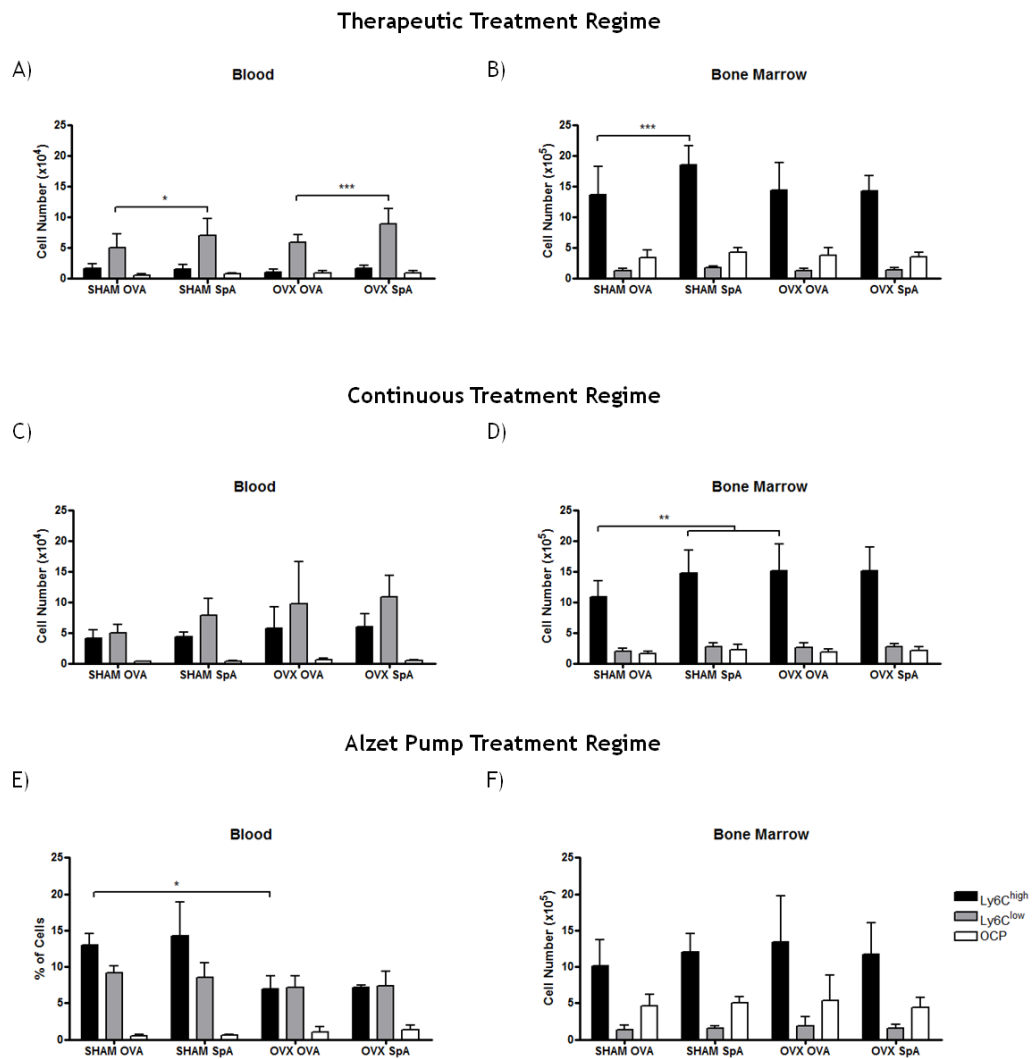


Figure 4-17: Monocyte subset cell numbers following OVX and treatment with SpA.

Continuing on from the data shown in Figure 4-16, the expression profiles of Ly6C and CD11b were used to identify monocyte subsets as described in Figure 4-15. The % of cells in each monocyte subset was used to calculate the absolute number of monocytes present in both the blood and BM. The subsets of interest were Ly6C^{high}, Ly6C^{low} and OCP. The absolute numbers of cells constituting these subsets in A) Blood and B) BM for the Therapeutic Treatment Regime is shown. The absolute numbers of cells constituting these subsets in C) Blood and D) BM for the Continuous Treatment Regime is shown. The percentage of, and absolute number of cells constituting these subsets in E) Blood and F) BM for the Alzet Pump™ Treatment Regime is shown. Two Way ANOVAs with Bonferroni's post-hoc test were used to compare individual monocyte subsets across treatment groups; p<0.05 (*), p<0.01 (**) and p<0.001 (***). Data represents mean ± SD, n=7-8.

4.2.9 Fcγ receptor profiles and oestrogen deficiency

Previously SpA has been shown to bind the monocytes *in vivo* (Figure 4-3) mediated by FcγRs³¹⁶. The effect of long term treatment with SpA and the absence of oestrogen could impact on the expression of FcγRI or II/III on the surface of monocyte subsets and this was examined.

First, expression of FcγRI on monocytes following OVX was examined. The Therapeutic Treatment Regime showed that OVX significantly decreased the expression of FcγRI on the surface of total monocytes in the blood ($p < 0.05$), but not on individual subsets (Figure 4-18A). In BM, OCP FcγRI expression was decreased following OVX (Figure 4-18B). Oestrogen deficiency was shown to have no effect on the expression of FcγRI on the surface of monocyte subsets in the blood and BM of Continuous or Alzet PumpTM Treatment Regimes (Figure 4-18C-F). This suggests that oestrogen deficiency had no overall effect on the expression of FcγRI as there was no consistent result.

Upon examining the expression pattern of FcγRII/III, OVX was shown to have no effect on the expression of FcγRII/III on monocytes in the Therapeutic Treatment Regime (Figure 4-19A-B). The Continuous Treatment Regime showed that Ly6C^{low} blood monocytes significantly decreased expression of FcγRII/III ($p < 0.05$) (Figure 4-19C). While in the Alzet PumpTM Treatment Regime, Ly6C^{low} BM monocytes had an increased expression of FcγRII/III following OVX (Figure 4-19F). These results show that oestrogen deficiency does not have a distinct effect on the expression of FcγRI or FcγRII/III on monocyte subsets. The control groups of each treatment regime are similar and comparison between OVA treated sham and OVX animals should be identical. Therefore, no conclusive effects have been shown.

Evaluation of SpA treatment showed that it had minimal effects on the expression of FcγRs. In particular, the expression of FcγRI and FcγRII/III on monocytes in Alzet PumpTM Treatment Regime was unaffected. A minor increase in FcγRII/III expression was observed in the Therapeutic Treatment Regime on Ly6C^{low} blood monocytes following treatment with SpA in OVX animals ($p < 0.05$) (Figure 4-20A). In the same treatment regime, SpA was able to decrease the surface expression of FcγRI on blood Ly6C^{low} monocytes and both BM Ly6C^{high} and Ly6C^{low} monocytes (Figure 4-20B-C). In the Continuous Treatment regime, SpA significantly increased the expression of FcγRII/III on BM Ly6C^{high} monocytes and OCP (Figure 4-20D). Examination of the expression patterns of FcγRI and II/III have shown that oestrogen deficiency does not conclusively alter the expression of these receptors on the surface of monocyte subsets and no reproducible effect was observed following SpA administration.

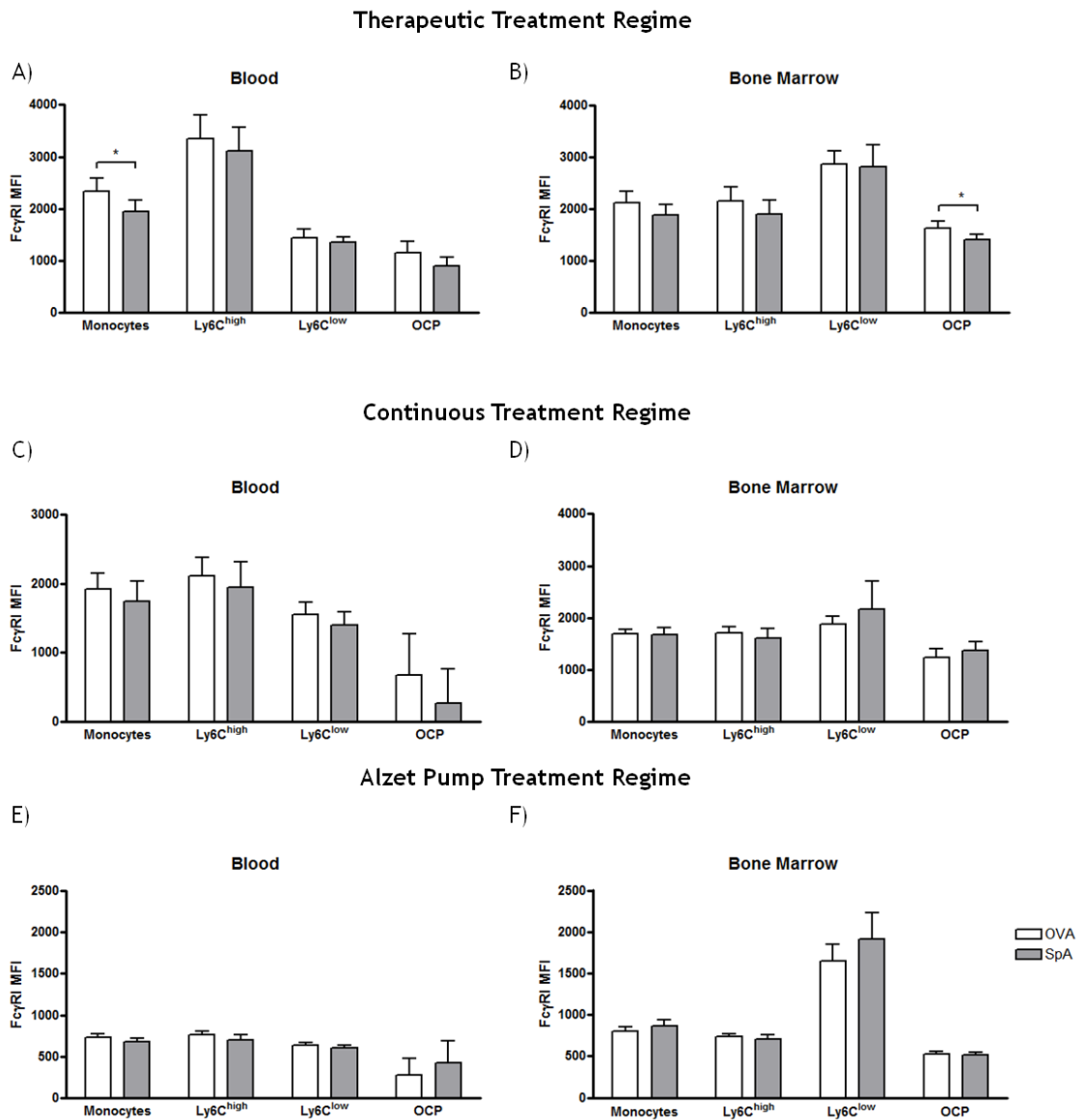
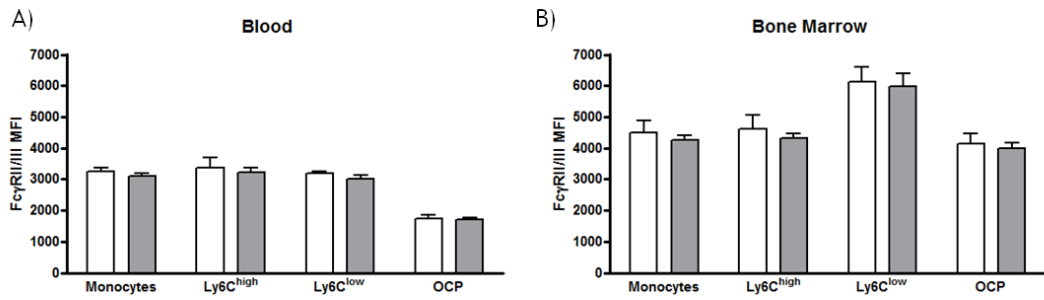


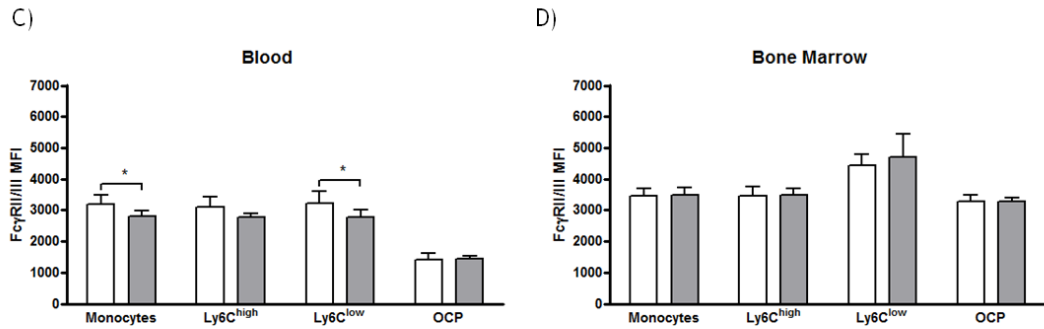
Figure 4-18: Expression of Fc γ RI on monocyte subsets in blood and bone marrow following OVX.

Continuing on from Figure 4-16, the expression of Fc γ RI was examined on the monocyte subsets identified (Figure 4-15). The subsets of interest were Ly6C^{high}, Ly6C^{low} and OCP and the expression of Fc γ RI on these subsets was recorded as MFI. The expression of Fc γ RI on monocyte subsets in A) Blood and B) BM for the Therapeutic Treatment Regime is shown. The expression of Fc γ RI on monocyte subsets in C) Blood and D) BM for the Continuous Treatment Regime is shown. The expression of Fc γ RI on monocyte subsets in E) Blood and F) BM for the Alzet PumpTM Treatment Regime is shown. Two Way ANOVAs with Bonferroni's post-hoc test were used to compare the effect of all treatment groups on individual monocyte subsets; $p < 0.05$ (*). Data represents mean \pm SD, $n = 7-8$.

Therapeutic Treatment Regime



Continuous Treatment Regime



Alzet Pump Treatment Regime

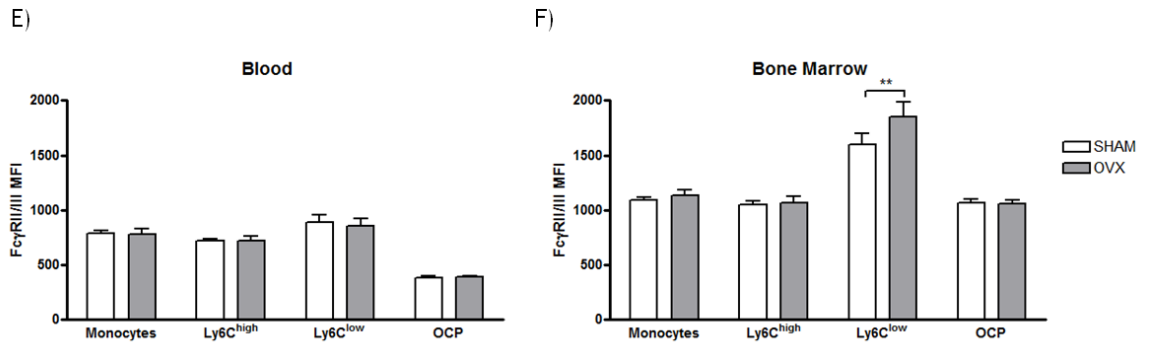


Figure 4-19: Expression of FcγRII/III on monocyte subsets in the blood and bone marrow following OVX.

Continuing on from Figure 4-16, the expression of FcγRII/III was examined on the monocyte subsets identified (Figure 4-15). The subsets of interest were Ly6C^{high}, Ly6C^{low} and OCP and the expression of FcγRII/III on these subsets was recorded as MFI. The expression of FcγRII/III on monocyte subsets in A) Blood and B) BM for the Therapeutic Treatment Regime is shown. The expression of FcγRII/III on monocyte subsets in C) Blood and D) BM for the Continuous Treatment Regime is shown. The expression of FcγRII/III on monocyte subsets in E) Blood and F) BM for the Alzet PumpTM Treatment Regime is shown. Two Way ANOVAs were used to compare the effect of all treatment groups on individual monocyte subsets; $p < 0.05$ (*) and $p < 0.01$ (**). Data represents mean \pm SD, $n = 7-8$.

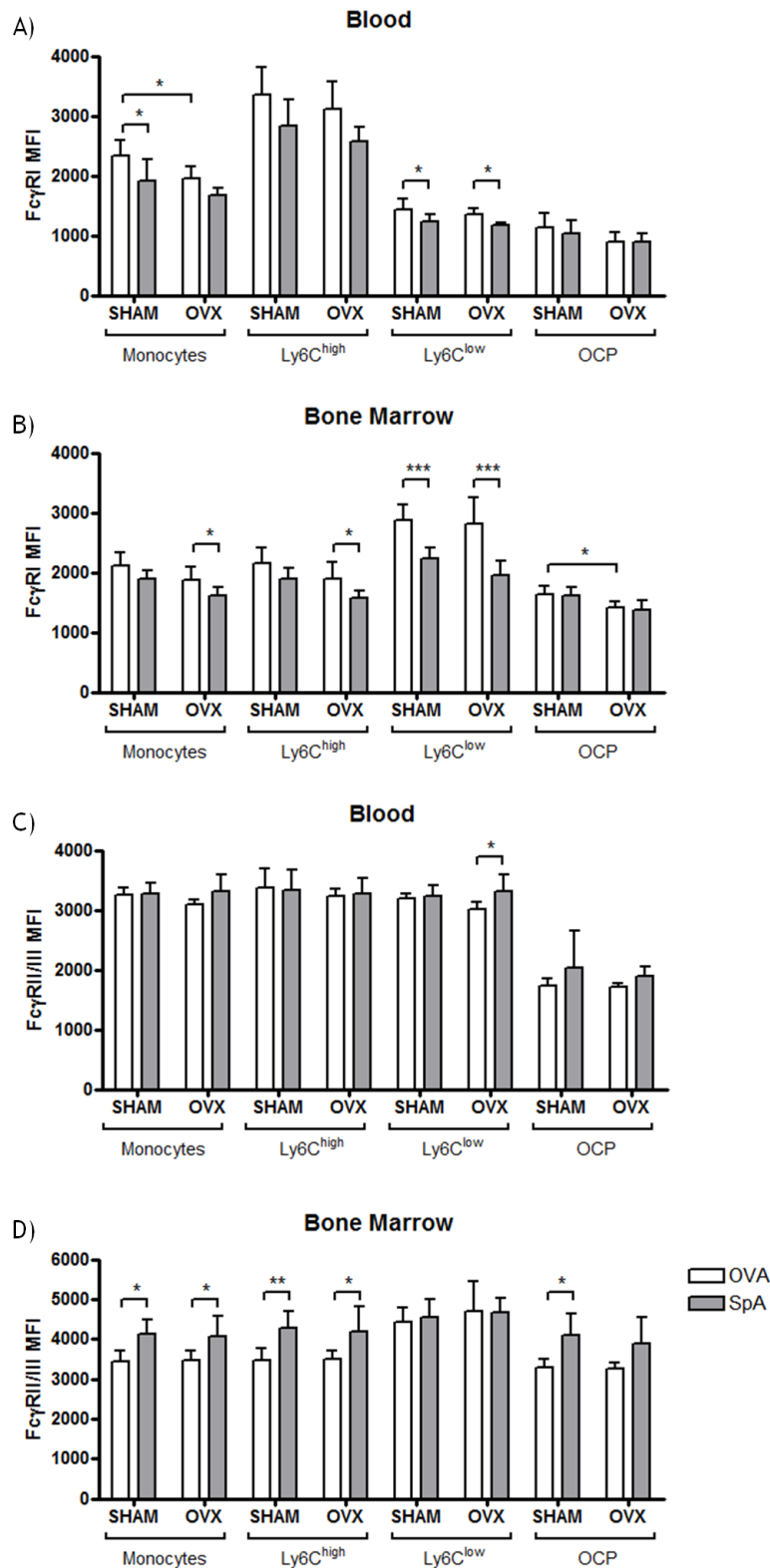


Figure 4-20: SpA modulates Fcγ receptors on monocytes.

Continuing on from Figure 4-16, the expression of both FcγRI and FcγRII/III was examined on the monocyte subsets identified (Figure 4-15). The subsets of interest were Ly6C^{high}, Ly6C^{low} and OCP and the expression of FcγRI and FcγRII/III on these subsets was recorded as MFI. The expression of FcγRI on monocyte subsets in A) Blood and B) BM and FcγRII/III in C) Blood in the Therapeutic Treatment Regime is shown. The expression of FcγRII/III on monocyte subsets in D) BM for the Continuous Treatment Regime is shown. Two Way ANOVAs were used to compare the effect of all treatment groups on individual monocyte subsets; p<0.05 (*), p<0.01 (**), and p<0.001 (***). Data represents mean ± SD, n=7-8.

4.3 Discussion

Osteoporosis is a pathology associated with the menopause and is an accumulation of multiple factors resulting in weakened bone integrity and increased risk of fracture³⁸⁰. PMO occurs in 30% of post-menopausal women and is a major cause of femoral head and vertebral fractures in the elderly³⁹¹. Animal models used to study PMO involve removal of the ovaries to simulate the oestrogen deficiency in humans⁴⁰. In the present study, the C57Bl/6 mouse model of osteoporosis was used as this strain is prone to oestrogen deficient bone loss³⁹. The mouse model of osteoporosis results in the rapid resorption of trabecular bone from the femur, tibia and vertebrae but does not resemble human disease because mice do not become prone to fractures⁴⁰. In mice, increasing age increases trabecular bone resorption and is more prominent in females than males due to an alteration in the pre-OC pool^{41,392,393}. However, as a model system, the OVX mouse model allows for the identification of potential drug targets to inhibit the rapid bone erosion in a non-inflammatory environment. As SpA has previously been shown to decrease the number of OCs in inflamed joints³¹⁶, it was hypothesised that SpA could reproduce this effect in the OVX model.

Monocytes are of particular interest as the different monocyte subsets have different roles during homeostasis and, when stimulated, are a potential pool of pre-OCs⁸⁹. Ablation of the monocyte lineage by clodronate has also been shown to halt osteoporotic disease in OVX animal models, highlighting not only that OCs are central to this disease pathology but also highlighting monocytes as a reservoir of pre-OCs³¹⁸. Research has already shown that the OCP population in the BM is a subset of monocytes which can repopulate OC deficient animals with mature functional OCs⁴. While in the blood, the same role was undertaken by Ly6C^{high} monocytes⁴. In the present study, we observed the effect of oestrogen on the regulation of these populations. It was also of interest to examine whether SpA could alter these pre-OC populations and prevent them from differentiation into OCs.

SpA is able to enter both the blood and BM following i.p. injection and interact with monocytes, possibly via FcγRI³¹⁶. Previously, SpA has been shown to bind highly to monocytes in the blood and BM and the low level of binding observed in this study may be due to a number of reasons. One particular example is that the conjugation of SpA and OVA to AF488 may have been unequal. A conjugation kit is used which can conjugate AF488 to proteins. However, each reaction varies slightly and as such the yield of labelled protein can differ between conjugations. The reaction can also produce proteins which have differing number of AF488 molecules conjugated to proteins; proteins with a high number of AF488 molecules conjugated to them fluoresce more

intensely than those with a low number of AF488 molecules. The ratio of AF488 molecules bound to OVA and SpA was normalised for in this study, however, if the previous studies had a high ratio of conjugation this may account for the heightened binding of SpA to monocytes. One important control which should be used in future experiments with these reagents is the use of a naive mouse which would have allowed the identification of the baseline expression of fluorescence, thus allowing determination of the effects of OVA-488 and SpA-488. Another discrepancy in this study was that OVA-488 was found to highly interact with BM Ly6C^{low} and OCP populations. This interaction was unexpected; however, it may be due to OVA-488 deposition in the tissue and uptake by phagocytes which have not been gated out using our gating strategy. This may also represent a clearance of OVA from the system, and had the spleen been examined it is likely that OVA-488 would be found at a high concentration. However, to fully determine whether this is a physiologically relevant interaction or due to phagocytosis, these cells would need to be viewed under a confocal microscope to observe whether the fluorescence was on the cell surface or within intracellular vesicles. This would also allow observation of SpA-488 treated cells and could provide evidence to demonstrate that SpA-488 IgG complexes interact with surface receptors on these cells. The difference in OVA-488 and SpA-488 interactions in blood and BM could also be examined by measuring their protein concentration within the tissue. Examination of protein concentration using western blots could demonstrate the protein concentration present in the BM and provide insight into the pharmacokinetics and distribution of SpA in the mouse.

In order to investigate whether monocyte subsets responded differently to ligation by FcγRs, Ly6C^{high} and Ly6C^{low} monocytes were sorted from the blood and BM. Because the BM provides a limited supply of Ly6C^{low} monocytes, blood was also used as a source of monocytes to increase the yield. Unfortunately, the OCP population could not be isolated at the same time. Had this population been cultured in the same conditions, published research suggests that it would have been highly osteoclastogenic¹⁰³. However, in comparison, Ly6C^{high} monocytes were more osteoclastogenic than Ly6C^{low} monocytes, and were inhibited from differentiation by FcγR modulation. As previously demonstrated, OC cultures derived from BM could be inhibited by addition of IgG or IgG complexes. The addition of Oplg and SIC to cultures of Ly6C^{high} monocytes was able to also inhibit OC differentiation. However, *in vivo* IgG is continually present and in its monomeric form has limited ability to influence cellular activity. Yet, IC have been shown to have a multitude of effects. In particular, IC have been shown to either inhibit or enhance osteoclastogenesis *in vitro* depending on the type of IC used^{262,317}. IC are also known to directly induce disease pathology, an example of this is systemic lupus erythematosus in which antibodies against DNA form IC and propagate the autoimmune

inflammation resulting in dysfunction of the kidney and neurological issues^{394,395}. Therefore, IC can have a multitude of effects *in vivo* and as SpA has been shown to be effective in reducing inflammatory derived OCs *in vivo*, the effect of SpA on pre-OC populations of the blood and BM was examined.

Oestrogen deficiency was shown to have inconsistent effects on the monocytes of the blood and BM. Over the course of three treatment regimes, oestrogen deficiency had alternating effects on the total monocytes present in the blood, while not effecting BM monocytes. In the rat OVX model, Erben *et al* (1998) showed that the ED1⁺ BM cells, which represent CD68⁺ myeloid cells were increased in OVX animals compared with sham as well as observing enhanced B cell lymphogenesis³⁹⁶. In rats, ED1 is a membrane marker found on monocytes and is also expressed on OCs^{397,398}. Research into the effects of oestrogen on monocytes is limited, however, the effects of oestrogen on other BM populations has been investigated. Katavic *et al* (2003) showed that in murine BM, CD45R⁺ B cells were increased two-fold following OVX compared to sham operated controls and that BM leukocytes were unaffected by OVX³⁹⁹. In the present study, CD45R/B220 was used in conjunction with CD3 to eliminate B and T cells from analysis of the monocyte subsets therefore analysis of the B cell compartment could not be done to verify this effect.

This study showed that OVX increased the number of Ly6C^{high} monocytes observed in the BM, but the OCP population was unaffected. The OCP population has been shown to be increased in a model of inflammatory bone loss¹⁰³. However, this present study suggests that the OCP population is not affected by oestrogen deficiency. SpA treatment increased Ly6C^{high} monocyte numbers in BM and Ly6C^{low} monocyte numbers in the blood. However these effects were not consistent across treatment regimes. One explanation for this inconsistency is that the dose of SpA given may not have been large enough to influence the disease progression. In the OVX models, SpA was injected i.p. at a dose of 100µg while to observe SpA-488 binding to monocytes, a dose of 600µg was used. This allowed determination of how SpA interacted with cells *in vivo*, but it can also result in rapid clearance of circulating immunoglobulin. SpA immediately engages with IgG in circulation, but it continually dissociates and reforms complexes with free IgG with a half life of 9 hours²⁹⁹. As a result, SpA given at high doses is able to reduce the concentration of IgG present in the serum²⁹⁹. However, a dose of 100µg of SpA per animal per 48 hours was chosen for long term studies because previously this concentration had been effective in treating the inflammatory model of disease CIA³¹⁶.

The effect of oestradiol on the expression of FcγRs has received some attention. Previous work has shown that oestrogen and ERα signalling complexes engage the

oestrogen response element (ERE) on the FcγRIII promoter and removal of this signal up-regulates FcγRIII transcription beyond untreated controls^{382,400}. Kramer *et al* (2004) also went onto demonstrate that direct ligation using mAb directed against the up-regulated FcγRIII resulted in heightened TNF-α, IL-6 and IL-1β secretion in human monocytes⁴⁰⁰. As mentioned, TNF-α, IL-6 and IL-1β are pro-OC cytokines which are up-regulated in the oestrogen deficiency model (Figure 4-1). Previous research on SIC showed that it can bind to the surface of MØ and increase the production of IL-10, while decreasing IL-12^{316,380}. This switch from IL-12 production to IL-10 is believed to identify a regulatory phenotype instead of inflammatory phenotype²⁷⁶. However, production of TNF-α, IL-6 and IL-1β was not investigated as part of that study and as such it is unknown whether SIC affects production of these inflammatory cytokines³¹⁶. This could have provided insight regarding the effect of SIC interactions with FcγRIII on monocytes and also indicate whether in the OVX model SIC could be interacting with monocytes to produce these inflammatory cytokines. In the OVX model, the concentration of TNF-α, IL-6, IL-1β and IFN-γ was examined in the serum of OVX and sham animals treated with SpA, however, the levels remained below the limit of detection. In order to fully evaluate the effect SIC exerts, SIC treated monocytes/MØ could have their production of TNF-α, IL-6 and IL-1β tested *in vitro*. This would be particularly interesting in FcγRIII^{-/-} cultures, as SIC does not require FcγRIII to inhibit osteoclastogenesis but may have an effect on MØ cytokine production.

The effect of the OVX model on the *in vivo* expression of FcγRs has not been previously addressed and so the present study examined whether oestrogen deficiency affected the expression of FcγRs. It was observed that in a state of oestrogen deficiency the expression of FcγRI and FcγRII/III remained relatively unchanged. However, the loss of distinction between FcγRII and FcγRIII due to use of an antibody which recognises both receptors could have masked any subtle changes that have been occurred in this model. The FcγRIII promoter is known to interact with the E/ER complex in human MØ and following removal of oestrogen from cultures FcγRIII transcription is up-regulated³⁸². Removal of oestrogen has also been shown to enhance the response of FcγRIII ligation and cytokine production³⁸². However, Kramer *et al* (2007) only used short term human cultures *in vitro* and there may also be species differences therefore this phenomenon must be verified in the murine system³⁸². The results of this present study would suggest that any increase in FcγRIII expression on monocytes that Kramer *et al* (2007) observed is short lived and in a model of oestrogen deficiency the expression levels of FcγRs remains unchanged³⁸². However, use of antibodies against FcγRII and FcγRIII would allow for distinct identification of changes in surface expression of these receptors. SpA treatment was also observed to have varied effects on monocyte subsets with the overall trend observed that FcγRI was down-regulated after SpA treatment and

FcγRII/III was up-regulated. The SpA IgG complexes may be interacting with FcγRI and thus masking its expression and increasing FcγRII/III in an attempt to clear IgG complexes from the system, however, these results were inconsistent across treatment regimes suggesting that overall long-term SpA treatment had no effect on the expression of FcγRs.

To assess whether SpA could alter bone metabolism in the OVX model, the concentrations of both Osteocalcin and CTX-1 were measured in the animal's plasma⁴⁰¹. It was found that oestrogen deficiency or treatment with SpA had no effect on the level of Osteocalcin in animal's plasma. Whereas animals undergoing oestrogen deficiency increased plasma CTX-1, which treatment with SpA did not effect. These results would indicate that bone resorption is increased in OVX animals, while bone formation remains unchanged. Published work has shown that due to the intimate nature of bone remodelling, an increase in bone resorption inherently results in an increase in bone formation⁴⁰². Yet, in osteoporosis bone resorption occurs at a faster rate than bone formation resulting in bone loss. This data suggests that the ELISA used to detect Osteocalcin was not sensitive enough to detect changes in the plasma samples. The use of serum may have provided a more concentrated sample for analysis however due to the technical requirements serum could not be used. EDTA was used to collect blood to allow analysis of cells by flow cytometry and also collection of plasma. EDTA chelates Ca²⁺ to prevent coagulation thus plasma contains extra proteins compared to serum. The results of the CTX-1 analysis showed that bone erosion was increased in these models while bone formation, as measured by Osteocalcin, was unaffected by OVX and SpA was unable to impact on these bone remodelling.

Three point bend testing was performed on the right femurs of sham and OVX operated animals. The results showed that there was no difference in bone strength, or quality, following OVX or treatment with SpA. However, this method of analysis is crude and destructive. Unfortunately, this experiment was underpowered with an 'n' of 4-6 which was too small to demonstrate any meaningful difference. Jämsä *et al* (1998) demonstrated that three point bend testing directly correlated with the cortical thickness and strength which requires up to 28 weeks following OVX to become notably altered^{387,403,404}. The observed results would therefore suggest that the cortical strength of bone has been unaffected by six weeks of oestrogen deficiency or treatment with SpA. A more sensitive method of analysing the bone integrity was required to assess the effect of oestrogen deficiency on the micro-architecture of the tibial bone and to observe trabecular bone lost following oestrogen deficiency.

μ CT was utilized to interrogate the micro-architecture of the trabecular bone in the proximal tibia and assess the presence of bone following oestrogen deficiency. A standardized method for the assessment of bone loss by μ CT was followed for each treatment regime⁴⁰⁵. As expected in all treatment regimes, OVX animals had less trabecular bone present than sham operated controls. The loss of oestrogen resulted in bone loss and treatment with SpA in OVX animals had no impact on the degree of bone loss. In this model of oestrogen deficiency an overall increase in pro-OC cytokines are produced which inadvertently drive monocytes to differentiate into OCs⁴⁰⁶. In this study, the data would suggest that SpA IgG complexes could interact with the monocytes but were unable to overcome the prevailing environment, which was driven towards osteoclastogenesis. Therapeutic treatments used to treat PMO, which have also been tested in OVX animal models, include denosumab (mAb direct to RANKL)⁴⁰⁷ and bisphosphonates (induce OC apoptosis)³³. These therapies have a direct effect on reducing osteoporotic disease^{408,409}, however, SpA had no effect on osteoporotic disease in the murine OVX model. Recently, SpA has been used in a safety trial, which provided evidence that SpA at low doses is safe for human use and could have beneficial effects in treating the disease⁴¹⁰. This finding couples with the CIA model of disease where treatment with SpA could reduce disease progression³¹⁶. Thus SpA appears to have the potential to become a therapeutic agent. However, the target diseases may remain inflammatory disorders as SpA could not alter disease progression in the OVX model of bone loss.

In summary, SpA passes into circulation via i.p. injection, and can interact with blood and BM monocytes which act as the pre-OC pool in homeostasis. However, SpA can not intervene to prevent bone loss during from oestrogen deficient OVX model. More research is required to determine whether SpA could be used as a therapeutic in treating PMO.

5 NF- κ B inhibitor Bcl-3 modulates bone remodelling

5.1 Introduction

Bone remodelling refers to the dynamic and tightly regulated process by which OCs erode bone matrix and OB's secrete new bone matrix¹³. OC's are large multinucleated cells which secrete enzymes such as MMP9, Cathepsin K and TRAP to erode the bone matrix^{240,264,336}. Cells of the monocyte/M ϕ cell lineage are pre-OCs³⁶⁶ and recent research has shown that certain subsets of monocytes found in the blood and BM are highly osteoclastogenic^{4,103,116}. Fusion of pre-OCs occurs following commitment to the OC lineage after stimulation with M-CSF and RANKL, acting via CD115 and RANK, respectively, on the cell surface^{6,324}. In fact animals deficient for M-CSF, CD115, RANKL or RANK develop osteopetrosis and fail to produce *in vivo* OCs^{102,119,137,411}. For effective osteoclastogenesis to occur, CD115 provides the survival signal which also up-regulates RANK expression on the surface of pre-OCs⁶. RANKL can then engage RANK allowing for a number of signalling molecules to be activated. One of the most important of these is NF- κ B, a ubiquitous signalling molecule vital for a variety of cellular functions. RANK is named for the receptor's ability to drive osteoclastogenesis via NF- κ B signalling^{145,156}. NF- κ B comprises of 5 subunits; p105 (p50), p100 (p52), p65, RelB and c-Rel¹⁵⁸⁻¹⁶². These subunits can form 15 combinations of homo- and hetero- dimers which can translocate to the nucleus and engage NF- κ B binding sites on the promoter regions of genes either activating/suppressing transcription^{163,164}.

In order to regulate this process, Inhibitor of κ B (I κ B) proteins sequester NF- κ B dimers in the cytoplasm and nucleus and suppress activation. Of particular interest is I κ B α which binds to the p65 subunit of the NF- κ B p50:p65 heterodimer and prevents activation of the canonical NF- κ B pathway¹⁶⁹. Interaction between RANKL and RANK on the surface of pre-OCs results in activation of the canonical NF- κ B pathway leading to rapid degradation of I κ B α and translocation of NF- κ B p50:p65 to the nucleus (Figure 5-1)¹⁷². There also exists a non-canonical NF- κ B pathway which upon activation leads to a gradual degradation and processing of the I κ B-like protein p100 into the NF- κ B subunit p52 (Figure 5-1)¹⁶⁰. p52 forms a heterodimer with RelB translocating to the nucleus for transcriptional activity¹⁷³. Bcl-3 is an I κ B-like protein which resides in the nucleus and is capable of binding homo- and hetero- dimers of p50 and p52^{170,171}. p50 and p52 are unlike other NF- κ B subunits because they lack transcriptional activation domains (TAD)¹⁶⁷. This results in homo- and hetero- dimers of p50 and p52 occupying NF- κ B sites on gene promoters suppressing transcription¹⁶⁷. Bcl-3 selectively binds to these complexes, stabilizing the dimers on NF- κ B binding sites, preventing their degradation and inhibiting activatory NF- κ B binding and transcription¹⁶⁷. The role of NF- κ B has been

studied extensively and demonstrated that p50, p52, p65 and RelB but not c-Rel are essential for osteoclastogenesis (see Section 1.2.4)^{145,162,174-177}.

Studies investigating the atypical I κ B protein, Bcl-3, have shown that in the absence of Bcl-3 M ϕ /DCs were highly responsive to TLR-4 stimulation as a result of aberrant NF- κ B activity due to the lack of p50 or p52 dimers in the nucleus¹⁶⁷. In addition, Bcl-3^{-/-} animals have altered immune responses because secondary lymphoid organs do not develop⁴¹². These animals develop advanced diabetes compared to WT animals in both spontaneous and induced diabetes models which results from Bcl-3's ability to control transcription of cytokine and chemokine mRNA in inflammatory conditions⁴¹³. Thus in the absence of Bcl-3, there is higher production of inflammatory cytokines which worsens the progression of inflammatory diseases⁴¹³. However, the role of Bcl-3 as an inhibitor of NF- κ B in osteoclastogenesis has not been investigated. Furthermore, it remains to be elucidated whether Bcl-3 deficiency has any impact on *in vivo* bone remodelling. It is proposed that the absence of Bcl-3 will allow transcription of OC essential genes to continue without regulation and result in excessive osteoclastogenesis (Figure 5-1). Another, yet to be defined, aspect of interest is how Bcl-3 deficient pre-OCs respond to IC mediated inhibition of osteoclastogenesis. As previously shown, SIC is able to inhibit *in vitro* osteoclastogenesis by Fc γ R engagement and examination into the role of Bcl-3 in this inhibitory mechanism is required.

The research presented in this chapter examines the role of Bcl-3 in osteoclastogenesis and phenotypes Bcl-3^{-/-} animals for skeletal abnormalities. The principal aims were to:

1. Investigate whether Bcl-3^{-/-} pre-OCs could differentiate into OCs *in vitro*.
2. Test the ability of SIC to inhibit osteoclastogenesis in Bcl-3^{-/-} cultures.
3. Determine whether Bcl-3^{-/-} animals have osteoimmune abnormalities *in vivo*.

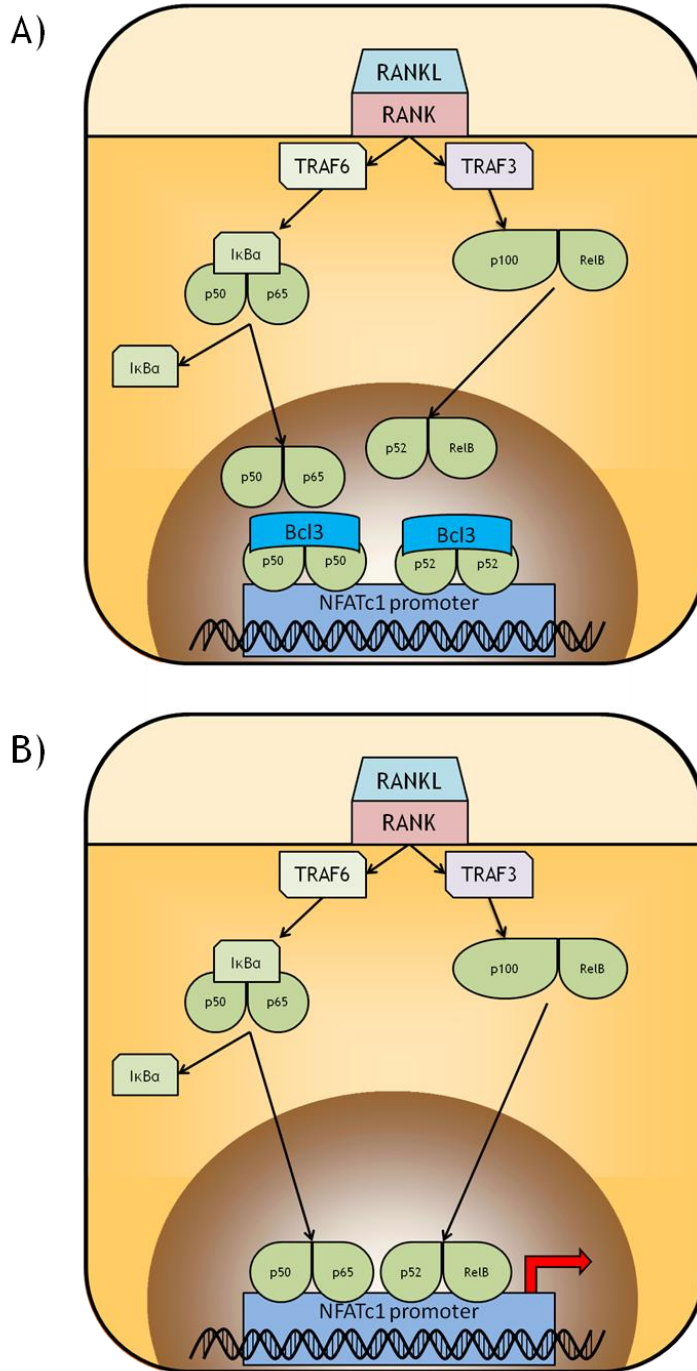


Figure 5-1: Schematic of Bcl-3's hypothesised role in RANKL-RANK mediated signal transduction.

Upon RANKL-RANK interaction, both the canonical and non-canonical pathways are activated by TRAF6 and TRAF3, respectively. Canonical signalling rapidly occurs and relies on TRAF6 mediated degradation of I κ B α which allows for nuclear translocation of NF- κ B heterodimer p50:p65 to bind NF- κ B binding domains in the nucleus. TRAF3 is degraded following RANK activation which allows processing of the p100 to the p52 NF- κ B subunit which dimerises with RelB and translocates to the nucleus. The non-canonical pathway requires hours to potentiate signalling and continues long term transcriptional processes after the canonical pathway ends. In this pathway, the proposed role of Bcl-3 is that it binds non-activatory homo- and hetero- dimers of p50 or p52 blocking NF- κ B domains on the promoters of essential osteoclastogenic genes (A). In the absence of Bcl-3 a shift in the ratio of non-activatory to activatory NF- κ B binding dimers occurs resulting in excessive transcription of osteoclastogenesis (B). Thus Bcl-3 is hypothesised to be a regulator of osteoclastogenesis.

5.2 Results

5.2.1 RANKL induces Bcl-3 mRNA transcription

Bcl-3 is known to be under the transcriptional control of NF- κ B⁴¹⁴ and to verify that Bcl-3 is involved in RANKL mediated signalling, the level of Bcl-3 mRNA was measured in OCs. NA BM cells were cultured with 75ng/ml M-CSF and/or 50ng/ml RANKL for 5 days. mRNA was extracted from cultures and probed for the presence of Bcl-3 mRNA by qPCR. M-CSF and RANKL treated cultures were compared to M-CSF alone cultures, revealing that OCs had significantly more Bcl-3 mRNA than M \emptyset s ($p < 0.001$) (Figure 5-2). This method of analysis shows that OCs have a higher level of Bcl-3 mRNA than M \emptyset and provides evidence that Bcl-3 is involved in RANKL mediated osteoclastogenesis.

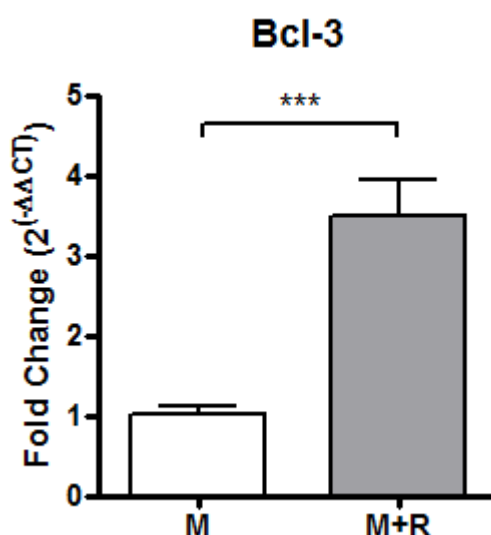


Figure 5-2: RANKL stimulation up-regulates Bcl-3 mRNA.

1×10^5 murine WT and Bcl-3^{-/-} NA BM cells were cultured with 75ng/ml M-CSF (M) and/or RANKL (M+R) for 5 days at 37°C. Media was refreshed on day 4. Cultures were lysed, mRNA extracted, cDNA generated and qPCR performed on all samples which were run in triplicate. GAPDH was used as the housekeeping control and non-template controls were run for each gene. Fold Change (2^(-ΔΔCT)) was measured by normalising samples of Bcl-3 primers to the housekeeping control (ΔCT). Subsequently M+R Bcl-3 ΔCT's were normalised to the average M ΔCT to obtain the ΔΔCT. This was then used to obtain the fold change (2^(-ΔΔCT)). To obtain the spread of M data, each M ΔCT was compared to the average M ΔCT and fold change calculated. Bcl-3 mRNA in M and M+R samples were compared using an unpaired two-tailed t test; $p < 0.001$ (***). Data represents mean \pm SD, $n=3$.

5.2.2 Bcl-3 deficient osteoclastogenesis

To investigate the effect of Bcl-3 deficiency on osteoclastogenesis, BM cultures were set up to differentiate non-adherent BM (NA BM) from C57Bl/6 (WT) or Bcl-3^{-/-} animals on a C57Bl/6 background. OCs were differentiated as previously described in the presence of 75ng/ml M-CSF and 50ng/ml RANKL. After 4, 5, 6 and 7 days of culture, cells were stained for the presence of TRAP. TRAP was used as an indicator of osteoclastogenesis and cells that were TRAP⁺ with 3 or more nuclei were considered as an OC. WT and Bcl-3^{-/-} OCs were present at each day examined (Figure 5-3). Interestingly, in WT and Bcl-3^{-/-} cultures the size of OCs appears to increase from day 4 to day 5, but then decrease on days 6 and 7 (Figure 5-3). Following the 5th day of culture there was evidence of cell death in the form of large cellular debris. The number of OCs was counted on each day which demonstrated that WT and Bcl-3^{-/-} NA BM cultures were able to differentiate into OCs at the same rate up until 6 days of culture (Figure 5-4A). At day 7, WT cultures had significantly more OCs present than Bcl-3^{-/-} cultures ($p < 0.01$). Due to the multinucleated nature of OCs, the average size of OCs was calculated to ensure that the difference in number was not due to a discrepancy in the size of the OCs. The average size of OCs over the course of experiment remained equal between WT and Bcl-3^{-/-} cultures, however, larger OCs were observed at day 5 compared to other days (Figure 5-4B). Differences between the numbers of OCs present over the course of this experiment may be due to differences in the pre-OC populations present in the BM. The BM contains a large number of myeloid precursors at a variety of differentiation stages and as such stimulation with M-CSF and RANKL could result in terminal differentiation to OCs occurring over a series of days. This could also account for the difference observed at day 7 between WT and Bcl-3^{-/-}, as it is possible that there are differences between the progenitors present in the BM of each animal and this could ultimately affect the OC differentiation (Figure 5-4). However, WT and Bcl-3^{-/-} NA BM cells are able to respond to RANKL and differentiate into OCs *in vitro*.

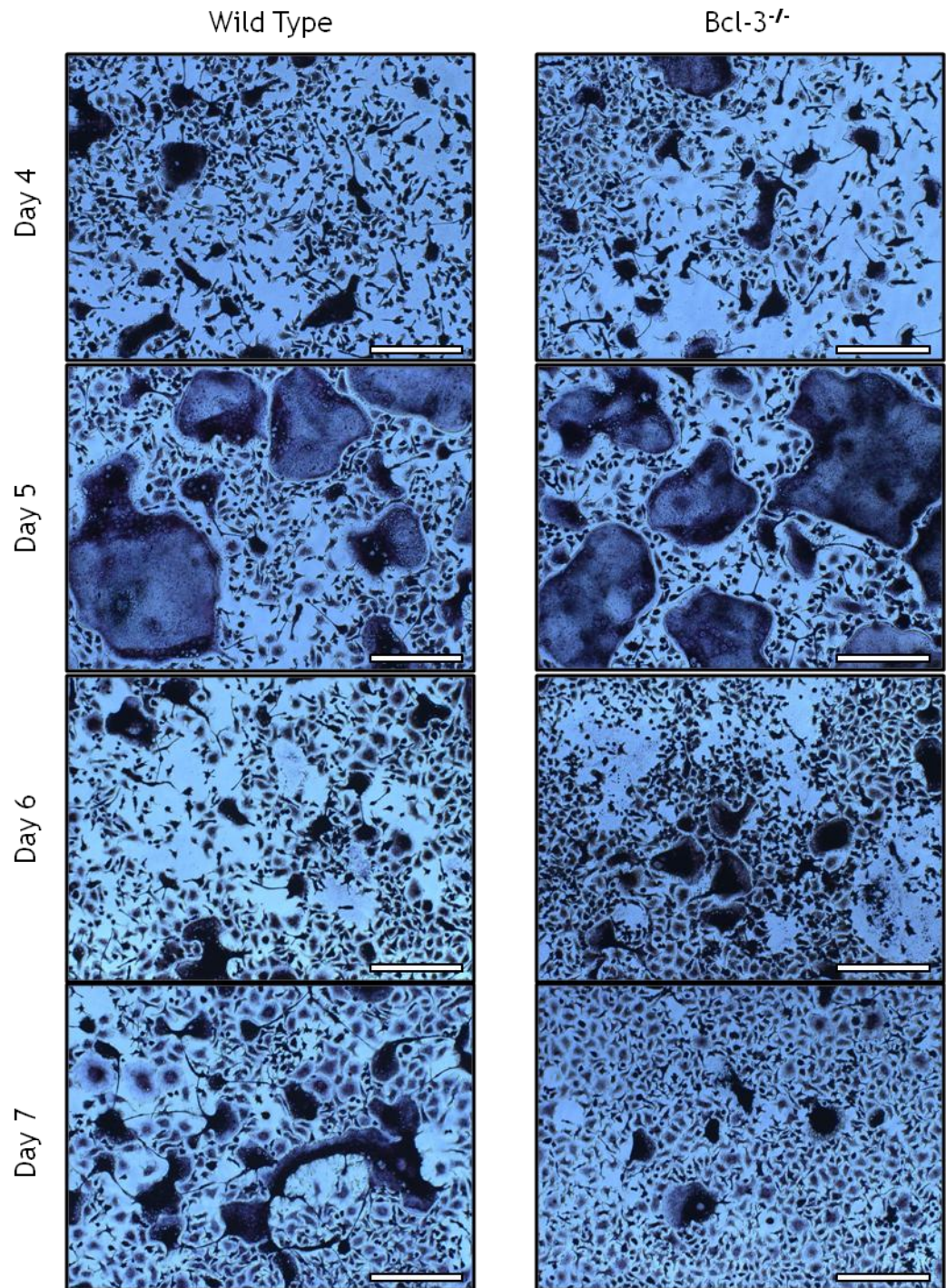


Figure 5-3: TRAP staining of osteoclast differentiation kinetics in WT and *Bcl-3*^{-/-} cultures. 1×10^5 NA BM cells from WT and *Bcl-3*^{-/-} animals were cultured, in triplicate or quadruplicate, in the presence of 75ng/ml M-CSF and 50ng/ml RANKL. Cells were maintained at 37°C in 5% CO₂ with media refreshed on day 4. Cultures were stained for the presence of TRAP at days 4, 5, 6 and 7. Representative images of WT and *Bcl-3*^{-/-} OC cultures are shown at each of these days. Scale bars; 200µm.

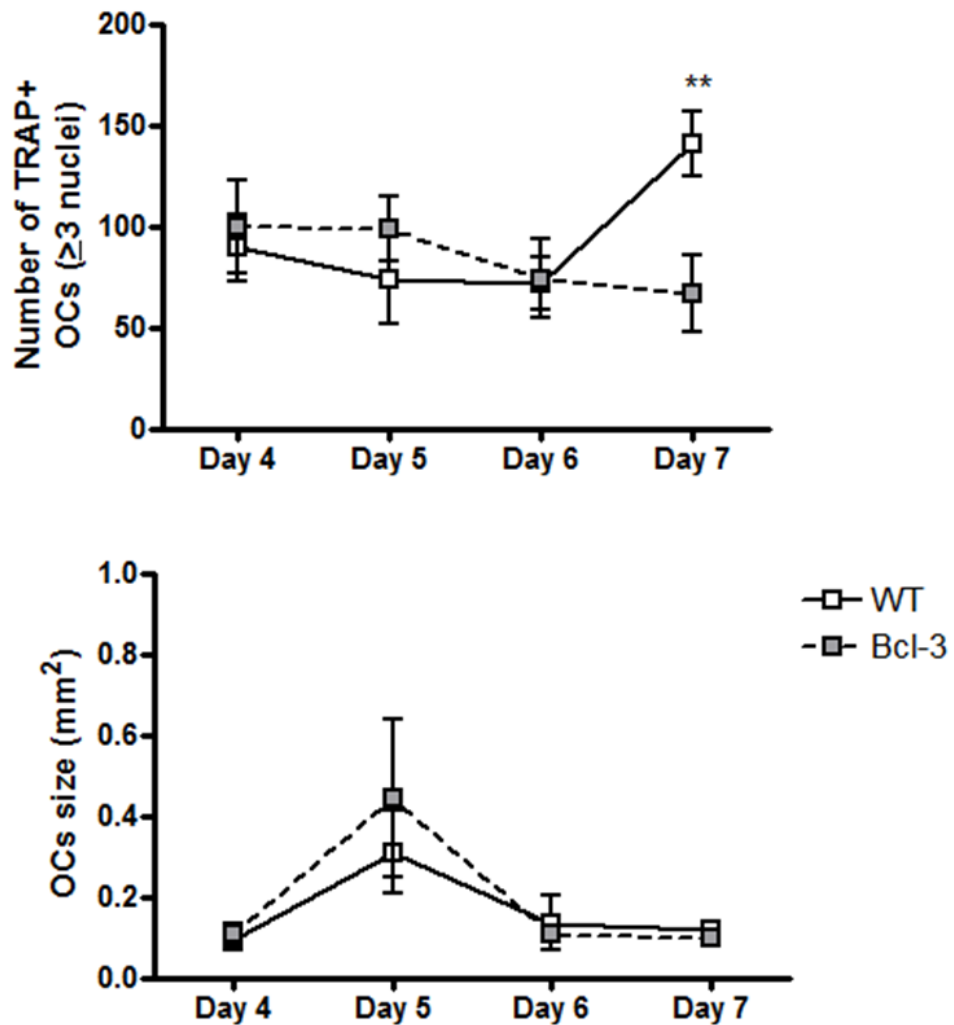


Figure 5-4: Osteoclast differentiation kinetics in WT and Bcl-3^{-/-} cultures.

1x10⁵ NA BM cells from WT and Bcl-3^{-/-} animals were cultured, in triplicate or quadruplicate, alongside 75ng/ml M-CSF and 50ng/ml RANKL. Cells were maintained at 37°C in 5% CO₂ with media refreshed on day 4. Cultures were stained for the presence of TRAP at days 4, 5, 6 and 7. Cells that stained positive for TRAP with ≥ 3 nuclei were defined as an OC and counted. A) OCs were counted and the sum total of 4 fields of view per condition, in triplicate or quadruplicate. B) Each OC that was counted had their size measured using Image J software and the mean size of OCs (mm²) was calculated. Two-way ANOVAs with Bonferroni's post-hoc tests were used to compare WT and Bcl-3^{-/-} cultures on each day; p<0.001 (***)). Data represents mean ± SD, n=3.

5.2.3 RANKL induced transcription in Bcl-3 deficient animals

RANKL can induce the terminal differentiation of OCs in Bcl-3^{-/-} NA BM. However, the transcriptional profile of Bcl-3^{-/-} OCs was examined to confirm that differentiation of mature OCs. OCs present at day 5 were selected because this time point was the first point at which a significant degree of osteoclastogenesis is observed. This will also eliminate the possibility of the cell death observed at later time points influencing the results.

In order to examine differences in transcriptional profile between WT and Bcl-3^{-/-} OCs, mRNA was extracted from day 5 cultures. Bcl-3^{-/-} OC culture mRNA was compared to that of the WT OC cultures. This revealed that at day 5 there was no difference in the transcription of CD115 or RANK, the two main inducers of osteoclastogenesis (Figure 5-5A, B). The transcription of two anti-apoptotic genes were also examined; Bcl-2 and Bcl-XL are responsible for preventing apoptosis and modulating OC differentiation^{415,416}. Both Bcl-2 and Bcl-XL were unaffected by the absence of Bcl-3 (Figure 5-5C, D). The effect of Bcl-3 deficiency on the levels of mRNA essential for osteoclastogenesis was also examined. mRNA for MMP9, Cathepsin K, DC-STAMP and TRAP, essential for multinucleation of pre-OCs¹⁰ and degradation of the bone matrix³³⁶, were all unchanged when Bcl-3^{-/-} OC were compared to WT (Figure 5-6A-D). This data suggests that at day 5 WT and Bcl-3^{-/-} OCs have a similar transcriptional profile, however, further work may be required to fully determine if any differences exist in the transcription of other genes. Comparison between WT and Bcl-3^{-/-} at day 6 and 7 in culture could also prove interesting as subsequent waves of osteoclastogenesis are evident from the kinetic experiments. Microarray analysis could provide insight into why there are less Bcl-3^{-/-} OCs present in day 7 cultures. However, further work would need to be done to dissect possible differences. However, the data presented here shows that by day 5 Bcl-3^{-/-} NA BM can differentiate mature OCs that are transcriptional similar to WT OCs.

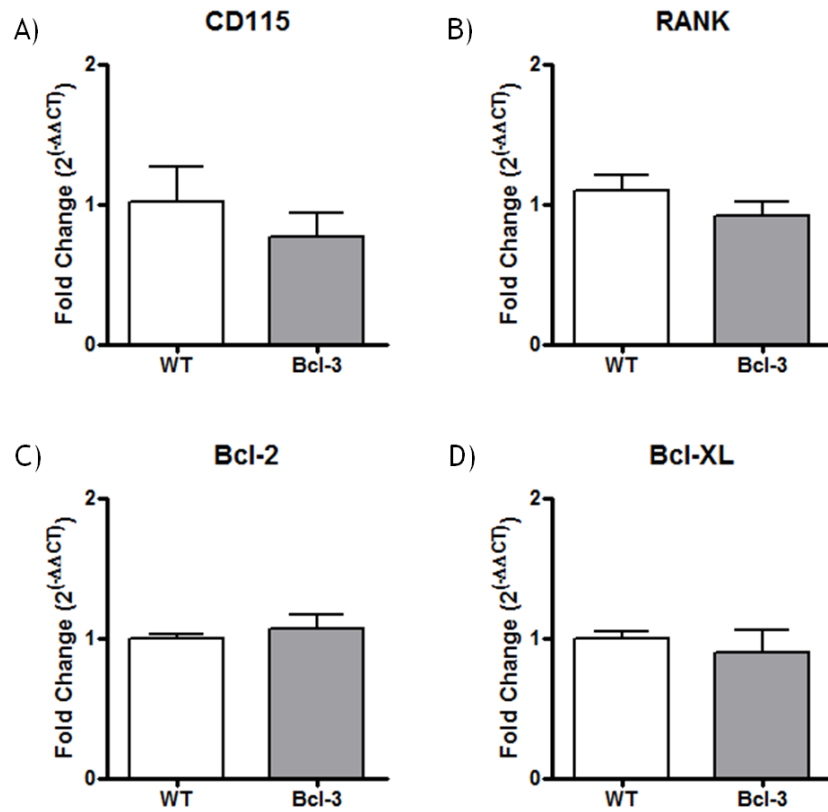


Figure 5-5: Osteoclast survival signals are unaffected in the absence of Bcl-3.

1×10^5 murine WT and Bcl-3^{-/-} NA BM cells were cultured with 75ng/ml M-CSF and RANKL for 5 days at 37°C to differentiate OCs. Media was refreshed on day 4. Cultures were lysed, mRNA extracted, cDNA generated and qPCR performed on all samples which were run in triplicate. GAPDH was used as the housekeeping control and non-template controls were run for each gene. Fold Change ($2^{(-\Delta\Delta CT)}$) was measured by normalising samples of each primer to the housekeeping control (ΔCT). Subsequently Bcl-3^{-/-} ΔCT 's were normalised to the average WT ΔCT to obtain the $\Delta\Delta CT$. This was then used to obtain the fold change ($2^{(-\Delta\Delta CT)}$). To obtain the spread of data, each WT ΔCT was compared to the average WT ΔCT and fold change calculated. WT and Bcl-3^{-/-} samples were compared using an unpaired two-tailed t-test. Data represents mean \pm SD, n=3.

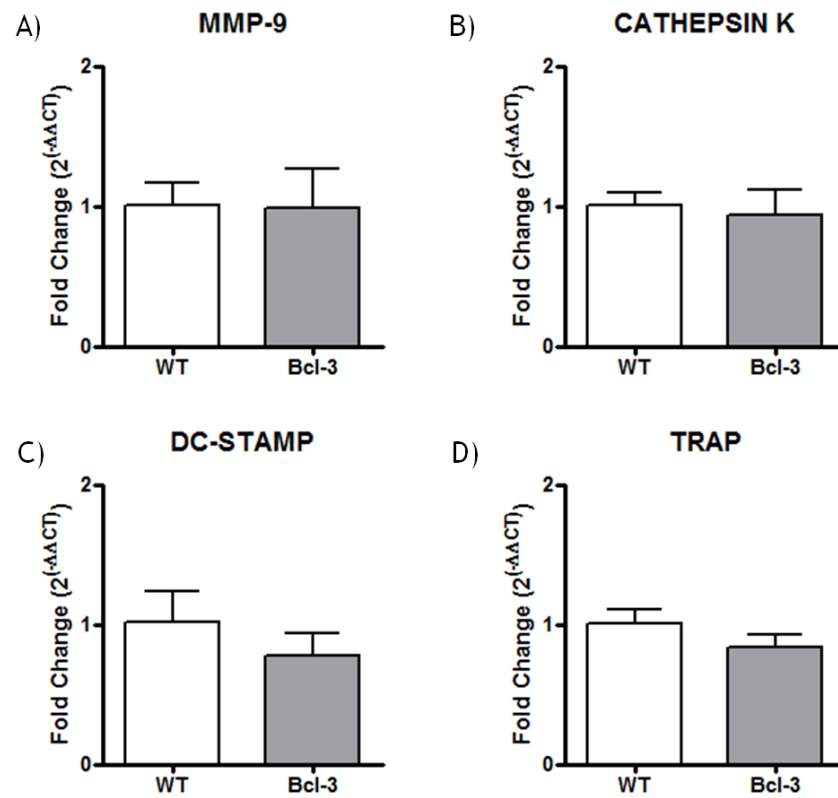


Figure 5-6: The transcription of osteoclast specific mRNA is unaffected in Bcl-3^{-/-} osteoclasts. 1x10⁵ murine WT and Bcl-3^{-/-} NA BM cells were cultured with 75ng/ml M-CSF and RANKL for 5 days at 37°C to differentiate OCs. Media was refreshed on day 4. Cultures were lysed, mRNA extracted, cDNA generated and qPCR performed on all samples which were run in triplicate. GAPDH was used as the housekeeping control and non-template controls were run for each gene. Fold Change (2^(-ΔΔCT)) was measured by normalising samples of each primer to the housekeeping control (ΔCT). Subsequently Bcl-3^{-/-} ΔCT's were normalised to the average WT ΔCT to obtain the ΔΔCT. This was then used to obtain the fold change (2^(-ΔΔCT)). To obtain the spread of data, each WT ΔCT was compared to the average WT ΔCT and fold change calculated. WT and Bcl-3^{-/-} samples were compared using an unpaired two-tailed t-test. Data represents mean ± SD, n=3

5.2.4 Fcγ receptor mediated osteoclast inhibition

To determine whether Bcl-3^{-/-} OCs could be inhibited by engagement of FcγRs, cultures of NA BM were incubated in the presence of 75ng/ml M-CSF and/or 50ng/ml RANKL for 5 days. SpA, Oplg and SIC were generated as previously described and cultured with OCs from day 1. When the number of TRAP⁺ OCs present in cultures were counted it was shown that with SIC treatment, WT and Bcl-3^{-/-} OC differentiation was inhibited (63%; p<0.001 and 62%; p<0.001, respectively) (Figure 5-7 and Figure 5-8A, B). Bcl-3^{-/-}, but not WT, cultures were inhibited by Oplg treatment (42% reduction; p<0.05) (Figure 5-8B). Previously, Oplg has been shown to inhibit the differentiation of WT OC cultures. However, Oplg contains monomeric IgG which is not capable of interacting with FcγRs in the same way as the IgG complexes which SIC generates. These results also demonstrate that the inhibitory potential of Oplg is not as consistent as SIC and as such shows that IgG complex interactions can consistently inhibit osteoclastogenesis. Overall, these results demonstrate that IgG and IgG complex interactions with FcγR do not require Bcl-3 to inhibit osteoclastogenesis.

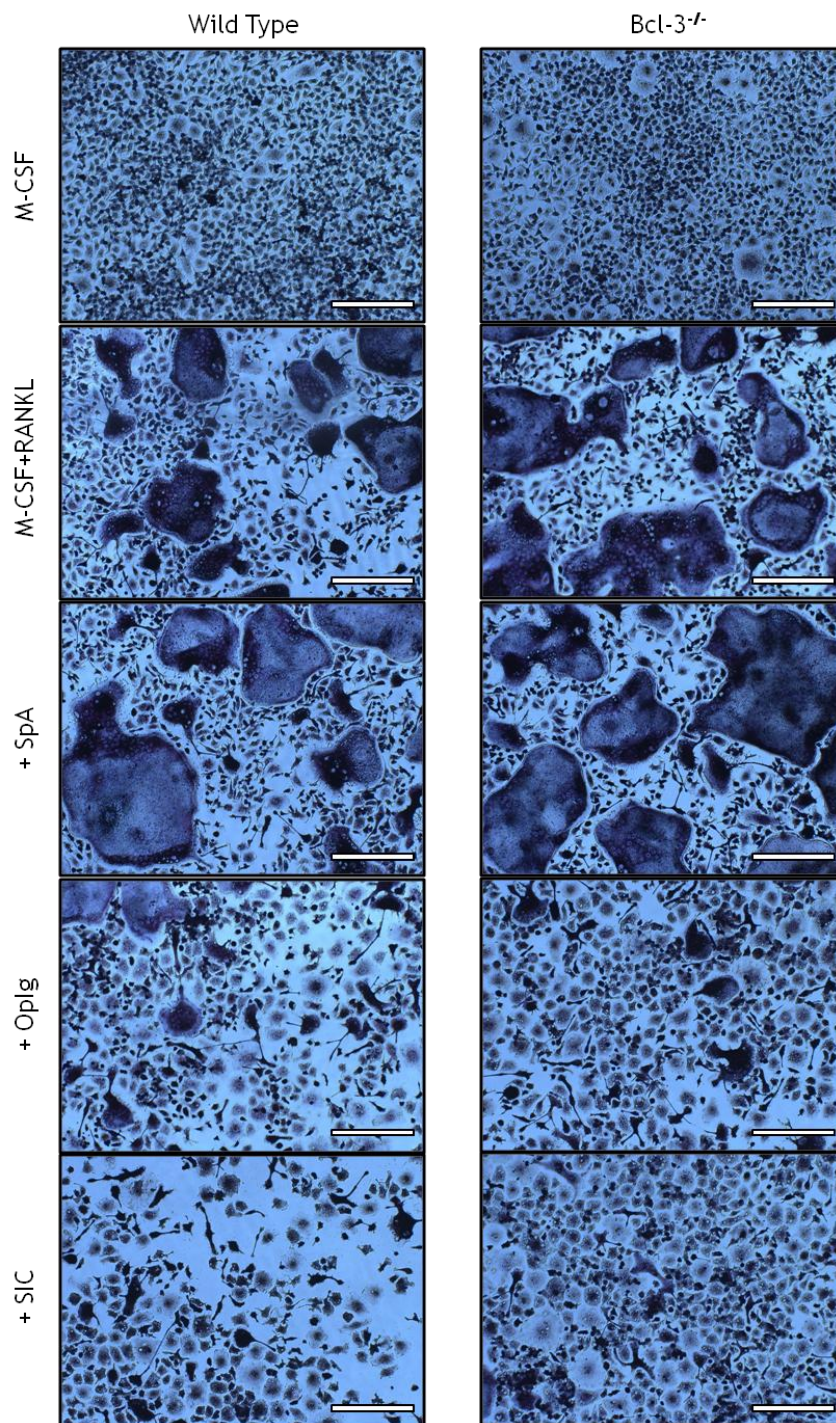


Figure 5-7: Representative TRAP staining for WT and Bcl-3^{-/-} osteoclasts. 1x10⁵ murine NA BM cells from WT and Bcl-3^{-/-} were cultured with 75ng/ml M-CSF and/or 50ng/ml RANKL for 5 days in 37°C with media renewed on day 4. Treatment with SpA, Oplg and SIC was given at day 1 and 4 alongside M-CSF and RANKL. Cultures were stained for the presence of TRAP and representative images of TRAP stained cultures are shown. Scale bar; 200µm.

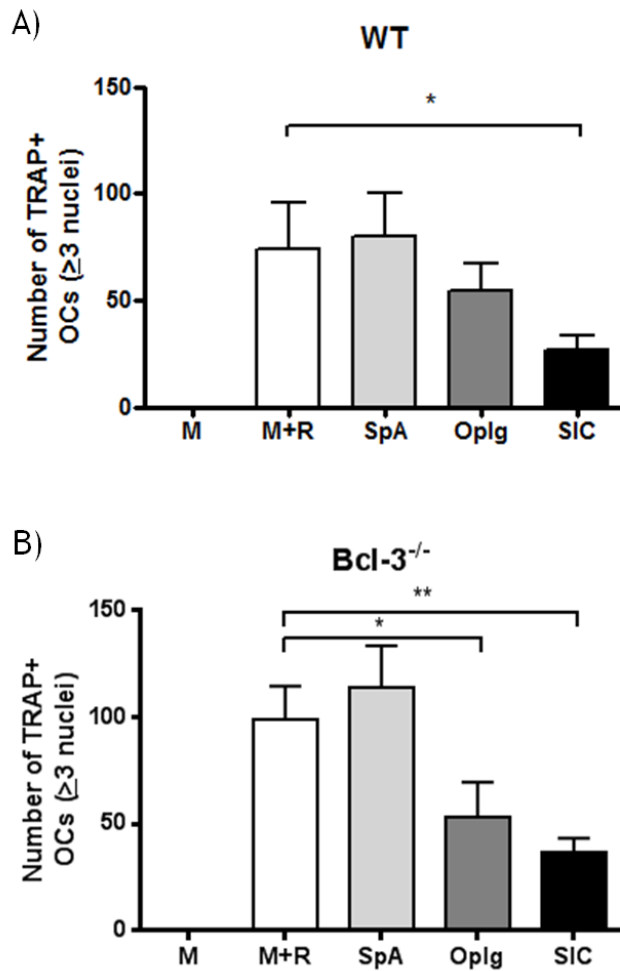


Figure 5-8: Fcγ receptor modulation inhibits WT and Bcl-3^{-/-} osteoclast differentiation. 1×10⁵ murine NA BM cells from WT and Bcl-3^{-/-} were cultured with 75ng/ml M-CSF and/or 50ng/ml RANKL for 5 days in 37°C with media renewed on day 4. Treatment with SpA, Oplg and SIC was given at day 1 and 4 alongside M-CSF and RANKL. Cultures were stained for the presence of TRAP (Figure 5-7). TRAP+ OCs with ≥3 nuclei were counted in A) WT and B) Bcl-3^{-/-} cultures and the sum total of 4 fields of view per condition in triplicate. Mean values of each condition were compared using a one way ANOVA with Bonferroni's post-hoc test; p<0.05 (*), p<0.001 (**). Data represents pooled mean ± SD of three individual experiments.

5.2.5 Bcl-3 is required for osteoclast precursor homeostasis

To evaluate the pre-OC populations present in Bcl-3^{-/-} animals we examined the monocyte subsets of the blood and BM from WT and Bcl-3^{-/-} animals. Monocytes are known to differentiate into OCs, however recent research has shown that subpopulations of monocytes can respond with greater efficacy to M-CSF and RANKL^{4,103,116}. Therefore, *ex vivo* analysis of blood and BM was done to examine these populations. 200µl of blood and BM from one femur were taken from WT and Bcl-3^{-/-} animals and stained for FACS analysis with CD3, B220, Ly6G, Ly6C, CD11b and CD115. This panel allowed the total population of blood and BM cells to be interrogated for the percentage of total monocytes (Ly6C⁺Ly6G⁻) and neutrophils (Ly6C⁺Ly6G⁺) (Figure 5-9A, B and Figure 5-10A). This also allowed the examination of the monocyte subsets present; Ly6C^{high} classical monocytes (Population 1 - Ly6C^{high} CD11b^{high}), Ly6C^{low} non-classical monocytes (Population 2 - Ly6C^{low} CD11b^{high}) and osteoprecursors (OCPs - Population 3 Ly6C^{high} CD11b^{low}) (Figure 5-10B). All three subsets are able to differentiate to OCs, however, in the BM, the OCP population is considered the most proficient pre-OC, while in the blood the Ly6C^{high} monocyte population is considered the most osteoclastogenic^{4,103,116}.

The percentage of cells obtained from FACS analysis was used to calculate the total number of cells present in each sample from cell counts. It was shown that the total number of monocytes present in the blood and BM was unaffected by the absence of Bcl-3 (Figure 5-10A and Figure 5-11A, B). Interestingly, the number of neutrophils in the blood and BM were significantly reduced in Bcl-3^{-/-} animals compared to WT animals (Figure 5-10A and Figure 5-11C, D). This data suggests that Bcl-3 might play a role in neutrophil biology, however, this is outwith the focus of this study and merits separate investigation.

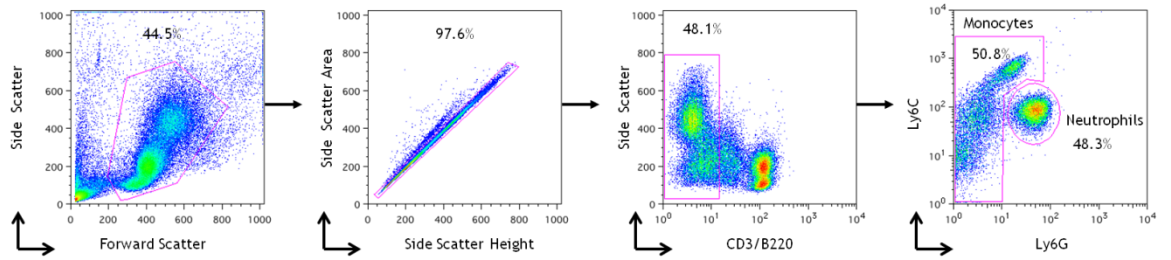
The three monocyte subsets in the blood and BM of WT and Bcl-3^{-/-} animals were examined. In the blood, Bcl-3 deficiency had no effect on the number of circulating monocyte subsets (Figure 5-12A). However, Bcl-3^{-/-} had fewer Ly6C^{high} and Ly6C^{low} monocytes in the BM (Figure 5-12B). In the BM, the OCP population is predominantly thought to be the main pre-OC^{4,103}, however, it has previously been observed that Ly6C^{high} BM monocytes can differentiate into OCs *in vitro*¹⁰³. Therefore, Bcl-3^{-/-} animals may have fewer pre-OCs present *in vivo* than WT controls.

The examination of CD115 expression on these pre-OC populations was also examined because CD115 is essential in the up-regulation of RANK and thus osteoclastogenesis⁶. Populations of CD115⁺ monocytes and monocyte subsets were identified based on their

forward scatter and expression of CD115 (Figure 5-13) and the percentage CD115⁺ cells was used to calculate the total number of CD115⁺ cells in each population. This revealed that Bcl-3^{-/-} animals had fewer CD115⁺ monocytes in the blood and BM, especially fewer Ly6C^{high} CD115⁺ monocytes when compared to WT controls (Figure 5-14A, B). As CD115 has an essential role in the differentiation of OCs *in vivo*, this data supports the idea that Bcl-3^{-/-} animals may have fewer pre-OCs present *in vivo*.

In order to ascertain whether the overall milieu of the BM was altered in Bcl-3^{-/-} animals mRNA was extracted from whole BM. mRNA for RANK and RANKL was quantified and revealed to be unchanged in Bcl-3^{-/-} animals compared to WT controls (Figure 5-15A, B). This would suggest that as an inducer of osteoclastogenesis the RANKL-RANK axis may be unaffected by Bcl-3 deficiency, however, further work needs to be done to validate this observation. At the same time, evaluation of the GM-CSF mRNA transcript level was examined. GM-CSF is a vital cytokine in the differentiation, chemotaxis and function of neutrophils^{417,418} and as such it was hypothesised that as the number of neutrophils present in the blood and BM are lower in Bcl-3^{-/-} animals the GM-CSF production may be altered. However, examination of GM-CSF mRNA showed that in Bcl-3^{-/-} BM had a slight, but significant, increase in the mRNA present compared to WT controls (p<0.01) (Figure 5-15C). This increase could be due to any population present in the BM up-regulating GM-CSF mRNA and due to the large number of cells present this increase has become diluted. Therefore, dissemination of which population up-regulates GM-CSF mRNA is required. Examination of day 5 OC mRNA showed that GM-CSF mRNA from WT and Bcl-3^{-/-} cultures were identical (Figure 5-15D). Thus, OCs are unlikely to be the cell responsible for this increase, however, further work will be required to determine if the increase in GM-CSF mRNA is physiologically relevant. An increase in GM-CSF is unlikely to induce the neutropenia observed in Bcl-3^{-/-} animals therefore further work must be done to understand this phenotype.

A) Blood



B) Bone Marrow

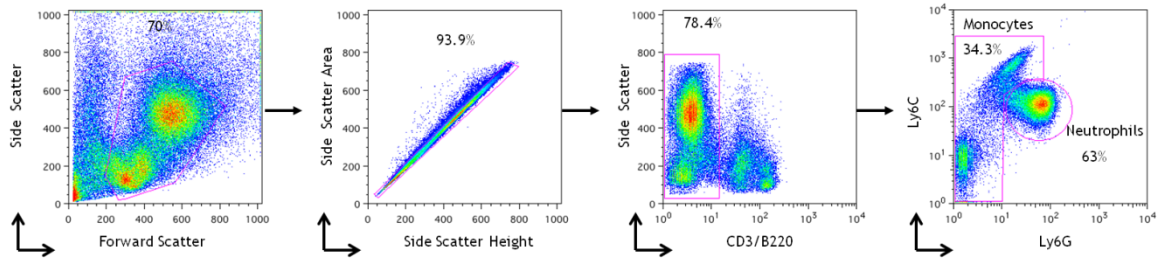


Figure 5-9: Gating strategy to identify blood and bone marrow monocytes.

A) Blood and B) BM cells were isolated from WT and *Bcl-3^{-/-}* animals. Per animal, 1×10^6 BM cells and the cells present in 200 μ l of blood were stained with CD3, B220, Ly6G, Ly6C and CD11b for FACS analysis. Representative FACS plots of gating strategies employed to distinguish monocytes are shown. Doublets were isolated from single cells by exclusion of events which had a non-linear relationship with Side Scatter Area versus Side Scatter Height and T and B cells were excluded by their expression of CD3 and B220. Monocytes and Neutrophils could then be identified based on their expression of Ly6C and Ly6G. Neutrophils express Ly6G and Ly6C, however, monocytes do not express Ly6G and can express Ly6C at high or low levels. Representative FACS plots shown are based on WT blood and BM cells. Percentages shown in FACS plots are of the percentage of cells present in the current gate.

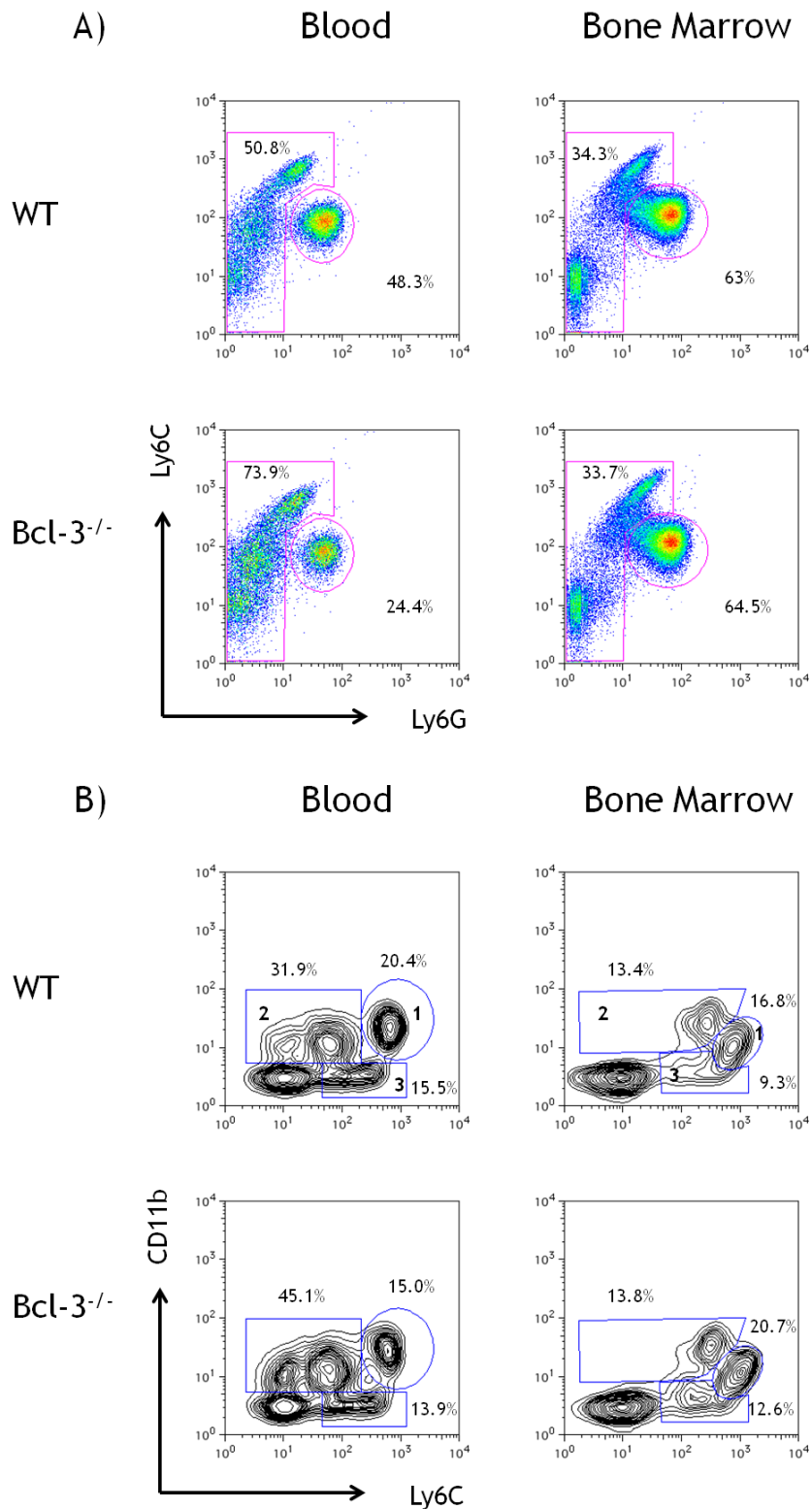


Figure 5-10: WT and Bcl-3^{-/-} blood and bone marrow monocyte and neutrophil populations. FACS analysis was performed as previously described (Figure 5-9). A) A comparison of representative FACS plots depicting monocyte (Ly6C⁺Ly6G⁻) and neutrophil (Ly6C⁺ Ly6G⁺) populations of the blood and BM from WT and Bcl-3^{-/-} animals. B) A comparison of representative FACS plots showing the three monocyte subset populations of the blood and BM based on their expression of Ly6C and CD11b. Ly6C^{high} classical monocytes (Population 1), Ly6C^{low} non-classical (Population 2) and OCP (Osteoprecursor - Population 3). Percentages shown are of the percentage of cells present in the current gate. All FACS plots are representative of one experiment.

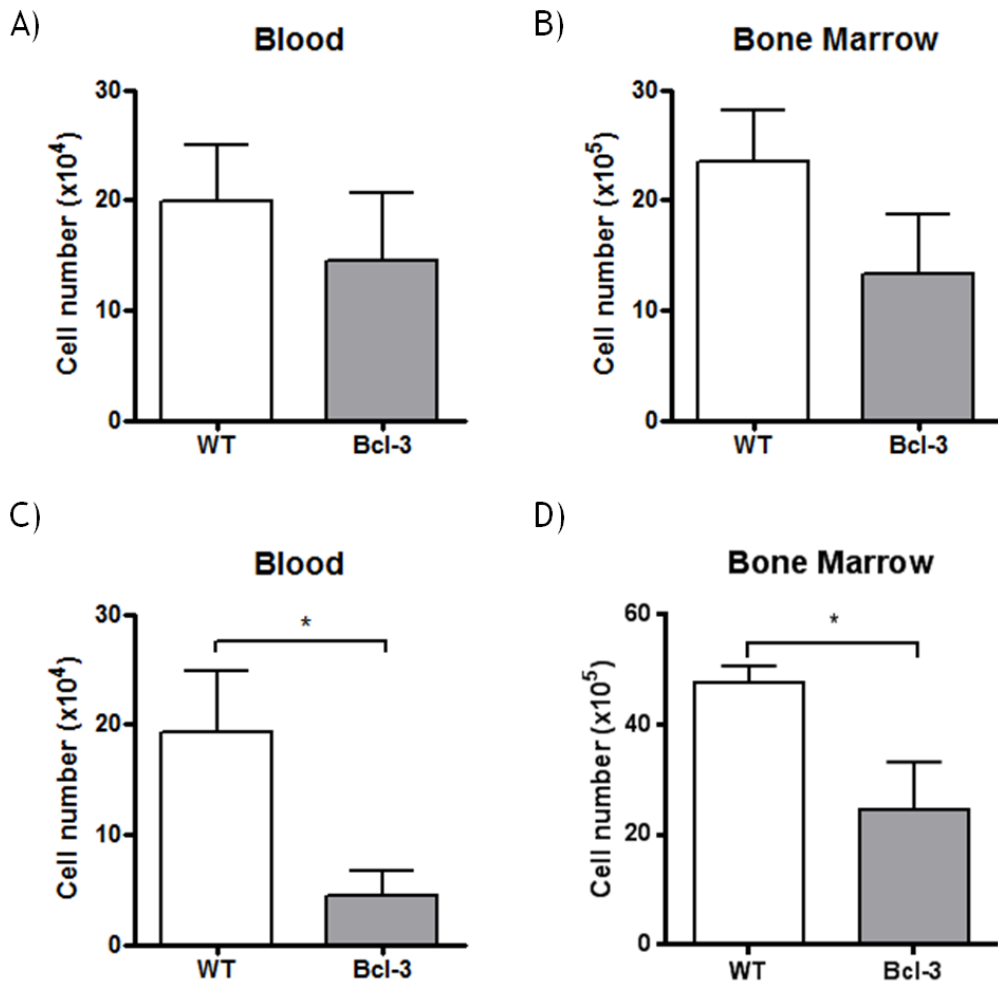


Figure 5-11: Number of total monocytes and neutrophils in WT and Bcl-3^{-/-} animals. Blood and BM were taken from WT and Bcl-3^{-/-} animals and prepared for analysis by flow cytometry. Cells were counted prior to staining for FACS analysis and a gating strategy previously shown (Figure 5-9) was used to isolate the number of total monocytes (Ly6C⁺ Ly6G⁻) and neutrophils (Ly6C⁺ Ly6G⁺) (Figure 5-10A). The % of monocytes or neutrophils defined by FACS analysis were used to calculate the absolute number of monocytes present in blood and BM. The number of monocytes from WT and Bcl-3^{-/-} animals in A) Blood and B) BM are shown. The number of neutrophils from WT and Bcl-3^{-/-} animals in C) Blood and D) BM are shown. WT and Bcl-3^{-/-} animals were compared using an unpaired two-tailed t-test; p < 0.05 (*). Data represents mean ± SD, n=3. Data representative of two separate experiments.

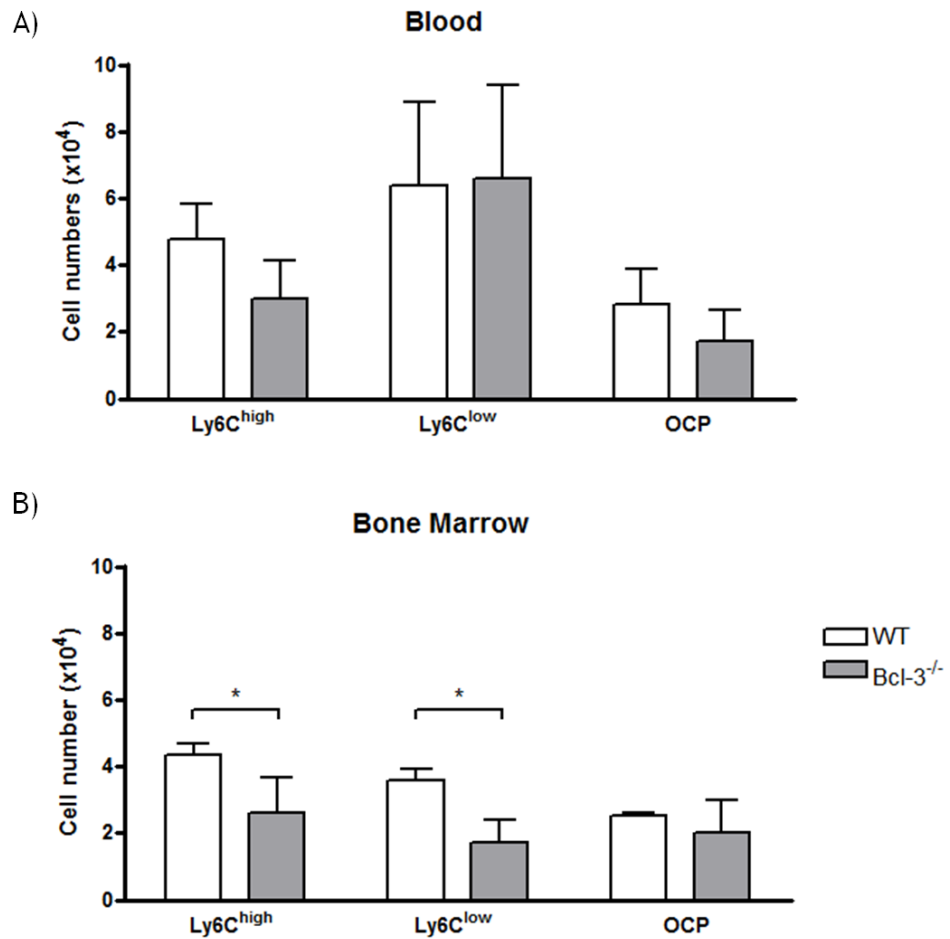


Figure 5-12: Monocyte subsets cell number in WT and Bcl-3^{-/-} animals.

Continuing on from the data shown in Figure 5-11, the expression of Ly6C and CD11b was used to identify monocyte subsets as described in Figure 5-10B. The % of cells in each monocyte subset was used to calculate the absolute number of monocytes present in both the blood and BM. The subsets of interest were the Ly6C^{high} monocytes, Ly6C^{low} monocytes and the OCP population (Ly6C^{high} CD11b^{low}). The absolute numbers of cells constituting these subsets in A) Blood and B) BM for WT and Bcl-3^{-/-} animals were calculated. Individual monocyte subsets from WT and Bcl-3^{-/-} animals were compared using a Two Way ANOVAs with Bonferroni's post-hoc test; $p < 0.05$ (*). Data represents mean \pm SD, $n = 3$.

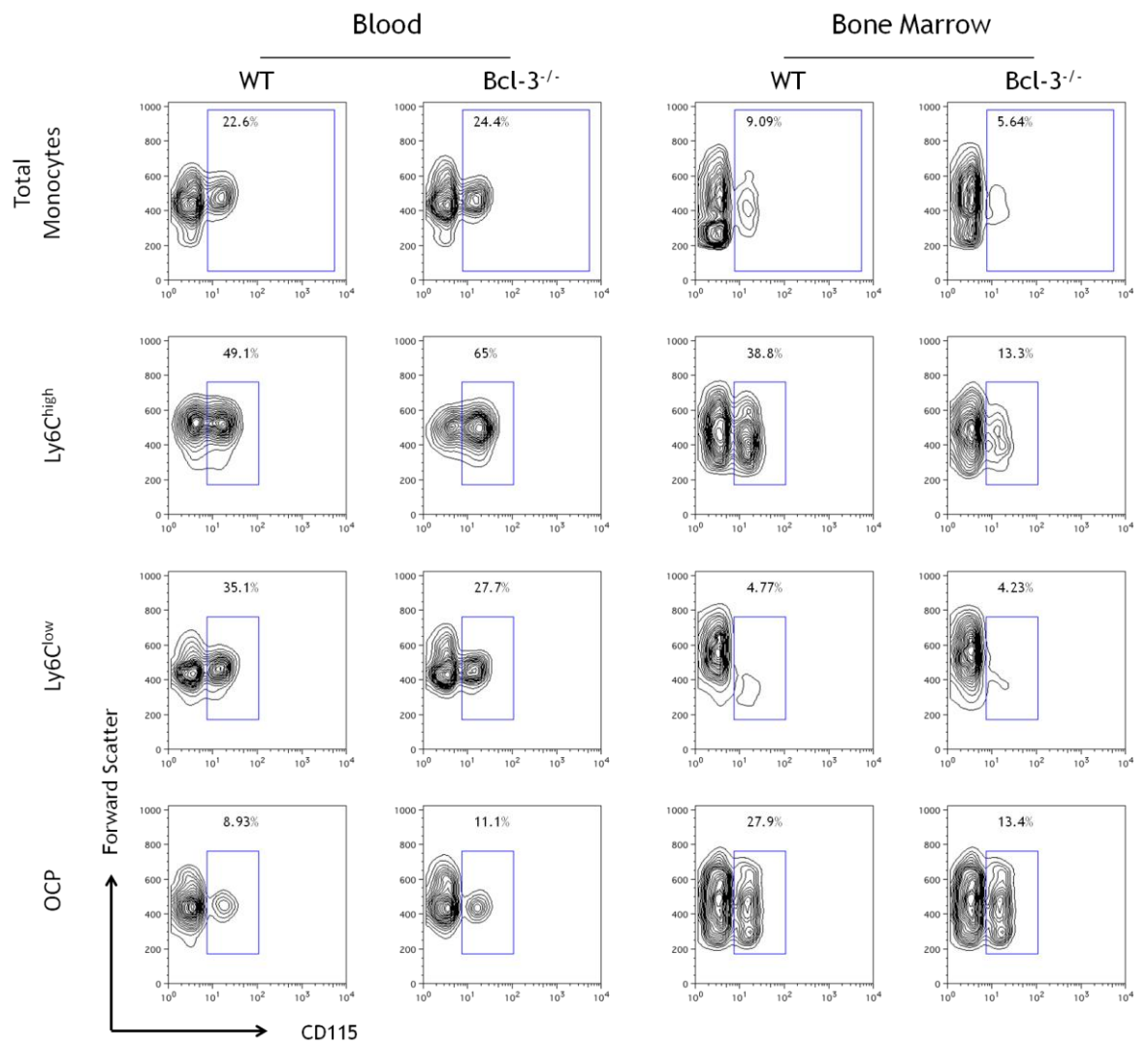


Figure 5-13: Representative FACS plots of CD115 expression on monocytes and monocytes subsets.

FACS analysis was performed on blood and BM from WT and Bcl-3^{-/-} animals. Monocytes and monocyte subsets were identified as previously described (Figure 5-9 and Figure 5-10). Fluorescence minus one (FMO) control was used to identify the CD115 expressing cells in each monocyte population. Representative FACS plots of CD115⁺ cells in blood and BM monocytes and monocytes subsets are shown from WT and Bcl-3^{-/-} animals. Percentages shown are of cells present in the current gate. All FACS plots are representative of one experiment.

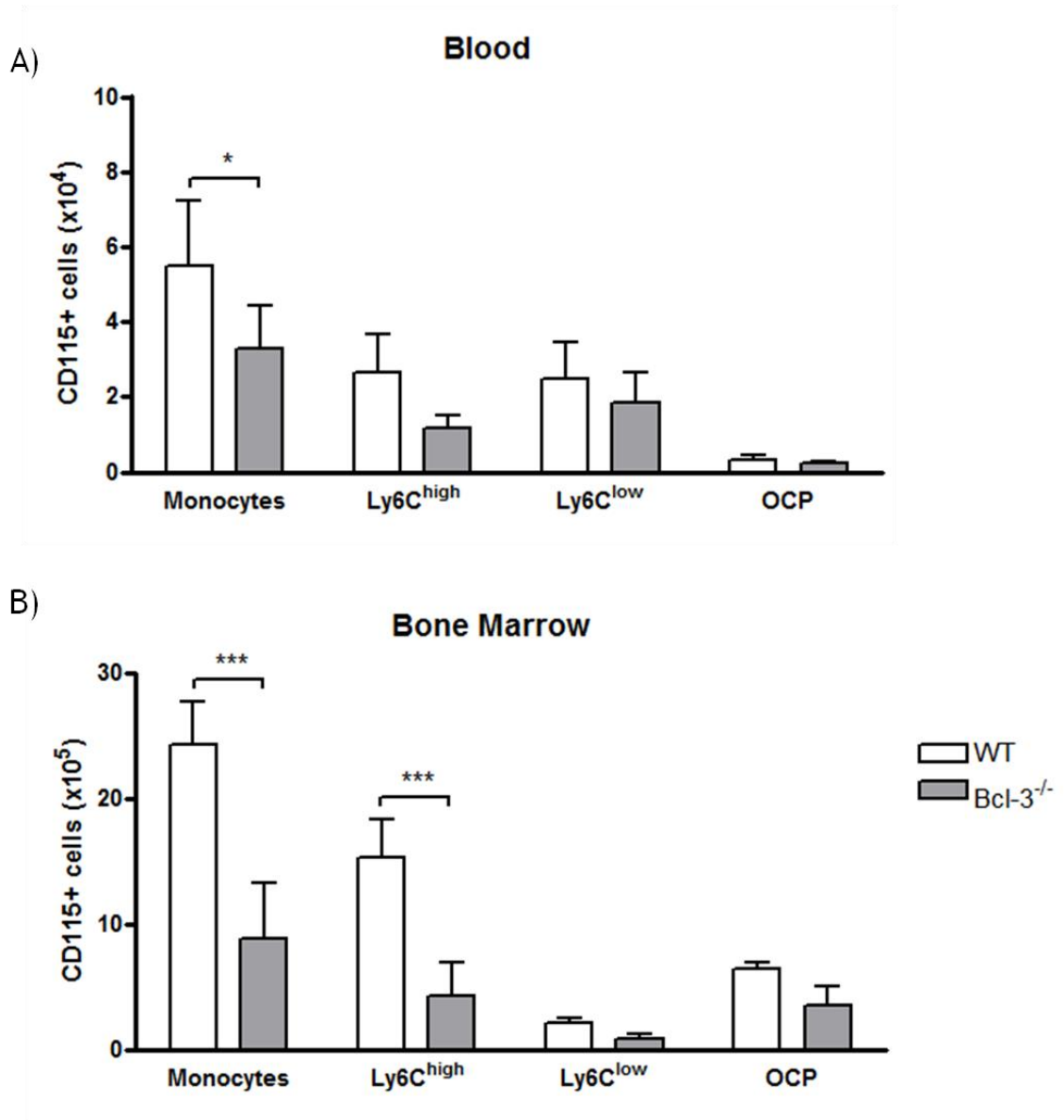


Figure 5-14: CD115 expressing monocytes in WT and Bcl-3^{-/-} animals.

Blood and BM taken from WT and Bcl-3^{-/-} animals were isolated and prepared for flow cytometry. The gating strategy shown (Figure 5-9 and Figure 5-10) was used to isolate total monocytes and monocyte subsets for analysis of CD115 (Figure 5-13). The number of CD115⁺ cells in A) Blood and B) BM monocytes and monocyte subset populations was calculated from the % of CD115⁺ cells and the total number of cells isolated from each animal. Individual monocyte populations of WT and Bcl-3^{-/-} animals were compared using a two way ANOVA's with Bonferroni's post-hoc tests; p<0.05 (*) and p<0.001 (***). Data represents mean ± SD, n=3. Data represents one experiment.

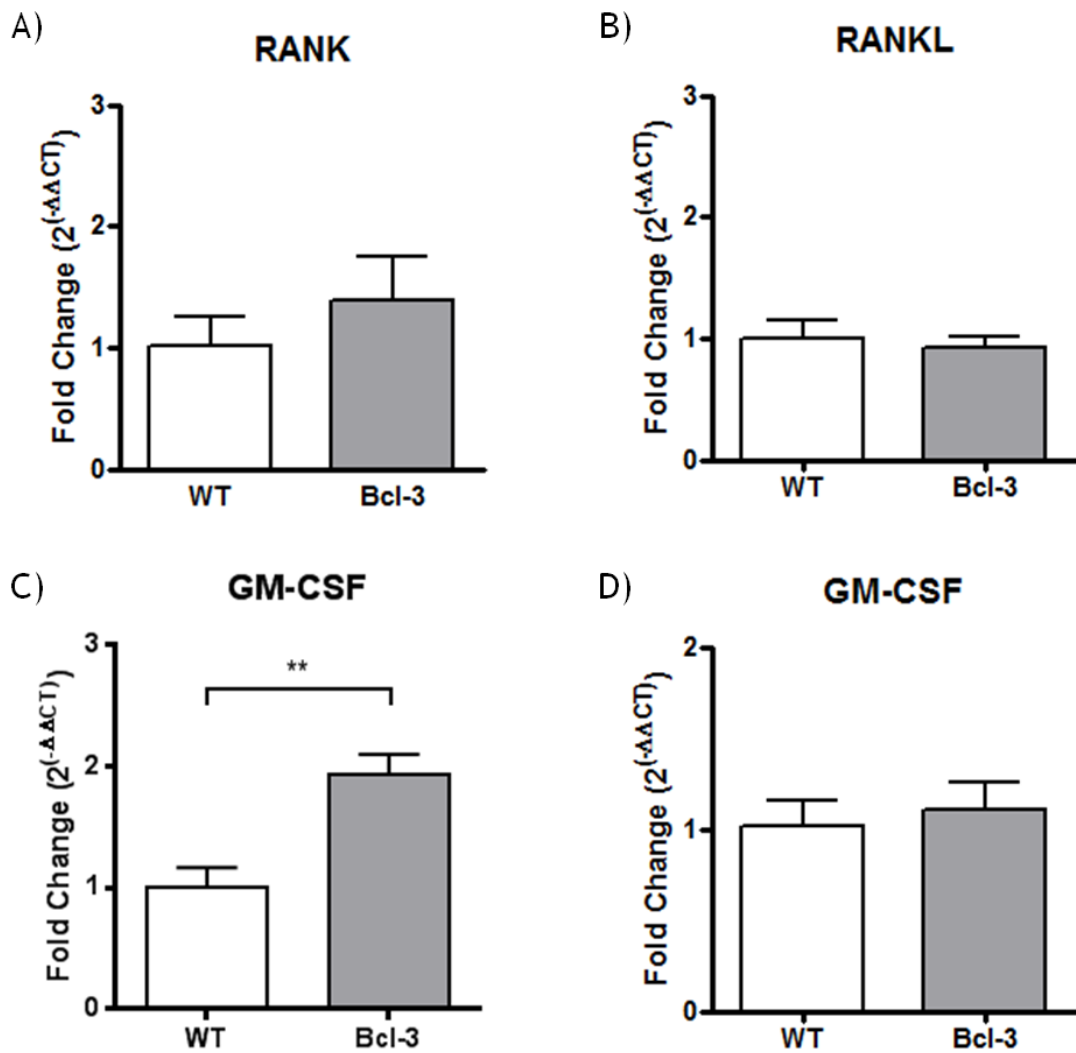


Figure 5-15: GM-CSF mRNA transcript is up-regulated in Bcl-3 bone marrow.

A-C) 1×10^6 murine WT and Bcl-3^{-/-} BM cells were lysed, mRNA extracted, cDNA generated and qPCR performed on all samples which were run in triplicate. D) NA BM cells cultured for 5 days in the presences of 75ng/ml M-CSF and 50ng/ml RANKL were lysed, mRNA extracted, cDNA generated and qPCR performed on all samples which were run in triplicate. For all samples, GAPDH was used as the housekeeping control and non-template controls were run for each gene. Fold Change ($2^{(-\Delta\Delta CT)}$) was measured by normalising samples of each primer to the housekeeping control (ΔCT). Subsequently Bcl-3^{-/-} ΔCT 's were normalised to the average WT ΔCT to obtain the $\Delta\Delta CT$. This was then used to obtain the fold change ($2^{(-\Delta\Delta CT)}$). To obtain the spread of WT data, each WT ΔCT was compared to the average WT ΔCT and fold change calculated. WT and Bcl-3^{-/-} samples were compared using an unpaired two-tailed t-test; $p < 0.01$ (**). Data represents mean \pm SD, $n=3$.

5.2.6 Bcl-3 deficiency results in perturbed bone remodelling

Although we observed no overt difference in osteoclastogenesis, due to the previously described role of NF- κ B signalling in bone remodelling the *in vivo* architecture of the tibial trabecular bone was examined. Tibias were removed from 12 week old WT and Bcl-3^{-/-} male mice. The age of the animals was selected because at this point male mice have a fully mature skeletal system which removes any variance that younger mice might introduce into the study as their skeletal system develops at a rapid rate⁴¹⁹. Male mice have higher bone mass than female mice and also less variance due to limited exposure to oestrogen which can influence bone remodelling⁴¹.

μ CT was used to interrogate the trabecular bone present in the proximal tibia (Figure 5-16A). Analysis of the trabecular region revealed that Bcl-3^{-/-} animals had significantly more bone present than WT, as measured by BV/TV (WT - 18.9% versus Bcl-3^{-/-} - 23.1%; $p < 0.001$) (Figure 5-16B). Further analysis of the trabecular bone showed that the number of trabecular structures was increased ($p < 0.05$) and the space between trabeculae was decreased ($p < 0.05$) when compared to WT controls (Figure 5-16C, D). Interestingly, there was no difference in the structural model index, thickness of trabeculae or the intersection surface (Figure 5-16E-G). Other parameters of trabecular structure were measured to examine the differences between WT and Bcl-3^{-/-} animals (Table 5-1). These results revealed that Bcl-3^{-/-} animals had normal trabecular structure compared to WT, yet the increase in bone volume suggests that there is an uncoupling in the bone remodelling process between WT and Bcl-3^{-/-} animals.

In order to test whether the increase in bone volume in Bcl-3^{-/-} animals was due to a deficiency in *in vivo* OCs, histology was undertaken on μ CT scanned tibias. Sections were stained with haematoxylin and eosin (H&E) which showed that WT and Bcl-3^{-/-} tibias had a similar trabecular bone and growth plate structure (Figure 5-17A). TRAP staining was performed on these sections which revealed the presence of OCs in Bcl-3^{-/-} tibias (Figure 5-17B). Therefore, the increase in bone present in the trabecular region of the tibia in Bcl-3^{-/-} animals was not due to an absence of OCs. In order to fully examine the histomorphometry of these animals more research needs to be done to count the number of OCs and OBs present in the trabecular bone. This could provide insight in the *in vivo* differentiation of OCs and OBs in the Bcl-3^{-/-} animals and using a larger sample size could definitively prove whether Bcl-3^{-/-} animals have differences in bone remodelling.

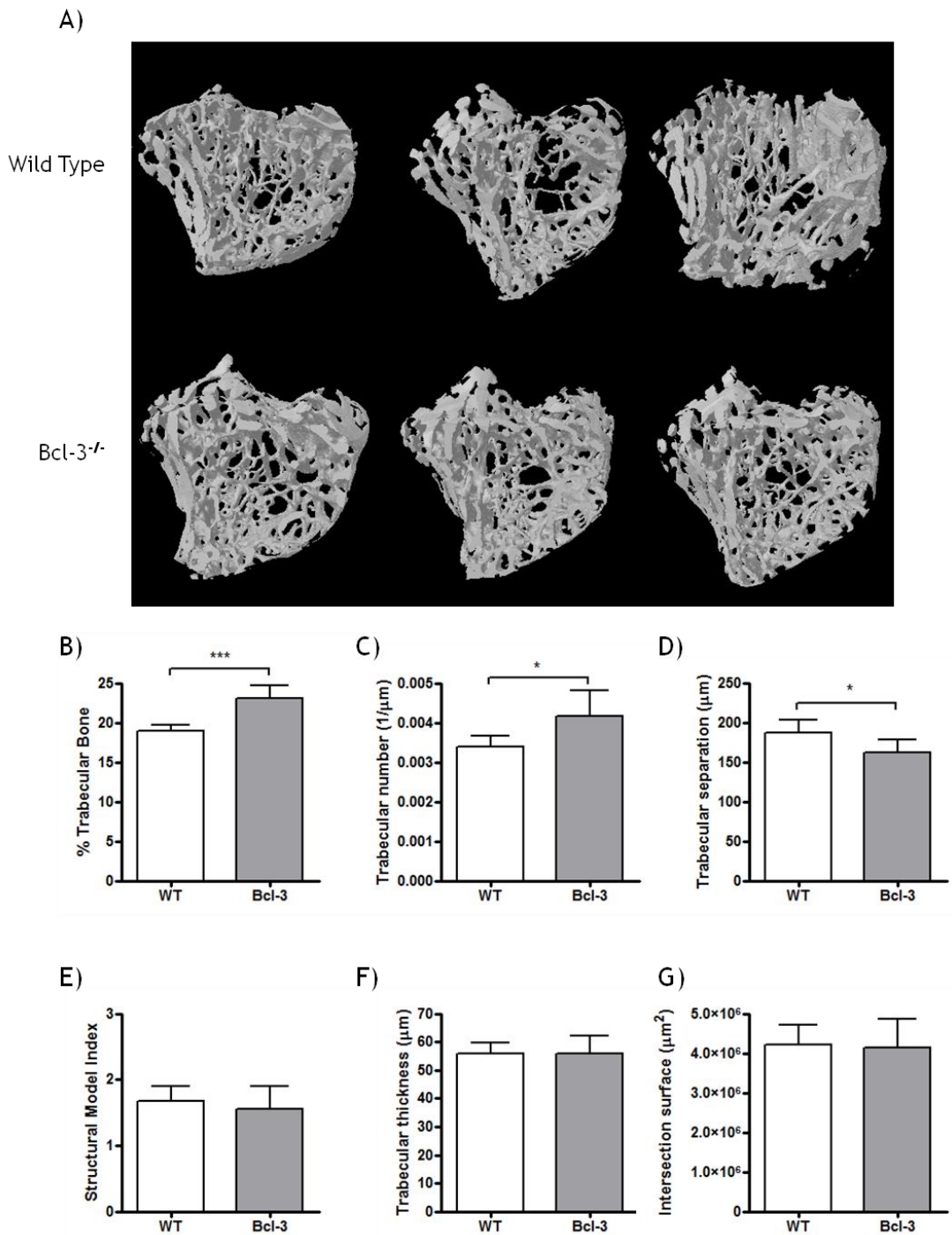


Figure 5-16: μ CT analysis of trabecular bone of proximal tibia from WT and Bcl-3^{-/-} animals. The left tibias of WT and Bcl-3^{-/-} animals were taken at 12 weeks of age. Tibias were fixed overnight in 4% para-formaldehyde before storing bones in 70% ethanol. To analyse the bone volume in the tibia, bones were scanned using a SkyScan 1172 μ CT scanner. Trabecular bone was identified and analysed using SkyScan CTAn software. A) Representative images of trabecular bone reconstructions of WT (top panel) and Bcl-3^{-/-} (bottom panel) animals, B) % of Trabecular bone (BV/TV), C) Trabecular number (1/ μ m), D) Trabecular separation (μ m), E) Structural Model Index (SMI), F) Trabecular thickness (μ m) and G) Intersection surface (μ m²). WT and Bcl-3^{-/-} animals were compared using an unpaired two-tailed t-test; $p < 0.05$ (*), $p < 0.001$ (***)). Data shown represents mean \pm SD, n=6.

Parameter	Units	μ CT Analysis	
		WT	Bcl-3 ^{-/-}
Bone volume / tissue volume	%	18.9 \pm 0.81	23.1 \pm 0.71 ***
Bone volume	μm^3	4.08E+08 \pm 4.94E+07	5.46E+08 \pm 3.972E+07 **
Tissue volume	μm^3	2.15E+09 \pm 1.89E+08	2.36E+09 \pm 1.01E+08
Tissue surface	μm^2	1.23E+07 \pm 857321	1.25E+07 \pm 782304
Bone surface	μm^2	2.98E+07 \pm 3.65E+06	3.51E+07 \pm 6.04E+06
Intersection surface	μm^2	4.22E+06 \pm 481020	4.15E+06 \pm 723174
Bone surface / Bone volume	1/ μm	0.0673 \pm 0.005558	0.06922 \pm 0.004409
Bone surface density	1/ μm	0.01338 \pm 0.0009311	0.01528 \pm 0.00215
Trabecular thickness	μm	56.02 \pm 3.879	55.98 \pm 6.048
Trabecular separation	μm	187 \pm 15.75	161.6 \pm 16.64 *
Trabecular number	1/ μm	0.003394 \pm 0.0002643	0.004176 \pm 0.0006491 *
Trabecular pattern factor		0.01584 \pm 0.003009	0.01482 \pm 0.00399
Structural model index		1.682 \pm 0.2235	1.556 \pm 0.3369
Connectivity		1005 \pm 442.4	1147 \pm 243.7
Degree of anisotropy		2.306 \pm 0.1889	2.482 \pm 0.4008
Connectivity density	1/ μm^3	4.56E-07 \pm 2.10E-07	4.97E-07 \pm 7.35E-08

Table 5-1: All μ CT analysis parameters of trabecular bone of the proximal tibia in WT and Bcl-3^{-/-} animals.

As previously outline (Figure 5-16), all μ CT analysis parameters are provided. Unpaired two-tailed t-tests were used to compare WT and Bcl-3^{-/-} animals; p<0.05 (*), p<0.01 (**) and p<0.001 (***). Data shown is the mean \pm SD, n=6.

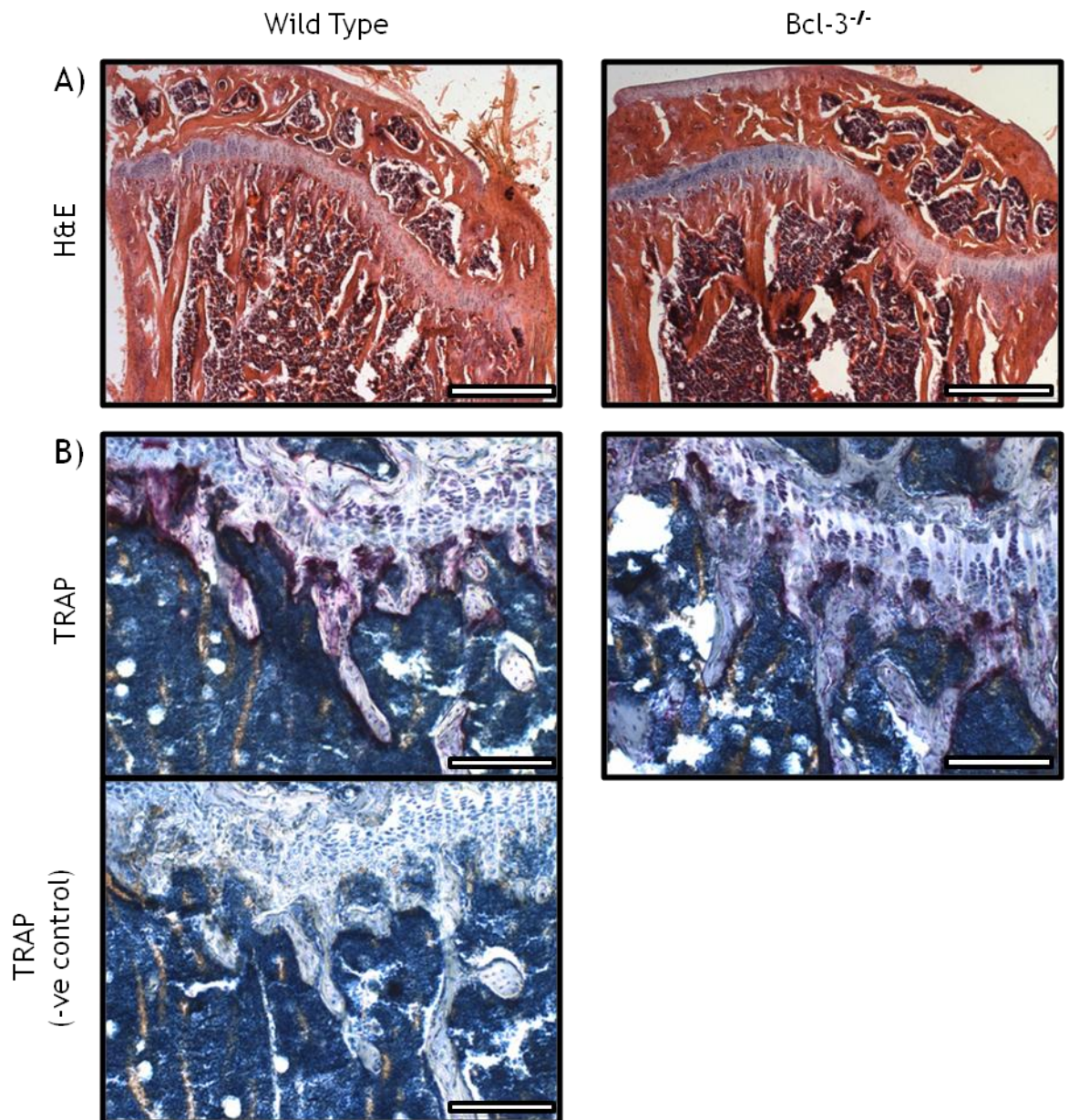


Figure 5-17: The presence of osteoclasts in Bcl-3^{-/-} tibias.

The left tibias of WT and Bcl-3^{-/-} animals were taken at 12 weeks of age. Tibias were fixed overnight in 4% para-formaldehyde before decalcification in 14% EDTA pH 8 until bones were pliable. 20µm coronal sections of the proximal tibia were following paraffin wax embedding. A) Representative images of Haematoxylin and Eosin (H&E) staining of tibial sections. Scale bar is 500µm. B) Representative images of TRAP staining of tibial sections (Purple - TRAP and Blue - Haematoxylin). Negative control for TRAP stain was included. 3-5 serial sections per tibia, n=3. Scale bar; 200µm.

5.3 Discussion

NF- κ B is an essential regulator of osteoclastogenesis via the roles of p50, p52, p65 and RelB^{145,162,176}. These components bridge both the canonical and non-canonical NF- κ B pathways which are essential in the *in vitro* and *in vivo* differentiation of fully functional OCs. Following stimulation of RANK by RANKL, these subunits translocate to the nucleus and initiate transcription of OC essential genes¹⁶⁴. The role of the negative regulator of NF- κ B signalling, Bcl-3, has not been examined as an osteoclastogenic regulator. Thus this investigation aimed to examine whether Bcl-3 influenced *in vitro* and *in vivo* osteoclastogenesis.

In response to stimuli, various receptors can activate NF- κ B signalling resulting in the transcription of a huge number of genes¹⁶⁷. As Bcl-3 is under NF- κ B control, transcription of Bcl-3 acts in a negative feedback loop to dampen the primary response and limit a possible secondary response from stimuli⁴²⁰. Therefore, the absence of Bcl-3 can result in uncontrolled NF- κ B mediated transcription. In the present study, RANKL was used as the activator of NF- κ B and as such, was shown to induce Bcl-3 transcription (Figure 5-2). However, RANKL stimulation of WT and Bcl-3^{-/-} NA BM induced the differentiation of OCs (Figure 5-4). This differentiation of OCs was also inhibited by stimulation of Fc γ Rs by IgG alone and in IgG complexes with SpA (Figure 5-8). This suggests the mechanism used by Fc γ Rs to inhibit osteoclastogenesis in response to IgG does not utilise Bcl-3 and that WT and Bcl-3^{-/-} pre-OCs respond in a similar manner to stimulation. Evaluation of essential OC mRNA transcription failed to show any differences between WT and Bcl-3^{-/-} *in vitro* cultures (Figure 5-5 and Figure 5-6). Importantly, WT and Bcl-3^{-/-} cultures were not tested for OC activity on bovine bone, therefore it remains to be confirmed whether Bcl-3^{-/-} pre-OCs differentiate into functional OCs.

One noticeable difference between WT and Bcl-3^{-/-} OC cultures was that by day 7, there were nearly twice as many OCs present in WT than Bcl-3^{-/-} cultures (Figure 5-4). One possible explanation for this is the variety of progenitors present in the BM at different differentiation stages responding to M-CSF and RANKL over a series of days. This would suggest that Bcl-3^{-/-} cells have a deficit in one of these progenitor populations and thus could not differentiate into OCs to the same degree as WT cells. Further work would need to be done to evaluate the effect of Bcl-3 on myelopoiesis and whether there was a defect in the BM progenitor populations. In order to do this, FACS analysis could investigate the populations of progenitors which are lineage negative and CD117 and CD135 positive. This would give a good insight into the progenitor populations present. These differences may also be caused by Bcl-3's ability to act as a pro-survival factor,

as Bcl-3 can enhance adjuvant driven T cell proliferation and survival⁴²¹. In the absence of Bcl-3, stimulated T cells have increased levels of the pro-apoptotic factor Bim, while over expression of Bcl-3 lowers the concentration of Bim present and enhances T cell survival⁴²². Due to the availability of reagents examination of anti-apoptotic mediators, Bcl-2 and Bcl-XL, was done and showed that at day 5 there was no difference between WT and Bcl-3^{-/-} OCs. However, examination of pro- and anti-apoptotic factors at later time points, day 6 and 7, could provide insight into Bcl-3's role as a survival factor in OCs. Examination of Bim on these days could demonstrate whether there are differences in the ability of Bcl-3 to act as a survival factor in T cells and myeloid cells. Interplay may exist following OC stimulation, whereby Bcl-3 enhances the survival of OCs in long term cultures; however, this remains to be investigated.

To fully evaluate the role of Bcl-3 in the differentiation of OCs it would be essential to investigate the early response of cells to RANKL. This is possible by culturing NA BM cells and examining the effect of RANKL induced p50:p65 nuclear translocation and the processing of p100:RelB to p52:RelB. ChIP analysis could also be conducted to examine the ability of Bcl-3:p50/p52 and NF-κB subunits to bind to NF-κB sites on the gene promoters of OC essential genes such as *NFATc1* following RANKL stimulation. The transcription of mRNA at an earlier time point could indicate whether Bcl-3 acts as an osteoclastogenic regulator. Further examination gene promoters like *nfatc1*, *rank* and even OC specific genes like *dc-stamp* and *trap* may reveal potential Bcl-3:NF-κB binding sites and infer an activatory or suppressive activity of this complex⁴²³. This could be done using ChIP analysis to reveal which NF-κB subunits bind to amplified regions of the gene promoters. It should be appreciated that the view of Bcl-3 as an NF-κB regulator is evolving. Bcl-3 is capable of interacting with AP1 to drive expression of AP1 specific targets⁴²⁴. Deletion of *c-fos*, a component of AP1, results in osteopetrosis and prevention of RANKL induced osteoclastogenesis¹⁴⁴. AP1 promotes cell survival⁴²⁵ and drives the differentiation of OCs¹⁴⁴, thus Bcl-3 may have a role in this interaction. Examination of these interactions following RANKL stimulation would reveal whether Bcl-3 has a role in regulating the initial stages of osteoclastogenesis.

Monocytes serve as a pool of pre-OCs and can be used *ex vivo* to generate OCs³⁶⁶. Therefore, examination of Bcl-3^{-/-} animals for defects in this population was undertaken. Blood and BM monocytes were identified on the basis of their expression of Ly6C^{+/-} Ly6G⁻³⁸⁴ allowing discrimination with Ly6C⁺ Ly6G⁺ neutrophils. Interestingly, identification of the neutrophil population revealed fewer blood and BM neutrophils in Bcl-3^{-/-} animals compared to WT counterparts (Figure 5-11). Bcl-3 may also have an effect at an early stage of differentiation and influence the myelopoiesis of neutrophils from progenitors in the BM. As mentioned, identification of BM stem cells would allow

further comparison of the effects that the absence of Bcl-3 incurs. The presence of GM-CSF mRNA present in BM was examined, because of its pleiotropic effects on neutrophils and bone biology. GM-CSF is involved in stimulating neutrophil differentiation from BM progenitors and acts as a chemotactic during inflammation^{417,418}. It is also a known pro-OC factor and stimulates the differentiation and activity of OCs⁴²⁶, but it also increases the proliferation and activity of OBs^{427,428}, enhancing bone remodelling. When examined there was an increase in GM-CSF mRNA in the BM of Bcl-3^{-/-} animals was observed compared to WT animals. This is counter-intuitive as an increase in GM-CSF should result in the production of neutrophils. It could be speculated that the gene encoding GM-CSF, *csf2* is transcribed under NF- κ B or AP1 control and thus in the absence of Bcl-3, *csf2* transcription becomes dysregulated leading to an increase in transcription. Cultured OCs do not alter expression of GM-CSF mRNA, therefore another cell type may be responsible for this increase *in vivo*. Protein concentration of GM-CSF needs to be examined to ensure that the difference in mRNA relates to a physiologically relevant change. Another cytokine that is known to influence neutrophil differentiation is G-CSF and this could also be investigated to further elucidate the link between Bcl-3 and neutrophil biology.

However, following examination of neutrophils, the number of monocytes and monocyte subsets in WT and Bcl-3^{-/-} animals was examined. This revealed that there were fewer Ly6C^{high} and Ly6C^{low} monocytes present in the BM of Bcl-3^{-/-} animals (Figure 5-12). Following further examination of this population, the number of CD115⁺ monocytes were deficient in the blood and BM of Bcl-3^{-/-} animals compared to WT controls. As the receptor for M-CSF, CD115 can be used as an identifier of pre-OCs⁴ and has been shown to be essential in driving RANK expression in pre-OCs⁶. With a decrease in the cells expressing this receptor there is the potential for an *in vivo* defect in the cells differentiating to OCs. This may itself provide an explanation for the difference in bone volume observed in WT and Bcl-3^{-/-} animals' trabecular bone and the difference in *in vitro* OC numbers at day 7.

Following the observation that there was a defect in the CD115⁺ monocytes the micro-architecture of the tibial bone was examined to determine whether Bcl-3 had an effect on bone remodelling. This revealed that Bcl-3^{-/-} animals had increase in bone volume in the trabecular region of the proximal tibia (Figure 5-16). This increase in bone density would indicate that bone remodelling had become perturbed in Bcl-3^{-/-} animals, suggesting that Bcl-3^{-/-} may have roles in bone remodelling beyond OCs. Further work needs to be done to fully identify further changes in trabecular and cortical bone architecture, as well as the potential gender and age differences. However, this increase in bone volume was not due to an absence of OCs *in vivo* (Figure

5-17). Further work would need to be undertaken to determine the number of TRAP+ cells present in the tibial trabecular region of WT and Bcl-3^{-/-} animals, this would have shown if Bcl-3^{-/-} animals had a deficit in the number of *in vivo* OCs. Bcl-3^{-/-} BM also had similar levels of RANK and RANKL mRNA present compared to WT, suggesting that this axis is unaffected by Bcl-3 deficiency (Figure 5-15). However, the presence of OPG could be measured to ensure that there was no increase in OPG which would inhibit OC differentiation and could account for the increase in bone volume.

The Bcl-3^{-/-} animals have a global deletion of the *bcl3* gene which will exert effects on all cell types. Therefore, to dissect the effect that Bcl-3 has on bone remodelling, OBs must also be examined. The role of NF-κB in the differentiation of OBs is complex as activation of NF-κB during differentiation inhibits maturation⁴²⁹. However, OBs require the NF-κB subunit p50 for TNF-α mediated secretion of M-CSF⁴³⁰. Yet, Yao *et al* (2014) demonstrated that RelB was a negative regulator of OB differentiation and function⁴²⁹. Indicating that the role of Bcl-3 in regulating OBs may be complex and the differentiation of OBs from WT and Bcl-3^{-/-} animals would dissect the differences between these genotypes. The differentiation of OBs and OCs in co-cultures could also reveal if there are cell specific abnormalities. By using cultures of mixed genotype WT or Bcl-3^{-/-} OBs could be co-cultured with WT or Bcl-3^{-/-} pre-OCs. The level of osteoclastogenesis could demonstrate if the absence of Bcl-3 alters the relationship between these cell types. To further examine the capacity of OBs to function *in vivo*, bone formation can be measured by use of calcein double labelling, as calcein only binds to newly formed matrix. By administering two doses of calcein and visualisation of the bone matrix by histology the rate of bone formation can be measured by the distance between layers of calcein. This would indicate whether OBs from Bcl-3^{-/-} animals can form bone at a higher rate than WT animals and may be the reason for the increased tibial bone volume in Bcl-3^{-/-} animals.

However, as a global gene deletion the Bcl-3^{-/-} genotype is known to effect the activity of a number of other cells including B cells. B cells are known to be a major contributor to OPG production within the BM and if Bcl-3 were to influence B cell production of OPG there could be ramifications on bone remodelling. As such, the generation of two transgenic mouse strains with OC and OB specific Bcl-3 gene deficiencies would allow absolute observation of the effect of Bcl-3 in these cells *in vivo*. The use of *Cre-lox* technology to generate an OC specific Bcl-3 deletion under the control of the Cathepsin K promoter and osteocalcin promoter for OBs would be an excellent tool to examine the effects of Bcl-3 deficiency in an otherwise ordinary environment.

Studies have shown that Bcl-3 modulates NF- κ B activation by sequestering p50/p52 homo- and hetero- dimers on NF- κ B sites and the absence of Bcl-3 can result in enhanced production of pro-inflammatory cytokines following stimulation with TNF- α or LPS¹⁶⁷. This present study demonstrated that RANKL could induce Bcl-3 transcription and result in the differentiation of OCs in Bcl-3^{-/-} cells. The role of Bcl-3 *in vivo* was shown to influence CD115⁺ monocytes and neutrophils numbers, however further work is required to examine this observation. Interestingly, Bcl-3 deficiency increased trabecular bone volume compared to WT animals. This confirmed that Bcl-3 had an impact on bone remodelling, however further work is required to understand the role of Bcl-3 in this process.

6 General discussion

This thesis examined the potential for SpA IgG complexes as a novel therapeutic in osteoporotic disease. Osteoporosis is a condition resulting from a disruption between the immune and skeletal system due to menopausal oestrogen deficiency³⁸⁰. The animal model used to study this disease was the OVX model which was induced by the removal of the ovaries to simulate the menopause⁴⁰. The result is a species and strain specific bone loss in the femur, tibia and vertebrae, emulating human disease³⁹. Every second day following surgery animals were treated with 100µg SpA or OVA. We observed that SpA had no effect on the bone loss in the OVX model. Previous work had shown that 100µg SpA was able to reduce inflammation and OCs numbers in inflamed joints of CIA animals³¹⁶. A dose of 100µg SpA may have been optimal for treating inflammation in the CIA model, however, we hypothesis that a higher dose may be required to combat osteoclastogenesis in the OVX model. Further research is required to discover the optimal dose of SpA to exert an *in vivo* anti-osteoclastogenic effect. It has been shown that high doses of SpA (1.5mg) can reduce the serum IgG concentration²⁹⁹, thus the dose must be carefully monitored to ensure that there is no detrimental effects on serum IgG concentration following long term treatment. These pharmacokinetic experiments could inform the correct dose to test SpA's ability to treat the OVX model of disease and determine whether SpA mediated FcγR modulation is capable of treating osteoporotic disease.

The bioavailability of SpA is also an important factor as SpA can induce B cell apoptosis via the Fab VH3 domain of surface IgM^{271,308,309}. However, SpA's ability to interact with von Willebrand factor and, in particular, TNFRI is also important^{431,432}. TNFRI is expressed on multiple cell types including epithelial cells, keratinocytes and OBS^{431,433,434}. In animals models, *S. aureus* interacts directly with OBs in an SpA dependent manner⁴³⁵. This interaction can result in enhanced RANKL production and decreases OPG secretion by OBs⁴³⁵. It is currently believed that SpA triggers TNFRI NF-κB signalling, resulting in secretion of inflammatory cytokines and contributing to diseases like osteomyelitis^{435,436}. However, this particular interaction requires the IgG binding domain and as SpA treated systemically co-opts circulating IgG, the interaction between SpA and OBs may not be physiologically relevant, but may require further investigation^{316,431}.

Recently, a highly purified form of SpA (PRTX-100) has been used in clinical trials⁴¹⁰. In these safety trials, intravenous low doses of SpA (0.3-0.45µg/kg) were safe with only a small number of individuals presenting with adverse effects, while individuals given higher doses (5,10 and 20µg/kg) were more likely to suffer side effects⁴¹⁰. Side effects

included headaches, myalgia and nausea⁴¹⁰. At low doses, patients given SpA had a decrease in circulating lymphocytes, however, the effect on monocyte populations were not studied⁴¹⁰. Clinical trials are on-going and aimed at determining the effect of PRTX-100 in RA patients⁴¹⁰. It should be appreciated that this study observed the production of anti-SpA antibodies after treatment with PRTX-100, which resulted in enhanced clearance of SpA following administration⁴¹⁰. To use SpA clinically a novel SpA mimetic needs to be developed that can engage FcγRs, while removing SpA's immunogenicity.

The inability of SpA to alter disease progression in the OVX model was not mirrored *in vitro* because SpA was able to form IgG complexes that inhibit murine osteoclastogenesis. The differentiation of OCs from BM cells isolated from mice and cultured with M-CSF and RANKL could be inhibited by treatment with SIC or Oplg. Importantly, SIC was able to inhibit osteoclastogenesis in an FcγRIII independent manner. Yet, Oplg required the presence of FcγRIII to inhibit osteoclastogenesis suggesting that aggregates are present in the Oplg preparation that have the capacity to interact with this low affinity receptor to inhibit osteoclastogenesis. Importantly, SIC but not Oplg, was able to limit *in vitro* OC-mediated bone erosion.

Although in the murine system, both Oplg and SIC were able to inhibit osteoclastogenesis, previous studies have demonstrated that Oplg could not inhibit the differentiation of human OCs³¹⁶. Why there is a difference between murine and human *in vitro* systems is not fully understood. The only constituents of Oplg are IgG and OVA, and OVA should be an inert protein in this system: unable to be bound by polyclonal IgG and unable to bind to any monocyte receptors. Given the unexplained result, even though the combination of OVA and IgG might seem to be the ideal control, further studies should be undertaken to categorically determine the effect of purified polyclonal IgG in the murine system. In addition, use of antibody:antigen complexes provide a more physiologically relevant method of FcγR engagement. Complexes consisting of OVA and anti-OVA IgG would have the ability to interact with FcγRs and the ratio of antigen to antibody would inform the FcγR binding affinity²⁷⁹. Therefore, studies using SpA IgG complexes, OVA immune complexes and monomeric polyclonal IgG (Oplg) to modulate OC differentiation would yield valuable insight into effect of FcγR modulation during osteoclastogenesis.

FcγR modulation alters the mRNA transcription of pre-OC resulting in decreased levels of mRNA for genes such as Cathepsin K, DC-STAMP, OSCAR and TRAP which are required for the maturation of OCs^{7,154,242,336}. Studies that examined siRNA mediated down-regulation of DC-STAMP mRNA revealed that DC-STAMP is essential for the fusion

of pre-OC^{220,363}. Treatment with SIC and Oplg prevented RANKL induced DC-STAMP up-regulation and thus pre-OC fusion was inhibited. However, to confirm that the observed changes in mRNA transcription represented a physiological change the protein level of each corresponding mRNA transcript should be quantified. In this thesis, only OC specific mRNA transcription was investigated, yet, examination of MØ specific mRNA levels may identify the differentiation pathway FcγR modulated cells undertake. Previously, Grevers *et al* (2013) used heat-aggregated rabbit IgG to inhibit murine osteoclastogenesis while demonstrating that this form of FcγR modulation down-regulated mRNA transcription for DC-STAMP, TRAP and Cathepsin K, but also increased F4/80 mRNA³¹⁷. F4/80 is a MØ marker associated with MØ maturation, suggesting that heat-aggregated rabbit IgG can skew the differentiation of progenitors from OCs to MØ^{317,437}. Examination of this marker and others could identify similarities between SIC/Oplg and heat-aggregated rabbit IgG modulation of FcγRs.

The final section of this thesis was an examination into the role of Bcl-3, a negative regulator of NF-κB, on bone remodelling. NF-κB is essential for osteoclastogenesis and the subunits p50, p52, p65 and Rel-B have been identified as mediators in OC differentiation^{145,162,176}. Bcl-3^{-/-} animals are highly responsive to TLR4 and cytokine stimulation and produce aberrant and excessive responses to stimulation¹⁶⁷. We hypothesised that due to Bcl-3's regulatory role in NF-κB signalling, it would regulate RANKL-RANK signalling and influence OC differentiation. Examination of day 5 OCs produced by WT and Bcl-3^{-/-} animals showed that the OCs were similar in number, appearance and transcriptional profile, however, by day 7 there were fewer Bcl-3^{-/-} OCs than WT OCs. There may be intrinsic differences in the progenitor populations present in the BM resulting in varied responses to M-CSF and RANKL. As such, examination of the BM monocyte subsets revealed that Bcl-3 deficient animals had fewer CD115⁺ monocytes. These cells are able to differentiate into OCs⁴ and may be responsible for the difference in OC numbers *in vitro*. Further examination of progenitor populations to identify HSCs, MDPs, and CMPs in Bcl-3 deficient animals would provide information regarding the involvement of Bcl-3 in myelopoiesis. This would not only help understand Bcl-3's role in monocyte homeostasis but also our understanding of Bcl-3's role in neutropenia, as Bcl-3 deficiency resulted in fewer neutrophils in the blood and BM. Due to the decrease in CD115⁺ monocytes in Bcl-3^{-/-} animals, further studies were undertaken to assess the role Bcl-3 has in bone remodelling. The trabecular bone microarchitecture was examined by μCT and Bcl-3^{-/-} animals were discovered to have increased bone compared to WT controls. This data suggests that there may be defect in OC erosion or OB bone formation that remains to be elucidated, however, Bcl-3 appears to have a role in bone remodelling.

6.1 Future work

It was shown in Chapter 3 that SpA IgG complexes are able to engage FcγRs and inhibit osteoclastogenesis. Yet, the signalling mechanism utilised by these complexes remains undefined. Activatory FcγRs signal via the FcRγ which has been implicated in OSCAR signalling along with the DAP12 adaptor protein. Classically, FcRγ and DAP12 signal via ITAM motifs and are regarded as an activatory signal enhancing osteoclastogenesis through Ca²⁺ responses and NFATc1¹⁵⁴. Yet, TREM2-DAP12 ITAM signalling negatively regulates osteoclastogenesis and bone remodelling²¹⁶, providing evidence that ITAM signalling can activate and inhibit cellular functions. Recently, ITAMi signalling has been shown to inhibit cellular abilities; one example of this is the interaction between monomeric IgG and FcγRIII which inhibits MØ Ca²⁺ responses, endocytosis and phagocytosis²⁵⁷. Typically FcγRIII-FcRγ signal via SYK which activates Ca²⁺ responses and NFATc1, yet, ITAMi signalling by FcγRIII-FcRγ can result in SHP-1 activation which is associated with the inhibitory FcγRIIB ITIM signalling^{257,330}. In our system, SIC treatment is believed to act through FcγRI-FcRγ³¹⁶. Examination of the molecular machinery associated with FcRγ following SIC engagement would reveal the initial signalling events resulting in the inhibition of OC differentiation. To do this, SIC treatment of pre-OCs followed by co-immunoprecipitation to 'pull-out' FcγRI would reveal the identity of receptors and signalling molecules associated with the FcγRI/SIC complex. Co-immunoprecipitation allows a molecule to be targeted by antibody and subsequently removed from the sample. This isolated molecule can then be run on a gel and probed to determine which proteins it associates with. This could identify whether SIC can induce FcγRI-FcRγ to signal via ITAM, ITIM or ITAMi pathways. This could reveal the signalling pathway used by SIC to inhibit osteoclastogenesis and also provide further targets which could be used to prevent osteoclastogenesis.

The results from Chapter 5 demonstrate that *in vitro* WT and Bcl-3^{-/-} OCs are fundamentally similar. However, these animals differ in their bone structure revealing that Bcl-3 has a role in bone remodelling. In order to continue this research further work must be undertaken to characterise the erosive potential of *in vitro* OCs. While *in vivo* examination of OCs could reveal whether there is a deficit in the number of OC present in the trabecular region. Examination of cortical and trabecular bone in the femur or vertebrae could be used to verify that the increase in bone is observed at other anatomical sites. As demonstrated, oestrogen has a marked effect on bone remodelling and its effect in Bcl-3^{-/-} animals must be examined. Oestrogen deficiency has been shown to increase Bcl-3 mRNA and thus inhibit NF-κB activity⁴³⁸. The bone microarchitecture of Bcl-3^{-/-} animals was only studied in male mice as female mice are exposed to higher levels of oestrogen. It is hypothesised that female Bcl-3^{-/-} mice would

be more responsive to NF- κ B activation than males, resulting in female Bcl-3^{-/-} mice with more severe osteopetrosis. The examination and comparison of OCs and OBs produced from male and female animals would be useful in identifying interplay between oestrogen and Bcl-3 in bone remodelling. The use of OB maturation and nodule formation assays would provide insight in the role of Bcl-3 in osteoblastogenesis. Analysis of the secreted extracellular matrix would provide clues to the functionality of Bcl-3^{-/-} OBs and thus allude to whether *in vivo* Bcl-3^{-/-} OBs are dysfunctional. These studies would demonstrate the extent to which Bcl-3 is involved in bone remodelling and provide necessary information to determine whether Bcl-3 has therapeutic potential.

6.2 Conclusion

SpA IgG complexes and Bcl-3 were investigated to determine their potential as novel avenues of therapeutic intervention in osteoporotic disease. *In vitro*, SpA generating IgG complexes of a discreet size that interacted with Fc γ R_s on the surface of murine pre-OCs inhibiting their differentiation to mature OCs in the presence of M-CSF and RANKL. Treatment of animals with SpA induced the formation of IgG complexes in circulation with the ability to interact with monocyte subsets in the blood. However, in the murine model of osteoporosis, therapeutic and prophylactic treatment of animals with SpA failed to prevent oestrogen deficient bone loss. Thus further work must be done to determine whether SpA at higher doses has the potential to prevent oestrogen deficient bone loss, yet, the data presented in this thesis demonstrates that SpA is unable to treat osteoporotic disease.

The role of Bcl-3 in bone remodelling is yet to be fully elucidated; current observations demonstrate that Bcl-3 deficiency perturbs the intimate nature of bone remodelling resulting in increased trabecular bone. This novel target could potentially be used to treat osteoporotic diseases, however, whether the increase in bone in Bcl-3^{-/-} mice is a result of increased bone formation or decreased bone erosion remains to be verified.

Appendix - Media, buffers and reagents

Roswell Park Memorial Institute Medium (RPMI 1640)

500 ml of RPMI 1640, 50 ml Fetal Bovine Serum (FBS), 5 ml L-glutamine and 5 ml Penicillin/Streptomycin.

Complete Dulbecco's Modified Eagle Medium (D-MEM)

500 ml of D-MEM, 50 ml Fetal Bovine Serum (FBS), 5 ml L-glutamine and 5 ml Penicillin/Streptomycin.

Complete alpha Minimum Essential Media (α -MEM)

500 ml of α -MEM, 50 ml Fetal Bovine Serum (FBS), 5 ml L-glutamine and 5 ml Penicillin/Streptomycin.

1x Phosphate Buffered Saline pH 7.4 (PBS)

8 g NaCl, 0.2 g KCl, 0.2 g KH_2PO_4 and 1.74 g Na_2HPO_4 in 1 litre dH_2O .

Separation Media

500 ml 1x PBS, 10 ml Fetal Bovine Serum (FBS) and 0.146g EDTA.

PBS - 0.01% Tween-20 (PBST 0.01%)

100 μl Tween-20 in 1 litre 1x PBS.

FACS Buffer

10 ml Foetal Bovine Serum (FBS, PAA Cell Culture Company), 2 g NaN_3 and 1.68 g EDTA in 1 litre 1x PBS.

0.5M EDTA Solution

168.12 g EDTA in 1 litre dH_2O .

Tris-Acetate-EDTA (TAE) pH 8 Buffer

4.84 g Tris Base, 1.14 ml glacial acetic acid and 0.37 g EDTA in 1 litre dH_2O .

TRAP Fixative Solution (Acid Phosphatase Leukocyte (TRAP) kit, Sigma-Aldrich)

12.5 ml Citrate Solution, 32.5 ml Acetone and 4 ml 37% formaldehyde.

TRAP Staining Solution (Acid Phosphatase Leukocyte (TRAP) kit, Sigma-Aldrich)

125 µl Fast Garnet GBC Base solution and 125 µl NaNO₂ solution, mixed for 2 minutes.
11.25 ml 37°C dH₂O with 250 µl Fast Garnet/NaNO₂ mixture, 125 µl Naphthol As-Bi Phosphoric acid solution, 250 µl Acetate solutions and 250 µl Tartrate solution.

Decalcification Solution (14% EDTA pH 8)

140 g EDTA in 1 litre dH₂O with pH adjusted to 8 using NaOH.

ELISA Assay Diluent - 1x PBS (10% FBS)

5 ml FBS in 50 ml 1x PBS.

Sodium Carbonate Coating Buffer (pH 9.5)

7.13 g NaHCO₃ and 1.59 g Na₂CO₃ in litre of dH₂O and pH to 9.5 with NaOH

Sodium Phosphate Coating Buffer (pH 6.5)

12.94 g Na₂HPO₄ and 15.47 g NaH₂PO₄ in 1 litre of dH₂O and pH to 6.5

Scott's Tap Water Substitute

2 g NaHCO₃ and 20 g MgSO₄ in 1 litre of dH₂O.

1% Acid/Alcohol Solution

700 ml Ethanol, 10 ml concentrated HCl and 290 ml dH₂O.

2% Agarose Solution

2 g Agarose in 100 ml 1x TAE, heated to dissolve agarose.

References

1. Takayanagi H. Osteoimmunology: shared mechanisms and crosstalk between the immune and bone systems. *Nat. Rev. Immunol.* 2007;7(4):292-304.
2. Rudolf R, Busch R, Patra AK, et al. Architecture and Expression of the Nfatc1 Gene in Lymphocytes. *Front. Immunol.* 2014;5(21):1-4.
3. Fu Y-X, Gu J-H, Zhang Y-R, et al. Inhibitory effects of osteoprotegerin on osteoclast formation and function under serum-free conditions. *J. Vet. Sci.* 2013;14(4):405-412.
4. Jacome-Galarza C, Lee S-K, Lorenzo J, Aguila H. Identification, characterization, and isolation of a common progenitor for osteoclasts, macrophages, and dendritic cells from murine bone marrow and periphery. *J. Bone Miner. Res.* 2013;28(5):1203-1213.
5. Clowes JA, Riggs BL, Khosla S. The role of the immune system in the pathophysiology of osteoporosis. *Immunol. Rev.* 2005;208(1):207-227.
6. Arai F, Miyamoto T, Ohneda O, et al. Commitment and Differentiation of Osteoclast Precursor Cells by the Sequential Expression of C-Fms and Receptor Activator of Nuclear Factor kb (Rank) Receptors. *J. Exp. Med.* 1999;190(12):1741-1754.
7. Mensah K, Ritchlin C, Schwarz E. RANKL induces heterogeneous DC-STAMP hi and DC-STAMP lo osteoclast precursors of which the DC-STAMP hi precursors are the master fusogens. *J. Cell. Physiol.* 2009;223(1):76-83.
8. Aeschlimann D, Evans B. The vital osteoclast: how is it regulated? *Cell Death Differ.* 2004;11:S5-S7.
9. Lacey D., Timms E, Tan H-L, et al. Osteoprotegerin Ligand Is a Cytokine that Regulates Osteoclast Differentiation and Activation. *Cell.* 1998;93(2):165-176.
10. Kukita T. RANKL-induced DC-STAMP Is Essential for Osteoclastogenesis. *J. Exp. Med.* 2004;200(7):941-946.
11. Oursler M. Recent advances in understanding the mechanisms of osteoclast precursor fusion. *J. Cell. Biochem.* 2010;110(5):1058-1062.
12. Boyle WJ, Simonet WS, Lacey DL. Osteoclast differentiation and activation. *Nature.* 2003;423(6937):337-342.
13. Crockett J, Rogers M, Coxon F, Hocking L, Helfrich M. Bone remodelling at a glance. *J. Cell Sci.* 2011;124(7):991-998.
14. Urry DW. Neutral sites for calcium ion binding to elastin and collagen: a charge neutralization theory for calcification and its relationship to atherosclerosis. *Proc. Natl. Acad. Sci. U. S. A.* 1971;68(4):810-814.
15. Heino TJ, Kurata K, Higaki H, Väänänen HK. Evidence for the role of osteocytes in the initiation of targeted remodeling. *Technol. Health Care.* 2009;17(1):49-56.
16. Jilka RL. Biology of the basic multicellular unit and the pathophysiology of osteoporosis. *Med. Pediatr. Oncol.* 2003;41(3):182-185.
17. Seeman E. Bone Modeling and Remodeling. *Crit. Rev. Eukaryot. Gene Expr.* 2009;19(3):219-233.
18. Kalu DN. The ovariectomized rat model of postmenopausal bone loss. *Bone Miner.* 1991;15(3):175-191.
19. Lerner UH. Bone Remodeling in Post-menopausal Osteoporosis. *J. Dent. Res.* 2006;85(7):584-595.
20. Lukert BP, Raisz LG. Glucocorticoid-Induced Osteoporosis: Pathogenesis and Management. *Ann. Intern. Med.* 1990;112(5):352-364.
21. Center JR, Nguyen TV, Schneider D, Sambrook PN, Eisman JA. Mortality after all major types of osteoporotic fracture in men and women: an observational study. *The Lancet.* 1999;353(9156):878-882.
22. Kanis J, McCloskey E, Johansson H, et al. A reference standard for the description of osteoporosis. *Bone.* 2008;42(3):467-475.
23. Sherman BM, Korenman SG. Hormonal characteristics of the human menstrual cycle throughout reproductive life. *J. Clin. Invest.* 1975;55(4):699-706.
24. Martini F. Fundamentals of anatomy and physiology. Prentice Hall; 1989.

25. Goldman JM, Murr AS, Cooper RL. The rodent estrous cycle: characterization of vaginal cytology and its utility in toxicological studies. *Birth Defects Res. Part B.* 2007;80(2):84-97.
26. Byers SL, Wiles MV, Dunn SL, Taft RA. Mouse Estrous Cycle Identification Tool and Images. *PLoS ONE.* 2012;7(4):e35538.
27. Powers JB. Hormonal control of sexual receptivity during the estrous cycle of the rat. *Physiol. Behav.* 1970;5(8):831-835.
28. Cui J, Shen Y, Li R. Estrogen synthesis and signaling pathways during aging: from periphery to brain. *Trends Mol. Med.* 2013;19(3):197-209.
29. Zittermann A, Schwarz I, Scheld K, et al. Physiologic fluctuations of serum estradiol levels influence biochemical markers of bone resorption in young women. *J. Clin. Endocrinol. Metab.* 2000;85(1):95-101.
30. Al-Azzawi F, Palacios S. Hormonal changes during menopause. *Maturitas.* 2009;63(2):135-137.
31. Nelson HD, Humphrey LL, Nygren P, Teutsch SM, Allan JD. Postmenopausal hormone replacement therapy: Scientific review. *JAMA.* 2002;288(7):872-881.
32. Cranney A, Adachi JD. Benefit-risk assessment of raloxifene in postmenopausal osteoporosis. *Drug Saf. Int. J. Med. Toxicol. Drug Exp.* 2005;28(8):721-730.
33. Reszka AA, Halasy-Nagy JM, Masarachia PJ, Rodan GA. Bisphosphonates Act Directly on the Osteoclast to Induce Caspase Cleavage of Mst1 Kinase during Apoptosis: a link between inhibition of the mevalonate pathway and regulation of an apoptosis-promoting kinase. *J. Biol. Chem.* 1999;274(49):34967-34973.
34. Kennel KA, Drake MT. Adverse Effects of Bisphosphonates: Implications for Osteoporosis Management. *Mayo Clin. Proc.* 2009;84(7):632-638.
35. Brown JP, Reid IR, Wagman RB, et al. Effects of Up to 5 Years of Denosumab Treatment on Bone Histology and Histomorphometry: The FREEDOM Study Extension. *J. Bone Miner. Res.* 2014;29(9):2051-2056.
36. Recker R, Benson C, Matsumoto T, et al. A randomized, double-blind phase 2 clinical trial of blosozumab, a sclerostin antibody, in postmenopausal women with low bone mineral density. *J. Bone Miner. Res.* 2014;n/a-n/a.
37. Téletchéa S, Stresing V, Hervouet S, et al. Novel RANK Antagonists for the Treatment of Bone Resorptive Disease: Theoretical Predictions and Experimental Validation. *J. Bone Miner. Res.* 2014;n/a-n/a.
38. Saville PD. Changes in skeletal mass and fragility with castration in the rat; a model of osteoporosis. *J. Am. Geriatr. Soc.* 1969;17(2):155-166.
39. Bouxsein ML, Myers KS, Shultz KL, et al. Ovariectomy-Induced Bone Loss Varies Among Inbred Strains of Mice. *J. Bone Miner. Res.* 2005;20(7):1085-1092.
40. Turner AS. Animal models of osteoporosis--necessity and limitations. *Eur. Cell. Mater.* 2001;1:66-81.
41. Glatt V, Canalis E, Stadmeier L, Bouxsein ML. Age-Related Changes in Trabecular Architecture Differ in Female and Male C57BL/6J Mice. *J. Bone Miner. Res.* 2007;22(8):1197-1207.
42. Shen V, Dempster DW, Birchman R, Xu R, Lindsay R. Loss of cancellous bone mass and connectivity in ovariectomized rats can be restored by combined treatment with parathyroid hormone and estradiol. *J. Clin. Invest.* 1993;91(6):2479-2487.
43. Williams DC, Paul DC, Black LJ. Effects of estrogen and tamoxifen on serum osteocalcin levels in ovariectomized rats. *Bone Miner.* 1991;14(3):205-220.
44. Kalu DN, Salerno E, Liu CC, et al. A comparative study of the actions of tamoxifen, estrogen and progesterone in the ovariectomized rat. *Bone Miner.* 1991;15(2):109-123.
45. Babaei P, Mehdizadeh R, Ansar MM, Damirchi A. Effects of ovariectomy and estrogen replacement therapy on visceral adipose tissue and serum adiponectin levels in rats. *Menopause Int.* 2010;16(3):100-104.
46. Espeland MA, Stefanick ML, Kritz-Silverstein D, et al. Effect of postmenopausal hormone therapy on body weight and waist and hip girths. Postmenopausal Estrogen-Progestin Interventions Study Investigators. *J. Clin. Endocrinol. Metab.* 1997;82(5):1549-1556.

47. Ettinger B, Genant H, Cann C. Long-Term Estrogen Replacement Therapy Prevents Bone Loss and Fractures. *Ann. Intern. Med.*. 1985;102(3):319-324.
48. Simonet W., Lacey D., Dunstan C., et al. Osteoprotegerin: A Novel Secreted Protein Involved in the Regulation of Bone Density. *Cell*. 1997;89(2):309-319.
49. Cenci S, Toraldo G, Weitzmann MN, et al. Estrogen deficiency induces bone loss by increasing T cell proliferation and lifespan through IFN- γ -induced class II transactivator. *Proc. Natl. Acad. Sci.*. 2003;100(18):10405-10410.
50. Gao Y, Grassi F, Ryan M, et al. IFN-gamma stimulates osteoclast formation and bone loss in vivo via antigen-driven T cell activation. *J. Clin. Invest.*. 2007;117(1):122-132.
51. Duque G, Huang DC, Dion N, et al. Interferon- γ plays a role in bone formation in vivo and rescues osteoporosis in ovariectomized mice. *J. Bone Miner. Res.*. 2011;26(7):1472-1483.
52. Fry TJ, Mackall CL. Interleukin-7: from bench to clinic. *Blood*. 2002;99(11):3892-3904.
53. Roggia C, Gao Y, Cenci S, et al. Up-regulation of TNF-producing T cells in the bone marrow: A key mechanism by which estrogen deficiency induces bone loss in vivo. *Proc. Natl. Acad. Sci.*. 2001;98(24):13960-13965.
54. Weitzmann MN, Cenci S, Rifas L, Brown C, Pacifici R. Interleukin-7 stimulates osteoclast formation by up-regulating the T-cell production of soluble osteoclastogenic cytokines. *Blood*. 2000;96(5):1873-1878.
55. Toraldo G, Roggia C, Qian W-P, Pacifici R, Weitzmann MN. IL-7 induces bone loss in vivo by induction of receptor activator of nuclear factor kappa B ligand and tumor necrosis factor alpha from T cells. *Proc. Natl. Acad. Sci.*. 2003;100(1):125-130.
56. Weitzmann MN, Roggia C, Toraldo G, Weitzmann L, Pacifici R. Increased production of IL-7 uncouples bone formation from bone resorption during estrogen deficiency. *J. Clin. Invest.*. 2002;110(11):1643-1650.
57. Lee S-K, Kalinowski JF, Jacquin C, et al. Interleukin-7 Influences Osteoclast Function In Vivo but Is Not a Critical Factor in Ovariectomy-Induced Bone Loss. *J. Bone Miner. Res.*. 2006;21(5):695-702.
58. Lee S-K, Kalinowski JF, Jastrzebski SL, Puddington L, Lorenzo JA. Interleukin-7 is a direct inhibitor of in vitro osteoclastogenesis. *Endocrinology*. 2003;144(8):3524-3531.
59. Kim OY, Chae JS, Paik JK, et al. Effects of aging and menopause on serum interleukin-6 levels and peripheral blood mononuclear cell cytokine production in healthy nonobese women. *AGE*. 2012;34(2):415-425.
60. Ishimi Y, Miyaura C, Jin CH, et al. IL-6 is produced by osteoblasts and induces bone resorption. *J. Immunol.*. 1990;145(10):3297-3303.
61. Galien R, Garcia T. Estrogen receptor impairs interleukin-6 expression by preventing protein binding on the NF-kappaB site. *Nucleic Acids Res.*. 1997;25(12):2424-2429.
62. Poli V, Balena R, Fattori E, et al. Interleukin-6 deficient mice are protected from bone loss caused by estrogen depletion. *EMBO J.*. 1994;13(5):1189-1196.
63. Roggia C, Tamone C, Cenci S, Pacifici R, Isaia GC. Role of TNF-alpha producing T-cells in bone loss induced by estrogen deficiency. *Minerva Med.*. 2004;95(2):125-132.
64. Ammann P, Rizzoli R, Bonjour J, et al. Transgenic mice expressing soluble tumor necrosis factor-receptor are protected against bone loss caused by estrogen deficiency. *J. Clin. Invest.*. 1997;99(7):1699-1703.
65. Schett G, Redlich K, Hayer S, et al. Osteoprotegerin protects against generalized bone loss in tumor necrosis factor-transgenic mice. *Arthritis Rheum.*. 2003;48(7):2042-2051.
66. Li P, Schwarz EM. The TNF-alpha transgenic mouse model of inflammatory arthritis. *Springer Semin. Immunopathol.*. 2003;25(1):19-33.
67. Axmann R, Bohm C, Kronke G, et al. Inhibition of interleukin-6 receptor directly blocks osteoclast formation in vitro and in vivo. *Arthritis Rheum.*. 2009;60(9):2747-2756.

68. Wei S, Kitaura H, Zhou P, Ross FP, Teitelbaum SL. IL-1 mediates TNF-induced osteoclastogenesis. *J. Clin. Invest.*. 2005;115(2):282-290.
69. Kimble RB, Srivastava S, Ross FP, Matayoshi A, Pacifici R. Estrogen Deficiency Increases the Ability of Stromal Cells to Support Murine Osteoclastogenesis via an Interleukin-1 and Tumor Necrosis Factor-mediated Stimulation of Macrophage Colony-stimulating Factor Production. *J. Biol. Chem.*. 1996;271(46):28890-28897.
70. Kimble R, Vannice J, Bloedow D, et al. Interleukin-1 receptor antagonist decreases bone loss and bone resorption in ovariectomized rats. *J. Clin. Invest.*. 1994;93(5):1959-1967.
71. Cenci S, Weitzmann MN, Gentile MA, Aisa MC, Pacifici R. M-CSF neutralization and Egr-1 deficiency prevent ovariectomy-induced bone loss. *J. Clin. Invest.*. 2000;105(9):1279-1287.
72. Toh M-L, Bonnefoy J-Y, Accart N, et al. A CSF-1 receptor monoclonal antibody has potent bone and cartilage protective effects in experimental arthritis. *Arthritis Rheumatol.*. 2014;Epub ahead of print:
73. Lorenzo J, Naprta A, Rao Y, et al. Mice Lacking the Type I Interleukin-1 Receptor Do Not Lose Bone Mass after Ovariectomy. *Endocrinology.* 1998;139(6):3022-3025.
74. Deshpande R, Khalili H, Pergolizzi RG, Michael SD, Chang M-DY. Estradiol Down-Regulates LPS-Induced Cytokine Production and NF κ B Activation in Murine Macrophages. *Am. J. Reprod. Immunol.*. 1997;38(1):46-54.
75. Ra L, Ja L, Ml P. Ovarian steroids modulate human monocyte tumor necrosis factor alpha messenger ribonucleic acid levels in cultured human peripheral monocytes. *Fertil. Steril.*. 1992;58(4):733-739.
76. Morishita M, Miyagi M, Iwamoto Y. Effects of Sex Hormones on Production of Interleukin-1 by Human Peripheral Monocytes. *J. Periodontol.*. 1999;70(7):757-760.
77. Ben-Hur H, Mor G, Insler V, et al. Menopause Is Associated With a Significant Increase in Blood Monocyte Number and a Relative Decrease in the Expression of Estrogen Receptors in Human Peripheral Monocytes. *Am. J. Reprod. Immunol.*. 1995;34(6):363-369.
78. Thongngarm T, Jenkins JK, Ndebele K, McMurray RW. Estrogen and Progesterone Modulate Monocyte Cell Cycle Progression and Apoptosis. *Am. J. Reprod. Immunol.*. 2003;49(3):129-138.
79. Imai Y, Youn M-Y, Inoue K, et al. Nuclear receptors in bone physiology and diseases. *Physiol. Rev.*. 2013;93(2):481-523.
80. Dai R, Phillips RA, Ahmed SA. Despite inhibition of nuclear localization of NF-kappa B p65, c-Rel, and RelB, 17-beta estradiol up-regulates NF-kappa B signaling in mouse splenocytes: the potential role of Bcl-3. *J. Immunol.*. 2007;179(3):1776-1783.
81. Hsu S-M, Chen Y-C, Jiang M-C. 17 β -Estradiol Inhibits Tumor Necrosis Factor- α -Induced Nuclear Factor- κ B Activation by Increasing Nuclear Factor- κ B p105 Level in MCF-7 Breast Cancer Cells. *Biochem. Biophys. Res. Commun.*. 2000;279(1):47-52.
82. Razandi M. Plasma Membrane Estrogen Receptors Exist and Functions as Dimers. *Mol. Endocrinol.*. 2004;18(12):2854-2865.
83. Haynes MP, Sinha D, Russell KS, et al. Membrane Estrogen Receptor Engagement Activates Endothelial Nitric Oxide Synthase via the PI3-Kinase-Akt Pathway in Human Endothelial Cells. *Circ. Res.*. 2000;87(8):677-682.
84. Patten RD, Pourati I, Aronovitz MJ, et al. 17 β -Estradiol Reduces Cardiomyocyte Apoptosis In Vivo and In Vitro via Activation of Phospho-Inositide-3 Kinase/Akt Signaling. *Circ. Res.*. 2004;95(7):692-699.
85. Brubaker KD, Gay CV. Depolarization of Osteoclast Plasma Membrane Potential by 17 β -Estradiol. *J. Bone Miner. Res.*. 1999;14(11):1861-1866.
86. Okabe K, Okamoto F, Kajiya H, Takada K, Soeda H. Estrogen directly acts on osteoclasts via inhibition of inward rectifier K⁺ channels. *Naunyn. Schmiedebergs Arch. Pharmacol.*. 2000;361(6):610-620.
87. Imai Y, Youn M-Y, Kondoh S, et al. Estrogens maintain bone mass by regulating expression of genes controlling function and life span in mature osteoclasts. *Ann. N. Y. Acad. Sci.*. 2009;1173(Suppl 1):E31-39.

88. Nakamura T, Imai Y, Matsumoto T, et al. Estrogen Prevents Bone Loss via Estrogen Receptor α and Induction of Fas Ligand in Osteoclasts. *Cell*. 2007;130(5):811-823.
89. Udagawa N, Takahashi N, Akatsu T, et al. Origin of osteoclasts: mature monocytes and macrophages are capable of differentiating into osteoclasts under a suitable microenvironment prepared by bone marrow-derived stromal cells. *Proc. Natl. Acad. Sci.*. 1990;87(18):7260-7264.
90. Geissmann F, Manz MG, Jung S, et al. Development of monocytes, macrophages and dendritic cells. *Science*. 2010;327(5966):656-661.
91. Francke A, Herold J, Weinert S, Strasser RH, Braun-Dullaeus RC. Generation of Mature Murine Monocytes from Heterogeneous Bone Marrow and Description of Their Properties. *J. Histochem. Cytochem.*. 2011;59(9):813-825.
92. Doulatov S, Notta F, Rice KL, et al. PLZF is a regulator of homeostatic and cytokine-induced myeloid development. *Genes Dev.*. 2009;23(17):2076-2087.
93. Scott EW, Simon MC, Anastasi J, Singh H. Requirement of transcription factor PU.1 in the development of multiple hematopoietic lineages. *Science*. 1994;265(5178):1573-1577.
94. Tondravi MM, McKercher SR, Anderson K, et al. Osteopetrosis in mice lacking haematopoietic transcription factor PU.1. *Nature*. 1997;386(6620):81-84.
95. Zhang DE, Hetherington CJ, Chen HM, Tenen DG. The macrophage transcription factor PU.1 directs tissue-specific expression of the macrophage colony-stimulating factor receptor. *Mol. Cell. Biol.*. 1994;14(1):373-381.
96. Tsou C-L, Peters W, Si Y, et al. Critical roles for CCR2 and MCP-3 in monocyte mobilization from bone marrow and recruitment to inflammatory sites. *J. Clin. Invest.*. 2007;117(4):902-909.
97. Geissmann F, Jung S, Littman D. Blood Monocytes Consist of Two Principal Subsets with Distinct Migratory Properties. *Immunity*. 2003;19(1):71-82.
98. Grainger JR, Wohlfert EA, Fuss IJ, et al. Inflammatory monocytes regulate pathologic responses to commensals during acute gastrointestinal infection. *Nat. Med.*. 2013;19(6):713-721.
99. Ziegler-Heitbrock L, Ancuta P, Crowe S, et al. Nomenclature of monocytes and dendritic cells in blood. *Blood*. 2010;116(16):e74-e80.
100. Auffray C, Fogg D, Garfa M, et al. Monitoring of Blood Vessels and Tissues by a Population of Monocytes with Patrolling Behavior. *Science*. 2007;317(5838):666-670.
101. Landsman L, Bar-On L, Zerneck A, et al. CX3CR1 is required for monocyte homeostasis and atherogenesis by promoting cell survival. *Blood*. 2009;113(4):963-972.
102. Dai X-M, Ryan GR, Hapel AJ, et al. Targeted disruption of the mouse colony-stimulating factor 1 receptor gene results in osteopetrosis, mononuclear phagocyte deficiency, increased primitive progenitor cell frequencies, and reproductive defects. *Blood*. 2002;99(1):111-120.
103. Charles J, Hsu L-Y, Niemi E, et al. Inflammatory arthritis increases mouse osteoclast precursors with myeloid suppressor function. *J. Clin. Invest.*. 2012;122(12):4592-605.
104. Fossati-Jimack L, Ling GS, Cortini A, et al. Phagocytosis Is the Main CR3-Mediated Function Affected by the Lupus-Associated Variant of CD11b in Human Myeloid Cells. *PLoS ONE*. 2013;8(2):e57082.
105. Ashman LK. The biology of stem cell factor and its receptor C-kit. *Int. J. Biochem. Cell Biol.*. 1999;31(10):1037-1051.
106. Lyman SD, Jacobsen SEW. c-kit Ligand and Flt3 Ligand: Stem/Progenitor Cell Factors With Overlapping Yet Distinct Activities. *Blood*. 1998;91(4):1101-1134.
107. Harada S, Kimura T, Fujiki H, et al. Flt3 ligand promotes myeloid dendritic cell differentiation of human hematopoietic progenitor cells: possible application for cancer immunotherapy. *Int. J. Oncol.*. 2007;30(6):1461-1468.
108. Yamane T, Kunisada T, Yamazaki H, et al. Development of Osteoclasts From Embryonic Stem Cells Through a Pathway That Is c-fms but not c-kit Dependent. *Blood*. 1997;90(9):3516-3523.

109. Dolence JJ, Gwin KA, Shapiro MB, Medina KL. Flt3 signaling regulates the proliferation, survival, and maintenance of multipotent hematopoietic progenitors that generate B cell precursors. *Exp. Hematol.*. 2014;42(5):380-393.
110. Mackarehtschian K, Hardin JD, Moore KA, et al. Targeted disruption of the flk2/flt3 gene leads to deficiencies in primitive hematopoietic progenitors. *Immunity*. 1995;3(1):147-161.
111. Servet-Delprat C, Arnaud S, Jurdic P, et al. Flt3+ macrophage precursors commit sequentially to osteoclasts, dendritic cells and microglia. *BMC Immunol.*. 2002;3(1):15.
112. Kotani M, Kikuta J, Klauschen F, et al. Systemic Circulation and Bone Recruitment of Osteoclast Precursors Tracked by Using Fluorescent Imaging Techniques. *J. Immunol.*. 2013;190(2):605-612.
113. Fuller K, Wong B, Fox S, Choi Y, Chambers TJ. TRANCE Is Necessary and Sufficient for Osteoblast-mediated Activation of Bone Resorption in Osteoclasts. *J. Exp. Med.*. 1998;188(5):997-1001.
114. Susa M, Luong-Nguyen N-H, Cappellen D, Zamurovic N, Gamse R. Human primary osteoclasts: in vitro generation and applications as pharmacological and clinical assay. *J. Transl. Med.*. 2004;2(1):6.
115. Wittrant Y, Theoleyre S, Couillaud S, et al. Regulation of osteoclast protease expression by RANKL. *Biochem. Biophys. Res. Commun.*. 2003;310(3):774-778.
116. Jacquin C, Gran D, Lee S, Lorenzo J, Aguila H. Identification of multiple osteoclast precursor populations in murine bone marrow. *J. Bone Miner. Res.*. 2006;21(1):67-77.
117. Takayanagi H. The Unexpected Link Between Osteoclasts and the Immune System. *Osteoimmunology*. 2010;658:61-68.
118. Marks SC, Lane PW. Osteopetrosis, a New Recessive Skeletal Mutation on Chromosome 12 of the Mouse. *J. Hered.*. 1976;67(1):11-18.
119. Wiktor-Jedrzejczak W, Bartocci A, Ferrante AW, et al. Total absence of colony-stimulating factor 1 in the macrophage-deficient osteopetrotic (op/op) mouse. *Proc. Natl. Acad. Sci.*. 1990;87(12):4828-4832.
120. Van Wesenbeeck L, Odgren PR, MacKay CA, et al. The osteopetrotic mutation toothless (tl) is a loss-of-function frameshift mutation in the rat *Csf1* gene: Evidence of a crucial role for CSF-1 in osteoclastogenesis and endochondral ossification. *Proc. Natl. Acad. Sci. U. S. A.*. 2002;99(22):14303-14308.
121. Chihara T, Suzu S, Hassan R, et al. IL-34 and M-CSF share the receptor Fms but are not identical in biological activity and signal activation. *Cell Death Differ.*. 2010;17(12):1917-1927.
122. Nakamichi Y, Mizoguchi T, Arai A, et al. Spleen serves as a reservoir of osteoclast precursors through vitamin D-induced IL-34 expression in osteopetrotic op/op mice. *Proc. Natl. Acad. Sci. U. S. A.*. 2012;109(25):10006-10011.
123. Kodama H, Yamasaki A, Nose M, et al. Congenital osteoclast deficiency in osteopetrotic (op/op) mice is cured by injections of macrophage colony-stimulating factor. *J. Exp. Med.*. 1991;173(1):269-272.
124. Hamilton JA. CSF-1 signal transduction. *J. Leukoc. Biol.*. 1997;62(2):145-155.
125. Ross FP. M-CSF, c-Fms, and Signaling in Osteoclasts and their Precursors. *Ann. N. Y. Acad. Sci.*. 2006;1068(1):110-116.
126. Bourette RP, Rohrschneider LR. Early Events in M-CSF Receptor Signaling. *Growth Factors*. 2000;17(3):155-66.
127. Weilbaecher KN, Motyckova G, Huber WE, et al. Linkage of M-CSF Signaling to Mitf, TFE3, and the Osteoclast Defect in Mitfmi/mi Mice. *Mol. Cell*. 2001;8(4):749-758.
128. Fuller K, Owens JM, Jagger CJ, et al. Macrophage colony-stimulating factor stimulates survival and chemotactic behavior in isolated osteoclasts. *J. Exp. Med.*. 1993;178(5):1733-1744.
129. Hodge JM, Collier FM, Pavlos NJ, Kirkland MA, Nicholson GC. M-CSF Potently Augments RANKL-Induced Resorption Activation in Mature Human Osteoclasts. *PLoS ONE*. 2011;6(6):e21462.

130. Ishii J, Kitazawa R, Mori K, et al. Lipopolysaccharide suppresses RANK gene expression in macrophages by down-regulating PU.1 and MITF. *J. Cell. Biochem.*. 2008;105(3):896-904.
131. Kawai T, Matsuyama T, Hosokawa Y, et al. B and T lymphocytes are the primary sources of RANKL in the bone resorptive lesion of periodontal disease. *Am. J. Pathol.*. 2006;169(3):987-998.
132. Kameda T, Mano H, Yamada Y, et al. Calcium-Sensing Receptor in Mature Osteoclasts, Which Are Bone Resorbing Cells. *Biochem. Biophys. Res. Commun.*. 1998;245(2):419-422.
133. Nakashima T, Kobayashi Y, Yamasaki S, et al. Protein Expression and Functional Difference of Membrane-Bound and Soluble Receptor Activator of NF- κ B Ligand: Modulation of the Expression by Osteotropic Factors and Cytokines. *Biochem. Biophys. Res. Commun.*. 2000;275(3):768-775.
134. Ikeda T. Determination of Three Isoforms of the Receptor Activator of Nuclear Factor kappa B Ligand and Their Differential Expression in Bone and Thymus. *Endocrinology*. 2001;142(4):1419-1426.
135. Kong Y-Y, Yoshida H, Sarosi I, et al. OPG is a key regulator of osteoclastogenesis, lymphocyte development and lymph-node organogenesis. *Nature*. 1999;397(6717):315-323.
136. Bodmer J-L, Schneider P, Tschopp J. The molecular architecture of the TNF superfamily. *Trends Biochem. Sci.*. 2002;27(1):19-26.
137. Dougall WC, Glaccum M, Charrier K, et al. RANK is essential for osteoclast and lymph node development. *Genes Dev.*. 1999;13(18):2412-2424.
138. Kim H-H, Lee DE, Shin JN, et al. Receptor activator of NF- κ B recruits multiple TRAF family adaptors and activates c-Jun N-terminal kinase. *FEBS Lett.*. 1999;443(3):297-302.
139. Winograd-Katz SE, Brunner MC, Mirlas N, Geiger B. Analysis of the signaling pathways regulating Src-dependent remodeling of the actin cytoskeleton. *Eur. J. Cell Biol.*. 2011;90(2-3):143-156.
140. Lomaga MA, Yeh W-C, Sarosi I, et al. TRAF6 deficiency results in osteopetrosis and defective interleukin-1, CD40, and LPS signaling. *Genes Dev.*. 1999;13(8):1015-1024.
141. Li X, Udagawa N, Itoh K, et al. p38 MAPK-Mediated Signals Are Required for Inducing Osteoclast Differentiation But Not for Osteoclast Function. *Endocrinology*. 2002;143(8):3105-3113.
142. Matsumoto M, Sudo T, Saito T, Osada H, Tsujimoto M. Involvement of p38 Mitogen-activated Protein Kinase Signaling Pathway in Osteoclastogenesis Mediated by Receptor Activator of NF- κ B Ligand (RANKL). *J. Biol. Chem.*. 2000;275(40):31155-31161.
143. He Y, Staser K, Rhodes SD, et al. Erk1 Positively Regulates Osteoclast Differentiation and Bone Resorptive Activity. *PLoS ONE*. 2011;6(9):e24780.
144. Grigoriadis AE, Wang ZQ, Cecchini MG, et al. c-Fos: a key regulator of osteoclast-macrophage lineage determination and bone remodeling. *Science*. 1994;266(5184):443-448.
145. Yamashita T, Yao Z, Li F, et al. NF- κ B p50 and p52 Regulate Receptor Activator of NF- κ B Ligand (RANKL) and Tumor Necrosis Factor-induced Osteoclast Precursor Differentiation by Activating c-Fos and NFATc1. *J. Biol. Chem.*. 2007;282(25):18245-18253.
146. Balkan W, Martinez AF, Fernandez I, et al. Identification of NFAT binding sites that mediate stimulation of cathepsin K promoter activity by RANK ligand. *Gene*. 2009;446(2):90-98.
147. Asagiri M, Sato K, Usami T, et al. Autoamplification of NFATc1 expression determines its essential role in bone homeostasis. *J. Exp. Med.*. 2005;202(9):1261-1269.
148. Khosla S. Minireview: The OPG/RANKL/RANK System. *Endocrinology*. 2001;142(12):5050-5055.

149. Wagner EF, Karsenty G. Genetic control of skeletal development. *Curr. Opin. Genet. Dev.*. 2001;11(5):527-532.
150. Li Y, Toraldo G, Li A, et al. B cells and T cells are critical for the preservation of bone homeostasis and attainment of peak bone mass in vivo. *Blood*. 2007;109(9):3839-3848.
151. Udagawa N. Osteoprotegerin Produced by Osteoblasts Is an Important Regulator in Osteoclast Development and Function. *Endocrinology*. 2000;141(9):3478-3484.
152. Morony S, Capparelli C, Shimamoto G, et al. A Chimeric Form of Osteoprotegerin Inhibits Hypercalcemia and Bone Resorption Induced by IL-1beta, TNF-alpha, PTH, PTHrP, and 1,25(OH)2D3. *J. Bone Miner. Res.*. 1999;14(9):1478-85.
153. Steeve KT, Marc P, Sandrine T, Dominique H, Yannick F. IL-6, RANKL, TNF-alpha/IL-1: interrelations in bone resorption pathophysiology. *Cytokine Growth Factor Rev.*. 2004;15(1):49-60.
154. Barrow A, Raynai N, Anderson T, et al. OSCAR is a collagen receptor that costimulates osteoclastogenesis in DAP12-deficient humans and mice. *J. Clin. Invest.*. 2011;121(9):1-12.
155. Jarry CR, Duarte PM, Freitas FF, et al. Secreted osteoclastogenic factor of activated T cells (SOFAT), a novel osteoclast activator, in chronic periodontitis. *Hum. Immunol.*. 2013;74(7):861-866.
156. Nakagawa N, Kinosaki M, Yamaguchi K, et al. RANK Is the Essential Signaling Receptor for Osteoclast Differentiation Factor in Osteoclastogenesis. *Biochem. Biophys. Res. Commun.*. 1998;253(2):395-400.
157. Chen F, Castranova V, Shi X, Demers LM. New Insights into the Role of Nuclear Factor- κ B, a Ubiquitous Transcription Factor in the Initiation of Diseases. *Clin. Chem.*. 1999;45(1):7-17.
158. Ryseck RP, Bull P, Takamiya M, et al. RelB, a new Rel family transcription activator that can interact with p50-NF-kappa B. *Mol. Cell. Biol.*. 1992;12(2):674-684.
159. Fan C-M, Maniatis T. Generation of p50 subunit of NF-kB by processing of p105 through an ATP-dependent pathway. *Nature*. 1991;354(6352):395-398.
160. Maruyama T, Fukushima H, Nakao K, et al. Processing of the NF-kB2 precursor p100 to p52 is critical for RANKL-induced osteoclast differentiation. *J. Bone Miner. Res.*. 2010;25(5):1058-1067.
161. Köntgen F, Grumont RJ, Strasser A, et al. Mice lacking the c-rel proto-oncogene exhibit defects in lymphocyte proliferation, humoral immunity, and interleukin-2 expression. *Genes Dev.*. 1995;9(16):1965-1977.
162. Vaira S, Alhawagri M, Anwisyte I, et al. RelA/p65 promotes osteoclast differentiation by blocking a RANKL-induced apoptotic JNK pathway in mice. *J. Clin. Invest.*. 2008;118(6):2088-97.
163. Perkins ND, Schmid RM, Duckett CS, et al. Distinct combinations of NF-kappa B subunits determine the specificity of transcriptional activation. *Proc. Natl. Acad. Sci.*. 1992;89(5):1529-1533.
164. Hayden MS, Ghosh S. Shared Principles in NF-kB Signaling. *Cell*. 2008;132(3):344-362.
165. Ghosh S, May MJ, Kopp EB. NF-kB AND REL PROTEINS: Evolutionarily Conserved Mediators of Immune Responses. *Annu. Rev. Immunol.*. 1998;16(1):225-260.
166. Soysa NS, Alles N. NF-kappaB functions in osteoclasts. *Biochem. Biophys. Res. Commun.*. 2009;378(1):1-5.
167. Carmody R, Ruan Q, Palmer S, Hilliard B, Chen Y. Negative regulation of toll-like receptor signaling by NF-kappaB p50 ubiquitination blockade. *Science*. 2007;317(5838):675-8.
168. Xu J, Wu HF, Ang ESM, et al. NF-kB modulators in osteolytic bone diseases. *Cytokine Growth Factor Rev.*. 2009;20(1):7-17.
169. Ernst MK, Dunn LL, Rice NR. The PEST-like sequence of I kappa B alpha is responsible for inhibition of DNA binding but not for cytoplasmic retention of c-Rel or RelA homodimers. *Mol. Cell. Biol.*. 1995;15(2):872-882.
170. Kerr LD, Duckett CS, Wamsley P, et al. The proto-oncogene bcl-3 encodes an I kappa B protein. *Genes Dev.*. 1992;6(12A):2352-2363.

171. Nolan GP, Fujita T, Bhatia K, et al. The bcl-3 proto-oncogene encodes a nuclear I kappa B-like molecule that preferentially interacts with NF-kappa B p50 and p52 in a phosphorylation-dependent manner. *Mol. Cell. Biol.*. 1993;13(6):3557-3566.
172. Gray CM, Remouchamps C, McCorkell KA, et al. Noncanonical NF-kB Signaling Is Limited by Classical NF-kB Activity. *Sci. Signal.*. 2014;7(311):ra13.
173. Dobrzanski P, Ryseck RP, Bravo R. Specific inhibition of RelB/p52 transcriptional activity by the C-terminal domain of p100. *Oncogene*. 1995;10(5):1003-1007.
174. Iotsova V, Caamaño J, Loy J, et al. Osteopetrosis in mice lacking NF-kappaB1 and NF-kappaB2. *Nat. Med.*. 1997;3(11):1285-1289.
175. Xing L, Bushnell TP, Carlson L, et al. NF-kappaB p50 and p52 expression is not required for RANK-expressing osteoclast progenitor formation but is essential for RANK- and cytokine-mediated osteoclastogenesis. *J. Bone Miner. Res.*. 2002;17(7):1200-1210.
176. Vaira S, Johnson T, Hirbe AC, et al. RelB is the NF-kappaB subunit downstream of NIK responsible for osteoclast differentiation. *Proc. Natl. Acad. Sci. U. S. A.*. 2008;105(10):3897-3902.
177. Ruocco M, Maeda S, Park J, et al. I kappa B kinase (IKK), but not IKKalpha, is a critical mediator of osteoclast survival and is required for inflammation-induced bone loss. *J. Exp. Med.*. 2005;201(10):1677-1687.
178. Hijdra D, Vorselaars AD, Grutters JC, Claessen AM, Rijkers GT. Differential expression of TNFR1 (CD120a) and TNFR2 (CD120b) on subpopulations of human monocytes. *J. Inflamm.*. 2012;9(1):38.
179. Fuller K, Murphy C, Kirstein B, Fox SW, Chambers TJ. TNFalpha Potently Activates Osteoclasts, through a Direct Action Independent of and Strongly Synergistic with RANKL. *Endocrinology*. 2002;143(3):1108-1118.
180. Li J, Sarosi I, Yan X-Q, et al. RANK is the intrinsic hematopoietic cell surface receptor that controls osteoclastogenesis and regulation of bone mass and calcium metabolism. *Proc. Natl. Acad. Sci.*. 2000;97(4):1566-1571.
181. Yao Z, Xing L, Boyce BF. NF-kappaB p100 limits TNF-induced bone resorption in mice by a TRAF3-dependent mechanism. *J. Clin. Invest.*. 2009;119(10):3024-3034.
182. Belardelli F. Role of interferons and other cytokines in the regulation of the immune response. *APMIS*. 1995;103(1-6):161-179.
183. Yao Z, Li P, Zhang Q, et al. Tumor Necrosis Factor- α Increases Circulating Osteoclast Precursor Numbers by Promoting Their Proliferation and Differentiation in the Bone Marrow through Up-regulation of c-Fms Expression. *J. Biol. Chem.*. 2006;281(17):11846-11855.
184. Charles P, Elliott MJ, Davis D, et al. Regulation of Cytokines, Cytokine Inhibitors, and Acute-Phase Proteins Following Anti-TNF- α Therapy in Rheumatoid Arthritis. *J. Immunol.*. 1999;163(3):1521-1528.
185. Feldmann M. Development of anti-TNF therapy for rheumatoid arthritis. *Nat. Rev. Immunol.*. 2002;2(5):364-371.
186. Dinarello CA. Immunological and Inflammatory Functions of the Interleukin-1 Family. *Annu. Rev. Immunol.*. 2009;27(1):519-550.
187. Kobayashi K, Takahashi N, Jimi E, et al. Tumor Necrosis Factor α Stimulates Osteoclast Differentiation by a Mechanism Independent of the Odf/Rankl-Rank Interaction. *J. Exp. Med.*. 2000;191(2):275-286.
188. Xing L, Carlson L, Story B, et al. Expression of either NF-kappaB p50 or p52 in osteoclast precursors is required for IL-1-induced bone resorption. *J. Bone Miner. Res.*. 2003;18(2):260-269.
189. Shih C, Huang MY. Interleukin-1 alpha stimulates osteoclast formation from peripheral blood monocytes and increases osteoclastic activity. *Zhonghua Yi Xue Za Zhi Chin. Med. J. Free China Ed.* 1996;57(2):85-92.
190. Moon S-J, Ahn IE, Jung H, et al. Temporal differential effects of proinflammatory cytokines on osteoclastogenesis. *Int. J. Mol. Med.*. 2013;31(4):769-777.
191. Lee ZH, Lee SE, Kim C-W, et al. IL-1alpha stimulation of osteoclast survival through the PI 3-kinase/Akt and ERK pathways. *J. Biochem. (Tokyo)*. 2002;131(1):161-166.

192. Scheller J, Chalaris A, Schmidt-Arras D, Rose-John S. The pro- and anti-inflammatory properties of the cytokine interleukin-6. *Biochim. Biophys. Acta.* 2011;1813(5):878-888.
193. Kurihara N, Bertolini D, Suda T, Akiyama Y, Roodman GD. IL-6 stimulates osteoclast-like multinucleated cell formation in long term human marrow cultures by inducing IL-1 release. *J. Immunol.* 1990;144(11):4226-4230.
194. Yokota K, Sato K, Miyazaki T, et al. Combination of Tumor Necrosis Factor α and Interleukin-6 Induces Mouse Osteoclast-like Cells With Bone Resorption Activity Both In Vitro and In Vivo. *Arthritis Rheumatol.* 2014;66(1):121-129.
195. Yoshitake F, Itoh S, Narita H, Ishihara K, Ebisu S. Interleukin-6 directly inhibits osteoclast differentiation by suppressing receptor activator of NF-kappaB signaling pathways. *J. Biol. Chem.* 2008;283(17):11535-11540.
196. Korn T, Bettelli 1 Estelle, Oukka 2 Mohamed, et al. IL-17 and Th17 Cells. *Annu. Rev. Immunol.* 2009;27(1):485-517.
197. Kotake S, Udagawa N, Takahashi N, et al. IL-17 in synovial fluids from patients with rheumatoid arthritis is a potent stimulator of osteoclastogenesis. *J. Clin. Invest.* 1999;103(9):1345-1352.
198. Jovanovic DV, Battista JAD, Martel-Pelletier J, et al. IL-17 Stimulates the Production and Expression of Proinflammatory Cytokines, IL-6 and TNF- α , by Human Macrophages. *J. Immunol.* 1998;160(7):3513-3521.
199. Zhao R. Immune regulation of bone loss by Th17 cells in oestrogen-deficient osteoporosis. *Eur. J. Clin. Invest.* 2013;43(11):1195-1202.
200. Zhang F, Tanaka H, Kawato T, et al. Interleukin-17A induces cathepsin K and MMP-9 expression in osteoclasts via celecoxib-blocked prostaglandin E2 in osteoblasts. *Biochimie.* 2011;93(2):296-305.
201. Cheng J, Liu J, Shi Z, et al. Molecular mechanisms of the biphasic effects of interferon- γ on osteoclastogenesis. *J. Interferon Cytokine Res.* 2012;32(1):34-45.
202. Schroder K, Hertzog PJ, Ravasi T, Hume DA. Interferon- γ : an overview of signals, mechanisms and functions. *J. Leukoc. Biol.* 2004;75(2):163-189.
203. Rifas L, Weitzmann MN. A novel T cell cytokine, secreted osteoclastogenic factor of activated T cells, induces osteoclast formation in a RANKL-independent manner. *Arthritis Rheum.* 2009;60(11):3324-3335.
204. Nemeth K, Schoppet M, Al-Fakhri N, et al. The Role of Osteoclast-Associated Receptor in Osteoimmunology. *J. Immunol.* 2010;186(1):13-18.
205. Kim N, Takami M, Rho J, Josien R, Choi Y. A novel member of the leukocyte receptor complex regulates osteoclast differentiation. *J. Exp. Med.* 2002;1-9.
206. Ivashkiv L. Cross-regulation of signaling by ITAM-associated receptors. *Nat. Immunol.* 2009;10(4):340-7.
207. Humphrey MB, Lanier LL, Nakamura MC. Role of ITAM-containing adapter proteins and their receptors in the immune system and bone. *Immunol. Rev.* 2005;208(1):50-65.
208. Mócsai A, Humphrey MB, Ziffle JAGV, et al. The immunomodulatory adapter proteins DAP12 and Fc receptor gamma chain (FcRgamma) regulate development of functional osteoclasts through the Syk tyrosine kinase. *Proc. Natl. Acad. Sci. U. S. A.* 2004;101(16):6158-6163.
209. Merck E. OSCAR is an FcRgamma-associated receptor that is expressed by myeloid cells and is involved in antigen presentation and activation of human dendritic cells. *Blood.* 2004;104(5):1386-1395.
210. Kim Y. Contribution of Nuclear Factor of Activated T Cells c1 to the Transcriptional Control of Immunoreceptor Osteoclast-associated Receptor but Not Triggering Receptor Expressed by Myeloid Cells-2 during Osteoclastogenesis. *J. Biol. Chem.* 2005;280(38):32905-32913.
211. Kim G, Koh J-M, Chang J, et al. Association of the OSCAR Promoter Polymorphism With BMD in Postmenopausal Women. *J. Bone Miner. Res.* 2005;20(8):1342-1348.
212. Andersson M, Lundberg P, Ohlin A, et al. Effects on osteoclast and osteoblast activities in cultured mouse calvarial bones by synovial fluids from patients with a

- loose joint prosthesis and from osteoarthritis patients. *Arthritis Res. Ther.* 2007;9(1):R18.
213. Herman S, Muller R, Kronke G, et al. Induction of osteoclast-associated receptor, a key osteoclast costimulation molecule, in rheumatoid arthritis. *Arthritis Rheum.* 2008;58(10):3041-3050.
 214. Humphrey MB, Daws MR, Spusta SC, et al. TREM2, a DAP12-associated receptor, regulates osteoclast differentiation and function. *J. Bone Miner. Res.* 2006;21(2):237-245.
 215. Paloneva J, Mandelin J, Kiialainen A, et al. DAP12/TREM2 deficiency results in impaired osteoclast differentiation and osteoporotic features. *J. Exp. Med.* 2003;198(4):669-675.
 216. Otero K, Shinohara M, Zhao H, et al. TREM2 and β -catenin regulate bone homeostasis by controlling the rate of osteoclastogenesis. *J. Immunol.* 2012;188(6):2612-2621.
 217. Humphrey MB, Ogasawara K, Yao W, et al. The signaling adapter protein DAP12 regulates multinucleation during osteoclast development. *J. Bone Miner. Res.* 2004;19(2):224-234.
 218. Zou W, Reeve JL, Liu Y, Teitelbaum SL, Ross FP. DAP12 Couples c-Fms Activation to the Osteoclast Cytoskeleton by Recruitment of Syk. *Mol. Cell.* 2008;31(3):422-431.
 219. Zawawi MSF, Dharmapatni AASSK, Cantley MD, et al. Regulation of ITAM adaptor molecules and their receptors by inhibition of calcineurin-NFAT signalling during late stage osteoclast differentiation. *Biochem. Biophys. Res. Commun.* 2012;427(2):404-409.
 220. Hartgers F, Vissers J, Looman M, et al. DC-STAMP, a novel multimembrane-spanning molecule preferentially expressed by dendritic cells. *Eur. J. Autoimmun.* 2000;30(12):3585-3590.
 221. Kim K, Lee S-H, Kim JH, Choi Y, Kim N. NFATc1 Induces Osteoclast Fusion Via Up-Regulation of Atp6v0d2 and the Dendritic Cell-Specific Transmembrane Protein (DC-STAMP). *Mol. Endocrinol.* 2008;22(1):176-185.
 222. Takahashi A, Kukita A, Li Y, et al. Tunneling nanotube formation is essential for the regulation of osteoclastogenesis. *J. Cell. Biochem.* 2013;114(6):1238-1247.
 223. Zeng Z-Y, Chen J-M. Cell-cell fusion: human multinucleated osteoclasts. *Cent. Eur. J. Biol.* 2009;4(4):543-548.
 224. Yang M, Birnbaum M, MacKay C, et al. Osteoclast stimulatory transmembrane protein (OC-STAMP), a novel protein induced by RANKL that promotes osteoclast differentiation. *J. Cell. Physiol.* 2008;215(2):497-505.
 225. Kim M, Park M, Baek S, Kim H, Kim S. Molecules and signaling pathways involved in the expression of OC-STAMP during osteoclastogenesis. *Amino Acids.* 2011;40(5):1447-1459.
 226. Lakkakorpi PT, Horton MA, Helfrich MH, Karhukorpi EK, Väänänen HK. Vitronectin receptor has a role in bone resorption but does not mediate tight sealing zone attachment of osteoclasts to the bone surface. *J. Cell Biol.* 1991;115(4):1179-1186.
 227. Lakkakorpi PT, Helfrich MH, Horton MA, Vaananen HK. Spatial organization of microfilaments and vitronectin receptor, α v β 3, in osteoclasts. A study using confocal laser scanning microscopy. *J. Cell Sci.* 1993;104(3):663-670.
 228. Chin SL, Johnson SA, Quinn J, et al. A role for α V integrin subunit in TGF- β -stimulated osteoclastogenesis. *Biochem. Biophys. Res. Commun.* 2003;307(4):1051-1058.
 229. Faccio R, Takeshita S, Zallone A, Ross F, Teitelbaum S. c-Fms and the α v β 3 integrin collaborate during osteoclast differentiation. *J. Clin. Invest.* 2003;111(5):749-758.
 230. Nyman J, Vaananen, Kalervo K. A Rationale for Osteoclast Selectivity of Inhibiting the Lysosomal V-ATPase α 3 Isoform. *Calcif. Tissue Int.* 2010;87(3):273-283.
 231. Rousselle A-V, Heymann D. Osteoclastic acidification pathways during bone resorption. *Bone.* 2002;30(4):533-540.

232. David JP, Rincon M, Neff L, Horne WC, Baron R. Carbonic anhydrase II is an AP-1 target gene in osteoclasts. *J. Cell. Physiol.*. 2001;188(1):89-97.
233. Kartner N, Yao Y, Li K, et al. Inhibition of Osteoclast Bone Resorption by Disrupting Vacuolar H⁺-ATPase α 3-B2 Subunit Interaction. *J. Biol. Chem.*. 2010;285(48):37476-37490.
234. Perez-Castrillon JL, Pinacho F, Luis DD, Lopez-Menendez M, Laita AD. Odanacatib, a New Drug for the Treatment of Osteoporosis: Review of the Results in Postmenopausal Women. *J. Osteoporos.*. 2010;2010:401581.
235. Skoumal M, Haberhauer G, Kolarz G, et al. Serum cathepsin K levels of patients with longstanding rheumatoid arthritis: correlation with radiological destruction. *Arthritis Res. Ther.*. 2004;7(1):R65.
236. Pennypacker BL, Duong LT, Cusick TE, et al. Cathepsin K inhibitors prevent bone loss in estrogen-deficient rabbits. *J. Bone Miner. Res.*. 2011;26(2):252-262.
237. Motyckova G, Weilbaecher KN, Horstmann M, et al. Linking osteopetrosis and pycnodysostosis: Regulation of cathepsin K expression by the microphthalmia transcription factor family. *Proc. Natl. Acad. Sci.*. 2001;98(10):5798-5803.
238. Roberts HC, Knott L, Avery NC, et al. Altered Collagen in Tartrate-Resistant Acid Phosphatase (TRAP)-Deficient Mice: A Role for TRAP in Bone Collagen Metabolism. *Calcif. Tissue Int.*. 2007;80(6):400-410.
239. Mansky KC, Sulzbacher S, Purdom G, et al. The microphthalmia transcription factor and the related helix-loop-helix zipper factors TFE-3 and TFE-C collaborate to activate the tartrate-resistant acid phosphatase promoter. *J. Leukoc. Biol.*. 2002;71(2):304-310.
240. Minkin C. Bone acid phosphatase: Tartrate-resistant acid phosphatase as a marker of osteoclast function. *Calcif. Tissue Int.*. 2006;34:285-290.
241. Angel N, Walsh N, Forwood M, et al. Transgenic Mice Overexpressing Tartrate-Resistant Acid Phosphatase Exhibit an Increased Rate of Bone Turnover. *J. Bone Miner. Res.*. 1999;15:103-110.
242. Hayman A, Cox T. Tartrate-Resistant Acid Phosphatase Knockout Mice. *J. Bone Miner. Res.*. 2003;18(10):1905-1907.
243. Hamano Y, Zeisberg M, Sugimoto H, et al. Physiological levels of tumstatin, a fragment of collagen IV α 3 chain, are generated by MMP-9 proteolysis and suppress angiogenesis via α V B3 integrin. *Cancer Cell.* 2003;3(6):589-601.
244. Nagase H, Visse R, Murphy G. Structure and function of matrix metalloproteinases and TIMPs. *Cardiovasc. Res.*. 2006;69(3):562-573.
245. Kim KC, Lee CH. MAP Kinase activation is required for the MMP-9 induction by TNF-stimulation. *Arch. Pharm. Res.*. 2005;28(11):1257-1262.
246. Fanger MW, Shen L, Graziano RF, Guyre PM. Cytotoxicity mediated by human Fc receptors for IgG. *Immunol. Today.* 1989;10(3):92-99.
247. Aderem A, Underhill DM. Mechanisms of phagocytosis in macrophages. *Annu Rev Immunol.* 1999;17:593-623.
248. Karsten CM, Köhl J. The immunoglobulin, IgG Fc receptor and complement triangle in autoimmune diseases. *Immunobiology.* 2012;217(11):1067-1079.
249. Nimmerjahn F, Ravetch JV. Fc γ Receptors: Old Friends and New Family Members. *Immunity.* 2006;24(1):19-28.
250. Janeway C, Travers P, Walport M, Shlomchik MJ. Immunobiology 5th Edition. 2001.
251. Poel CE van der, Spaapen RM, Winkel JGJ van de, Leusen JHW. Functional Characteristics of the High Affinity IgG Receptor, Fc γ RI. *J. Immunol.*. 2011;186(5):2699-2704.
252. Gessner J, Heiken H, Tamm A, Schmidt R. The IgG Fc Receptor Family. *Ann Hematol.* 1998;76(6):231-48.
253. Barrow AD, Trowsdale J. You say ITAM and I say ITIM, let's call the whole thing off: the ambiguity of immunoreceptor signalling. *Eur. J. Immunol.*. 2006;36(7):1646-1653.
254. Hogarth M. Immunoglobulin (Fc) Receptors. *Encycl. Biol. Chem.*. 2013;568-573.
255. Daëron M, Vivier E. Immunoreceptor Tyrosine Based Inhibition Motifs. Springer; 1999.

256. Worth RG, Schreiber AD. Fc Receptor Phagocytosis. *Mol. Mech. Phagocytosis*. 2005;33-48.
257. Administrator, Aloulou M, Mkaddem S, et al. IgG1 and IVIg induce inhibitory ITAM signaling through Fc gamma RIII controlling inflammatory responses. *Blood*. 2012;119(13):3084-3096.
258. Pfirsch-Maisonnas S, Aloulou M, Xu T, et al. Inhibitory ITAM Signaling Traps Activating Receptors with the Phosphatase SHP-1 to Form Polarized "Inhibisome" Clusters. *Sci. Signal.*. 2011;4(169):ra24.
259. Williams M, Bruhns P, Saeys Y, Hammad H, Lambrecht BN. The function of Fcγ receptors in dendritic cells and macrophages. *Nat. Rev. Immunol.*. 2014;14(2):94-108.
260. Bruhns P. Properties of mouse and human IgG receptors and their contribution to disease models. *Blood*. 2012;119(24):5640-5649.
261. Pierce AM, Lindskog S. Evidence for capping of Fc gamma receptors on osteoclasts. *Calcif. Tissue Int.*. 1986;39(2):109-116.
262. Seeling M, Hillen hoff U, David JP, et al. Inflammatory monocytes and Fcγ receptor IV on osteoclasts are critical for bone destruction during inflammatory arthritis in mice. *Proc. Natl. Acad. Sci.*. 2013;110(26):10729-34.
263. Hogg N, Shapiro IM, Jones SJ, Slusarenko M, Boyde A. Lack of Fc receptors on osteoclasts. *Cell Tissue Res.*. 1980;212(3):509-516.
264. Wang W, Ferguson DJP, Quinn JMW, Simpson AHRW, Athanasou NA. Osteoclasts Are Capable of Particle Phagocytosis and Bone Resorption. *J. Pathol.*. 1997;182(1):92-98.
265. Vugt M van, Heijnen AF, Capel PJ, et al. FcR gamma-chain is essential for both surface expression and function of human Fc gamma RI (CD64) in vivo. *Blood*. 1996;87(9):3593-3599.
266. Kuo TT, Aveson VG. Neonatal Fc receptor and IgG-based therapeutics. *mAbs*. 2011;3(5):422-430.
267. Huber AH, Kelley RF, Gastinel LN, Bjorkman PJ. Crystallization and stoichiometry of binding of a complex between a rat intestinal Fc receptor and Fc. *J. Mol. Biol.*. 1993;230(3):1077-1083.
268. Tzaban S, Massol RH, Yen E, et al. The recycling and transcytotic pathways for IgG transport by FcRn are distinct and display an inherent polarity. *J. Cell Biol.*. 2009;185(4):673-684.
269. Vidarsson G, Stemerding AM, Stapleton NM, et al. FcRn: an IgG receptor on phagocytes with a novel role in phagocytosis. *Blood*. 2006;108(10):3573-3579.
270. Kennedy MA. A Brief Review of the Basics of Immunology: The Innate and Adaptive Response. *Vet Clin Small Anim*. 2010;40(3):369-379.
271. Silverman GJ, Goodyear CS, Siegel DL. On the mechanism of staphylococcal protein A immunomodulation. *Transfusion (Paris)*. 2005;45(2):274-280.
272. Liu H, May K. Disulfide bond structures of IgG molecules. *mAbs*. 2012;4(1):17-23.
273. Wines BD, Powell MS, Parren PWHI, Barnes N, Hogarth PM. The IgG Fc Contains Distinct Fc Receptor (FcR) Binding Sites: The Leukocyte Receptors FcγRI and FcγRIIa Bind to a Region in the Fc Distinct from That Recognized by Neonatal FcR and Protein A. *J. Immunol.*. 2000;164(10):5313-5318.
274. Kaneko Y, Nimmerjahn F, Ravetch JV. Anti-Inflammatory Activity of Immunoglobulin G Resulting from Fc Sialylation. *Science*. 2006;313(5787):670-673.
275. Jefferis R. Aggregation, immune complexes and immunogenicity. *mAbs*. 2011;3(6):503-504.
276. Mosser D, Edwards J. Exploring the full spectrum of macrophage activation. *Nat. Rev. Immunol.*. 2008;8(12):958-969.
277. Loke P, Nair MG, Parkinson J, et al. IL-4 dependent alternatively-activated macrophages have a distinctive in vivo gene expression phenotype. *BMC Immunol.*. 2002;3(1):7.
278. Fleming BD, Mosser DM. Regulatory macrophages: Setting the Threshold for Therapy. *Eur. J. Immunol.*. 2011;41(9):2498-2502.

279. Lux A, Yu X, Scanlan CN, Nimmerjahn F. Impact of Immune Complex Size and Glycosylation on IgG Binding to Human FcγRs. *J. Immunol.*. 2013;190(8):4315-4323.
280. Ostreiko KK, Tumanova IA, Sykulev YuK. Production and characterization of heat-aggregated IgG complexes with pre-determined molecular masses: light-scattering study. *Immunol. Lett.*. 1987;15(4):311-316.
281. Torbinejad M, Clagett DJ, Engel D. A cat model for the evaluation of mechanisms of bone resorption: Induction of bone loss by simulated immune complexes and inhibition by indomethacin. *Calcif. Tissue Int.*. 1979;29(1):207-214.
282. Kuramoto A, Yoshinaga Y, Kaneko T, et al. The formation of immune complexes is involved in the acute phase of periodontal destruction in rats. *J. Periodontal Res.*. 2012;47(4):455-462.
283. Berger S, Balló H, Stutte HJ. Immune complex-induced interleukin-6, interleukin-10 and prostaglandin secretion by human monocytes: a network of pro- and anti-inflammatory cytokines dependent on the antigen: antibody ratio. *Eur. J. Immunol.*. 1996;26(6):1297-1301.
284. Ambarus CA, Santegoets KCM, van Bon L, et al. Soluble Immune Complexes Shift the TLR-Induced Cytokine Production of Distinct Polarized Human Macrophage Subsets towards IL-10. *PLoS ONE*. 2012;7(4):e35994.
285. Dwyer JM. Manipulating the Immune System with Immune Globulin. *N. Engl. J. Med.*. 1992;326(2):107-116.
286. Mandell BF. Intravenous gamma-globulin therapy. *J. Clin. Rheumatol.*. 1996;2(6):317-324.
287. Samuelsson A. Anti-inflammatory Activity of IVIG Mediated Through the Inhibitory Fc Receptor. *Science*. 2011;291(5503):484-486.
288. Li N, Zhao M, Hilario-Vargas J, et al. Complete FcRn dependence for intravenous Ig therapy in autoimmune skin blistering diseases. *J. Clin. Invest.*. 2005;115(12):3440-3450.
289. Schwab I, Nimmerjahn F. Intravenous immunoglobulin therapy: how does IgG modulate the immune system? *Nat. Rev. Immunol.*. 2013;13(3):176-189.
290. Lambris J, Ricklin D, Geisbrecht B. Complement evasion by human pathogens. *Nat. Rev. Microbiol.*. 2008;6(2):132-142.
291. Lowy FD. Staphylococcus aureus Infections. *N. Engl. J. Med.*. 1998;339(8):520-532.
292. Tashiro M, Montelione GT. Structures of bacterial immunoglobulin-binding domains and their complexes with immunoglobulins. *Curr. Opin. Struct. Biol.*. 1995;5(4):471-481.
293. Roben PW, Salem AN, Silverman GJ. VH3 family antibodies bind domain D of staphylococcal protein A. *J. Immunol.*. 1995;154(12):6437-6445.
294. Virgilio, Gonzalez, Munoz, Mendoza. Ability of Staphylococcus aureus cells to bind normal human immunoglobulin G. *Infect. Immun.*. 2003;2(3):342-344.
295. Ey PL, Prowse SJ, Jenkin CR. Isolation of pure IgG1, IgG2a and IgG2b immunoglobulins from mouse serum using protein A-Sepharose. *Immunochemistry*. 1978;15(7):429-436.
296. Lindmark R, Thorén-Tolling K, Sjöquist J. Binding of immunoglobulins to protein A and immunoglobulin levels in mammalian sera. *J. Immunol. Methods*. 1983;62(1):1-13.
297. Chalon MP, Milne RW, Vaerman J-P. Interactions between Mouse Immunoglobulins and Staphylococcal Protein A. *Scand. J. Immunol.*. 1979;9(4):359-364.
298. Snyder Jr. HW, Ernst NR, Grosmaire LS, et al. Selective removal of antigen-complexed IgG from cat plasma by adsorption onto a protein A-silica matrix. *J. Immunol. Methods*. 1987;101(2):209-217.
299. Dima S, Medeşan C, Moţa G, et al. Effect of protein A and its fragment B on the catabolic and Fc receptor sites of IgG. *Eur. J. Immunol.*. 1983;13(8):605-614.
300. Langone JJ, Das C, Mainwaring R, Shearer WT. Complexes prepared from protein A and human serum, IgG, or Fcγ fragments: characterization by immunochemical analysis of ultracentrifugation fractions and studies on their interconversion. *Mol. Cell. Biochem.*. 1985;65(2):159-170.

301. Atkins KL, Burman JD, Chamberlain ES, et al. S. aureus IgG-binding proteins SpA and Sbi: Host specificity and mechanisms of immune complex formation. *Mol. Immunol.*. 2008;45(6):1600-1611.
302. Sasso EH, Merrill C, Furst DE. Immunoglobulin Binding Properties of the Prosorba Immunoadsorption Column in Treatment of Rheumatoid Arthritis. *Ther. Apher.*. 2001;5(2):84-91.
303. Bosch T. Recent Advances in therapeutic apheresis. *J. Artif. Organs.* 2003;6(1):1-8.
304. Wiesenhutter CW, Irish BL, Bertram JH. Treatment of patients with refractory rheumatoid arthritis with extracorporeal protein A immunoadsorption columns: a pilot trial. *J. Rheumatol.*. 1994;21(5):804-812.
305. Mugnier B, Poullin P, Lefevre P, Roudier J. Clinical improvement in a patient with severe rheumatoid arthritis and chronic hepatitis B after prosorba column immunoadsorption: A one-year followup. *Arthritis Care Res.*. 2003;49(5):722-723.
306. Silverman GJ, Sasano M, Wormsley SB. Age-associated changes in binding of human B lymphocytes to a VH3-restricted unconventional bacterial antigen. *J. Immunol.*. 1993;151(10):5840-5855.
307. Silverman GJ, Nayak JV, Warnatz K, et al. The Dual Phases of the Response to Neonatal Exposure to a VH Family-Restricted Staphylococcal B Cell Superantigen. *J. Immunol.*. 1998;161(10):5720-5732.
308. Goodyear CS, Corr M, Sugiyama F, Boyle DL, Silverman GJ. Cutting Edge: Bim Is Required for Superantigen-Mediated B Cell Death. *J. Immunol.*. 2007;178(5):2636-2640.
309. Goodyear C, Silverman G. Death by a B Cell Superantigen: In Vivo VH-targeted Apoptotic Supraclonal B Cell Deletion by a Staphylococcal Toxin. *J. Exp. Med.*. 2003;197(9):1125-1139.
310. Shaw T, Quan J, Totoritis M. B cell therapy for rheumatoid arthritis: the rituximab (anti-CD20) experience. *Ann. Rheum. Dis.*. 2003;62(Suppl 2):ii55-ii59.
311. Deisenhofer J. Crystallographic refinement and atomic models of a human Fc fragment and its complex with fragment B of protein A from Staphylococcus aureus at 2.9- and 2.8-A resolution. *Biochemistry (Mosc.)*. 1981;20(9):2361-2370.
312. Jefferis R, Lund J. Interaction sites on human IgG-Fc for FcγR: current models. *Immunol. Lett.*. 2002;82(1-2):57-65.
313. Kim JK, Tsen MF, Ghetie V, Ward ES. Identifying amino acid residues that influence plasma clearance of murine IgG1 fragments by site-directed mutagenesis. *Eur. J. Immunol.*. 1994;24(3):542-548.
314. Medesan C, Matesoi D, Radu C, Ghetie V, Ward ES. Delineation of the amino acid residues involved in transcytosis and catabolism of mouse IgG1. *J. Immunol.*. 1997;158(5):2211-2217.
315. Silverman G. Confounding B-cell defences: lessons from a staphylococcal superantigen. *Nat. Rev. Immunol.*. 2006;6(6):465-475.
316. MacLellan L, Montgomery J, Sugiyama F, et al. Co-opting endogenous immunoglobulin for the regulation of inflammation and osteoclastogenesis in humans and mice. *Arthritis Rheum.*. 2011;63(12):3897-3907.
317. Grevers LC, Vries TJ de, Everts V, et al. Immune complex-induced inhibition of osteoclastogenesis is mediated via activating but not inhibitory Fcγ receptors on myeloid precursor cells. *Ann. Rheum. Dis.*. 2013;72(2):278-285.
318. Kippo K, Hannuniemi R, Virtamo T, et al. The effects of clodronate on increased bone turnover and bone loss due to ovariectomy in rats. *Bone*. 1995;17(6):533-542.
319. Schwarz EM, Krimpenfort P, Berns A, Verma IM. Immunological defects in mice with a targeted disruption in Bcl-3. *Genes Dev.*. 1997;11(2):187-197.
320. Hazenbos WLW, Gessner JE, Hofhuis FMA, et al. Impaired IgG-Dependent Anaphylaxis and Arthus Reaction in FcγRIII (CD16) Deficient Mice. *Immunity*. 1996;5(2):181-188.
321. Weischenfeldt J, Porse B. Bone Marrow-Derived Macrophages (BMM): Isolation and Applications. *Cold Spring Harb. Protoc.*. 2008;2008(12):1-6.

322. Englen MD, Valdez YE, Lehnert NM, Lehnert BE. Granulocyte/macrophage colony-stimulating factor is expressed and secreted in cultures of murine L929 cells. *J. Immunol. Methods.* 1995;184(2):281-283.
323. Yamamoto-Yamaguchi Y, Tomida M, Hozumi M. Effect of mouse interferon on growth and differentiation of mouse bone marrow cells stimulated by two different types of colony-stimulating factor. *Blood.* 1983;62(3):597-601.
324. Quinn JMW, Elliott J, Gillespie MT, Martin TJ. A Combination of Osteoclast Differentiation Factor and Macrophage-Colony Stimulating Factor Is Sufficient for both Human and Mouse Osteoclast Formation in Vitro. *Endocrinology.* 1998;139(10):4424-4427.
325. Nakagawa N, Kinoshita M, Yamaguchi K, et al. RANK Is the Essential Signaling Receptor for Osteoclast Differentiation Factor in Osteoclastogenesis. *Biochem. Biophys. Res. Commun.* 1998;253(2):395-400.
326. Lam J, Takeshita S, Barker J, et al. TNF-alpha induces osteoclastogenesis by direct stimulation of macrophages exposed to permissive levels of RANK ligand. *J. Clin. Invest.* 2000;106(12):1481-8.
327. Kobayashi K, Takahashi N, Jimi E, et al. Tumor Necrosis Factor α Stimulates Osteoclast Differentiation by a Mechanism Independent of the Odf/Rankl-Rank Interaction. *J. Exp. Med.* 2000;191(2):275-286.
328. Yao Z, Xing L, Qin C, Schwarz EM, Boyce BF. Osteoclast Precursor Interaction with Bone Matrix Induces Osteoclast Formation Directly by an Interleukin-1-mediated Autocrine Mechanism. *J. Biol. Chem.* 2008;283(15):9917-9924.
329. Kudo O, Sabokbar A, Pocock A, et al. Interleukin-6 and interleukin-11 support human osteoclast formation by a RANKL-independent mechanism. *Bone.* 2003;32(1):1-7.
330. Ishikawa S. Involvement of FcR gamma in signal transduction of osteoclast-associated receptor (OSCAR). *Int. Immunol.* 2004;16(7):1019-1025.
331. Yamashita T, Yao Z, Li F, et al. NF- κ B p50 and p52 Regulate Receptor Activator of NF- κ B Ligand (RANKL) and Tumor Necrosis Factor-induced Osteoclast Precursor Differentiation by Activating c-Fos and NFATc1. *J. Biol. Chem.* 2007;282(25):18245-18253.
332. Beinke S, Ley SC. Functions of NF- κ B1 and NF- κ B2 in immune cell biology. *Biochem. J.* 2004;382(2):393-409.
333. Takayanagi H, Kim S, Koga T, et al. Induction and Activation of the Transcription Factor NFATc1 (NFAT2) Integrate RANKL Signaling in Terminal Differentiation of Osteoclasts. *Dev. Cell.* 2002;3(6):889-901.
334. Sundaram K, Nishimura R, Senn J, et al. RANK ligand signaling modulates the matrix metalloproteinase-9 gene expression during osteoclast differentiation. *Exp. Cell Res.* 2007;313(1):168-178.
335. Shi Z, Silveira A, Patel P, Feng X. YY1 is involved in RANKL-induced transcription of the tartrate-resistant acid phosphatase gene in osteoclast differentiation. *Gene.* 2004;343(1):117-126.
336. Delaissé J-M, Andersen TL, Engsig MT, et al. Matrix metalloproteinases (MMP) and cathepsin K contribute differently to osteoclastic activities. *Microsc. Res. Tech.* 2003;61(6):504-513.
337. Fujisaki K, Tanabe N, Suzuki N, et al. Receptor activator of NF- κ B ligand induces the expression of carbonic anhydrase II, cathepsin K, and matrix metalloproteinase-9 in osteoclast precursor RAW264.7 cells. *Life Sci.* 2007;80(14):1311-1318.
338. Ravetch JV, Kinet JP. Fc Receptors. *Annu. Rev. Immunol.* 1991;9(1):457-492.
339. Krutmann J, Kirnbauer R, Köck A, et al. Cross-linking Fc receptors on monocytes triggers IL-6 production. Role in anti-CD3-induced T cell activation. *J. Immunol.* 1990;145(5):1337-1342.
340. Grevers L, Vries T, Everts V, et al. Immune complex-induced inhibition of osteoclastogenesis is mediated via activating but not inhibitory Fc gamma receptors on myeloid precursor cells. *Ann. Rheum. Dis.* 2013;72(2):278-85.

341. Eliasson M, Andersson R, Olsson A, Wigzell H, Uhlén M. Differential IgG-binding characteristics of staphylococcal protein A, streptococcal protein G, and a chimeric protein AG. *J. Immunol.* 1989;142(2):575-581.
342. Eliasson M, Olsson A, Palmcrantz E, et al. Chimeric IgG-binding receptors engineered from staphylococcal protein A and streptococcal protein G. *J. Biol. Chem.* 1988;263(9):4323-4327.
343. Langone JJ. Immune complex formation enhances the binding of staphylococcal protein A to immunoglobulin G. *Biochem. Biophys. Res. Commun.* 1980;94(2):473-479.
344. Mocsai A. The immunomodulatory adapter proteins DAP12 and Fc receptor γ -chain (FcR γ) regulate development of functional osteoclasts through the Syk tyrosine kinase. *Proc. Natl. Acad. Sci.* 2004;101(16):6158-6163.
345. Zaiss M, Kurowska-Stolarska M, Böhm C, et al. IL-33 Shifts the Balance from Osteoclast to Alternatively Activated Macrophage Differentiation and Protects from TNF α -Mediated Bone Loss. *J. Immunol.* 2011;186(11):6097-6105.
346. Collin-Osdoby P, Osdoby P. RANKL-Mediated Osteoclast Formation from Murine RAW 264.7 cells. *Bone Res. Protoc.* 2012;816:187-202.
347. He X, Andersson G, Lindgren U, Li Y. Resveratrol prevents RANKL-induced osteoclast differentiation of murine osteoclast progenitor RAW 264.7 cells through inhibition of ROS production. *Biochem. Biophys. Res. Commun.* 2010;401(3):356-362.
348. Hsu H, Lacey DL, Dunstan CR, et al. Tumor necrosis factor receptor family member RANK mediates osteoclast differentiation and activation induced by osteoprotegerin ligand. *Proc. Natl. Acad. Sci.* 1999;96(7):3540-3545.
349. Takahashi N, Yamana H, Yoshiki S, et al. Osteoclast-Like Cell Formation and its Regulation by Osteotropic Hormones in Mouse Bone Marrow Cultures. *Endocrinology.* 1988;122(4):1373-1382.
350. Burger EH, Meer JWV der, Gevel JS van de, et al. In vitro formation of osteoclasts from long-term cultures of bone marrow mononuclear phagocytes. *J. Exp. Med.* 1982;156(6):1604-1614.
351. Jandinski JJ. Osteoclast activating factor is now interleukin-1 beta: historical perspective and biological implications. *J. Oral Pathol. Med.* 1988;17(4):145-152.
352. Englen MD, Valdez YE, Lehnert NM, Lehnert BE. Granulocyte/macrophage colony-stimulating factor is expressed and secreted in cultures of murine L929 cells. *J. Immunol. Methods.* 1995;184(2):281-283.
353. Back JW, de Jong L, Muijsers AO, de Koster CG. Chemical Cross-linking and Mass Spectrometry for Protein Structural Modeling. *J. Mol. Biol.* 2003;331(2):303-313.
354. Quinn JM., Whitty G., Byrne R., Gillespie M., Hamilton J. The generation of highly enriched osteoclast-lineage cell populations. *Bone.* 2002;30(1):164-170.
355. Tushinski RJ, Oliver IT, Guilbert LJ, et al. Survival of mononuclear phagocytes depends on a lineage-specific growth factor that the differentiated cells selectively destroy. *Cell.* 1982;28(1):71-81.
356. Suzu S, Hiyoshi M, Yoshidomi Y, et al. M-CSF-mediated macrophage differentiation but not proliferation is correlated with increased and prolonged ERK activation. *J. Cell. Physiol.* 2007;212(2):519-525.
357. Celada A, Borrás F, Soler C, et al. The transcription factor PU.1 is involved in macrophage proliferation. *J. Exp. Med.* 1996;184(1):61-69.
358. Kwon OH, Lee C-K, Lee YI, Paik S-G, Lee H-J. The hematopoietic transcription factor PU.1 regulates RANK gene expression in myeloid progenitors. *Biochem. Biophys. Res. Commun.* 2005;335(2):437-446.
359. Lancet D, Isenman D, Sjö Dahl J, Sjöquist J, Pecht I. Interactions between staphylococcal protein A and immunoglobulin domains. *Biochem. Biophys. Res. Commun.* 1978;85(2):608-614.
360. Whaley K, Lappin D, McPhaden AR, Riches DW, Sandilands GP. A comparison of the effects of heat-aggregated and chemically cross-linked IgG on monocyte C2 production. *Immunology.* 1983;49(3):457-461.

361. Rankin CT, Veri M-C, Gorlatov S, et al. CD32B, the human inhibitory Fc- γ receptor IIB, as a target for monoclonal antibody therapy of B-cell lymphoma. *Blood*. 2006;108(7):2384-2391.
362. Yagi M, Miyamoto T, Sawatani Y, et al. DC-STAMP is essential for cell-cell fusion in osteoclasts and foreign body giant cells. *J. Exp. Med.*. 2005;202(3):345-351.
363. Chiu Y-H, Mensah KA, Schwarz EM, et al. Regulation of Human Osteoclast Development by Dendritic Cell-Specific Transmembrane Protein (DC-STAMP). *J. Bone Miner. Res. Off. J. Am. Soc. Bone Miner. Res.*. 2012;27(1):79-92.
364. Ravetch JV, Bolland S. Igg Fc Receptors. *Annu. Rev. Immunol.*. 2001;19(1):275-290.
365. Muto A, Mizoguchi T, Udagawa N, et al. Lineage-committed osteoclast precursors circulate in blood and settle down into bone. *J. Bone Miner. Res.*. 2011;26(12):2978-2990.
366. Quinn JM, Neale S, Fujikawa Y, McGee JO, Athanasou NA. Human osteoclast formation from blood monocytes, peritoneal macrophages, and bone marrow cells. *Calcif. Tissue Int.*. 1998;62(6):527-531.
367. Kitaura H, Sands MS, Aya K, et al. Marrow Stromal Cells and Osteoclast Precursors Differentially Contribute to TNF- α -Induced Osteoclastogenesis In Vivo. *J. Immunol.*. 2004;173(8):4838-4846.
368. Kaneda T, Nojima T, Nakagawa M, et al. Endogenous Production of TGF beta is essential for osteoclastogenesis induced by a combination of receptor activator of NF-kappa B Ligand and Macrophages colony stimulating Factor. *J. Immunol.*. 2000;165(8):4254-4263.
369. Lin SL, Castaño AP, Nowlin BT, Luper ML, Duffield JS. Bone Marrow Ly6Chigh Monocytes Are Selectively Recruited to Injured Kidney and Differentiate into Functionally Distinct Populations. *J. Immunol.*. 2009;183(10):6733-6743.
370. Strauss-Ayali D, Conrad SM, Mosser DM. Monocyte subpopulations and their differentiation patterns during infection. *J. Leukoc. Biol.*. 2007;82(2):244-252.
371. Yang J, Zhang L, Yu C, Yang X-F, Wang H. Monocyte and macrophage differentiation: circulation inflammatory monocyte as biomarker for inflammatory diseases. *Biomark. Res.*. 2014;2(1):1-27.
372. Michaud J-P, Bellavance M-A, Préfontaine P, Rivest S. Real-Time In Vivo Imaging Reveals the Ability of Monocytes to Clear Vascular Amyloid Beta. *Cell Rep.*. 2013;5(3):646-653.
373. Burke B, Ahmad R, Staples KJ, et al. Increased TNF expression in CD43⁺⁺ murine blood monocytes. *Immunol. Lett.*. 2008;118(2):142-147.
374. Majeska RJ, Ryaby JT, Einhorn TA. Direct modulation of osteoblastic activity with estrogen. *J. Bone Joint Surg. Am.*. 1994;76(5):713-721.
375. Krum SA, Miranda-Carboni GA, Hauschka PV, et al. Estrogen protects bone by inducing Fas ligand in osteoblasts to regulate osteoclast survival. *EMBO J.*. 2008;27(3):535-545.
376. Lindsay R, Aitken JM, Anderson LB, et al. Long term prevention of postmenopausal osteoporosis by oestrogen: evidence for an increased bone mass after delayed onset of oestrogen treatment. *The Lancet*. 1976;307(7968):1038-1041.
377. Jee WS, Yao W. Overview: animal models of osteopenia and osteoporosis. *J. Musculoskelet. Neuronal Interact.*. 2001;1(3):193-207.
378. Duque G, Huang DC, Dion N, et al. Interferon- γ plays a role in bone formation in vivo and rescues osteoporosis in ovariectomized mice. *J. Bone Miner. Res.*. 2011;26(7):1472-1483.
379. Kitazawa R, Kimble RB, Vannice JL, Kung VT, Pacifici R. Interleukin-1 receptor antagonist and tumor necrosis factor binding protein decrease osteoclast formation and bone resorption in ovariectomized mice. *J. Clin. Invest.*. 1994;94(6):2397-2406.
380. McNamara LM. Perspective on post-menopausal osteoporosis: establishing an interdisciplinary understanding of the sequence of events from the molecular level to whole bone fractures. *J. R. Soc. Interface*. 2010;7(44):353-372.

381. Phiel KL, Henderson RA, Adelman SJ, Elloso MM. Differential estrogen receptor gene expression in human peripheral blood mononuclear cell populations. *Immunol. Lett.*. 2005;97(1):107-113.
382. Kramer PR, Winger V, Kramer SF. 17 beta-estradiol utilizes the estrogen receptor to regulate CD16 expression in monocytes. *Mol. Cell. Endocrinol.*. 2007;279(1-2):16-25.
383. Biburger M, Aschermann S, Schwab I, et al. Monocyte Subsets Responsible for Immunoglobulin G-Dependent Effector Functions In Vivo. *Immunity*. 2011;35(6):932-944.
384. Rose S, Misharin A, Perlman H. A novel Ly6C/Ly6G-based strategy to analyze the mouse splenic myeloid compartment. *Cytometry A*. 2012;81A(4):343-350.
385. Lajeunesse D, Kiebzak GM, Frondoza C, Sacktor B. Regulation of osteocalcin secretion by human primary bone cells and by the human osteosarcoma cell line MG-63. *Bone Miner.*. 1991;14(3):237-250.
386. Reichel H, Roth H-J, Schmidt-Gayk H. Evaluation of serum beta-carboxy-terminal cross-linking telopeptide of type I collagen as marker of bone resorption in chronic hemodialysis patients. *Nephron Clin. Pract.*. 2004;98(4):c112-118.
387. Jämsä T, Jalovaara P, Peng Z, Väänänen HK, Tuukkanen J. Comparison of three-point bending test and peripheral quantitative computed tomography analysis in the evaluation of the strength of mouse femur and tibia. *Bone*. 1998;23(2):155-161.
388. Volpon JB, Shimano AC. Methods in Bone Biology in Animals: Biomechanics. *Osteoporos. Res.*. 2011;29-36.
389. Turner CH, Burr DB. Basic biomechanical measurements of bone: a tutorial. *Bone*. 1993;14(4):595-608.
390. Borah B, Gross GJ, Dufresne TE, et al. Three-dimensional microimaging (MRI and μ CT), finite element modeling, and rapid prototyping provide unique insights into bone architecture in osteoporosis. *Anat. Rec.*. 2001;265(2):101-110.
391. Melton JL. Perspectives: How many women have osteoporosis now? *J. Bone Miner. Res.*. 1995;10(2):175-177.
392. Halloran BP, Ferguson VL, Simske SJ, et al. Changes in Bone Structure and Mass With Advancing Age in the Male C57BL/6J Mouse. *J. Bone Miner. Res.*. 2002;17(6):1044-1050.
393. Cao JJ, Wronski TJ, Iwaniec U, et al. Aging Increases Stromal/Osteoblastic Cell-Induced Osteoclastogenesis and Alters the Osteoclast Precursor Pool in the Mouse. *J. Bone Miner. Res.*. 2005;20(9):1659-1668.
394. Mehra S, Fritzler MJ. The Spectrum of Anti-Chromatin/Nucleosome Autoantibodies: Independent and Interdependent Biomarkers of Disease. *J. Immunol. Res.*. 2014;2014:368274.
395. Li Y, Lee PY, Kellner ES, et al. Monocyte surface expression of Fc γ receptor RI (CD64), a biomarker reflecting type-I interferon levels in systemic lupus erythematosus. *Arthritis Res. Ther.*. 2010;12(3):R90.
396. Erben RG, Raith S, Eberle J, Stangassinger M. Ovariectomy augments B lymphopoiesis and generation of monocyte-macrophage precursors in rat bone marrow. *Am. J. Physiol. - Endocrinol. Metab.*. 1998;274(3):476-83.
397. Grau V, Scriba A, Stehling O, Steiniger B. Monocytes in the rat. *Immunobiology*. 2000;202(1):94-103.
398. Kuroda H, Nakamura M, Kamiyama K. Effects of calcitonin and parathyroid hormone on the distribution of F-actin in the clear zone of osteoclasts in vivo. *Bone*. 1996;19(2):115-120.
399. Katavić V, Grčević D, Lee SK, et al. The surface antigen CD45R identifies a population of estrogen-regulated murine marrow cells that contain osteoclast precursors. *Bone*. 2003;32(6):581-590.
400. Kramer PR, Kramer SF, Guan G. 17 β -estradiol regulates cytokine release through modulation of CD16 expression in monocytes and monocyte-derived macrophages. *Arthritis Rheum.*. 2004;50(6):1967-1975.

401. Srivastava AK, Bhattacharyya S, Castillo G, et al. Development and Application of a Serum C-Telopeptide and Osteocalcin Assay to Measure Bone Turnover in an Ovariectomized Rat Model. *Calcif. Tissue Int.*. 2000;66(6):435-442.
402. Rissanen JP, Suominen MI, Peng Z, et al. Short-Term Changes in Serum PINP Predict Long-Term Changes in Trabecular Bone in the Rat Ovariectomy Model. *Calcif. Tissue Int.*. 2008;82(2):155-161.
403. Martin-Millan M, Almeida M, Ambrogini E, et al. The estrogen receptor-alpha in osteoclasts mediates the protective effects of estrogens on cancellous but not cortical bone. *Mol. Endocrinol.*. 2010;24(2):323-334.
404. Comelekoglu U, Bagis S, Yalin S, et al. Biomechanical evaluation in osteoporosis: ovariectomized rat model. *Clin. Rheumatol.*. 2007;26(3):380-384.
405. Bouxsein M, Boyd S, Christiansen B, et al. Guidelines for assessment of bone microstructure in rodents using micro-computed tomography. *J. Bone Miner. Res.*. 2010;25(7):1468-1486.
406. Khosla S, Melton LJ, Riggs BL. The unitary model for estrogen deficiency and the pathogenesis of osteoporosis: Is a revision needed? *J. Bone Miner. Res.*. 2011;26(3):441-451.
407. Ominsky MS, Stouch B, Schroeder J, et al. Denosumab, a fully human RANKL antibody, reduced bone turnover markers and increased trabecular and cortical bone mass, density, and strength in ovariectomized cynomolgus monkeys. *Bone*. 2011;49(2):162-173.
408. Dempster DW, Lambing CL, Kostenuik PJ, Grauer A. Role of RANK ligand and denosumab, a targeted RANK ligand inhibitor, in bone health and osteoporosis: a review of preclinical and clinical data. *Clin. Ther.*. 2012;34(3):521-536.
409. Watkins MP, Norris JY, Grimston SK, et al. Bisphosphonates improve trabecular bone mass and normalize cortical thickness in ovariectomized, osteoblast connexin43 deficient mice. *Bone*. 2012;51(4):787-794.
410. Ballow C, Leh A, Slentz-Kesler K, et al. Safety, Pharmacokinetic, Immunogenicity, and Pharmacodynamic Responses in Healthy Volunteers Following a Single Intravenous Injection of Purified Staphylococcal Protein A. *J. Clin. Pharmacol.*. 2013;53(9):909-918.
411. Kim N, Odgren PR, Kim D-K, Marks SC, Choi Y. Diverse roles of the tumor necrosis factor family member TRANCE in skeletal physiology revealed by TRANCE deficiency and partial rescue by a lymphocyte-expressed TRANCE transgene. *Proc. Natl. Acad. Sci.*. 2000;97(20):10905-10910.
412. Poljak L, Carlson L, Cunningham K, Kosco-Vilbois MH, Siebenlist U. Distinct activities of p52/NF-kappa B required for proper secondary lymphoid organ microarchitecture: functions enhanced by Bcl-3. *J. Immunol.*. 1999;163(12):6581-6588.
413. Ruan Q, Zheng S-J, Palmer S, Carmody R, Chen Y. Roles of Bcl-3 in the pathogenesis of murine type 1 diabetes. *Diabetes*. 2010;59(10):2549-57.
414. Brasier AR, Lu M, Hai T, Lu Y, Boldogh I. NF-kappa B-inducible BCL-3 expression is an autoregulatory loop controlling nuclear p50/NF-kappa B1 residence. *J. Biol. Chem.*. 2001;276(34):32080-32093.
415. Iwasawa M, Miyazaki T, Nagase Y, et al. The antiapoptotic protein Bcl-xL negatively regulates the bone-resorbing activity of osteoclasts in mice. *J. Clin. Invest.*. 2009;119(10):3149-3159.
416. Viatour P, Bentires-Alj M, Chariot A, et al. NF-kappa B2/p100 induces Bcl-2 expression. *Leukemia*. 2003;17(7):1349-1356.
417. Bober LA, Grace MJ, Pugliese-Sivo C, et al. The effect of GM-CSF and G-CSF on human neutrophil function. *Immunopharmacology*. 1995;29(2):111-119.
418. Lang RA, Metcalf D, Cuthbertson RA, et al. Transgenic mice expressing a hemopoietic growth factor gene (GM-CSF) develop accumulations of macrophages, blindness, and a fatal syndrome of tissue damage. *Cell*. 1987;51(4):675-686.
419. Ferguson VL, Ayers RA, Bateman TA, Simske SJ. Bone development and age-related bone loss in male C57BL/6J mice. *Bone*. 2003;33(3):387-398.

420. Walker T, Adamson A, Jackson DA. BCL-3 attenuation of TNFA expression involves an incoherent feed-forward loop regulated by chromatin structure. *PLoS One*. 2013;8(10):e77015.
421. Mitchell TC, Hildeman D, Kedl RM, et al. Immunological adjuvants promote activated T cell survival via induction of Bcl-3. *Nat. Immunol.*. 2001;2(5):397-402.
422. Bauer A, Villunger A, Labi V, et al. The NF- κ B regulator Bcl-3 and the BH3-only proteins Bim and Puma control the death of activated T cells. *Proc. Natl. Acad. Sci.*. 2006;103(29):10979-10984.
423. Wang VY-F, Huang W, Asagiri M, et al. The Transcriptional Specificity of NF- κ B Dimers Is Coded within the κ B DNA Response Elements. *Cell Rep.*. 2012;2(4):824-839.
424. Na SY, Choi JE, Kim HJ, et al. Bcl3, an I κ B protein, stimulates activating protein-1 transactivation and cellular proliferation. *J. Biol. Chem.*. 1999;274(40):28491-28496.
425. Liebermann DA, Gregory B, Hoffman B. AP-1 (Fos/Jun) transcription factors in hematopoietic differentiation and apoptosis. *Int. J. Oncol.*. 1998;12(3):685-1385.
426. Lee M, Kim H, Yeon J-T, et al. GM-CSF regulates fusion of mononuclear osteoclasts into bone-resorbing osteoclasts by activating the Ras/ERK pathway. *J. Immunol.*. 2009;183(5):3390-9.
427. Postiglione L, Domenico GD, Montagnani S, et al. Granulocyte-Macrophage Colony-Stimulating Factor (GM-CSF) Induces the Osteoblastic Differentiation of the Human Osteosarcoma Cell Line SaOS-2. *Calcif. Tissue Int.*. 2003;72(1):85-97.
428. Modrowski D, Lomri A, Marie PJ. Endogenous GM-CSF is involved as an autocrine growth factor for human osteoblastic cells. *J. Cell. Physiol.*. 1997;170(1):35-46.
429. Yao Z, Li Y, Yin X, et al. NF- κ B RelB Negatively Regulates Osteoblast Differentiation and Bone Formation. *J. Bone Miner. Res.*. 2014;29(4):866-877.
430. Yao GQ, Sun BH, Insogna KL, Weir EC. Nuclear factor-kappaB p50 is required for tumor necrosis factor-alpha-induced colony-stimulating factor-1 gene expression in osteoblasts. *Endocrinology*. 2000;141(8):2914-2922.
431. Gomez M. Staphylococcus aureus Protein A Activates TNFR1 Signaling through Conserved IgG Binding Domains. *J. Biol. Chem.*. 2006;281(29):20190-20196.
432. Hartleib J, Herrmann M. Protein A is the von Willebrand factor binding protein on Staphylococcus aureus. *Blood*. 2000;96:2149-2156.
433. Gómez MI, Lee A, Reddy B, et al. Staphylococcus aureus protein A induces airway epithelial inflammatory responses by activating TNFR1. *Nat. Med.*. 2004;10(8):842-848.
434. Claßen A, Kalali BN, Schnopp C, et al. TNF receptor I on human keratinocytes is a binding partner for staphylococcal protein A resulting in the activation of NF kappa B, AP-1, and downstream gene transcription. *Exp. Dermatol.*. 2011;20(1):48-52.
435. Claro T, Widaa A, O'Seaghdha M, et al. Staphylococcus aureus Protein A Binds to Osteoblasts and Triggers Signals That Weaken Bone in Osteomyelitis. *PLoS ONE*. 2011;6(4):e18748.
436. Widaa A, Claro T, Foster TJ, O'Brien FJ, Kerrigan SW. Staphylococcus aureus Protein A Plays a Critical Role in Mediating Bone Destruction and Bone Loss in Osteomyelitis. *PLoS ONE*. 2012;7(7):e40586.
437. Austyn JM, Gordon S. F4/80, a monoclonal antibody directed specifically against the mouse macrophage. *Eur. J. Immunol.*. 1981;11(10):805-815.
438. Pratt MAC, Bishop TE, White D, et al. Estrogen withdrawal-induced NF-kappaB activity and bcl-3 expression in breast cancer cells: roles in growth and hormone independence. *Mol. Cell. Biol.*. 2003;23(19):6887-6900.